Graz University of Technology

Niels Buchhold, Dipl.-Ing.

3-axes sensor for highly sensitive control of medical devices with dynamic and adaptive adjustment to the existing force and range of motion

DISSERTATION

Submitted in fulfillment of the requirements for the degree of

Doctor of Technological Science

to

Technische Universität Graz

Supervisor

Univ.-Prof. Dipl.-Ing. Dr. techn., Christian Baumgartner

Institute of Health Care Engineering with

European Testing Center of Medical Devices

Graz, August 2017

STATUTORY DECLARATION

I declare that I have authored this thesis independently, that I have not used other than the declared sources / resources, and that I have explicitly marked all material which has been quoted either literally or by content from the used sources.

Graz, ...
date (signature)

I explicitly point to the fact that female and male persons are represented in this thesis as one gender for ease of communication without any intention of discrimination.

Acknowledgments

This thesis summarizes my research of alternative sensor systems for medical devices. The studies have been conducted during my time at the TU-Graz, Institute of Health Care Engineering. I want to give my thanks to all for the time, assistance and patience given to me so generously. I would like to express my sincere gratitude to Univ.-Prof. Dipl.-Ing. Dr. techn. Christian Baumgartner for his trust and for the opportunity to work under the best possible inspiring research conditions. Above all, the unique culture and open-mindedness at this institute made this thesis possible.

My special thanks are given to Dipl. Chem. Günther Wagenknecht, former CEO of DeltaMed GmbH, Friedberg/Hessen, for the constant support and advice with respect to materials and polymer processing.

I would like to thank all fellow researchers and friends for the fruitful discussions and constructive criticisms. Special thanks to Faust Borlinghaus, Dr. Friedrich Hanser, Andreas Jaksch, Michael Lamer, Heidi Moser, Achim Szameitat, Thomas Thaler, Dr. Thomas Uchronski.

Moreover, I am indebted to my beloved wife Barbara for her patience, constant encouragement, proofreading and that she never complained about the many days, evenings and weekends which I spent full of work. Also thanks to my dear daughter Nina who is also studying, and to my mother-in-law Manuela not only for the fabulous nutrition every Sunday but also for her permanent support.

Last but not least, I would like to thank my parents, Renate and Claus Buchhold, for their optimism, trust and unconditional support.

Kurzfassung

Die Verbindung zwischen Mensch und Maschine stellt immer höhere Ansprüche an Forschung und Entwicklung. Dabei steht die Wandlung analoger Informationen in digital verwertbare Daten im Vordergrund. Forscher arbeiten weltweit mit hohem Ressourceneinsatz um die Kommunikation zwischen Mensch und Maschine zu realisieren und zu optimieren. Einige dieser Kommunikationswege wurden bereits geschaffen und erleichtern dadurch das Leben vieler Menschen. Insbesondere Menschen mit körperlichen Defiziten profitieren von dieser sehr beachtlichen Entwicklungsgeschwindigkeit.

Diese Thesis befasst sich mit der Umsetzung von Kraft und Bewegung in digitale Signale. Die Aufgabenstellung scheint längst gelöst zu sein, da bereits eine Vielzahl von Eingabegeräten das tägliche Leben der Menschen begleitet. Werden jedoch nicht nur gesunde Menschen, sondern ebenso Menschen mit gesundheitlichen Beeinträchtigungen in den Kreis der möglichen Nutzer aufgenommen wird die Umsetzung um ein vielfaches komplexer. Unterschiedlichste Krankheitsbilder bringen unterschiedliche Kraft- und Bewegungsmöglichkeiten mit sich. Zudem verändern sich diese Möglichkeiten nicht nur durch das Voranschreiten einer Krankheit, sondern auch durch viele andere Faktoren wie zum Beispiel der Umgebungstemperatur. Der Forschungsansatz dieser Thesis liegt unter anderem darin Sensoren zu entwickeln, welche sich an die verschiedenen Kraft- und Bewegungsmöglichkeiten der Nutzer anpassen können. Dieser Anpassungsprozess sollte durch den Nutzer selbst und zu jeder Zeit ausführbar sein. Dabei müssen die zu entwickelnden Sensoren intelligent sein um eine nutzeroptimierte und zugleich höchstzuverlässige Nutzung zu ermöglichen. Im Rahmen einer Machbarkeitsstudie wurden 3 unterschiedliche voll funktionstüchtige Prototypen entwickelt. Während innerhalb der ersten Version ein Laserstrahl durch die eingebrachte Kraft abgelenkt wird und eine Projektion auf einem Bildsensor erzeugt, bedient sich die zweite und dritte Variante der Verformung eines Bewegungsträgers. Diese Verformung wird mittels Dehnungsmessstreifen detektiert und in digitale Signale umgesetzt. Die Einsatzmöglichkeiten der entwickelten Sensoren sind selbstverständlich nicht nur auf den Einsatz medizinischer Geräte beschränkt. Da die optische Variante eine extrem hohe Auflösung verzeichnet und zudem weitestgehend resistent gegenüber Störstrahlung ist wird der Einsatz in

hochsensiblen Bereichen wie Militär, Luft- und Raumfahrt ebenso denkbar. Die hierbei generierten digitalen Signale werden abschließend einer komplexen Plausibilitätsprüfung unterzogen wodurch die Nutzungssicherheit nochmals gesteigert wird.

Die größten Herausforderungen lagen darin, höchste Sensibilität und Robustheit in einem Gerät zu vereinen. Winkelabweichungen der Sensorachse im Bereich von $20\ \mu°$ werden zuverlässig und reproduzierbar verarbeitet. Die durchgeführten Untersuchungen zeigen, dass mittels der entwickelten Prototypen die in der Aufgabenstellung geforderten Eigenschaften erfüllt werden konnten. Während einer Testphase mit verschiedenen Probanden wurde die Eignung und Verwendbarkeit der Sensoren eingehend untersucht und bestätigt.

Abstract

The man-machine interaction imposes high demands on research and development. The conversion of analog information to digitally usable data stands in the foreground. All researchers in the world work with intensive use of resources to execute and optimize the communication between humans and machines. Some of these communication channels have been created already and facilitate the life of many people. In particular, humans with physical deficits profit from this considerable development speed.

This thesis deals with the conversion of force and motion into digital signals. This task seems to have been solved already for a long time because there is already a large number of input devices which accompany people in their daily life. If, however, not only healthy people shall use these devices but also humans with physical defects then the task, and with it the conversion, will become much more complex. Different diseases involve different force and motion options. Furthermore, these options do not only vary with the progressing illness but are also impacted by many other factors, e.g. ambient temperature. The research approach is to develop sensors which are able to adapt to the difference force and motion options of the users. This adaptation process should be executable anytime by the user himself. The sensors to be developed need to be intelligent to enable a user-optimized and, simultaneously, a highly reliable application. In a feasibility study, 3 different fully working prototypes have been developed. While in the first version, a laser beam is deflected by the applied force and an image is projected on an image sensor, the second and third variants used the deformation of a motion carrier. This deformation is detected with the aid of strain-gauges and then converted into digital signals. These developed sensors are, of course, not limited to the use in medical devices. Since the optical variant is characterized by an extremely high resolution and, in addition, is highly resistant against interfering radiation, their use is also thinkable in highly sensitive areas, e.g. in the military area and in the aerospace industry. The generated digital signals finally pass a complex plausibility test which further increases the security of the used signals.

The biggest challenge is to combine sensitivity and robustness in one unit. Angle deviations of the sensor axis in a range of $20\ \mu°$ are processed reliably and reproducibly. Executed researches show that the developed prototypes and their properties satisfy the claims. In a test phase with different probands, the suitability and usability of the sensors were thoroughly investigated and confirmed.

Table of Contents

List of Figures

List of Tables

List of Abbreviations

A/D	Analog / digital
ADC	Analog digital converter
AFRP	Aramid fibre reinforced plastic
AOI	Area of interest
CAN	Controller area network
CFRP	Carbon fibre reinforced plastic
CNC	Computer numerically controlled
DSP	Digital signal processor.
EMI	Electromagnetic interferences
EPW	Electronic power wheelchair
FPS	Frames per second
GFRP	Glass fibre reinforced plastic
H	Horinzontal
H700	Class fine dust filter
I/O	Input / output
I2C	Inter-Integrated Circuit
MDPI	Multidisciplinary Digital Publishing Institute
MMI	Man-machine interface
MPG	German: Medizin Produktgesetz
PCT	Patent Cooperation Treaty
Piezo	Piezo element
PVC	Polyvinylchlorid
RFI	Radio frequency interferences
SG	Strain-gauge
SGD	Strain-gauge-disk
SPI	Serial Peripheral Interface
V	Vertical

1. Introduction

1.1 Sensors in joystick design and application areas

Sensors in form of joysticks were first found in the military area in the Second World War [1]. Different missiles could be remote controlled by sensors of joystick type after launching. In the post-war period, the intuitive handling was taken over by the industry. At this time, the joystick was designated “commander” when its former principle function resembled to its function today. In the post-war period, multi-axis machines such as cranes were controlled by joysticks. In the beginning of the 50s, joysticks were used in model series for remote control. After the computer-mouse came up in the 80s, the mouse replaced the joystick and the joystick migrated to the world of computer games. The built-in sensors became more and more robust and got further functions.

The use of the actual joysticks depends on different technologies (see Table 1). It is principally distinguished between analog and digital signal processing. The fields of application are categorized as follows.

Table 1: Application fields of joysticks and their technical executions

Consumer	Industrial	Automotive	Medical	Marine, Aerospace, Aviation, Military
Potentiometry Digital	Potentiometric, inductive, capacitive Digital (switches, keys) Pneumatic, hydraulic Hall principle Optical (analog)			

The security requirements vary by the purpose of use; this aspect can be omitted, however, in the consumer area.

Another important execution feature is the technical resolution. The general difference between digital and analog signals, however, is not uniquely defined

since normally, analog signals are converted into digital signals by A/D-converters (ADC) [2]. A computer system can only process analog values in a digital format. Potentiometric ally working joysticks are provided with potentiometers for every axis. This means, that an infinite number of analog values exists, depending on the modulated motion axis. The value is limited by the dimension of the ADC. If, for example, a 10 bit ADC is used then, theoretically, 1024 values (digits) can be distinguished. Since in this case, the analog values are generated by a sliding contact on the resisting surface, the ability to reproduce a value in relation to the targeted position is guaranteed only to a limited extent. Factors such as temperature, humidity, homogeneity of resisting material etc. are responsible for this situation. Most probably, the large number of different joystick models and active principles (see Table 1) will cover a major part of all possible applications. The largest possible areas of different users and their motion options are rather neglected. This thesis takes up this deficit and tries to close the gap.

1.2 Task and motivation

In application areas such as medical engineering, top security is required when using joysticks. Furthermore, a large spectrum of individual applications is necessary. Just for physically handicapped humans, e.g. quadriplegia, spastics or humans with muscle diseases, the use of a sensor (joystick) often becomes a problem since the motion spectrum (force and stroke) due to the illness is subject to permanent changes. Depending on the specification, a certain accuracy (resolution), force for steering and stroke is defined for off-the-shelf joysticks to master the necessary paths, or the application of joysticks rests within a few variables. In most cases, however, an individual adaptation of the sensor seems to be impossible although the spectrum of forces and motions of the handicapped user may vary again and again due to different factors in short-time intervals. An individual construction of the sensor, however, goes in line with high production costs. The legal regulations of individual production surpass the available cost frame, that’s why the performance carriers normally reject a reconstruction of this kind. Most European countries calculate by lump sums (Ex.: Germany) [3]. Amounts can be taken from corresponding clinical pictures which are available

for the case of illness in question. A repeated individualization of the tools in context with the input device treated here, is not taken into account and must be applied for and checked and approved in tedious single cases – in best case. Also, expensive medical reports need to be created.

Therefore, this task can only be assigned to the development of alternative sensor systems which will be able to adapt to the actual force, stroke and motion spectrum of the users without technical intervention and at any time. The necessity of this new development bases on the sad fact that solely in the area of muscular disease acc. to Walton‘ classification, 800 forms exist [4]. The illness, popularly called “loss of muscles”, shows different courses of disease. It can touch some muscle groups as well as the total muscular structure [4]. For both principle forms of this illness (muscle dystrophy and spinal muscle atrophy), a source-related medical treatment could unfortunately not yet have been established. Pursuant to the information from Deutsche Gesellschaft für Muskelkrankheiten e.V., 10 to 100000 people are suffering from this illness on the average worldwide. The division by gender turns out to the disadvantage of the male sufferers.

The Institute of Health Care Engineering [5] at TU Graz deals with the development, evaluation and validation of new sensor technologies with the objective to establish new technical approaches to support diagnoses and therapies. Special attention is given to the methodical, device-, operation-, organizational-, quality-assuring and economic aspects of health care. Here, the ideal development environment for this research topic was found.

Another reason of equal importance for this topic is the economic aspect which is of concern for health care and related service providers. Savings mostly lead to a strict shortening of services so that processes, systems and also medical devices should be optimized on a continuous basis. For example, an investment in the individual adaptation of the input device to a muscle illness can be a false investment since it may happen that the illness progresses during the adaptive reconstruction so that the just executed modification is obsolete. These ineffective costs must be avoided. The sensors described in this thesis will avoid those risks. A use in development countries would also be thinkable, since the robust and easy to use technology does not need special resources or experts.

Even if the technology is passed on to other persons, an individual adaptation will be executed within just a few seconds.

Finally, another important social aspect must still be outlined. People with a high physical disease are normally forced to a 24 h support or nursing. According to personal statements, the patients suffer from a completely missing private atmosphere. Without a suitable input medium, it is not possible to make an undisturbed phone call or to write down a text. Also here, tremendous surplus costs result since the nursing staff is permanently forced to help. This negative effect can be diminished in favor of all participants. If an optimally adapted input device is available, then the user can control his environment temporarily without foreign assistance. The necessary systems are available in sufficient variants at low cost. The input device must only be adapted to the environment control system. Standardized protocols via Wi-Fi, Bluetooth or Infrared facilitate this link.

1.3 Profit and target

The profit of this thesis is the ability to convert individual physical motions into machine-readable signals. If the sensors are used for medical reasons, the living with this illness or disease should be possible within an acceptable frame. If the sensors are used by healthy users then the sensors will recognize the motoric properties and improve the accuracy of use. An individual adaptation generally cares for a fatigue-free working. The cost-effective and maintenance-free construction should make it possible to also supply emerging and other countries with adequate input devices. The safe use is an actual novelty in comparison with off-the-shelf multi-axis sensors combined with the extremely high and reproducible resolution, especially with the optical variant. All known systems do not reach all of the advantages in the same scope as outlined in this thesis. A natural “force-feedback effect” results from the almost non-perceivable paths and exponential reset force which are needed to move the sensor. This positive effect is explained by the fact that the motion carrier and with it also the axis of the sensors can only be moved by < 1° in every direction. The user perceives this as a rigid system. If an input force is applied to such a rigid system then the skin feels a pressure proportionally to the applied input force. Users report of a very pleasant effect in

comparison with normal joysticks. Normal joysticks are usually provided with return springs. The effect of a proportionally increased counter force is very low. If such a joystick is used, then the user cannot derive the actual motion from the applied force without looking at the motion axis during application. The used optical procedure clearly increases the safe use. Disturbing influences, e.g. electromagnetic interference (EMI) or radio frequency interference (RFI), as well as temperature differences do not impact the sensor or only marginally. This enables to extend the application areas of the sensor as desired. In particular, application areas are thinkable such as Automotive, Aerospace, Marine and Military.

2. Problem analysis

2.1 Problem analysis, target development

The sensors used in medical engineering for positioning are mainly of conventional construction. Seeing the many variables in the severest inability with differently progressing illnesses and different factors of influence, the development of an input device for all application purposes seems to be hard to realize. In particular, the available force and stroke related ability of the user are of greatest importance. The problem of the different stroke motions can be compensated by a generally short stroke for all users. Test positions and questionnaires have shown that users with high stroke motion ability can work with the systems in a similar way as those with a small stroke motion ability. The opposite, however, is not possible. Unfortunately, the problem of the applied force cannot be solved in an analog way. The force spectrum needed to use the sensor must be adapted highly individually to the available force spectrum of the user. If a healthy user with a normal force spectrum would use a highly sensitive sensor, then this would principally be possible. The necessary fine motoric here, however, favors wrong inputs and a fatigue in concentration. Vice versa, a user with low force spectrum cannot use a sensor which responds to the applied force by a too high return force. Another special case can be found in the field of spastic illnesses. Spastics generate enormous forces during a spastic and can act outside a spastic with a

relatively fine motoric. Therefore, the used sensor must be able to cope with high forces and simultaneously respond sensitively to fine motoric inputs.

The explained specifications will first result in the needed basic properties of this sensor as follows:

- Low motion upward (stroke)
- Protection against overload

To be able to process an as large as possible spectrum of applied forces with an as small as possible motion stroke, the counter-force must be exponential to the applied force. Since the total stroke shall be executed in a maximum angle deviation of < 1°, the necessity of such a very high resolution becomes obvious. To cover the application areas listed in chapter 1.3, the reproduction of the output values must be guaranteed. This can be checked by an accuracy micrometer screw. For this purpose, the sensor and the micrometer screw is placed in a statically closed system. The rotation of the micrometer screw against the sensor axis generates a defined force. In principle, it is reasonable to execute this test construction with accuracy scales. But it was found out that the described test position allowed a clearly more precise gradation. Thinkable would be a combination of micrometer screws and scales. If a defined force is applied to the sensor axis, then an appropriately defined output value is generated. At any other time point, the sensor must generate the exact output value with the same input force. Also, different temperatures should not influence the result. Consequently, further primary properties are required:

- High resolution
- Temperature stability

To generate an output value with high resolution within the targeted low stroke, the used hardware needs to work with a similar high solution. In case of medical use for physically highly disabled humans, the sensor to be developed should provide min. 100 reproducible digits in every direction. This value cannot be reached with the hardware on the market because of the deflection angle of

<1°. If a 10 bit ADC per axis is used then theoretically 512 digits are generated in every direction. This value, however, refers to the total deflection stroke per direction. The deflection angle of an off-the-shelf joystick is normally approx. 30° [6]. This means, in case the targeted deflection is 1°, that max. 17 digits would be available. A hardware conceived in this form would not be able anymore to accept and convert an inhomogeneous force spectrum of a user, since the reached max. deflection could locate in a range of µ°. Another problem is the ability of the sensor axis to retrieve the zero-position with the necessary accuracy. This problem occurs with a deflection of 30° through a normal tension spring and a corresponding gate. If the max. deflection angle, however, is < 1°, and if simultaneously, a resolution greater than 100 is executed in any direction, then the relative zero-position must locate at least in the milli degree range. The latter problem refers to the protection against EMI and RFI. A system can only be protected against electromagnetic radiation by the screening properties of a metallic or a metalized housing. Since the major part of the industrial multi-axis sensors base on the inductive, capacitive and magnetic (hall) principles, the indicated form of radiation is of special relevance. To bypass this problem, only the following effective principles would be valid:

- Optic
- Acoustic
- Strain gauges (SG)

Also combinations of the indicated effective principles would be thinkable.

2.2 Scope of development and research

In this thesis, the hardware development is limited to the manufacture of two fully functioning prototypes. The software should prove the basic principles and the feasibility. Since the selection of the effective principles (refer to Chapter 2.1) consists of three solution approaches, these approaches are, of course, followed up. In the first investigation of these effective principles, the advantages and disadvantages of all possible approaches are worked out. The subsequent selection

will result in the final approach-related candidates. The scope of research of the final hardware to be developed should at least include the following criteria:

- Feasibility (technical feasibility in production)
- Usability (in a medical engineering context)
- Suitability (in a medical engineering context)

To secure the technical feasibility, every development step will be analyzed. The possibility of an industrial production must be given anytime. Absolutely necessary manual interventions in the production process should be avoided. To be able to renounce at an increased accuracy of production, the software uses calibration processes to compensate production tolerances.

The usability is secured by different test constructions. Specific control jobs are used and analyzed by different test persons. All feedbacks are incorporated in the actual development and will be considered in the technology, if possible, or at least be documented. Minimum the following test constructions are planned:

- Control of an electric power wheelchair (EPW)
- Control of a computer mouse

The suitability is determined by a questionnaire still to be conceived. Since the hardware will be in a prototype state at inquiry time, the questioning can only take place within a limited test field of max. 10 to 20 test positions. As far as possible, the prototypes will be modified later according to the collected requirements. If a modification within this thesis will not be possible anymore, then a job list for future development activities will be created from the open requirements. If possible, secondary problems will be assigned in form of master theses, which will contain, among others:

- Selection of suitable image sensors and signal processors
- New development of a circuit board layout
- Software revision
- Development of housing

- Commercial assessment of sensor
- Test of sensor as regulated by the medical product law (German: MPG).

2.3 State of the art technology

As can be seen from Table 1, the following effective principles are essentially used in multi-axis sensors:

- Potentiometric
- Inductive
- Capacitive
- Digital (keys)
- Pneumatic
- Hydraulic
- Hall principle
- Optical (analog)

The primary application fields, the effective principles and their advantages and disadvantages, will be shown below.

2.3.1 Potentiometric effective principle

The pivot of every axis of these multi-axis sensors is connected to a potentiometer. The deflection of the sensor axis generates a resistance value per motion axis. Technically conditioned, a sliding contact is moved across the resisting surface. This construction implies a wear as well as an imprecise reproducibility of the deflection ratio to the generated value of resistance. The sensors are relatively filigree and need to be protected against penetrating dust and humidity. In most cases, a rubber bellow encapsulates the sensors. It is fixed to the housing in the lower area and coats the sensor axis in the upper area. The rubber bellow (neoprene or santoprene) is also subject to natural wear and tends to crack formation when aging. Due to the deflection angle in a range of approx. 30°, a sealing can only be made by such a rubber bellow. In addition, the described re-

sistance tracks are extremely sensitive against temperatures. The resistance tolerance of series 4000 sensors of company APEM amounts to +/- 20% with a linearity of +/- 2% [6]. Here, the output voltage is available in an analog format.

2.3.2 Inductive effective principle

An inductive multi-axis sensor possesses air coils which are geometrically arranged on a circuit board. The coils can also be directly implemented in the layout of the conductor tracks [7]. Another air coil is firmly fixed to the sensor axis and swings over the coils on the circuit board during deflection. The movable air coil is impinged with an alternating field which induces a voltage in the coils below. In dependence on the proximity between the coils, the physically conditioned induction voltage will vary. The advantage here is the missing wear of the real sensors. In the technical documents of these sensors, the resolution is defined as infinite, since here – similar to all effective principles listed here (except the digital key) – the generated analog position values are concerned. If a subsequent ADC is used then the resolution is reduced according to the properties of the ADC. The alternating field is generated in the movable coil and is sensitive to interferences and can be manipulated by external influences. Built-in safety mechanisms can only recognize an error in a manipulation case and can then generate neutral output values. This measure prevents unintended actions, that's true, but simultaneously it prevents an operation by the user. The wear of the rubber bellow and the gate of all listed joysticks are identical and will therefore not be explicitly mentioned again.

2.3.3 Capacitive effective principle

The capacitive effective principle is not very wide-spread to multi-axis sensors since it is nearly impossible to compensate the interferences caused by electromagnetic radiation. The principle construction is similar to that of an inductive sensor, except that the coils are replaced by capacitor plates. Here, the dielectric is the air. The capacity is changed when changing the distance and when the firmly installed and the movable capacitor plates overlap. The capacity measured according to the known principles is also subject to other interferences such as

humidity. This sensor principle is more used for proximity sensors where the created analog values only process a hysteresis which generates a digital switch signal.

2.3.4 Digital effective principle

Sensors which follow the digital effective principle, change the switching states of built-in keys while the main sensor axis is deflected. A tumbling disk switches one or more keys, depending on the selected direction. The construction is very robust and free of interference. Since only one status change per direction is possible, the application field is restricted. The used keys have an average mechanical stability (switching operations) of 5 million cycles. The purely digital work represents a disadvantage. Interim values can only be generated by a subsequent microcontroller in form of ramps. Hereby, a counter is incremented depending on the scanning duration. The actual value of the counter can then be output as an analog value. If the scanning is interrupted then the counter is reset to its neutral value. The installation of a digital ramp in opposite direction can have critical consequences, since e.g. an EPW cannot be stopped directly.

2.3.5 Pneumatic effective principle

A pneumatic multi-axis sensor is equipped with a number of valves which conduct the compressed air depending on the deflection of the sensor axis. These valves can be set steplessly to regulate the quantity of the streaming air. The return force of the individual valves simultaneously realizes the zero-setting of the sensor axis. Since this effective principle refers to a purely mechanical execution, it will not be further commented in details.

2.3.6 Hydraulic effective principle

The hydraulic effective principle works analog to the pneumatic execution described in chapter 2.3.5 but it uses a hydraulic liquid instead of compressed air. An essential advantage vs. air can be found in the fact that liquids (in partic-

ular oil) cannot be compressed. In comparison with a pneumatic system, the inertia of the control is omitted which results from the compression of the air. To digitally evaluate the deflection of the axes, a hydraulic liquid is routed to a pressure sensor. Since in this execution, a direct mechanical connection is missing between the main sensor axis and the pressure sensor, the power consuming sensors are protected against damage by an overload. Overpressure valves offload the hydraulic liquid in case of overload.

2.3.7 Hall effective principle

The Hall effective principle can be compared in its mechanical construction with the inductive effective principle (refer to Chapter 2.3.2). The passive coils used here are replaced, however, by hall elements. The excitation can be executed with a permanent magnet or with an exciter coil. All advantages of the inductive effective principle and also its disadvantages become obvious in the hall effective principle. The interference here must be classified as more critical. While in the inductive effective principle, the passive coils are connected with a defined alternating field, the hall element is excited by a directed magnetic field. The interference of the inductive principle can be suppressed by suitable band filters, where against this protective function cannot be executed in the hall effective principle.

2.3.8 Optical effective principle

Optical, analog working multi-axis sensors are already installed in the industry. A large number of technical executions are used. In general, the penetrating light (normally infrared light or laser light) is radiated reasonably to geometrically arranged light-sensitive sensors. If the main sensor axis is deflected then the radiation intensity will change which results in the generation of an analog output signal. Optical and digitally working multi-axis sensors are only known from patent specifications [8–11]. Industrially manufactured or industrially used multi-axis sensors of this type could not be found. Optical processes for the positioning are basically well known. The main purpose of use is the measurement of large objects. Developments similar to the application fields outlined here are described

in their processes but not in their technical execution. If a technical execution is presented then the total construction is so complex that in no case the dimensions of the off-the-shelf joysticks are reached which makes a direct exchange impossible. At this time, no concrete execution is known since the problem of zero-positioning (refer to Chapter 2.1) could not be solved up to now. Another problem is the targeted size of construction and the related minimum distance available between the light source and the projection surface.

2.3.9 Strain gauge effective principle

Positioning systems with SG are also known. The US Patents [12–14] describe input devices with SG the shape of which resembles the off-the-shelf joysticks. The SGs are directly mounted on the main sensor axis. If a force is applied to the sensor then the axis material will deform and the measuring grid of the SG will change its resistance. Of advantage is the interference immunity against EMI and RFI. The used SG must be compensated with the used carrier material so that temperature changes will only impact the measuring result to a minor extent or not at all.

3. Research approaches

The initially determined research approaches (see Table 2) contained the following effective principles.

Table 2: Research approaches

Acoustical effective principle	Optical effective principle	Inductive effective principle	Capacitive effective principle

Detailed researches have shown that the actual development of inductive and capacitive effective principles is widely sophisticated. In addition, these systems do not represent any alternative effective principles. Therefore, the approaches will not be further treated.

Furthermore, analog working sensors are concerned which are highly susceptible to electromagnetic radiation due to their construction. To execute a research approach within this topic, minimum one of the following selection criteria should be fulfilled (see Table 3).

Table 3: Selection criteria

Fully digital processing	Alternative effective principle	Alternative construction or purpose of use

In the industrial use, the optical effective principle has only been used hitherto in the analog technology. A complete digital construction would therefore fulfill at least one of the selection criteria. Multi-axis sensors with acoustical effective principle are completely unknown which fulfills the selection criteria of an alternative effective principle. Since SG sensors use an analog technology and do not represent any alternative effective principle, the third selection criteria of the alternative construction or purpose of use should be applied (see Table 4).

Table 4: Research approaches to be executed

Acoustic research approach	Alternative effective principle
Optical research approach	Fully digital processing
SG research approach	Alternative construction or purpose of use

3.1 Determination of measures

3.1.1 Acoustical research approach

This approach implies the transfer of sound waves. Therefore, minimum one sound sender and one sound receiver must be assumed. To reach a high functionality, it was decided to use piezo sound converters (piezo element, piezo).

Piezos are available in many different types and sizes (see Figure 1) which allows a perfect consideration of construction-conditioned properties.

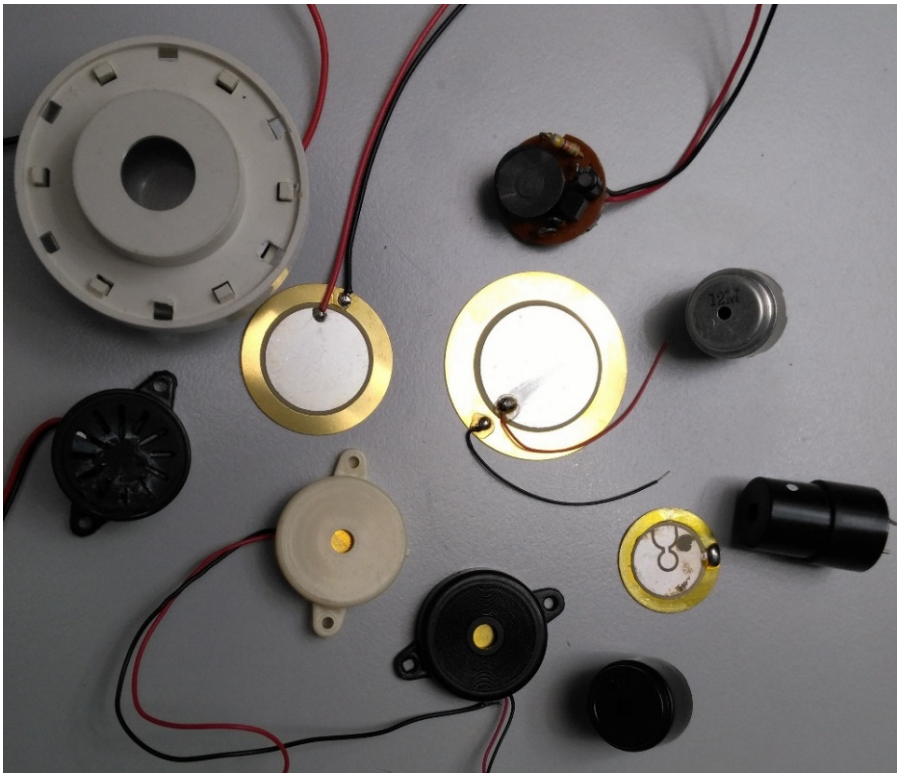

Figure 1: Piezo sound converters of different types

Piezo elements vibrate with a frequency of the applied voltage and are also able to generate voltage when receiving sound waves. This property bases on the piezo-electric effect. If the body of a piezo element is deformed then the electric polarity will change (direct piezo effect) and the voltage can be measured. If a voltage is applied then the piezo element will be deformed whereby the inverse piezo effect will become valid. For this research approach, disk-shaped piezo elements were selected. To be able to renounce at sensitive amplifiers in this research work, relatively large diameters were chosen. The advantage is the higher piezo voltage with same sound effect (see Figure 2). To better route the sound waves to the target, an addition cross-linked, cold vulcanized 2-component silicone material was provided. Since this material is available in many shore-hardness degrees and can also be mixed with each other, a stepless production of different hardness degrees is possible.

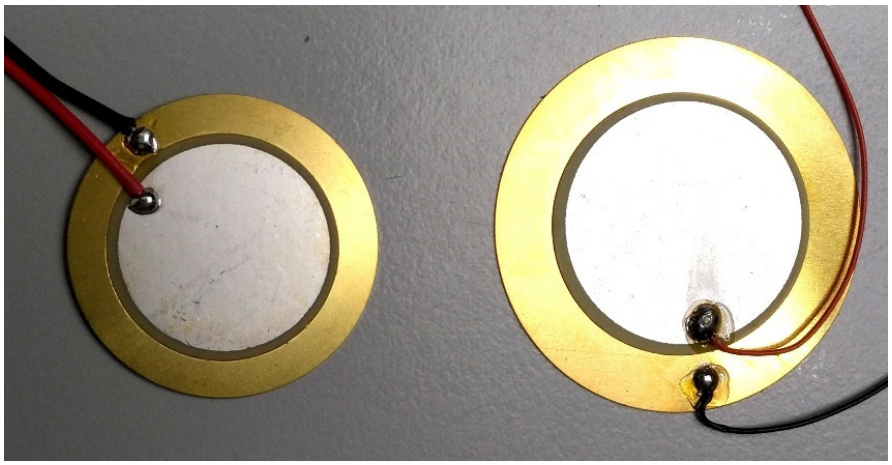

Figure 2: Piezo sound wave converters of 27 mm and 34 mm

The optical arrangement of the piezos to each other was determined in different test series.

3.1.2 Optical research approach

Since a novelty of this approach can only be found in a completely digital execution, the recording of the measuring values as well as the signal processing must exclusively be conceived on a digital basis. To be able to reach the targeted high resolution, a light beam shall hit an image sensor from which the position of the light and its influence can be determined. The size of the image sensor and its resolution (see Table 5) are of high relevance. The following popular sensor sizes are available.

Table 5: Popular image sensor sizes

Diagonal (inch) type	1/3.2“	1/2.7“	1/2.5“	1/1.8“	2/3“	1“
Width x height (mm)	4.5x3,4	5.4x4,0	5.8x4,3	7.2x5.4	8.8x6.6	13.2x8,8
Surface (mm²)	15.30	21.60	2.,94	38.88	58.08	116.16

Diagonal (inch) type	Four-thirds	Foveon	APS-C	DX	Small image	Middle for-mat
Width x height (mm)	17.3x13.0	20.7x13.8	22.2x14,8	23.7x15.6	36.0x24.0	48.0x36.0
Surface (mm²)	224.90	285.66	328.56	369.72	864.00	1728.00

The indicated image sensor sizes are delivered with different resolutions which results in a very large individual offering. To keep the size of the sensor to be developed within the range of normal diameters, the 1/1.8” format was favored. The image sensor to be used in the test construction (see Table 6) is further specified as follows.

Table 6: Image sensor specification UI-1241LE

Sensortype	Framerate	Resolution	Pixelsize	Diagonal
CMOS	25,8 fps	1280 x 1024	5.3 µm	1/1.8“

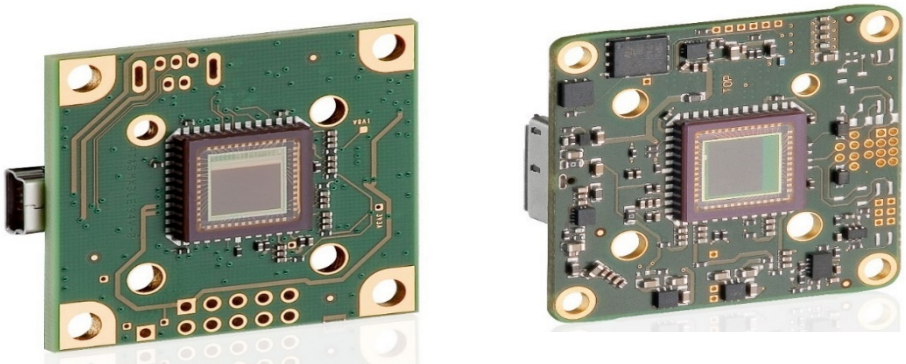

(a) *(b)*

Figure 3: (a) Camera module UI-1241LE, (b) UI-3591LE

The image sensor of manufacturer e2v is used as compact camera module UI-1241LE (see Figure 3 (a)) of company IDS [15]. A clearly higher resolution could be achieved by the camera module of same construction UI-3591LE (see Figure 3 (b)) [16] (see Table 7).

Table 7: Image sensor specification UI-3591LE

Sensortype	Framerate	Resolution	Pixelsize	Diagonal
CMOS	12.2 fps	4912 x 3684	1.25 µm	1/2.3“

Since the test construction does not change with the use of both modules, first module UI-1241LE is used. The modules have an USB-interface which reduces the development time of the prototype considerably. On the modules locates an image processor which takes over the total image sensor handling. The basing configuration of the module is parameterized by the delivered configuration program Ueye Cockpit [17]. The software to evaluate the image data will be developed in C++ and executed on a Windows platform. Since the objective of this thesis is to prove the functionality of a prototype, the software does not represent a necessary component of this thesis. The software function is realized in a development step outside this thesis using a microcontroller in the sensor housing. To return the main sensor axis after deflection to an exact rest position, a highly accurate construction needs to be developed. The execution with a spring mechanism has not revealed any acceptable result already in the upfront. The light emitting unit shall be deflected via a motion carrier which in turn shall enable a reset. To reach the highest possible accuracy here, an addition cross-linked hot and cold vulcanized 2-component accuracy polymer should be used. This material can principally be produced in several shore-hardness degrees but must be manufactured especially for this thesis by company Wacker Chemie AG [18]. In non-hardened state, this material has a dough-similar consistency and will be compressed under pressure in forms which must still be manufactured. The vul-

canizing is then made in an autoclave to remove the enclosed air and the resulting gasses from the material. The already mentioned motion carriers must be accurately positioned in the form prior to vulcanization.

3.1.3 SG research approach

Since a SG (see Figure 4) only changes the resistance in consequence of a deformation of its carrier material, the selection criteria of a completely digital measurement value creation cannot be fulfilled. Furthermore, the effective principle of SG positioning is known so that the alternative selection criterion is omitted. Thus, the SG research approach can only be accelerated by a constructive novelty and/or by a not yet known purpose of use.

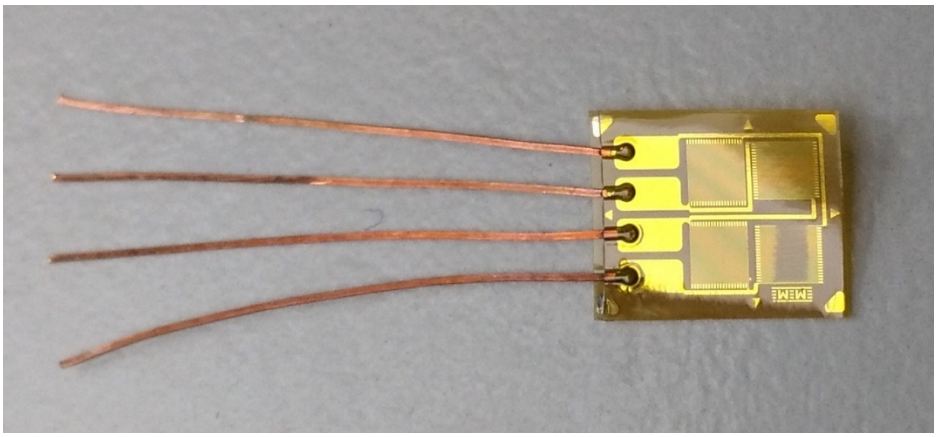

Figure 4: SG

4. Execution of research approaches

4.1 Prototyping and test series, acoustical approach

4.1.1 Function and construction

To secure the general functions of the acoustical approach, a prototype with three piezos was constructed. The mounting plate made of polyvinylchloride (PVC) was milled on a 2.5 D Computerized-Numerical-Control (CNC) tool machine. The used PVC material is made by a chained polymerization and belongs to the thermoplastic polymers.

The PVC material group is basically divided into hard and soft PVC from which the hard PVC variant was selected for the presented prototype construction. To exclude functional errors in the construction already in the upfront, the highest possible processing accuracy had to be secured. The used CNC-machine works with an accuracy of 1/100 mm which guarantees a sufficient production accuracy. The described accuracy does not only result from the resolution of the stepper motor in combination with the spindle axis thread pitch but also from the capability of the machine to accurately drive to a defined position several times.

To concentrate the sound distribution in a medium, the carrier plate was coated with an addition cross-linked 2-component, cold vulcanized silicon polymer. Silicone (chemical name Polyorganosiloxane) designates a product group of synthetic polymers, where the selenium atoms are linked via oxygen atoms.

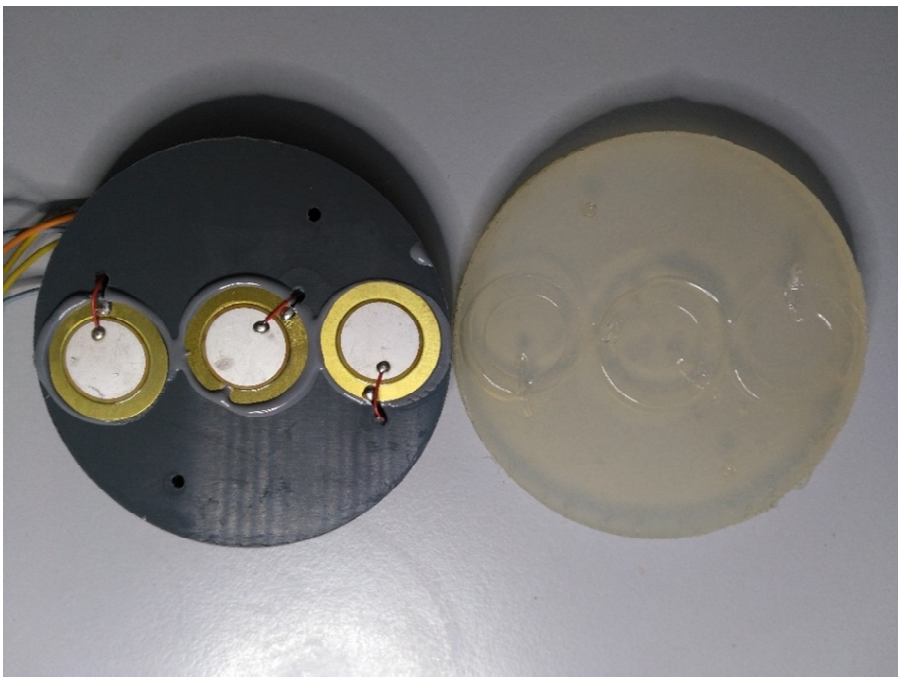

Figure 5: Acoustical prototype with 3 piezo elements (with removed silicone plate)

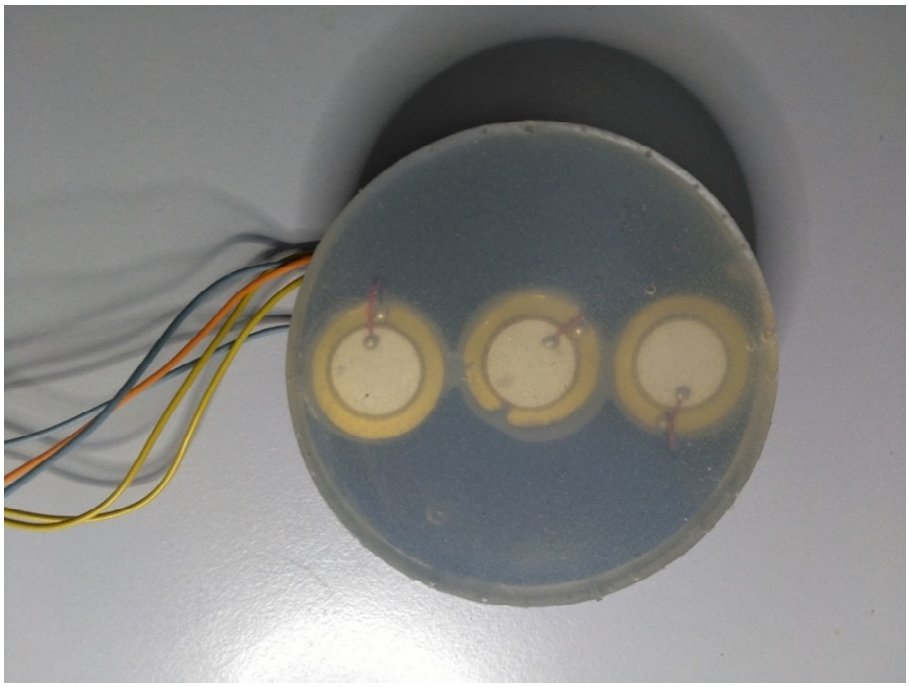

Figure 6: Acoustical prototype with 3 piezo elements

The relevant middle piezo element (see Figure 5 and Figure 6) is used as exciter by all prototypes and is first linked with a function generator. The used function generator is a SDG 1050 2-channel function / arbitrary waveform generator with 50 MHz bandwidth of company Siglent [19]. The receiver-piezos are directly connected to the mixed domain oscilloscope MDO 3024 of company Tektronix [20]. The voltage created by the piezo effect is visualized without further amplifier. Since the MDO 3024 disposes of 4 input channels, it is possible to record 4 measuring values fully digitally and simultaneously in parallel, in dependence on each other. Since the device provides a resolution of up to 200 MHz, it is possible to investigate a wide frequency spectrum. The initial test series seemed to promise success because the received piezo elements responded very well to the defined frequencies of the sent piezo. The change of the wave format from sinus to rectangular did not entail any relevant change of results. However, it was expected that the measuring results would clearly differ because the steepness of the edges of the rectangular pulses produces a by far higher energy in the system. Also other waveforms like saw tooth or pulse, always generate a measuring result of sinus-type. For test purposes, two piezos were rigidly combined with each other. Different waveforms were now accurately transferred which documented a significant damping effect of the silicon polymers. After a

suitable resonance frequency was found in a range of the used piezo elements of 5 kHz, it was possible to change the received height of amplitude and frequency by exercising pressure on the silicone polymer. Also, after application of a very soft force of about 0.2 N, reproducible changes of the measuring results could be stated. As already found out, every piezo element has its own resonance frequency. However, to get a nearly equal change of the measuring results of two piezos with the same force impact, the resonance frequency had to be set exactly to the relevant piezo. In the first prototype, a resonance frequency difference of 820 Hz could be stated, that's why a single exciter frequency was not sufficient. An overlapping of the two frequencies was not possible neither since a too strong wave effacement or overlay led to undefined measuring results. First, it should be determined why the resonance frequencies differ in this form. The piezos were glued with a tough 2-component Epoxy resin [21] in the PVC carrier (see Figure 7). After the piezos had been changed several times it was stated that the resonance frequency changed depending on the resin quantity and on the resin-wetting of the piezos.

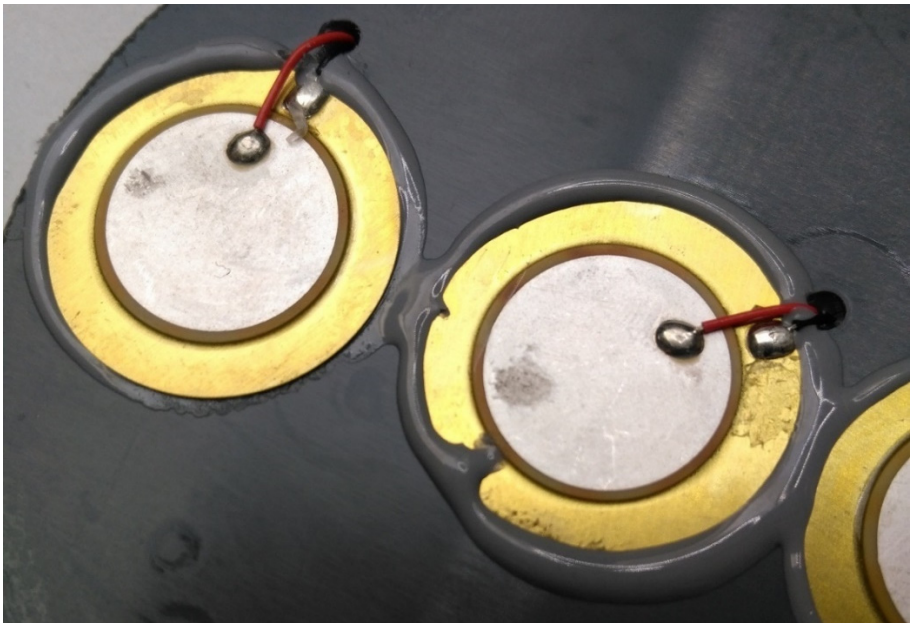

Figure 7: Epoxi resin glues piezo-elements

The piezo elements of the subsequent prototypes were fixed in one processing step by a silicone polymer coat. The deviations of the resonance frequen-

cies could be reduced by this procedure to +- 150 Hz. A consultation of the manufacturer revealed that this deviation is conditioned by the production technology and cannot be avoided. From 100 piezo elements 5 samples could be selected manually which showed a resonance frequency difference of max. +- 50 Hz. But also with this low deviation it was not possible to get nearly the same change of the measuring results with same exciter frequency and same applied force for each piezo.

The second prototype disposed of 4 receiver piezos (see Figure 8) which were placed in a circle around the exciter piezo. To guarantee an exact positioning, a chamfer was milled in the PVC to guarantee a defined supporting surface for the piezos. The chamfer was wetted with silicone polymer before insertion so that a direct piezo-PVC coupling could be avoided. This decoupling should prevent the exciter frequency from being directly transmitted to the receiver piezo.

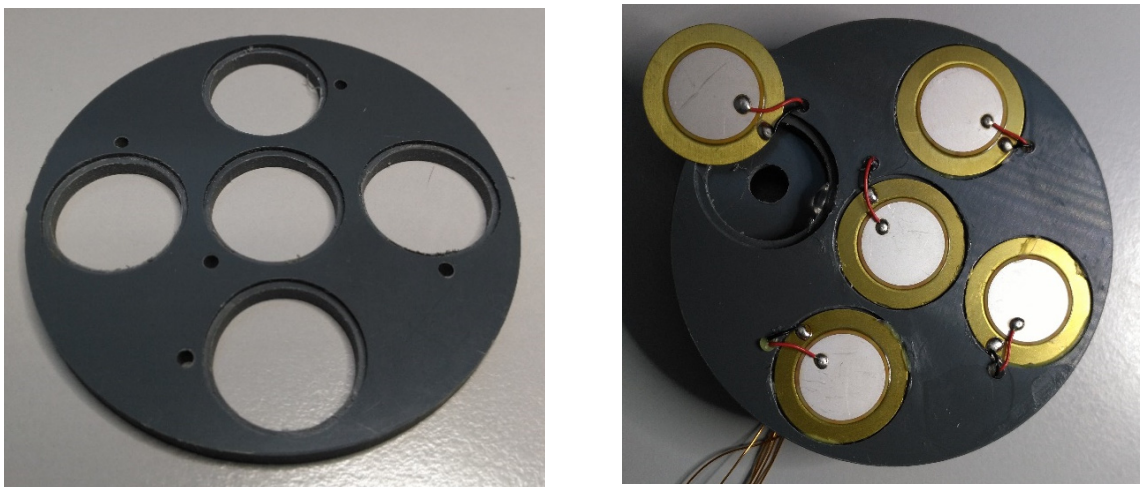

(a) *(b)*

Figure 8: (a) PVC-carrier plate with visible chamfers and (b) inserted piezo elements

Another problem was found in the climate chamber. The air which is densely enclosed among the piezo elements, pressed the piezos out of their holders when warming up. To solve this problem, a pressure balancing hole was provided below each piezo (see Figure 9 (a)). The general vibration response of the piezo was also improved which influenced the height of the receiver's amplitude.

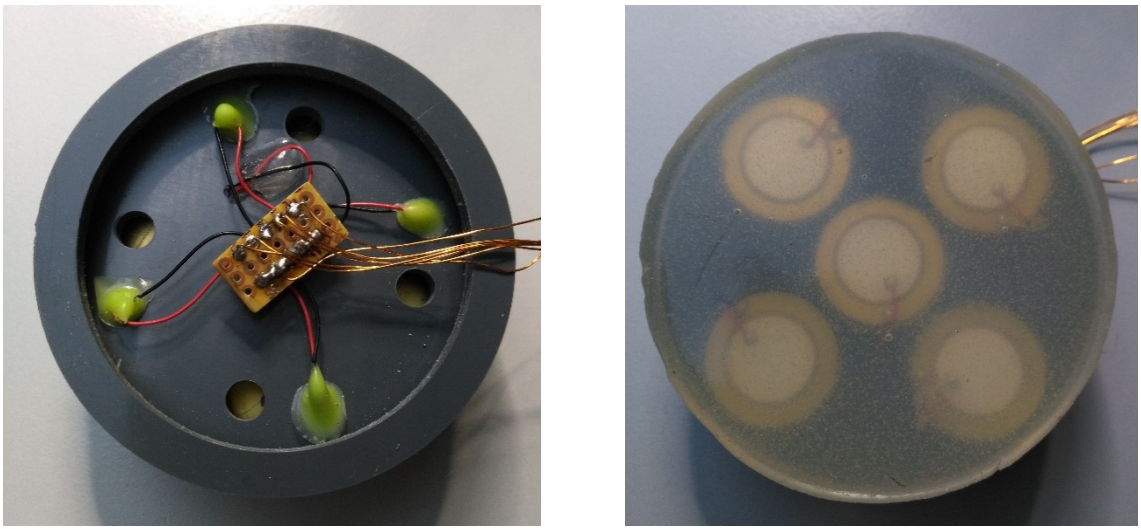

(a) *(b)*

Figure 9: (a) Prototype version 2, bottom view (b) with applied silicone polymer

To initialize prototype version 2, an operating plate with holding threads was mounted on top of the silicone polymer (see Figure 10). This guaranteed that forces from outside evenly impacted the sensor surface.

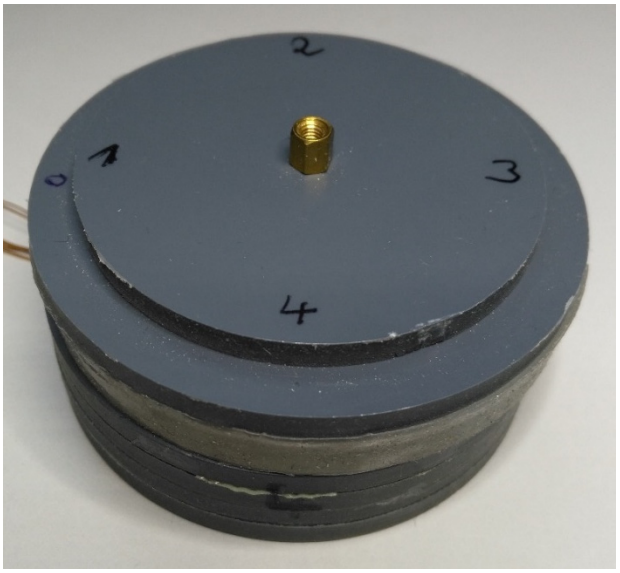

Figure 10: Prototype version 2 with applied operating plate and M3 holder

In the following test series, the acoustical prototype version 2 was connected to different frequencies and waveforms to determine the resonance frequencies

(see Table 8). The target was to generate the maximum amplitudes of the receiver piezos with a consistently applied force. To get a verifiable result, the force was executed with a micrometer screw or with placed weights.

Table 8: Resonance frequencies of receiver piezos

Piezo position	Piezo 1 left	Piezo 2 up	Piezo 3 right	Piezo 4 down
Resonance frequency	5040 Hz	4990 Hz	5030 Hz	5000 Hz

The following screenshots of the used memory oscilloscope show the significant and differently high amplitudes of the individual receiver piezos. Since the found resonance frequencies locate very close to each other (see Table 8) an optical change is not visible on the oscilloscope in this setting. The oscillations of the exciter piezo are derived to a very low extent also via the PVC carrier (Figure 8) whereby the basic oscillation is measured on every receiver piezo. As soon as the resonance frequency of a piezo is accurately set, its amplitude clearly increases in comparison with the other piezos (see Figure 11 and Figure 12).

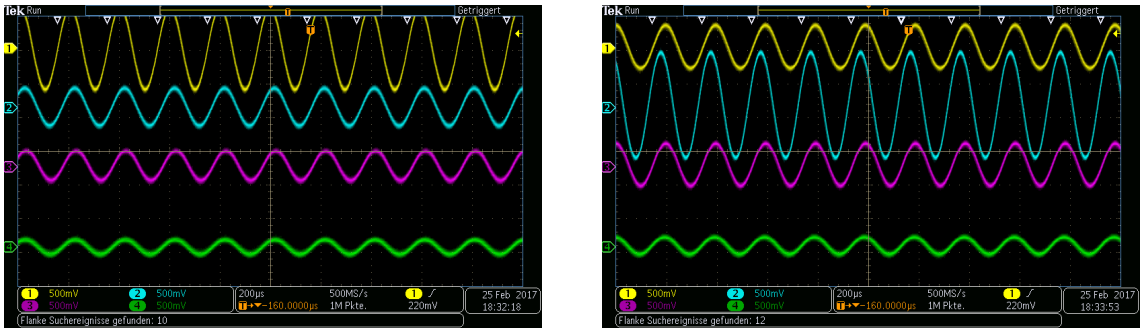

(a) *(b)*

Figure 11: (a) Resonance frequency piezo 1 yellow and (b) piezo 2 blue

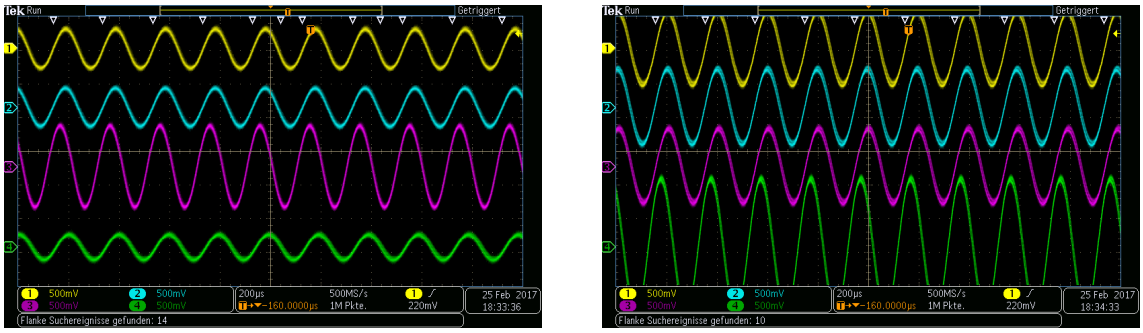

(a) *(b)*

Figure 12: (a) Resonance frequency piezo 3 purple and (b) piezo 4 green

A usable resonance response could also be measured with a multitude of the exciter frequency (see Figure 13).

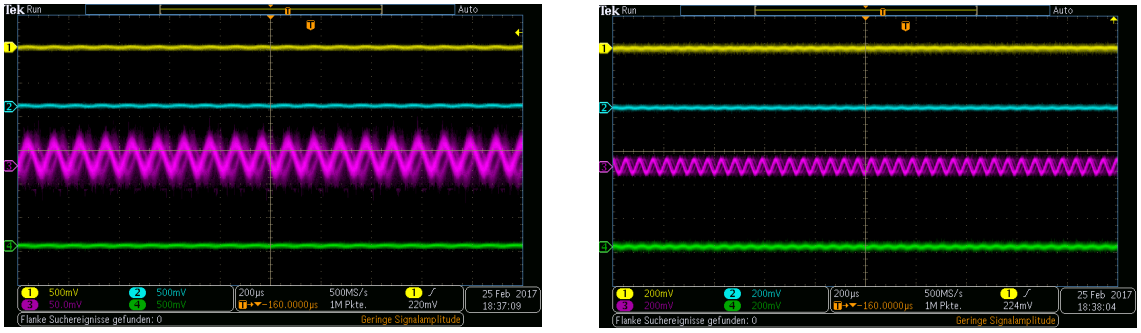

(a) *(b)*

Figure 13: (a) Resonance frequency piezo 3, 9.69 kHz and (b) 18.59 kHz

Since the measurements delivered a sinus-shaped result in a range of 5 kHz independent on the waveform of the input signal, the input signal could be identified in higher frequencies (see Figure 13). This fact can be explained by the damping response of the built-in silicone polymer. When a silicone polymer was used with a higher shore value (harder), the input waveform could already be recognized in lower frequencies. To get a shape of joystick-type, finally prototype version 3 (see Figure 14) has been developed.

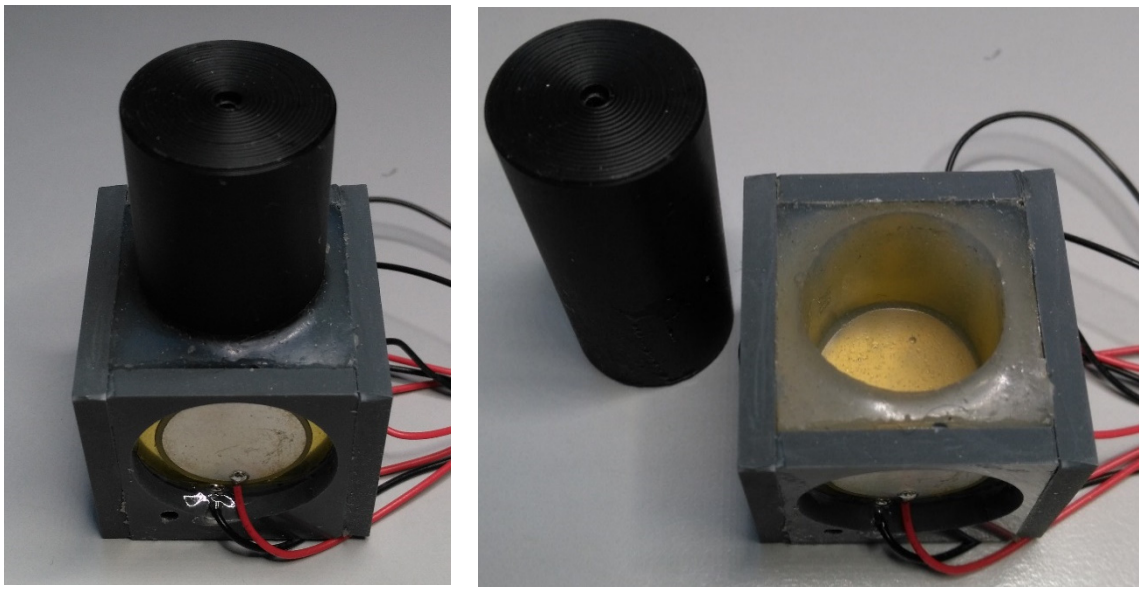

(a) *(b)*

Figure 14: (a) Acoustical prototype version 3 with axis and (b) inner view

The force on the sensor axis compresses the silicone polymer in front of the receiver piezo which allows to measure a proportional change of the height and the distance of the amplitudes. A centric force on the sensor axis damps the oscillation response of the centered exciter piezo. All receiver piezos will then induce a lower height of the amplitude which allows to uniquely identify a z-axis operation. A simultaneous force on the x-, y- and z-axis can also be measured.

4.1.2 Result and assessment, acoustic approach

The executed tests with three prototypes document that principally a multi-axis sensor is technically possible. A technical use in the indicated development phase, however, is not yet possible. The reason is primarily found in the production tolerances of the piezo elements. An automatic selection of these components would be thinkable but would considerably increase the costs of the production process. A later repair is rather impossible since only a piezo can be installed that fits. To compensate the problem of different resonance frequencies, the resonance frequency of every receiver piezo could be determined in an automatic calibration process. In a final test construction, the signal generator was replaced by a digital signal processor (DSP) of type ADAU1701 [22]. Company

Analog Devices provides a ready-to-use Evaluation Kit EVAL-ADAU1701MINIZ [23] (see Figure 15).

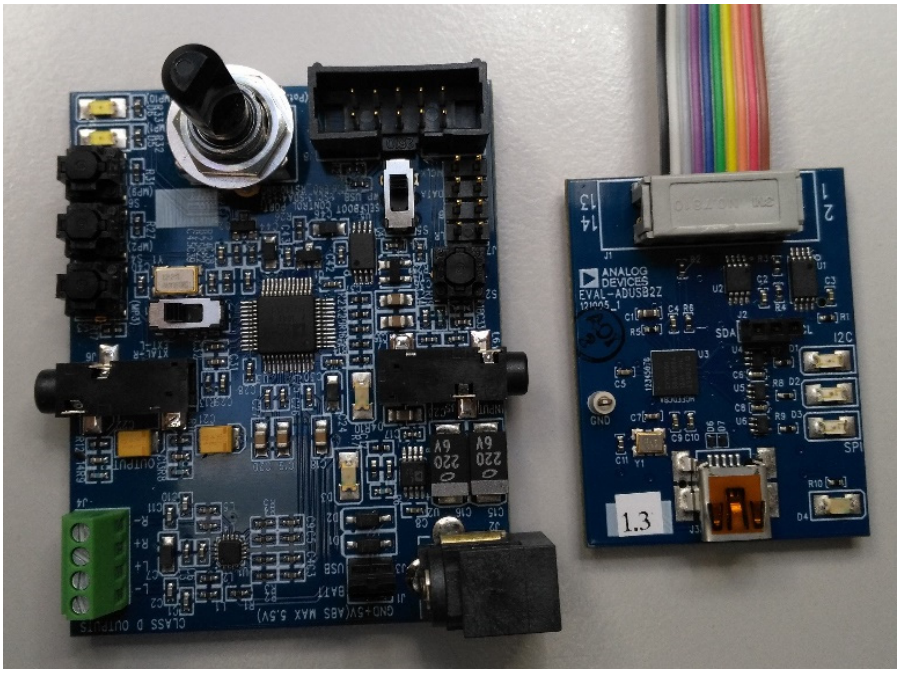

Figure 15: EVAL-ADAU1701MINIZ Analog Devices

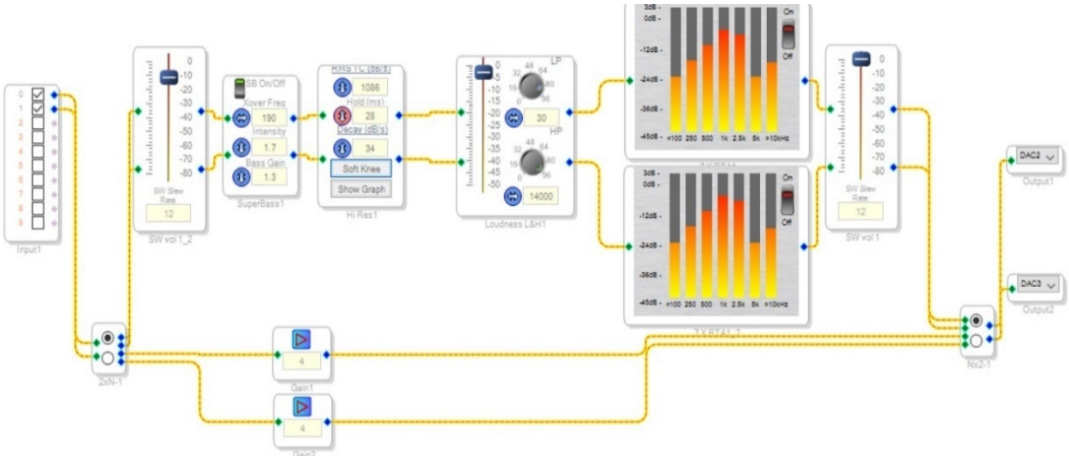

Figure 16: Sigma Studio

The delivered Software Sigma Studio [24] increases the velocity. It disposes of a graphical programming interface (see Figure 16). Signal sources, measuring and filtering elements, can be used and combined arbitrarily with each other. If an exciter frequency is used in a range from 4 kHz to 6 kHz where the maximum amplitude is checked with every receiver piezo continuously, then this calibration

process needs approx. 2.5 sec, once. In normal mode, every resonance frequency is generated one after the other within a defined period of time, and simultaneously the frequency and amplitude of the relevant receiver piezo is read out. If the exciter frequency is used in a range of 5 kHz then all four receiver piezos can be measured with a frequency of 62.5 Hz in every run. Here, 20 amplitudes, each, are measured per receiver piezo and their average value are then be further processed in terms of height and frequency of the amplitude. The scanning of the receiver piezos with a permanently varying frequency could prevent interferences from outside. It must be assumed that even an intended interference frequency will not vary the own frequency synchronously with a rotational frequency of 62.5 Hz. So, it can be uniquely stated that a foreign parasite frequency is radiated during signal evaluation. To avoid this improbable case entirely, the rotational frequency could be clocked by a random generator.

Another basic problem is the loudness of the working frequency. The noise level of 5 kHz locates in the middle of the listening spectrum of a human. That's why it is extremely unpleasant if the hearing is permanently exposed to this frequency (as personally experienced in this test series). Insulations could not achieve an acceptable improvement of loudness, neither. A possible multiplication of the exciter frequency would relieve the user but would be problematic for animals, e.g. pets.

4.2 Prototyping and test series, optical approach

The optical research approach (refer to Chapter 7.1.1) shall at least fulfill the selection criteria of a fully digital execution. In this sense, it is not possible in no case to base on known optical processes since these processes mainly use analog procedures. The known opto-digital multi-axis sensors just dispose of digital outputs in two operational states. Elaborate opto-digital systems with high resolution are not used as multi-axis sensors, all the more since their construction heights and construction features will not allow their use. The economic benefit and related technical execution should also be a focal point of this development. During the development work, two optical prototype constructions were realized.

The primary differences could be found in the suspension of the sensor axis which represented the major problem.

4.2.1 Functionality and construction

The optical sensor (see Figure 17) consists of a transducer (pos. 2) and a projection unit (pos. 3) which are rigidly connected to a motion carrier (pos. 4). In a defined distance below the projection unit locates the image sensor (pos. 6). The force on the transducer modifies the angle of the motion carrier to the image sensor. This shifts the position of projection on the image sensor. From this position, from the size and from the distortion of projection, the actual x-, y- and z-coordinates are calculated. This is done in relation to the modified angle and to the pressure on the axis. To be able to exchange the sensor by an off-the-shelf joystick [25] without further constructive problems, standard dimensions of construction were kept in the development phase. The 3-axis sensor housing has the dimensions (L x W x H) 40 mm x 40 mm x 37 mm. The lateral or rear connection cables can send digital and/or analog data, depending on the software configuration.

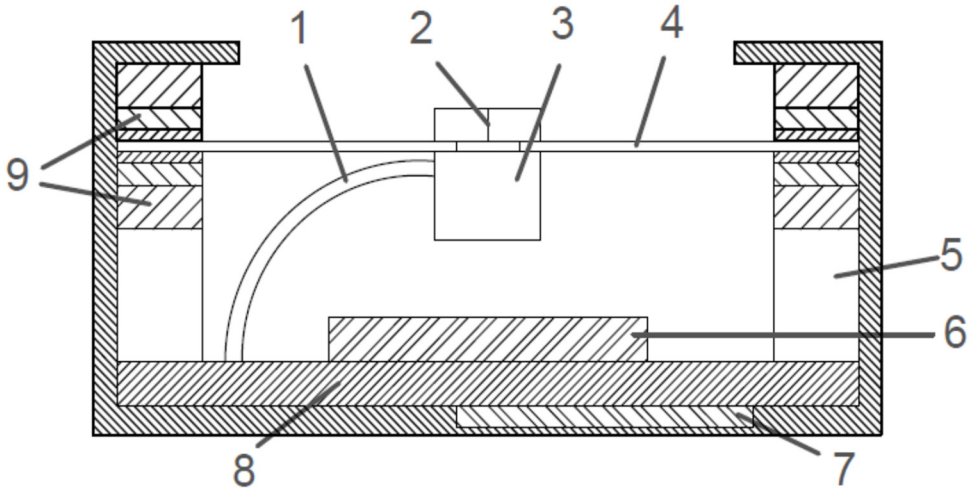

Figure 17: 3-axis sensor version 1

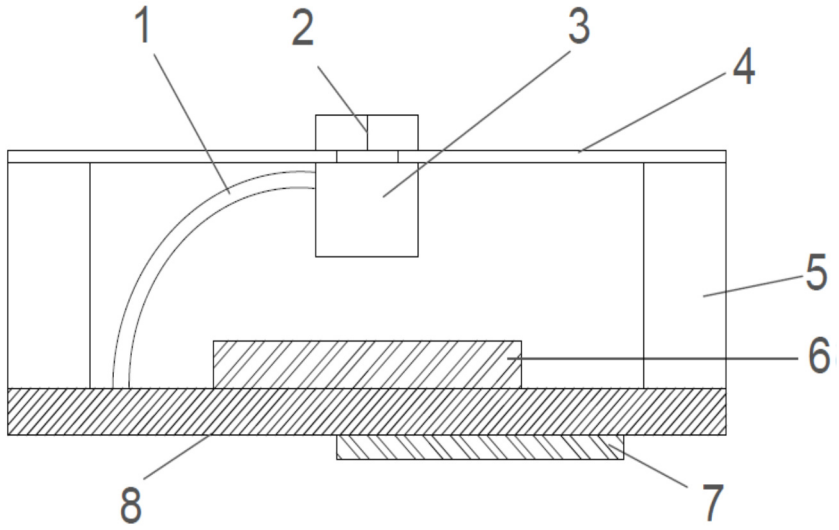

Figure 18: 3-axis sensor version 2

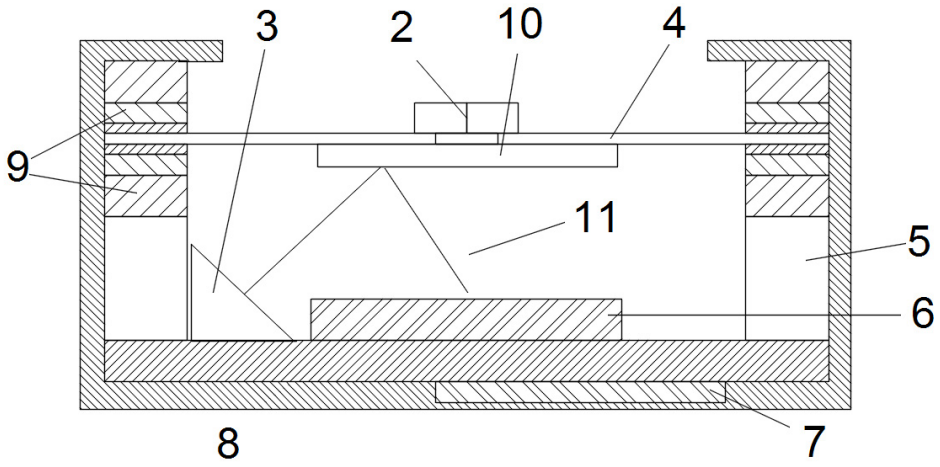

Figure 19: 3-axis sensor version 4

The 3-axis sensor consists of the following components:

1. Power supply cable, projection unit
2. Force transducer
3. Projection unit

4. Motion carrier
5. Spacer
6. Image sensor
7. Microcontroller
8. Circuit board
9. Polymer sandwich or firmly attached
10. Mirror
11. Laser beam

4.2.2 Projection unit and image sensor

The projection unit in its simplest version consists of a laser diode with subsequent plano-convex lens. This arrangement can be supplemented by a collimator lens [26] and figure templates. Depending on the software configuration and on the used image sensor, frame rates up to 180 images per second (fps) are reached. Also, the maximum resolution of the optical sensor depends on the type of image sensor. If e.g. a 1/1.8“ sensor is used with 1280 (H) x 1024 (V) pixels, SXGA / 1.3 MP [15] then 1280 (H) / 2 = 640 digits (H) and 1024 (V) / 2 = 512 digits (V) are reached for the relevant directions without further calculation. The construction scheme of the projection unit is shown in Figure 20.

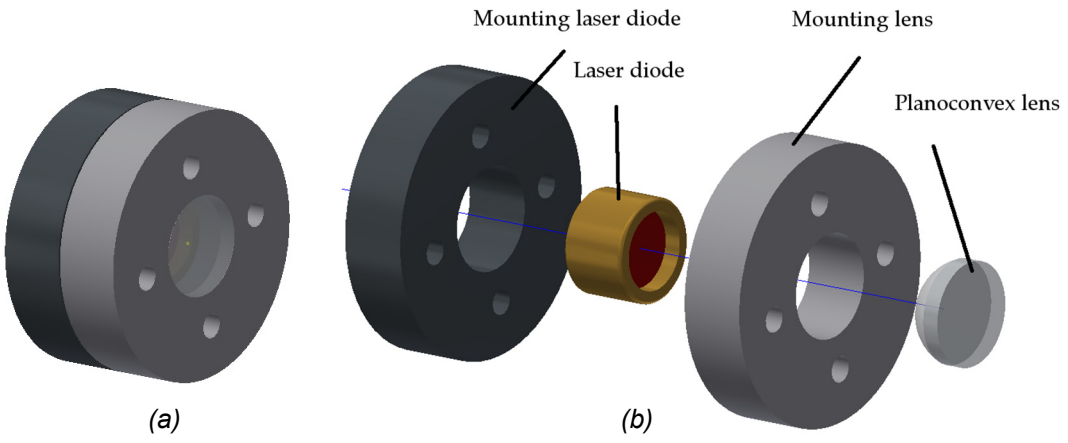

Figure 20: (a) Projection unit and (b) projection unit exploded view

The projection unit has a diameter of 17 mm and a height of 10 mm. The relatively large diameter of the mounting parts has no influence on the total size

of the sensor. Since the motion carrier and the projection unit should be connected with each other free of torsion, a support surface is needed. This enables to place the focal point in a distance of 10 mm below the light exit of the laser diode. If subpixels (gray shades) are used for calculation and if the resulting light circle is interpolated, then min. 2 valid digits after the decimal sign will be available. This increases the resolution by factor 100 and provides a resolution of 64000 digits horizontally (H) and 51200 digits vertically (V) in every direction. If an off-the-shelf 18.1 MP sensor is used with 4912 digits (H) x 3684 digits (V) [16], then – according to the calculation above – 245600 digits (H) x 184200 digits (V) will be resolved in every direction. These values should be sufficient also for measurements of extremely high sensitivity. For consumers (using a PC-joystick), a resolution of 0.36 MP and a framerate of 30 fps will perfectly do.

4.2.3 Different versions

The sensor can be executed in different versions depending on the purpose of use:

Version 1 (see Figure 17). The motion carrier locates in a polymer sandwich and consists of a rigid material, e.g. aluminum, steel or carbon-fiber-reinforced polymer (CFRP). The force from the transducer causes the motion carrier to decline. The declination depends on the applied force and on the shore-hardness of the polymer. This version was built as prototype.

Version 2 (see Figure 18). The motion carrier is made of an elastic material (e.g. CFRP in different thicknesses from 0.45 mm to 2 mm). The motion carrier is rigidly connected to the housing and is stressed with bending and torsion. A special milling arrangement favors the deformation response of the motion carrier. This version was built as prototype.

Version 3: Same as version 2, and with an additional polymer cushion above the motion carrier.

Version 4 (see Figure 19): The imaging projection unit is replaced by a mirror. To generate a projection on the image sensor, the projection unit is firmly mounted next to the image sensor on the circuit board and reflects the image to the image sensor via the mirror. A modification of the angle of the motion carrier repositions the projection in line with the applied forces.

4.2.4 Motion carrier and polymer sandwich

The necessary bearing accuracy of the motion carrier was worked-out by different procedures and test series. The motion carrier is centered, in version 1, by the bearing in polymer and consists of a rigid material, e.g. steel (thickness > 1 mm), aluminum (thickness > 1.5 mm) or CFRP (thickness > 1.5 mm) to redirect the force into the polymer. In this initial development phase, the motion carrier was first manufactured as a type of disk. The bearing was done by two polymer rings (see Figure 21 (a)) which were installed above and below the carrier. The used cast material was an addition cross-linked 2-component silicone polymer of different shore-hardness degrees.

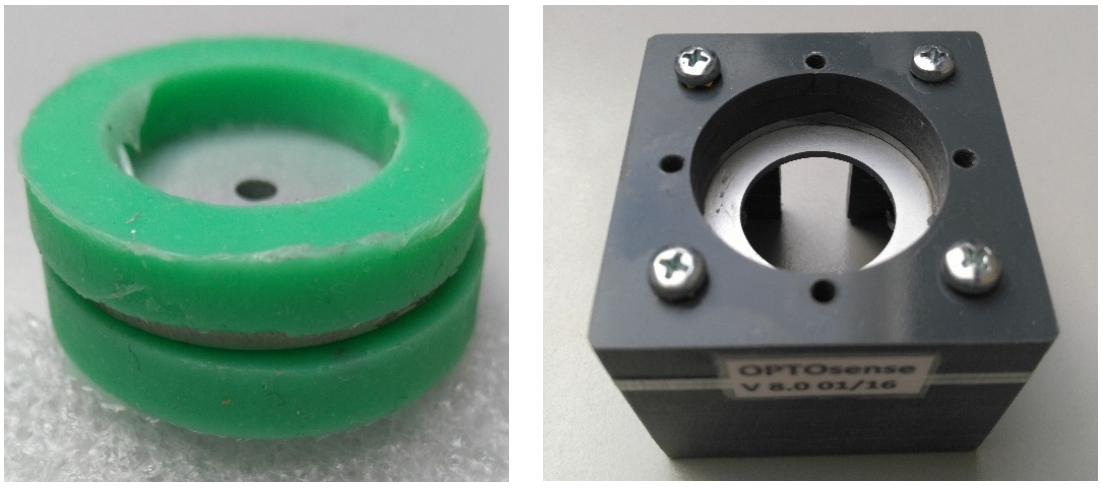

(a) *(b)*

Figure 21: (a) Motion carrier between two polymer rings and (b) housing

Due to the different shore-hardness degrees of the polymer rings, the sensor could be adapted to the desired force spectrum. This sandwich construction was inserted in the sensor housing (see Figure 21 (b)) and fixed with low compression

on top of the housing cover. With increasing force on the movement carrier, the ability to recover the rest position was deteriorated. The bearing had to be encapsulated in the test series, which made visual inspection impossible to find constructive disturbances. Since the motion carrier was a floating installation between the polymer disks, it was assumed that a minor lateral motion was possible. In addition, it could be stated that the motion carrier tilted in the housing in consequence of too strong forces (see Figure 22).

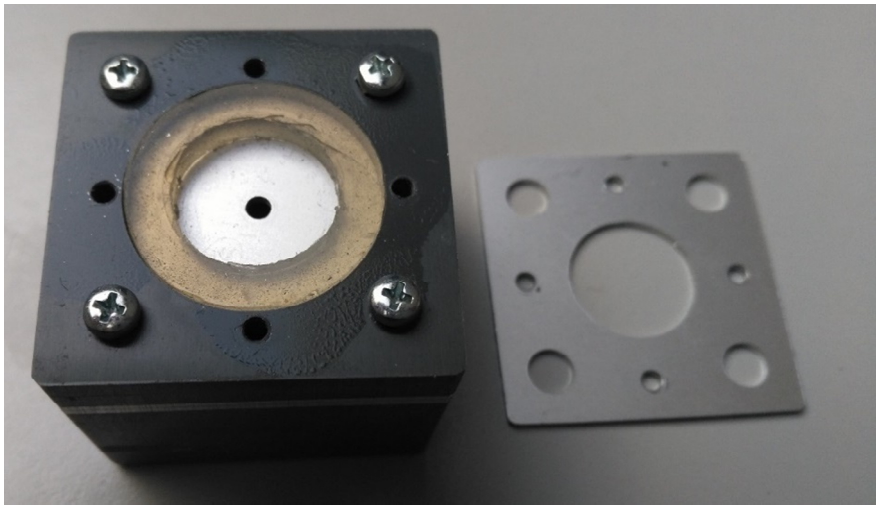

Figure 22: Housing with inserted polymer rings and cover

It has also been stated that a circular motion of the sensor axis caused the entire movement carrier to rotate between the polymer disks. It came to undesired derivations of the laser beam in different rotary angles. For this reason, the motion carrier was provided in the second development phase with holes and gear teeth (see Figure 23) and in addition was directly molded in the polymer (see Figure 24).

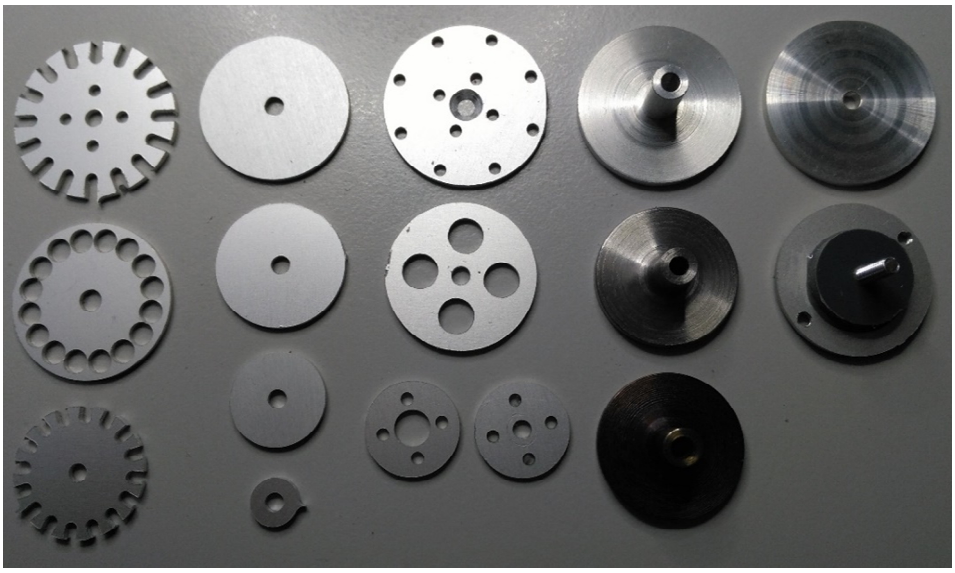

Figure 23: Motion carrier in different executions

Figure 24: Silicone polymer executions

This measure minimized the torsion of the motion carrier but could not exclude it entirely. Since the mandatorily accurate reset response of this construction was rated to be still dissatisfying, further modifications became necessary. Better results were achieved by mixed material and construction variants. Used were different shore-hardness degrees in different arrangements.

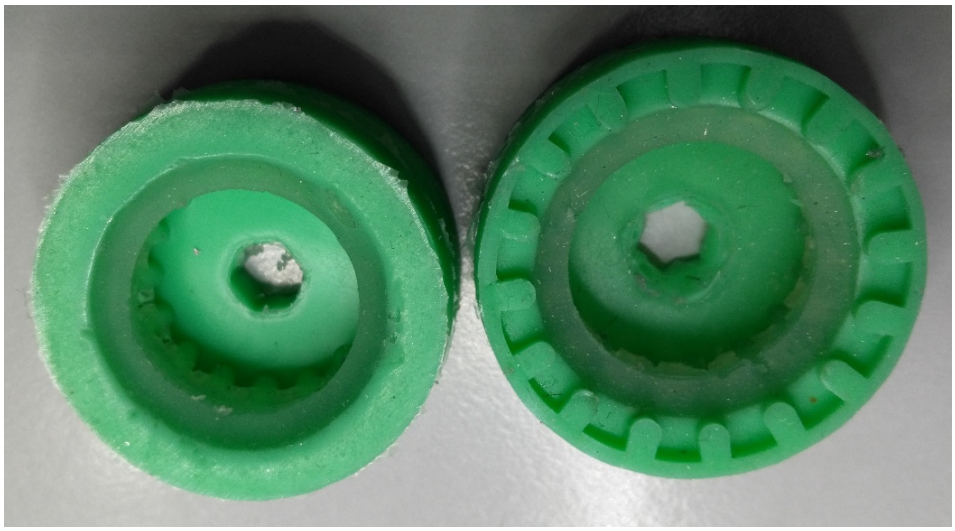

Figure 25: Use of different polymer materials

Figure 25 shows the different arrangement of different silicone polymers. The inner polymer ring (transparent) consists of a softer material than the outer ring (green). Therefore, the increasing force is first absorbed by the soft and then by the hard layers. This increases the spectrum of the applied force. The counter-acting reset force responds exponentially to the motion stroke. Since polymer is of low viscosity and no air was enclosed through the mixing in a compulsory mixer, the material could harden in a simple form (see Figure 26). Under pressure and with increased temperature, the hardening could be accelerated.

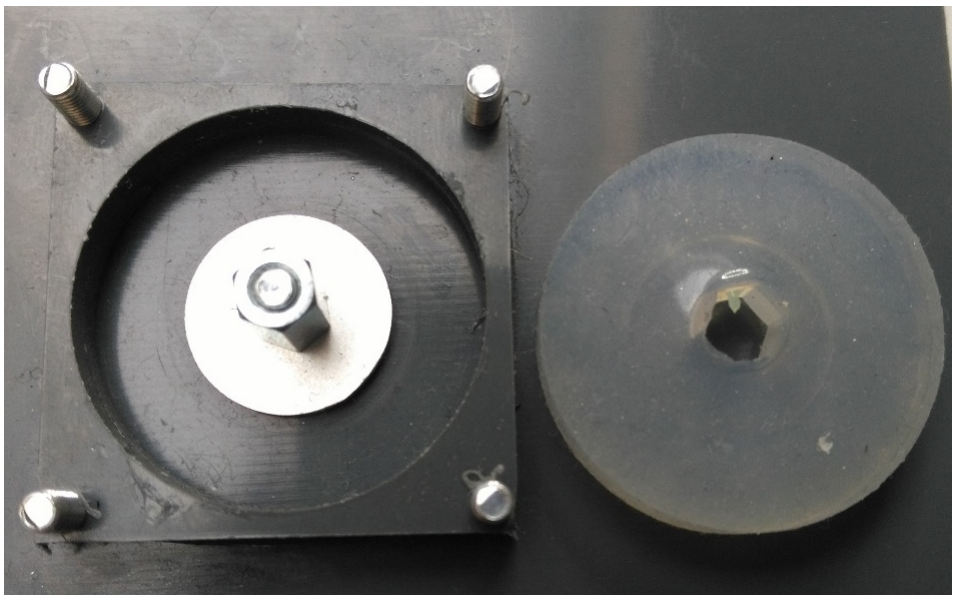

Figure 26: Cast form for silicone polymer of optical version 1

To avoid all possibilities of distortion of the main sensor axis and to further improve the reset accuracy, a third development step was necessary. Since the total result improved after direct pouring into the motion carrier, this construction step should be kept. The motion carrier and the bearing were now manufactured as one unit protected against distortion by 8 holes (see Figure 27 and Figure 28). Company Wacker Chemie in Munich [18] delivered a hot vulcanized 2-component polymer which was said to have extraordinary reset properties. This material, however, was much more complicated to process since its consistency resembles that of a tough modeling material. In addition, the material had to be pressed in form with min. 10.000 N and had to be finally hot vulcanized under this pressure. This reaction gasses (CO_2) resulted from the vulcanization process, an autoclave needed to be used in the following to remove the gas from the material in the hardening process. Because of the high compression force, the construction and manufacture of the forms turned out to be increasingly hard. Since the vulcanizing temperature was 250 °C, no PVC could be used as form material. Also, to deform the polymer, Teflon was selected as form, stabilized by an aluminum cover (see Figure 27). Thereafter, it was possible to execute different versions of the motion carrier and polymer mixtures (see Figure 29).

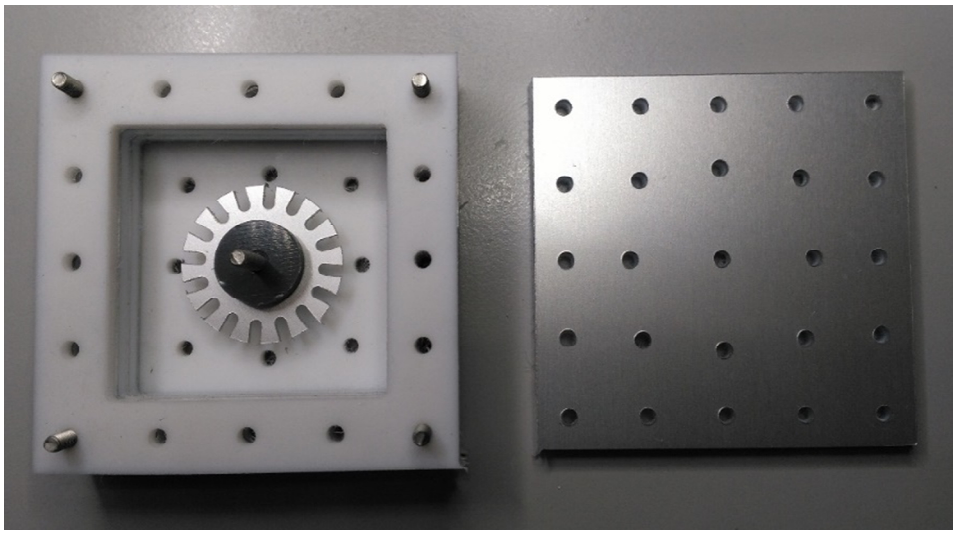

Figure 27: Pressure resistant mould made of Teflon

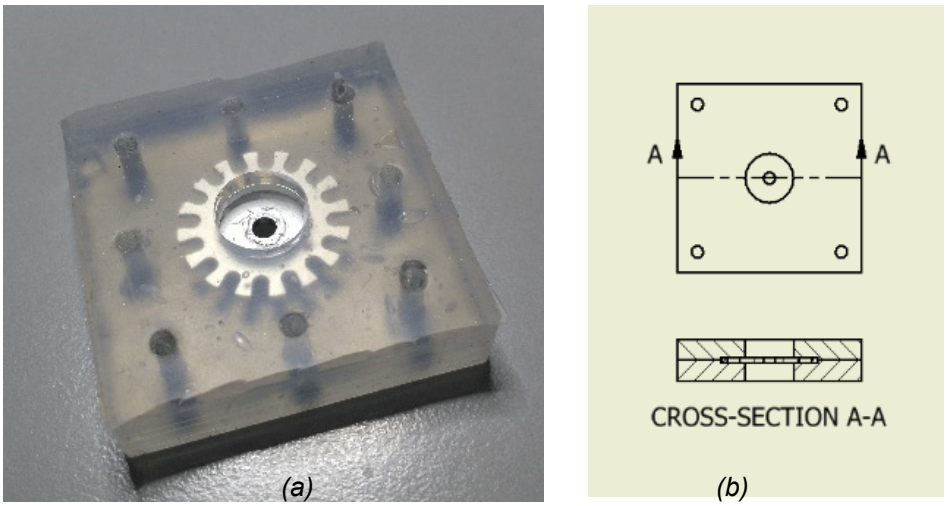

Figure 28: (a) Polymer with motion carrier version 2, (b) cross-section-view

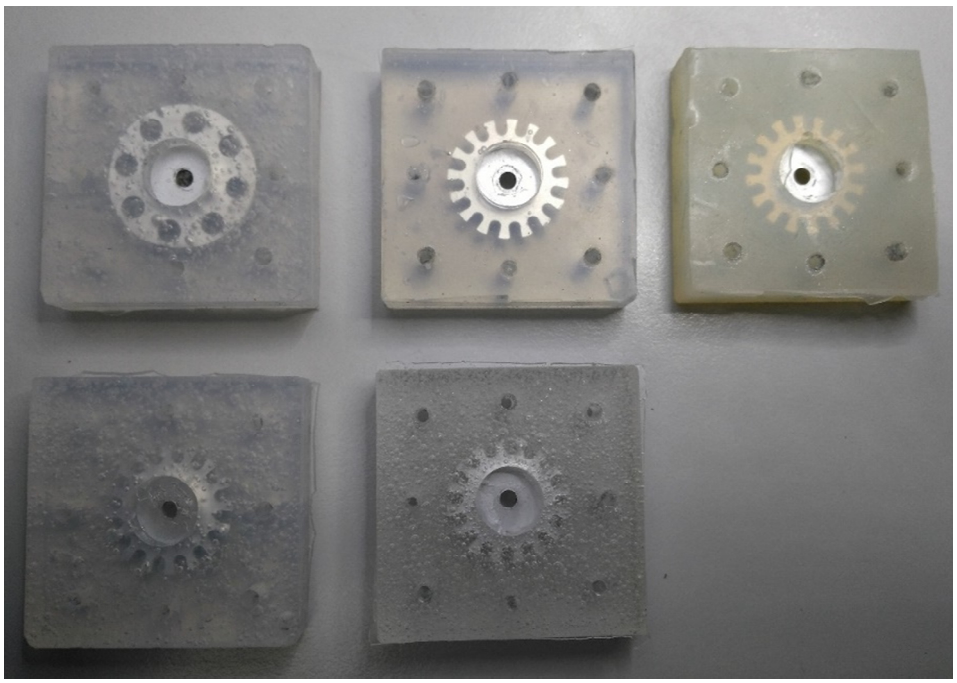

Figure 29: Silicone polymer with motion carrier, different forms

In versions 2 and 3, flexible materials (see Figure 30) in the thickness of 0.3 to 2 mm were used. The used materials should have an excellent reset response, where CFRP was predestined here.

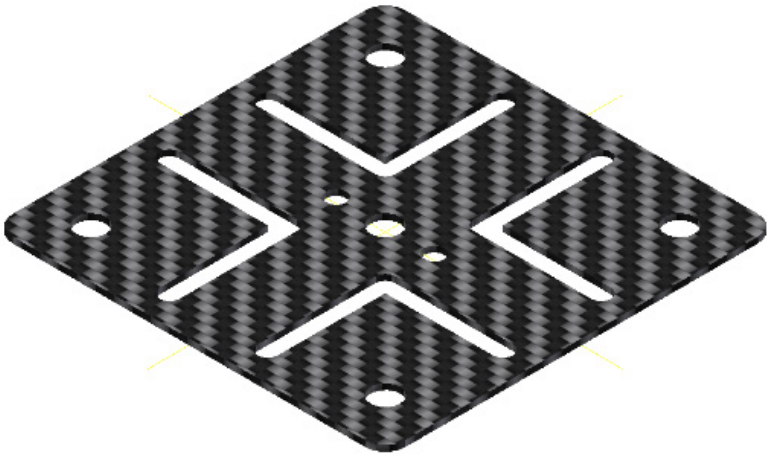

Figure 30: CFRP motion carrier

The bearing pivot locates at motion carrier level where the distance between the motion carrier and the image sensor surface is 17 mm. With a diagonal of the image sensor of 1/1.8“ (inch) (14.1 mm) and a resolution of 1.3 MPixel, the pixel size is 5.3 µm. From $x = r \sin(\varphi)$ results an angle deviation of $\sim 17{,}86° * 10^{-6}$ for the deflection of the laser beam on the image sensor by one pixel. The material and the form of the motion carrier was selected to retrieve the rest position after deflection of the laser beam across the total sensor surface, with a drift of +- 2 digits. Temperature influences from -30 °C to 80 °C generated an additional temperature drift of +- 1 digit. Consequently, a max. total drift of +- 3 digits is possible. The max. angle drift of the laser beam then amounts to $+- \ 53{,}58° * 10^{-6}$. To absorb this drift, the software considered a neutral window of +- 5 digits. The output signals only changed after the calculated coordinates have left the described neutral window.

The technical construction consists of three layers of CFRP tissue which have been installed unidirectional to each other in an angle of 120°. Below a material thickness of 0.8 mm, the motion carrier can only contain two layers, for technical reasons, which are executed unidirectional with 0°/90°. Essentially thinner motion carriers can also be manufactured with carbon fiber prepregs as UD-material (all chamfers longitudinal). Here, minimum two layers must be installed unidirectional with 0°/90° since else an asymmetric bending moment will result. The thickness of the won motion carrier could, however, also consist of a multiple of the carbon fiber thickness. The resin share amounts to 35 %, each. In the test construction,

the neutral drift did not surpass +- 2 digits even after 250000 maximum deflections. These stress tests were also executed in different temperatures and no change of the maximum neutral drift could be stated.

4.2.5 Basic operations

Impact from outside on the transducer of the motion carrier changes its inclination and/or distance to the lower image sensor. The projection unit which is firmly fixed to the motion carrier generates the image of a filled circle on the image sensor (see Figure 31 and Figure 32, as full image of a 1.3 MP image sensor).

Figure 31: Complete image sensor frame without image processing

The reset force of the motion carrier either comes from the arrangement of the defined polymer layers in version 1 or by the restoring force of the used material itself, refer to version 2 and 3.

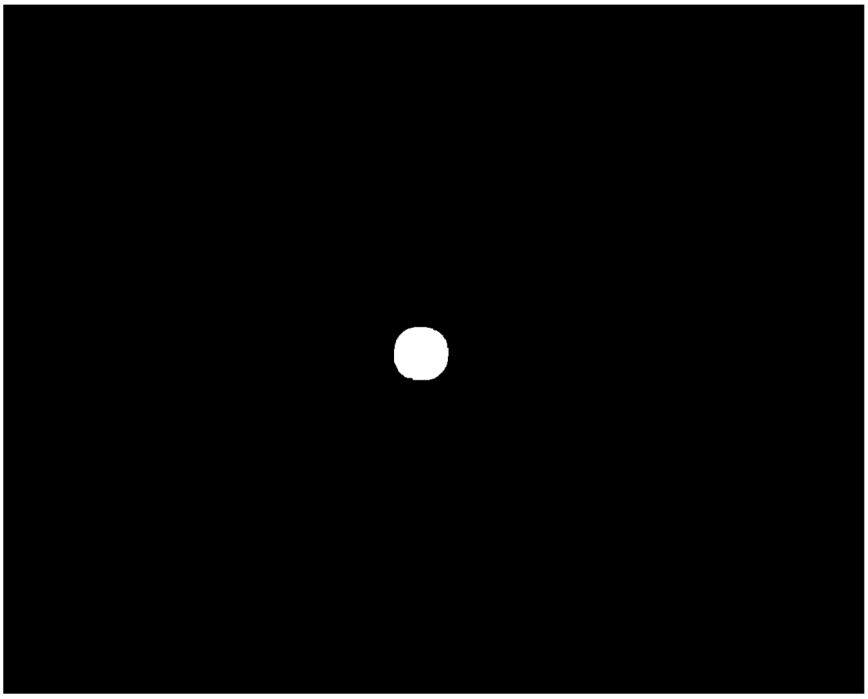

Figure 32: Complete frame with image processing in binary mode

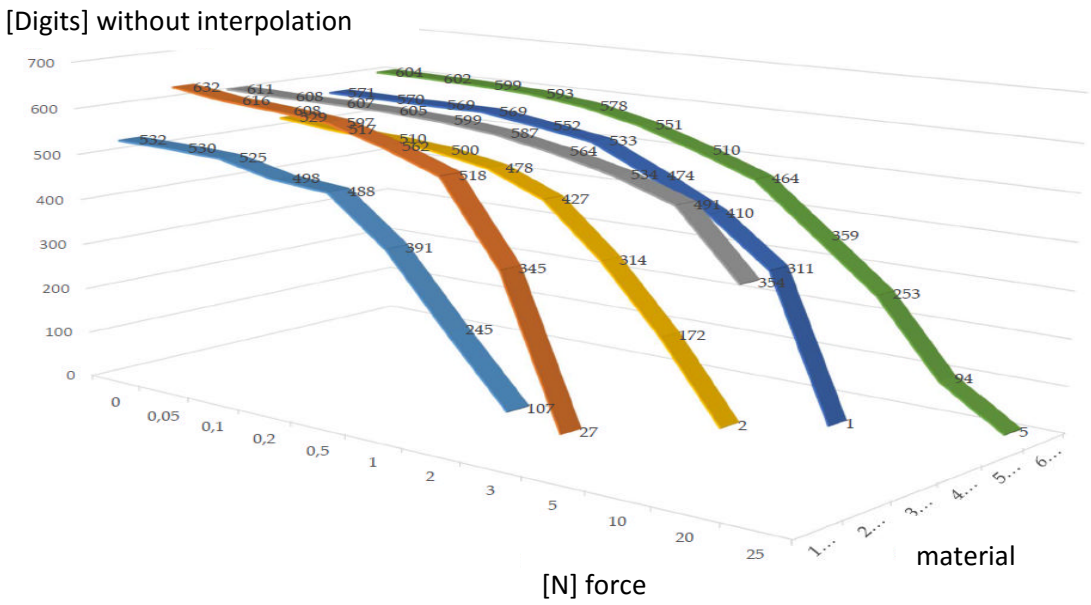

Figure 33: Visualized, measured values from Table 9

Figure 33 shows the deflection in relation to the acting force (measuring values from Table 9). Different polymer arrangements and also different polymer types are shown as examples. The material composition is declared in Table 10. Since the measuring curves are identical in every direction, the measurement

was only recorded in one direction. The force was applied via an axis of 45 mm in length. Relatively soft polymer layers were used, and forces were measured up to 25 N (“out” means that the light circuit has left the active sensor field).

Table 9: Selected measurements with different materials and versions

Excerpt test series / force (N) 45 mm lever	0	0,05	0,1	0,2	0,5	1	2	3	5	10	20	25
1 Mat.T13-44T1V11.0	532	530	525	498	488	391	245	107	out	out	out	out
2 Mat.T13-44T1V10.2	632	616	608	597	562	518	345	27	out	out	out	out
3 Mat.T11-55V10.2	611	608	607	605	599	587	564	534	491	354	out	out
4 Mat.T13i-T1a-V10.2	529	517	510	500	478	427	314	172	2	out	out	out
5 Mat.T1-V10.2	571	570	569	569	552	533	474	410	311	1	out	out
6 Mat.CFRP055-V12.2	604	602	599	593	578	551	510	464	359	253	94	5

Table 10: Material declaration

Material 1	Material 2	Material 3
Prototype version: 11.0	*Prototype version:* 10.2	*Prototype version:* 10.2
4 parts base shore 0	4 parts base shore 0	1 part base shore 22
4 parts mesh shore 0	4 parts mesh shore 0	1 part mesh shore 22
1 part base shore 20	1 part base shore 20	
1 part mesh shore 20	1 part mesh shore 20	

Material 4	Material 5	Material 6
Prototype version: 10.2	*Prototype version:* 10.2	*Prototype version:* 12.2
4 parts base shore 0 inside	1 part base shore 20	CFRP Carrier 0,55 mm
4 parts mesh shore 0 inside	1 part mesh shore 20	1 part base shore 0
1 part base shore 20 outside		1 part mesh shore 0
1 part mesh shore 20 outside		

4.2.6 Projection

As shown in Figure 34, any number of geometric forms can be used for projection. For the prototype presented here, the example of a geometric form has been selected which was the easiest one to execute (filled circle and/or disk Figure 34, lower left side and Figure 35).

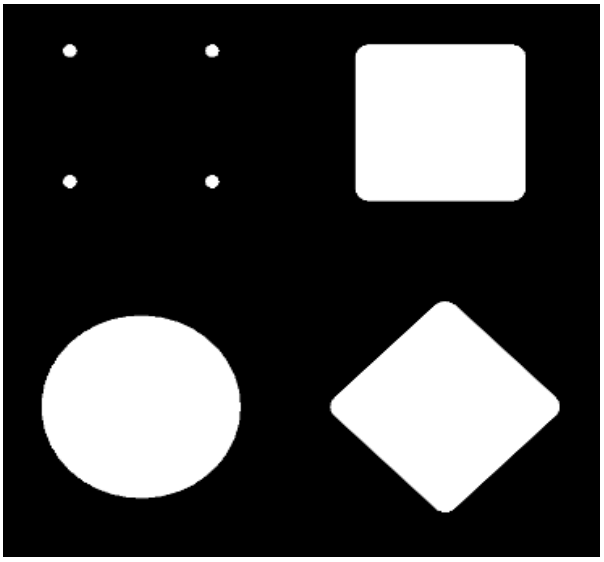

Figure 34: Various projection images schematically

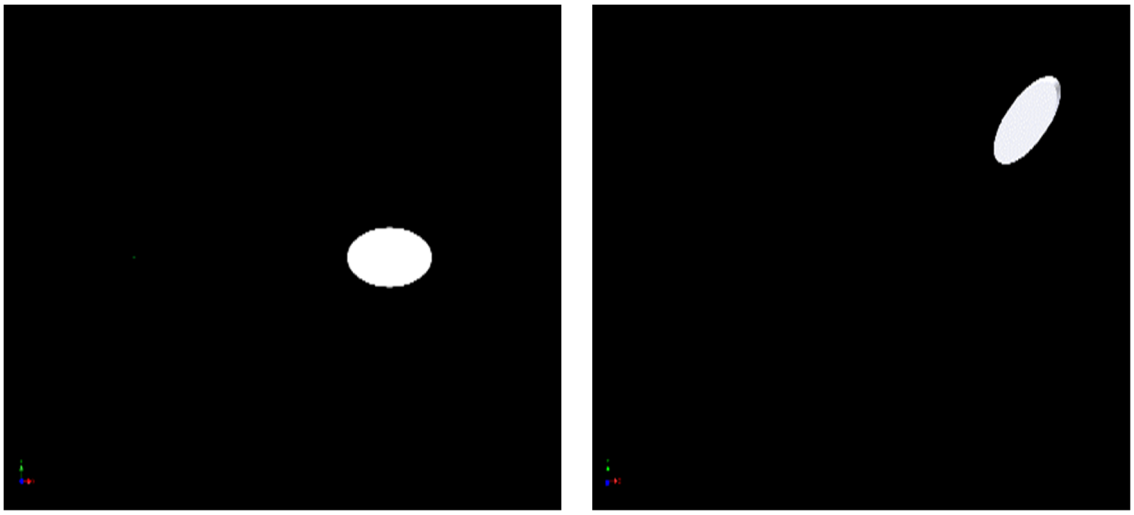

(a) *(b)*

Figure 35: (a) Deflection on the x-axis and (b) on the x- and y-axis, schematically

If 4 points are used (see Figure 34 upper left side), also here more than 3 axes can be measured. The measurement of the four points to each other as well as the measurement within the image sensor coordinate system, detects a change around any axis. Unfortunately, the measurement of the four points is very processor intensive, so that the framerate of the prototype decreases to approx. 12 fps. Faster processors may be of help. Figure 36 indicates the rest position.

(a) *(b)*

Figure 36: (a) Neutral z-axis and (b) pressed z-axis

It is of no importance in terms of production tolerances here, whether the projection of a circle locates exactly in the middle of the image sensor or somewhat outside this middle position. The absolute zero- and/or rest position is individually defined in a calibration process. Normally, this process is only executed once after production. In this way, increased production costs will be omitted since the production tolerances are relatively unimportant. Figure 35 shows a deflected motion carrier. Because of the radiation angle, a distorted ellipse will result.

4.2.7 Software, image analysis and data output

The image analysis software first searches the previously defined geometric form in the recorded image. After the image is found, only the area around the found image is investigated to save processor time, i.e. the “area of interest” AOI

[26,27]. This procedure increases the processing speed considerably. Thereafter, the brightness values of the subpixels are evaluated and the focus of projection is calculated by interpolation. The accuracy here is extended by two digits after the decimal sign.

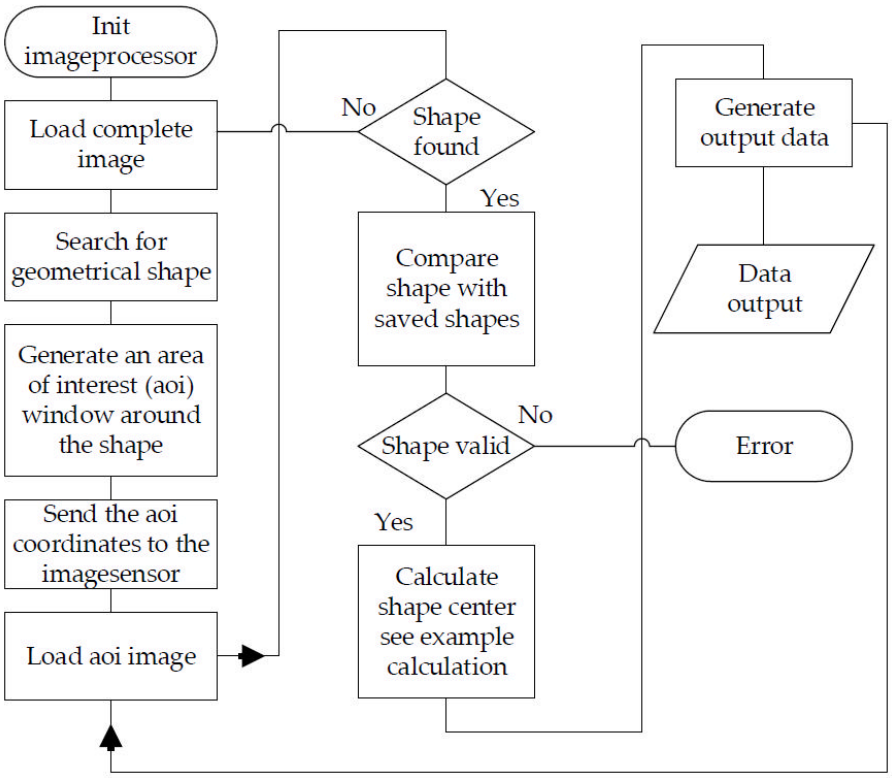

Figure 37: Schematic software procedure normal use

To start the learning process for the individual adaptation, a key must be pressed. Then, the microprocessor records the reached maximum coordinates in every direction. In addition, the distortion of the geometric shape is saved during the reached maximum coordinates. If the shape is a circle or an ellipse then the max. x- and y-extension of the shape is saved. In normal mode (see Figure 37) the found shape is compared with the saved figures and their coordinates. If there is a mismatch between the found shape and the expected shape on this position then an error is generated to protect the following systems against malfunctions. The focus of projection is set in such a way that the static state of the focal point (see Figure 38) is approx. 1 mm below the image sensor surface. This varies the size of the projected circle in z-direction depending on the applied force. Dragging

the z-axis will downsize the projection, while a pressure on the z-axis in direction to the image sensor will upsize the projection (see Figure 39).

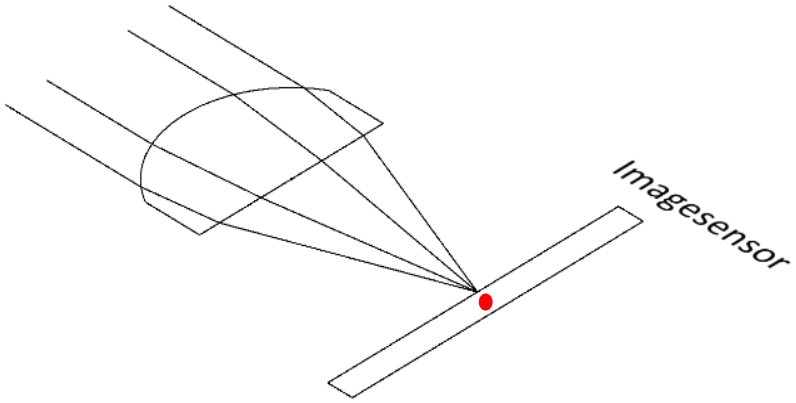

Figure 38: Focusing without pressure on the z-axis

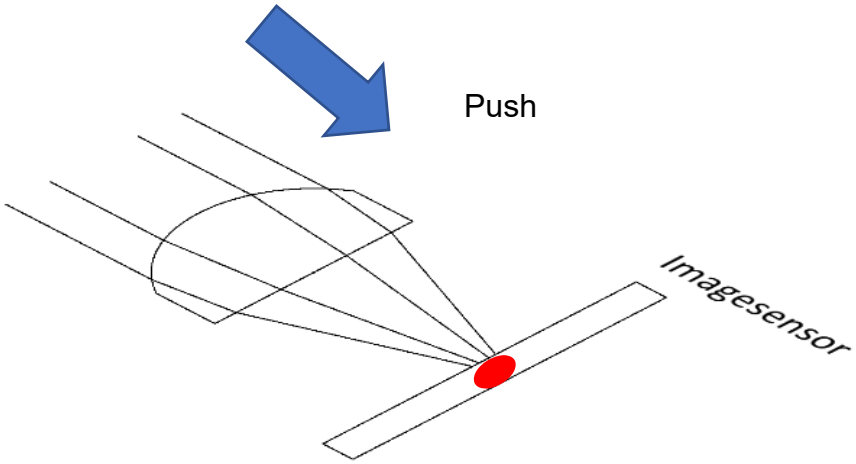

Figure 39: Focusing with pressure on the z-axis

The image analysis software recognizes a smaller and/or larger light circle from which the intensity of the z-axis movement can be calculated. If a threshold or a hysteresis is defined for the size of the light circle, then a mouse click can be generated, for example. The highly accurate coordinates won in this way, will then be forwarded to the next system. Serial values or different bus protocols can be generated (CAN, SPI, I2C) as well as analog voltages. To increase the processing speed (framerate), the x-, y- coordinates for the relevant AOI image section (see Figure 40) are transferred to the image processor. Thereafter, not the

total image is searched anymore to find the geometric shape, but only a section thereof. As soon as the found shape locates in the marginal area of the AOI, the position of the AOI will follow. If the shape cannot be found in the AOI image section then automatically the total image is searched to find the shape. Thereafter, the AOI-image section is set again.

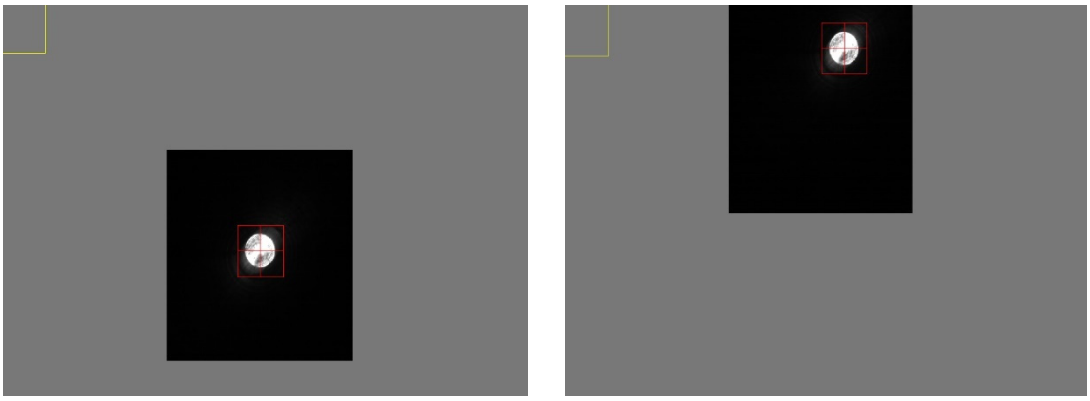

(a) *(b)*

Figure 40: Image with AOI window

4.2.8 Plausibility check

It is intended to use the sensor also in highly sensible and/or safety-relevant areas. For this reason, a plausibility check is executed. The basis among others is the natural distortion (Figure 35) of the projected shape while the main sensor axis is deflected. When the projection of a circle moves from the middle of the image sensor to the periphery, it takes on the shape of an ellipse. This ellipse disposes of two focal points – F1 and F2 – the resulting distance can be calculated. The distance between the focal points increases in the same way as the motion carrier is deflected. To learn the allowed maximum distance between F1 and F2, the motion carrier is moved with the allowed maximum force at least once in every direction. Ideally, this movement is a circular motion with allowed maximum force. This circular motion can be executed manually as well as with a calibration device. During this calibration, the allowed maximum distortions and their positions are analyzed and permanently saved. In normal mode, all recognized

projections are compared with the previously saved images. If a maximum position or a maximum distortion is surpassed then actions can be taken to protect the following system against malfunctions. Also, still further special cases can be intercepted. If the projection unit leaves the rest position due to a malfunction of the hardware without being deflected then the resulting projection would locate distortion-free at a position outside the expected rest position. This situation will then be recognized as hardware error since it is not possible to find a distortion-free projection on another coordinate than the originally learned rest position. Depending on the performance of the used image sensor and microcontroller, the plausibility check can still be extended. In this case, additional motion patterns or motion velocities can be analyzed and checked for plausibility.

4.2.9 Individually adjustment of the 3-axis sensor

Because of the different disease patterns, different input forces and input strokes are needed. Depending on the requirement, a certain accuracy (resolution), a certain force for deflection as well as a certain stroke for the mastering of the necessary paths are defined for off-the-shelf joysticks. As mentioned in the introduction, defined groups of humans with physical diseases cannot use standardized joysticks. The problem is found in the individual motion spectrum (force and stroke) of these persons. The available motion spectrum is also subject to external influences such as the ambient temperature [28]. To secure a sustainable use, a permanent re-adaptation of the sensor would be necessary. To adapt the sensor to the available motion and stroke properties of the patient, the user moves the 3-axis sensor minimum once with a circular motion in every direction. Also the z-axis can be learned by a vertically pushing and pulling the motion carrier. Thereafter, the reached maximum x-, y-, z-coordinates are saved. As an example, the force and/or stroke of a patient with a muscle illness was recorded. The result in Figure 41 shows an inhomogeneous course of the applied force in different directions.

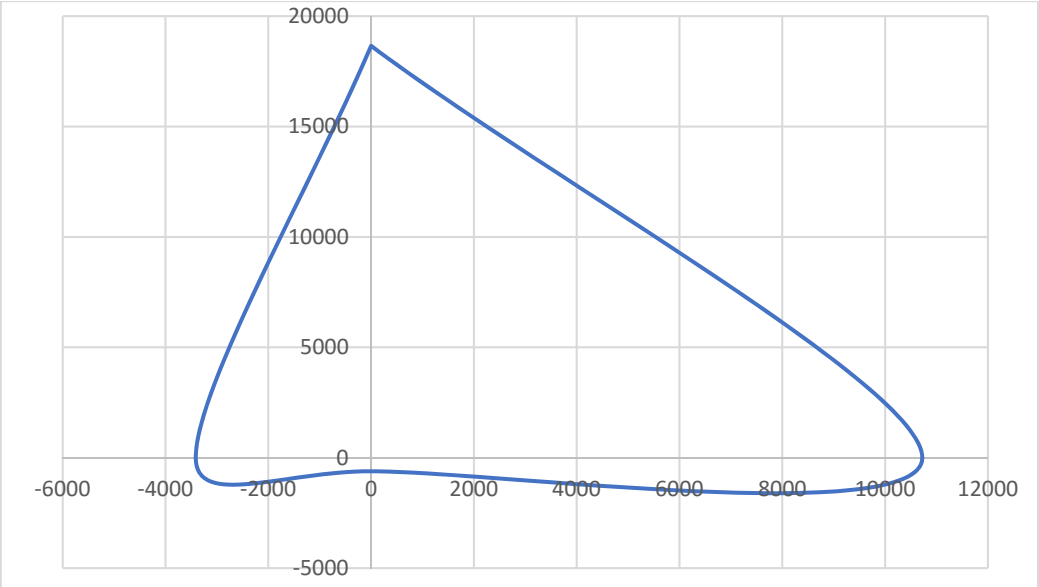

Figure 41: Force curve (force to digit), interpolated values

If a reference has been created previously (deflection and force onto digit), then the applied force (see Table 11) and the stroke of the patient can be directly derived from Figure 41. Of course, the ratio of stroke and changed coordinate also depends on the position of the lever. In this test case, the patient could apply the following deflection and/or forces (the z-axis is not considered here):

Table 11: Patient measurements and applied force

Direction	Max. digits	Approx. force (N)
forward	18653	3.92 N
back	611	0.07 N
left	3411	0.74 N
right	10724	2.12 N

These values cannot be sent directly to e.g. an EPW. The patient can only select the forward and right direction. The achieved values for back and left direction were not sufficient to move the EPW. This can be rectified by suitable factors and/or divisors to reach the desired even output signal. Example: Popular output values locate in the 10 bit range (measured value/1024) 2 = divisor; refer to Table 12).

Table 12: Patient measurements and calculated divisor

Direction	Max. digits	Divisor for each direction
forward	18653	36,43
back	611	1,19
left	3411	6,66
right	10724	20,95

All coordinates recorded during operation must then be calculated for this user with the determined divisor to get an even (homogenous) output signal.

Example of calculation:

All values are multiplied by 100 through the interpolation of the image (value for the right direction, Table 11; 10 bit output signal; image sensor 1280 x 1024).

X_{MaxRes} = 128000 digits; Maximum resolution in horizontal direction;

$X_{MaxResRight} = \frac{X_{MaxHorRes}}{2}$;

$X_{MaxResRight}$ = 64000 digits; Half resolution each direction;

$X_{Neutral}$ = 63891 digits; Measured neutral value;

$X_{NeutHysteresis}$ = 500 digits; Hysteresis for a neutral window in the middle position;

$X_{MaxRight}$ = 74615 digits; Learned maximum value to the right;

$X_{AbsolutMaxRight} = X_{MaxRight} - X_{Neutral}$;

$X_{AbsolutMaxRight}$ = 10724 digits; Absolut maximum value to the right;

$Resolution_{OutMax10bit}$ = 1024 digits; Desired maximum output value;

$$Resolution_{EachDirection} = \frac{Resolution_{OutMax10bit}}{2}$$

$Resolution_{EachDirection}$ = 512 digits; Desired maximum output value each direction;

$$X_{DiviRight} = \frac{X_{AbsolutMaxRight}}{512\ digits};$$

$X_{DiviRight}$ = 20,95; Calculated divisor;

$X_{RightExample}$ = 4200 digits; Example value to the right;

$X_{OutRight} = \frac{X_{RightExample}}{20,95}$;

$X_{OutRight}$ = 200 digits; Digital output value;

With the above mentioned algorithms, the coordinates of the inhomogeneous input forces (Figure 41) are converted into homogenous output data (see Figure 42). The user will then be able to move e.g. a computer mouse or an EPW with the same speed in all directions independently on his inhomogeneous force-stroke ratio. The output values calculated by the divisor were entered in Table 13 and shown in Figure 42.

Table 13: Maximum patient measurements and calculated output values

Direction	Max. digits	Divisor for each direction	Calculated output values
forward	18653	36,43	512
back	611	1,193	512
left	3411	6,66	512
right	10724	20,945	512

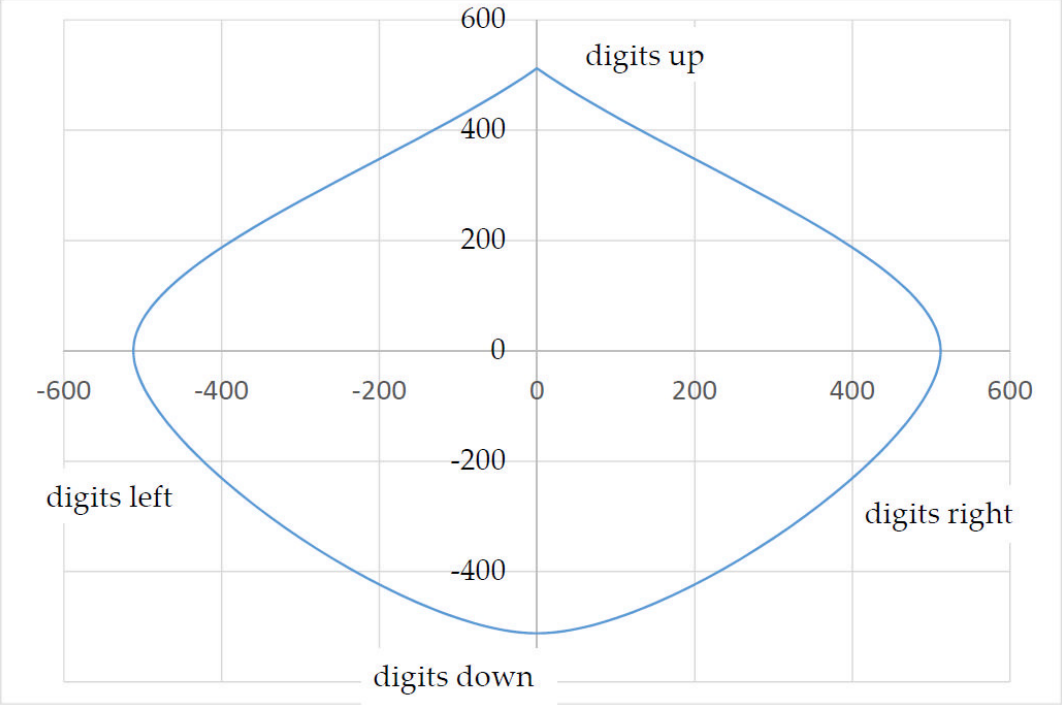

Figure 42: Output data curve

4.2.10 Hardware

The hardware (see Figure 43) consists of the image sensor, the image processor and another microprocessor. The microprocessor first configures the image processor and then receives image data for further processing (see Figure 37). Thereafter, the microprocessor generates the desired output data and receives the learning command, if desired, from an I/O-port. If an error is detected then an additional I/O-port can be activated to inform the subsequent system accordingly, also outside the agreed protocol.

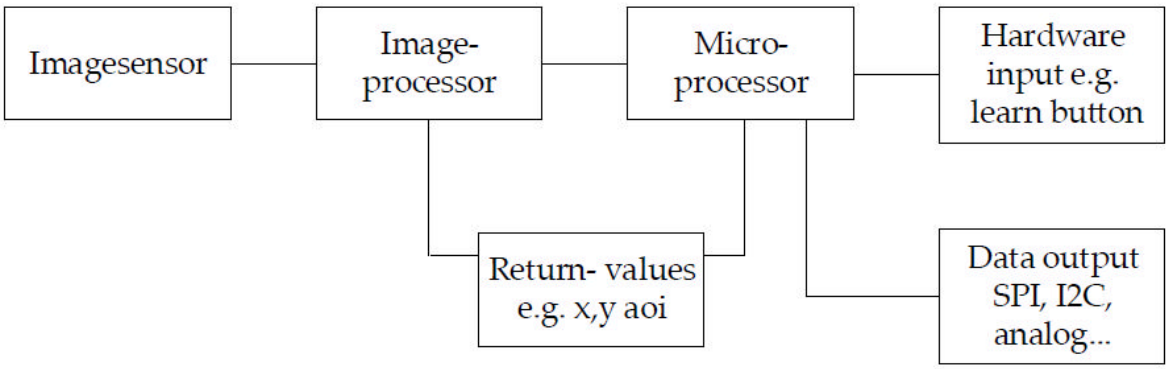

Figure 43: Schematic sensor hardware

4.2.11 Novelties against known systems

The optical research approach also fulfills the criteria of an alternative construction and purpose of use besides the selection criteria for a complete digital execution. To support this thesis, individual items are listed below which will explain the novelty in comparison with the known systems.

- Concrete construction of the projection unit: Since an optical construction could only be found with one lens and since complex lens systems with mandatory distances could be renounced at, the constructive size of an off-the-shelf input device can be executed. Without reaching this construction size, the actual application areas would be strongly restricted.
- Low distance of projection unit to image sensor: The executed distance results from the developed projection unit. Industrially manufactured laser

optics are generally equipped with collimator lenses to guarantee an optimized parallel guiding of the laser beam. Due to the low distance, these lens systems could be omitted.

- Construction and forming of motion carrier from CFRP: Due to the formation and material selection of the motion carrier, a sufficient bending capability could be reached in spite of the used material thickness. Also lowest force impacts in a 0.05 N range were sufficient to generate a useable deflection of the laser beam. Simultaneously, the motion carrier must also be stable enough to resist against overload to avoid an irreversible deformation or damage of the carrier material.
- Ability of motion carrier to return to the accurate rest position after deflection: This aspect represents the most time-consuming part of development. Only a combination of material quality, material strength and shaping enable this extraordinary capability. In all known publications, no execution feature could be found which describes – not even partially – the execution developed here.
- Observance of constructional standard dimension and related option to establish the sender in the different application areas.
- Algorithm for the individual adaptation to the user with changing disease pattern: Solely this property makes it possible to adapt the sensor to a changing disease pattern. This process can be initiated anytime by the user himself whereby the health system is financially discharged since no specialists are needed. This aspect should support the establishment of this sensor in the health care industry. Due to the individual adaptation process, the healthy users will work clearly more accurately and free of fatigue.
- Use of software AOI-function to increase the processing speed (framerate) up to 180 fps, which in turn increases the operability and the response of the sensor: Through this function, expensive image sensors with high image refresh rates (framerate) can be renounced at, resulting in less production costs.

- Plausibility check of projections and safe use: The permanent tests of data in operation tremendously increases the safe use of the sensor. Therefore, the use of this data in highly sensitive areas will meet the requirements.
- Use of construction-based natural “force feedback“ effect: This effect informs the user anytime of the strength of deflection via feedback. Since the main sensor axis is deflected in an angle that can hardly be perceived, the force receptors of the skin acknowledge a proportionally increasing feeling of pressure with increasing force impact.
- Increase of a valid and useable resolution by factor 100 by interpolation of the project mapping, using gray- and limit values.

4.2.12 Result and estimation, optical approach

The sensor described here is in prototype stage (see Figure 44). Due to the optical execution, the sensor should resist against external interferences such as EMI or RFI. In version 1, cold and hot vulcanized 2K silicone caoutchouc polymers were used which characterize by a good reset capability. Unfortunately, this capability was not sufficient to achieve a satisfying result. The missing of the neutral position increased with increasing axis deflection. Since, however, the achieved neutral values could be accurately reproduced depending on the executed axis deflection, this missing could be compensated by software. Because of the dissatisfying results, no further permanent tests were executed. Therefore, no verified statement about the stability of the material can be made. Since, in addition, the processing of silicone polymer is expensive, a further follow-up of this bearing was omitted.

In versions 3 and 4 the motion carrier was manufactured from a CFRP and firmly fixed to the housing. In comparison with the aramid fiber reinforced polymer (AFRP) and glass-fiber reinforced polymer (GFRP), CFRP has extraordinary dynamic properties. The dynamic damping ability with dynamic load of CFRP is 6 times higher than that of AFRP and 9 times higher than that of GFRP [29]. Through the use of CFRP, the above mentioned problem was solved, where the reset accuracy amounted to +- 2 digits (without interpolation, image sensor 1.3 MP).

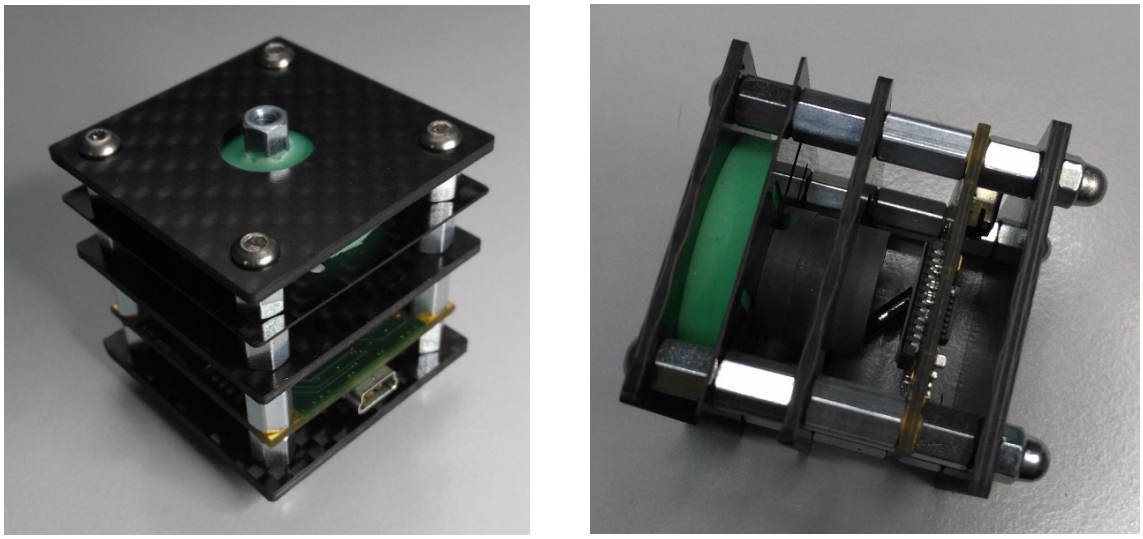

(a) (b)

Figure 44: (a) Optical prototype finale version and (b) side view

The climatic chamber was passed successfully (-30 °C to 80 °C). The deviation amounted to +- 1 digit (without interpolation, image sensor 1.3 MP). In the first test phase (see Table 14), the optical sensor was not deflected.

Table 14: Optical sensor, rest values in climate chamber

Temp. (° Celsius)	Rest values x-axis	Rest values y-axis	Rest values z-axis
-30	626	524	81
-20	626	524	81
-10	626	524	81
0	627	525	81
10	627	525	81
20	627	525	81
30	627	525	81
40	627	525	81
60	628	526	81
70	628	526	81
80	628	526	81

The total test period lasted 8 hours. The temperature dependent max. deviation of the rest values of +- 1 could only be reached with a motion carrier made of CFRP. During the second test (see Table 15), a fixed deflection of the sensor

was executed with a micrometer screw (test period 8 hours). The deviations also ranged within max. +- 1 (measured with a 10 bit ADC).

Table 15: Fixed deflection in climate chamber

Temp. (° Celsius)	Rest values x-axis	Rest values y-axis	Rest values z-axis
-30	839	614	80
-20	839	614	81
-10	839	614	81
0	839	615	81
10	840	615	81
20	840	615	81
30	840	615	81
40	840	615	81
60	840	616	82
70	841	616	82
80	841	616	82

Another test series investigated the reset accuracy (see Table 16) of the motion carrier after load of the optical sensor with different forces in every direction.

Table 16: Static position after load (temperature 21 °C)

Load (N)	Statis values x-axis	Statis values y-axis	Statis values z-axis
Statis value	626	524	81
forward 1	626	524	81
forward 2.5	626	524	81
forward 10	627	524	81
forward 25	627	524	82
backward 1	626	524	81
backward 2.5	626	524	81
backward 10	626	524	81
backward 25	625	524	82
right 1	626	524	81
right 2.5	626	524	81
right 10	626	525	81

right 25	626	525	82
left 1	626	524	81
left 2.5	626	524	81
left 10	626	523	82
left 25	626	523	82

The load test showed that the rest values of the motion carrier after different loads deviate by max. +- 1 digit. Since deviations may occur also in common after temperature impacts as well as after load, a deviation of max. +- 2 digits due to external influences must be taken into account. To overcome this problem, the measuring values of the optical sensor must deviate by min. +- 4 digits from the rest values before the subsequent system executes any action. Initial tests under laboratory conditions were passed successfully. The optical sensor was used as mouse substitute. If a physically diseased patient still possesses any remaining function (hand, finger, foot, head, shoulder [30] etc.) it should be possible to use this optical sensor. If the disease pattern deteriorates then the sensor can be adapted immediately to the new conditions. Because of the high resistance against interference, not only the medical area but also the application areas in the automotive-, aeronautical-, aerospace-, marine- and military-industry can be of major importance. The high resolution and the reproducibility of the measuring values allows to also replace geophysical sensors. A screwed rod or ball for the take-up of force may enter a resonance oscillation if a defined vibration frequency impacts the sensor. In the laboratory test, the resonance frequency of the optical sensor amounted to approx. 810 Hz. This can „build up“ the system. This condition which can hardly be expected under normal conditions, can also occur with off-the-shelf joysticks. To compensate this, a polymer ring is mounted on top of the motion carrier (version 3) which acts as shock absorber and damps the vibrations.

Another problem is the noise of the image sensor. In absolute static state, the coordinates change by up to 2/100 digits (with interpolation, image sensor 1.3 MP). The indicated results show the feasibility of the optical 3-axis sensor. In comparison with off-the-shelf high-resolution sensors (potentiometric, inductive or capacitive) the presented sensor works completely digitally. No compensation

is necessary to calibrate the sensor, e.g. in case of temperature changes. Depending on the intensity of the plausibility check, the software needs considerable processor time. In the present version, the calculation can either focus on the maximum framerate or to the maximum resolution. Since, normally, the different purposes of use only need one focal point, the sensor can be optimized for the relevant application by software. The actual prototype can process 60 full images per second. The AOI function accelerates the processing to up to 180 fps. This problem can be solved by faster image sensors and faster microcontrollers. The sensor is also able to present more than 3 axes, if e.g. 4 single points are used as projection shapes. The image analysis software then also states the rotary motion of the axis. The processor time here would, however, increase considerably. The needed minimum assemblies to manufacture the optical sensor are limited to the motion carrier, laser diode, and plan convex lens and to an image sensor unit with microcontroller (see Figure 45).

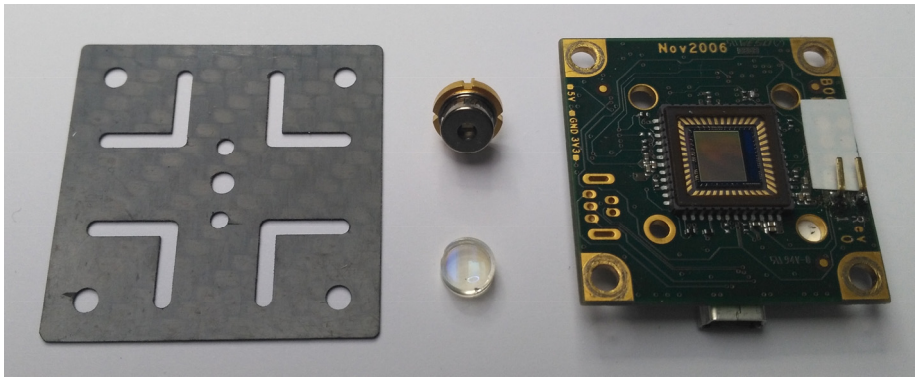

Figure 45: Minimum components

4.3 Prototyping and test series, SG approach, version 1

The SG research approach (refer to Chapter 7.1.2) fulfills the selection criterion of an alternative construction to develop new application areas. Similar to the optical research approach, the primary problem is the construction and the selection of material for the motion carrier. Since this development aims at covering especially the spastic illnesses, the construction must resist high impacting forces. This, however, must not deteriorate the sensitivity since the force and motion spectrum of this group of persons outside the spastic seizures resembles the spectrum of healthy people. For humans with spastic illnesses, the use of an off-the-shelf multi-axis sensor [31] is often a problem, since the motion spectrum

(force and stroke) in these illnesses is subject to permanent changes and unforeseen spastics. During the use of sensible systems, these spastic motions can result in non-controllable and dangerous situations. In addition, the user may be hurt when his hand cramps around the joystick and when bones and tendons are disproportionately stressed [32]. To bypass the described problems, the input device to be developed shall be executed as a flat disk which can be operated with any part of the body. The displacement of force (x- and y-axis) shall decline the disk to all sides while generating proportionate output signals. A centric pressure (z-axis), for example, could call a menu or execute a mouse click. If a spastic attack occurs then the user will not get caught by his input device since the input device is a flat disk and can be inserted, in addition, in an operating table. The relevant part of the body only slides across the disk which excludes a wrong handling to a far reaching extent. Strongly varying input forces must be filtered which the user only applies selectively with the objective to initiate an action of the connected system. Systems which support the user in his navigation [33,34] are reasonable but expensive. In addition, a “free use” is not possible since the navigation aid is activated in programmed situations. Controls which monitor the spastic motions for a defined period of time [35] and which generate an algorithm-based average value for the selected desired direction, can generally be combined with input devices. However, also in this case, a direct control would be prevented. For sportive activities such as EPW-hockey, preference is given to the direct control. If an EPW is used then new control systems such as eye-tracking, voice control and brain-computer-interfaces are rather problematic [36–39]. Also a control by tongue [40,41] is only of limited use for spastics. It is difficult to realize an accurate and simultaneously complex control of the mentioned input methods. Eye-tracking is subject to natural reflexes (eye reflex) and completely inappropriate for safety-relevant control tasks. The voice control normally only accepts single commands and do not work reliably in loud environments [42]. The selection criteria of alternative construction and innovative purpose of use is fulfilled. That’s why this research approach has been chosen.

4.3.1 Functionality and construction

The described gross motoric forces must first fulfill the stability criterion. It must be calculated with the fact that forces up to 1400 N can be applied which the sensor must resist without being damaged. As already explained, the construction of a flat disk (120 mm diameter) seems to be the most reasonable solution. The SG version 1 (strain-gauge-disk (SGD)) (see Figure 46) consists of a CFRP motion carrier (Pos. 2) to which four SG are fixed (Figure 47). Below the motion carrier locates the circuit board (see Figure 46, Pos. 4) with 4 differential amplifiers AD 623 [43] and an ADC AD 7811 [2] with integrated SPI (Serial Peripheral Interface) connection. This enables the user to decline the disk into every direction by displacing the weight (x-, y-axis) on the top cover (see Figure 46, Pos. 1). The CFRP motion carrier is operated differentially. If an edge of the CFRP motion carrier is pressed down then the opposite side of the CRRP motion carrier goes up which is a geometrically conditioned process. Therefore, a plausibility check can be executed (refer to Chapter 4.3.5). Also, the top cover can be operated centrally. Here, all 4 strain-gauges are deflected in one direction (z-axis) which enables further control options, e.g. the use of a computer mouse (mouse click). The components (see Figure 46, Pos. 3 and 5) of the sensor only serve as spacers. The total sensor can also be integrated in an operating table in front of the user (operating table of an EPW). The total operating table could be made of CFRP whereby the table simultaneously represents the sensor material. The meshing parts of the housing protect the sensor against splash water.

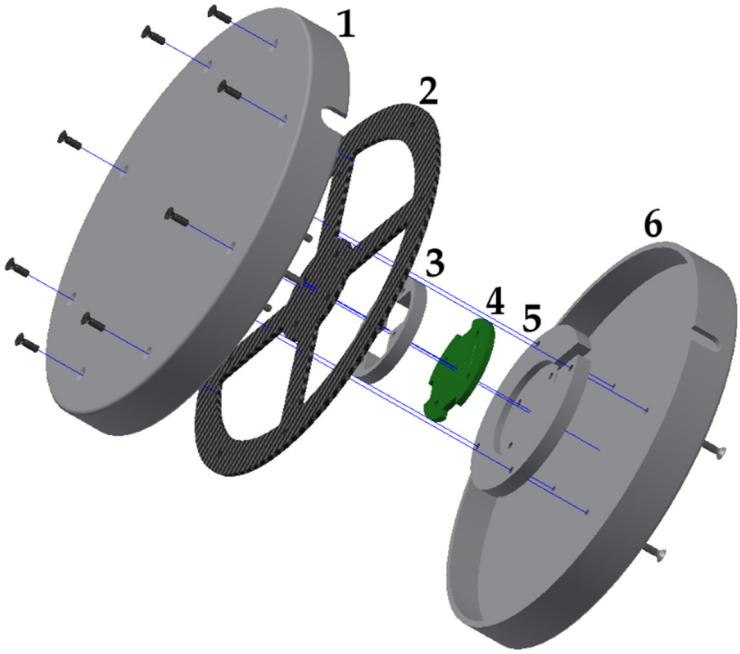

Figure 46: SGD exploded view drawing

The SGD consists of the following components:

1. Upper case
2. CFRP carrier
3. Spacer
4. Circuit board
5. Spacer
6. Lower case

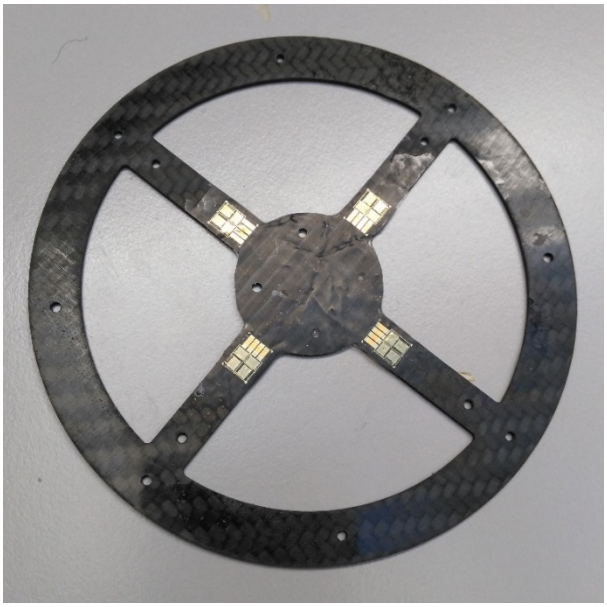

Figure 47: CFRP carrier with affixed strain-gauges

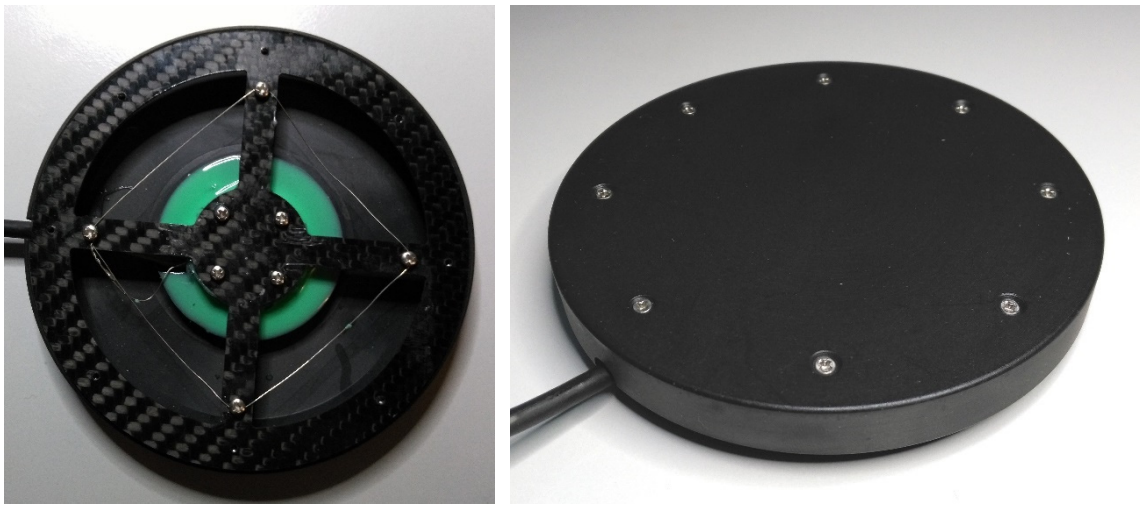

(a) *(b)*

Figure 48: (a) SGD without cover and (b) with cover

4.3.2 CFRP motion carrier

The CFRP motion carrier (see Figure 47) of the prototype consists of a CFRP plate with a thickness of 1.3 mm. The thickness of the material can be adapted to the purpose of use where a good relationship between the necessary resolution and the sustainability could be found. Of special importance was the accurate reset response of the CFRP motion carrier. In the test series, also aluminum and steel was used to construct the motion carrier. Aluminum changed its initial properties already after 120000 load cycles. The material fatigued obviously, that's why its further use was excluded. Steel did not fatigue, not even after 250000 load cycles. In a direct comparison, however, steel was by far not as flexible as CFRP with respect to the ratio of applied force to deformation. CFRP achieved a higher flexibility with comparable stability. So, the motion stroke is higher which increased the technical resolution of the sensor. CFRP did not change its initial properties, even not after 500000 load cycles. If the sensor is overloaded then the meshed parts of the housing protect the CFRP carrier against damages. The construction of the housing mechanically limits the maximum stroke. In case of too high load (max. 1400 N), the applied forces are derived to the CFRP carrier via the housing. The CFRP compensated strain-gauges are affixed and then soldered to the circuit board. The circuit board and the strain-gauges can finally be

sealed by an addition cross-linked silicone. So, the sensor can also be used in a humid environment. For test purposes, the CFRP carrier was also tensioned. The construction shown in Figure 48 with a material thickness of 1.3 mm broke, after a tensile load of 102 N had been applied. Without auxiliary tools, however, it is not possible to load the sensor housing in this tensile direction.

4.3.3 Different versions

The sensor can be executed in different variants depending on the desired purpose of use.

Version 1: The CFRP carrier and its shape is adapted to the expected requirements. Special attention is given to the material thickness and to the arrangement of the CFRP tissue layers. In addition, the shaping supports the stability and varies the bending load of the strain-gauges.

Version 2: The construction is analog to version 1. In addition, the CFRP carrier is encapsulated in an addition cross-linked, thermally vulcanizing silicone polymer. Depending on the shore-hardness, the damping properties are varied. Other damping materials such as compression springs or other polymers were not so successful as desired since their thermal expansion coefficient influenced the CFRP motion carrier counterproductively.

Version 3: The total operating table (e.g. an EPW) is made of CFRP. The strain-gauges are attached by adhesives below the table. The desired input forces by the users vary according to the corresponding milling pattern around the strain-gauges.

In the test series, the CFRP motion carriers with a material thickness of 0.45 mm to 2 mm are investigated. Also the sensitivity and the maximum load, in particular the tensile strength, can be additionally adapted by shaping.

4.3.4 Basics

If external forces impact the CFRP motion carrier on the upper side of the housing then the motion carrier slightly varies its inclination. This deflects the opposite strain-gauges differentially. The resulting differential measuring values can be added in the following microcontroller to increase the technical resolution. Example of calculation:

$X_{Neutral}$=512 digits; Measured neutral value;

$X_{Right\ t=1}$=640 digits; Measured value right strain-gauges at t = 1;

$X_{Left\ t=1}$=430 digits; Measured value left strain-gauges at t = 1;

$X_{t=1}=|X_{Neutral}-X_{Right\ t=1}|+|X_{Neutral}-X_{Left\ t=1}|$;

$X_{t=1}$=210 digits; Output x-value;

To further improve the technical resolution, also a 12 bit ADC with a higher resolution can be used. The reset force of the motion carrier depends on the used version and can be applied either via the CFRP motion carrier alone or additionally via the used silicone polymer. Table 17 and Figure 49 show the measuring values in relation to the applied force.

Table 17: Selected measurements (only X_{Right})

Test series force (N) / digits diameter disk 110 mm	0	0.05	0.1	0.2	0.5	1	2	3	5	10	20	25
1 Mat. CFRP 0,45 mm non silicon rubber	532	538	545	561	592	650	760	890	1024	1024	1024	1024
2 Mat. CFRP 0,90 mm non silicon rubber	535	537	540	551	569	622	698	810	903	1024	1024	1024
3 Mat. CFRP 1,30 mm non silicon rubber	510	511	513	516	529	550	611	675	776	895	1024	1024
4 Mat. CFRP 2,00 mm non silicon rubber	521	521	521	521	522	528	549	607	673	790	897	1024
5 Mat. CFRP 0,90 mm silicon rubber shore 20	505	506	507	511	558	611	670	796	881	982	1024	1024
6 Mat. CFRP 0,45 mm silicon rubber shore 30	535	537	542	561	614	666	791	873	970	1024	1024	1024

Different silicone polymer mixtures and also different material thicknesses (see Table 18) are listed as examples. The measuring curves in every direction

and for every strain-gauge are nearly identical, therefore only one strain-gauge measurement was recorded. In addition to the achievable max. 1024 digits further forces are derived from the housing.

Table 18: Material declaration SG version

Number of material	Thickness CFRP (mm)	Silicon rubber	Shore-hardness degree
1 Mat.	0,45	no	none
2 Mat.	0,90	no	none
3 Mat.	1,30	no	none
4 Mat.	2,00	no	none
5 Mat.	0,90	yes	20
6 Mat.	0,45	yes	30

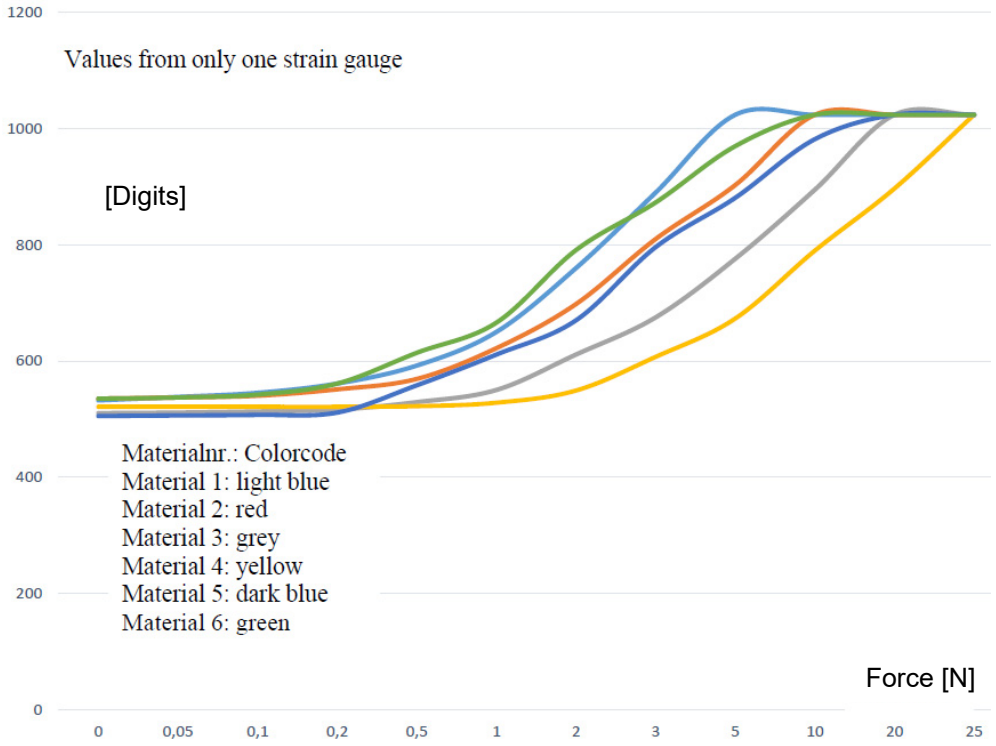

Figure 49: Visualized, measured values from Table 13

4.3.5 Plausibility check

Since the sensor is intended to be used also in highly sensible and/or safety-relevant areas, a plausibility check is executed. In an individual calibration process, all possible measuring value combinations of the individual strain-gauges are saved in a hash table. If a strain-gauge is detached from the CFRP carrier then a specific measuring value is recorded. For this measuring values, a previously saved opposite and differentially working strain-gauge is searched in the hash table. In case of mismatch (the value pair differs from the actually measured value pair), an entry is made in the error memory. In this case, immediate actions are taken to protect the next system against malfunctions (see Figure 54).

4.3.6 Individual adjustment of the SGD

To adapt the sensor to the existing motion and stroke properties of the patient, the user moves the SGD minimum once in a circular motion in every direction. A vertical pressure on the housing cover also learns the z-axis. The maximum values of the reached x-, y- and z-coordinates are saved. The absolute zero- and/or rest position is defined individually for every SGD in a calibration process. Normally, this process is executed only once after production. In this way, high production costs are omitted since the production tolerances are of relative minor importance. The force and/or stroke of the patient are recorded as an example. The result in Figure 50 shows an inhomogeneous course of the applied force in different directions.

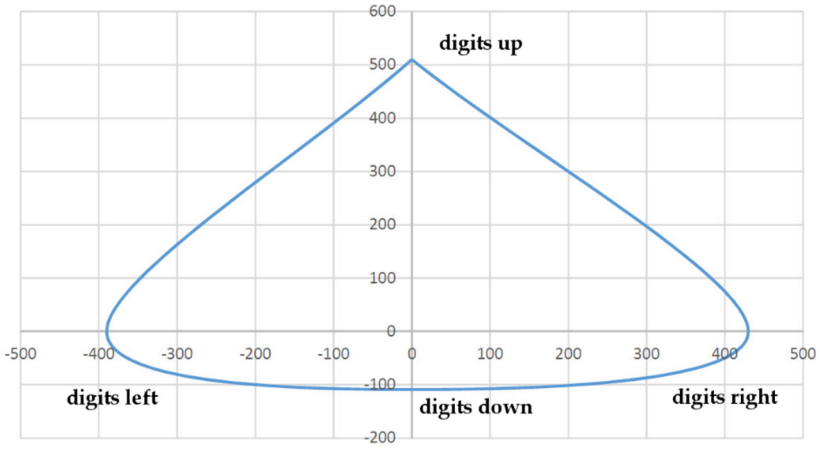

Figure 50: Force Curve (force to digit)

If formerly a reference was generated (deflection and force to measuring value), the applied force of the patient can be directly derived from Figure 50 (see Table 19). In this test case, the patient could apply the following deflections and/or forces (the z-axis is not considered here)

Table 19: Patient measurements and applied force

Direction	Maximum digits	Approximate force
forward	510	18.4 N
back	109	2.1 N
left	390	11 N
right	430	14.2 N

These values cannot be sent directly to an EPW. The patient would be able to drive forward, right and left with sufficient velocity. The achieved values for the back direction, however, are not enough to move the EPW with sufficient velocity in this direction. Suitable factors will help to achieve a desired and even output signal.

Example: Popular output values locate in a 10 bit range (1024 / measuring value = factor).

Table 20: Maximum patient measurements and calculated output values

Direction	Maximum digits	Factor	Calculated output values
forward	510	2,007	1024
back	109	9,394	1024
left	390	2.626	1024
right	430	2.381	1024

All coordinates recorded during operation must be calculated for this user, based on the determined factor (see Table 20), to get an even output signal.

Example of calculation:

(Right value see Table 20, 10 bit ADC output signal)

$X_{MaxRight}$ = 430 digits;	Maximum right direction;
$X_{FactorRight}$ = 2.381;	Calculated factor see Table 20;
$X_{RightExample}$ = 200 digits;	Example value to the right;
$X_{OutRight} = X_{RightExample} * X_{FactorRight}$;	Digital output value;
$X_{OutRight}$ = 476 digits;	Digital output;

Thereafter, the output signals are deducted from the differential output value of the opposite strain-gauge, see calculation example (refer to Chapter 4.3.4). In the meantime, the plausibility check is executed (refer to Chapter 4.3.5). By means of the algorithm shown above, the coordinates of the inhomogeneous input forces (see Figure 50) are converted into homogeneous output data (see Figure 51). The user can then, for example, move a computer mouse or an EPW with the same speed in all directions independently of its inhomogeneous force-stroke ratio. The output values calculated by the factor are denoted in Table 20 and visualized in Figure 51.

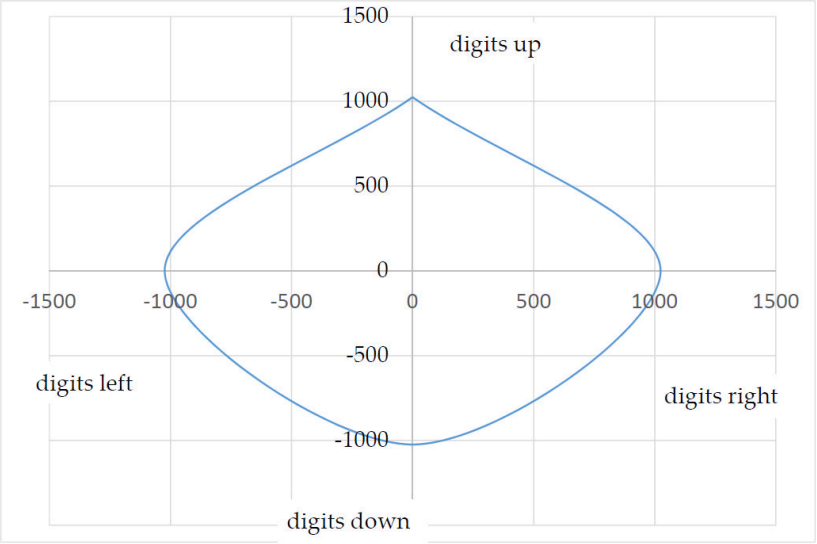

Figure 51: Output data curve

4.3.7 Software

The software is divided into two separate processes. To adapt the SGD to the user (see Figure 52), the teach-in-button need to be pressed. The microcontroller then saves the achieved maximum values for every direction of the previously defined rest values. It also saves possible value combinations to be used later for the plausibility check. After definition of all indicated values, the factors are calculated which are used to generate homogeneous output signals (see Figure 51) from the inhomogeneous input signals (see Figure 50). If the rest values are not in the previously defined range (theoretic rest value +- 100 digits) then an error is generated. This value-window serves to catch the production tolerances.

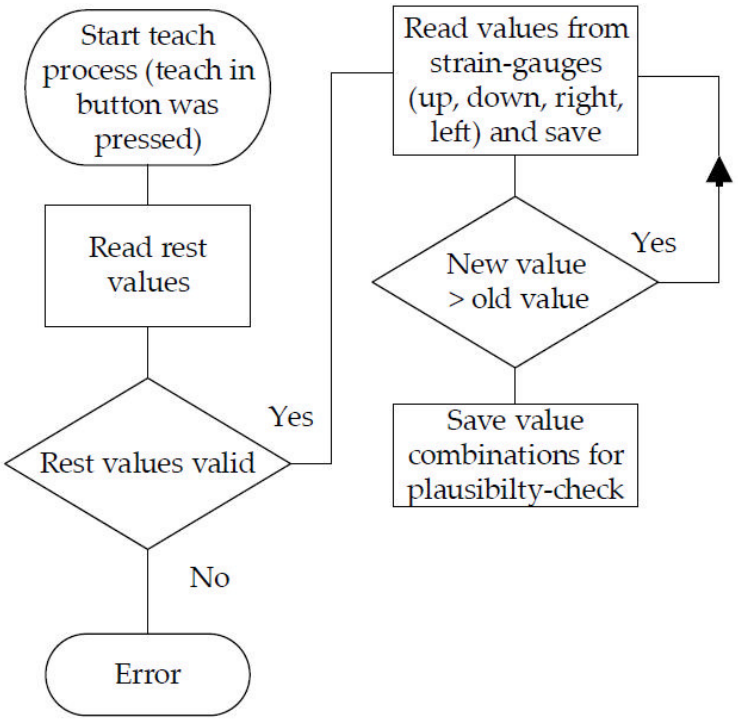

Figure 52: Schematic sensor software teach-in process

During normal use (see Figure 53), first the data of AD 7811 is input via SPI. In the permanent plausibility check, the relevant opposite strain-gauges are summarized as a value pair. These value pairs must match with the value paires saved in the teach-in-process. This enables to catch the major part of all possible errors. In case of error, the microcontroller sends neutral values to the connected system to prevent an action. Furthermore, a separate error message can be sent via an I/O pin.

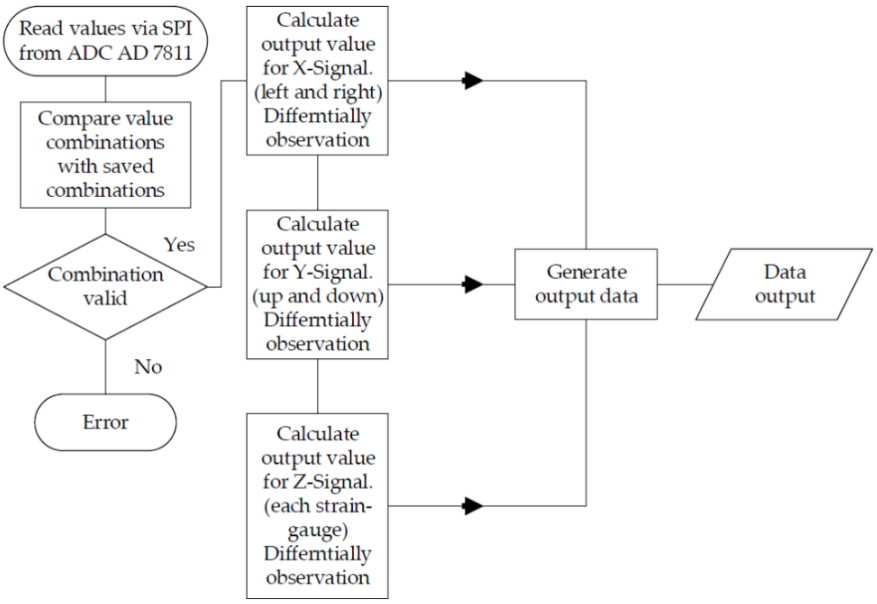

Figure 53: Schematic sensor software - normal use

4.3.8 Hardware

On the circuit board (see Figure 46, Pos. 4) locate 4 differential amplifiers, a 10 bit ADC as well as the voltage stabilizer. The amplification of the differential amplifier is firmly set with an external resistance. The measured output signals (differential voltages) (see Figure 54) of the 4 strain-gauges are amplified with the differential amplifiers AD 623 [43]. The so won analog voltage values are then input with an ADC AD 7811 [2] and converted into a SPI (slave) bus signal. A microcontroller SPI (master) receives the data and generates the desired output signals from it for the connected hardware. The microcontroller also handles different input and output signals which send e.g. emergency signals to an EPW if the SGD fails.

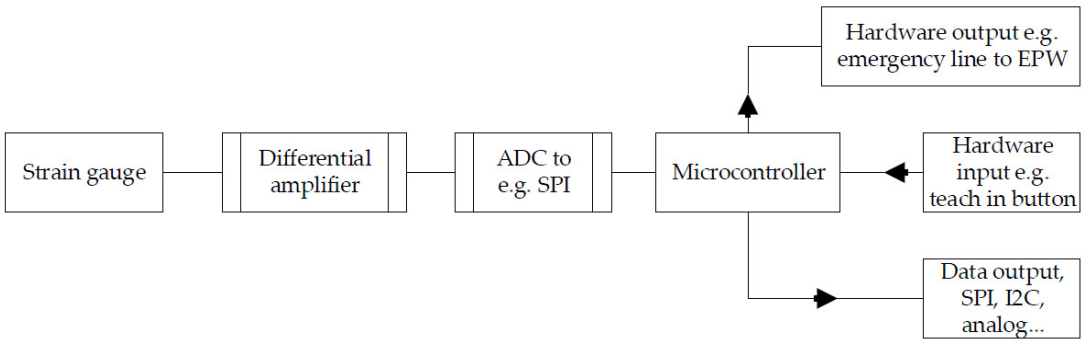

Figure 54: Schematic sensor hardware

4.3.9 Novelties against known systems

The SGD does not fulfill the selection criterion of a complete digital execution since analog signals are generated. To support the criteria of alternative construction and purposes of use, individual items will be listed below which demonstrate in how far a novelty and/or an alternative is justified in comparison with known systems.

- Concrete construction of sensor as flat disk: Only through the flat construction of the SGD and through the related input options, the person with spastic illnesses can handle also safety-relevant systems. A violation by spasms is also prevented.
- Construction and shaping of motion carrier from CFRP: The shaping and the selected material for the motion carrier favored a sufficient bending ability in spite of the used material thickness. Simultaneously, the motion carrier must be stable to resist overloads and to thus avoid an irreversible deformation or damage of the carrier material.
- Ability of motion carrier after deflection to return to an accurate rest position. Only the combination of material quality, material thickness and shaping allow these extraordinary capabilities. In all publications, no execution feature could be found which described the execution developed here, not even in part.
- Algorithm for an individual adaptation of the sensor to the user with changing illness pattern: This process can be initiated by the user himself anytime, which offloads the health care system since no experts are needed.
- Differential plausibility check of the strain-gauge values to increase the safety of use: Due to the permanent tests of the data in operation, the safety of use is increased considerably. A use in highly sensible areas will therefore be justified.
- Use of construction-based natural “force feedback“ effect: This effect informs the user anytime of the strength of deflection by a feedback. Since

the SGD is deflected in a nearly unperceivable angle, the pressure receptors of the skin acknowledge an increasing feeling of pressure in proportion to the increasing applied force.

4.3.10 Result and estimation, SG approach

The SGD described here is in a fully functioning prototype stage (see Figure 55).

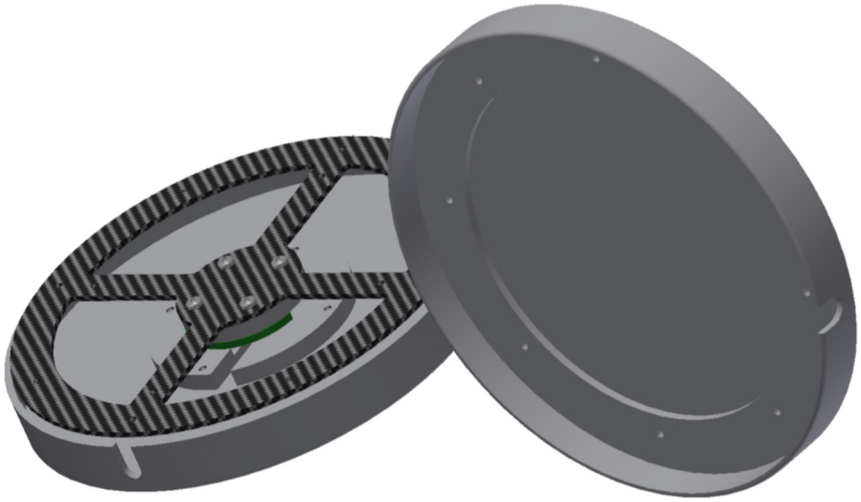

Figure 55: Drawing SGD prototype final version with open housing

The primary problem of this development was the execution of the motion carrier. First, the motion carrier was made of aluminum and steel. In spite of the special compensation of SG to aluminum and/or steel, the past test series in a climate chamber were not satisfying. The maximum deviation of aluminum amounted to +- 8 digits and of steel +- 5 digits (measured with a 10 bit ADC). In the climate test, the SGD in a climate chamber was exposed to a temperature range from -30 °C to +80 °C. In the first test phase (see Table 21) the SGD was not deflected. The total test period was 8 hours. The temperature dependent maximum deviation of the rest values of +- 1 digit could only be reached with a motion carrier made of CFRP.

Table 21: CFRP motion carrier, rest values in climate chamber

Temp. (° Celsius)	Rest values forward	Rest values backward	Rest values right	Rest values left
-30	509	499	502	504
-20	509	499	502	504
-10	510	499	502	504
0	510	499	502	504
10	510	499	502	504
20	510	499	502	504
30	510	499	502	504
40	510	499	502	504
60	511	500	502	504
70	511	500	502	505
80	510	500	502	505

In a second test (see Table 22) a rest was deflected with a clamp device (test period 8 hours). The deviations also ranged within max. +- 1 digit (measured with a 10 bit ADC).

Table 22: Fixed deflection of CFRP SGD in forward and right direction

Temp. (° Celsius)	Rest values forward	Rest values backward	Rest values right	Rest values left
-30	829	182	769	231
-20	829	182	769	231
-10	829	182	770	231
0	829	182	770	231
10	829	182	770	231
20	829	182	770	231
30	829	183	770	231
40	829	183	770	231
60	829	183	770	231
70	830	183	770	231
80	829	183	771	231

Another test series investigated the reset accuracy (see Table 23) of the motion carrier in every direction after load of SGD with different forces.

Table 23: Static position after load of CFRP (temperature 21 °C)

Load (N)	Rest values forward	Rest values backward	Rest values right	Rest values left
Rest values	510	499	502	504
forward 25	510	499	502	504
forward 100	510	499	502	504
forward 500	511	499	502	504
forward 1400	511	499	502	504
backward 25	510	499	502	504
backward 100	510	499	502	504
backward 500	509	498	502	504
backward 1400	509	498	502	504
right 25	510	499	502	504
right 100	510	499	502	504
right 500	510	499	503	503
right 1400	510	499	503	503
left 25	510	499	502	504
left 100	510	499	502	505
left 500	510	499	502	505
left 1400	510	499	502	505

The load test showed that the rest values of the motion carrier after different loads deviated by max. +- 1 digit. The aluminum variant deviated by +- 6 digits and the steel variant by +- 4 digits. Since deviations also can occur in common caused by temperature impacts as well as after load, a deviation of max. +- 2 digits by external influences must be taken into account. To counteract this problem, the measuring values of the SG must be deviated from the rest values by min. +- 4 digits, before the subsequent system executes an action. Initial tests under laboratory conditions were passed successfully. The sensor was used as mouse-substitute and to operate an EPW [44]. If a patient with physical disease still possesses any remaining function (hand, finger, foot, head, shoulder [30] etc.) it should be possible to use this SGD. If the illness pattern changes then the SGD can be immediately (without service personnel) be adapted to the new force and motion spectrum of the user. This learning process lasts max. 10 s. Through the own weight of the upper housing cover, the SGD may enter a resonance

vibration if a defined oscillation frequency impacts the sensor. In a laboratory test, the resonance frequency amounted to approx. 120 Hz. This can “build-up” the system. This special case which can hardly be expected under normal conditions, can be found also with off-the-shelf joysticks. To take preliminary actions to prevent this unlikely case, an addition cross-linked silicone rubber can be enclosed below the CFRP carrier (version 2) which acts as vibration damper and which catches this special case.

In summary, this sensor represents a new input option, in particular for spastics. Possible hurts or unintended initiating of commands by sudden spastic attacks are avoided to a far reaching extent. In combination with other actual developments described in the introduction, the man-machine interface (MMI) for this illness can be improved. Because of the simple construction of the SGD, the production costs will be moderate.

4.4 Prototyping, SG approach version 2

Since the constructive development of SG version 1 was conceived for spastic illnesses, the construction of SG version 2 was executed less specifically. Since the user prefers a traditional execution of a joystick with sensor axis, without having to spend a lot of time to get familiar with it, the SG version 2 concept was designed accordingly. The SG basic concept was kept, that’s why the presentation was compressed accordingly. SG version 2 shall be used with patients after successful verification by the actual medical product law for test series of patients. For this reason, a small series of 50 units will be produced within the scope of this work to detect possible problems in the production process. In this stage, the problems in production can be eliminated by constructive changes without major development costs.

4.4.1 Functionality and construction

The explosion drawing (see Figure 56 (a)) shows SG sensor, version 2. Synergy effects between both SG versions were utilized so that the circuit board was used in both versions. To establish a force coupling between the user and

the CFRP motion carrier, a hexagonal bolt is centrally screwed with a M3 inner thread. In the bottom of the PVC housing locate screwed-in thread inserts made of metal to guarantee a permanent fixing option for the sensor. The spacer between the motion carrier and the circuit board has no further function. The real sensor unit (see Figure 56 (b)) is screwed in the housing with four M2 stainless steel screws. The top cover of the sensor was provided with a grid to derive extreme force impacts via the housing. In the bottom of the housing locates a longitudinally milled hole to take-up the connection cable. The SGs are attached to the CFRP motion carrier from the bottom using an adhesive (see Figure 57) and soldered later onto the circuit board below. In a future production process, the soldering could be omitted by inserting gold-plated spring contacts between the circuit board and the SG.

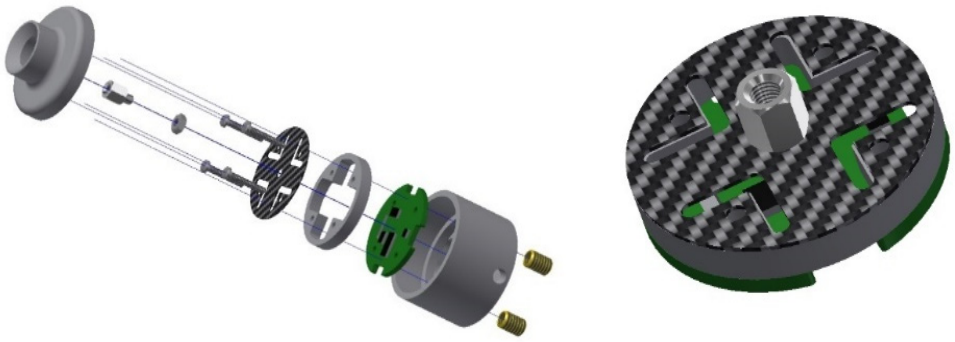

(a) *(b)*

Figure 56: (a) Exploded view SG version 2 and (b) sensor unit SG version 2

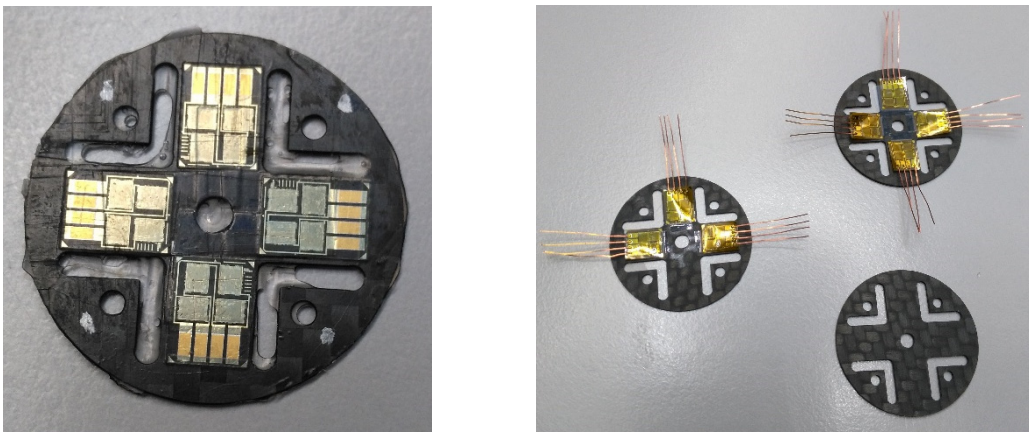

Figure 57: Movement carrier with attached strain-gauges

The total data processing was adopted without change and therefore all functions were kept.

4.4.2 Small series production, SG version 2

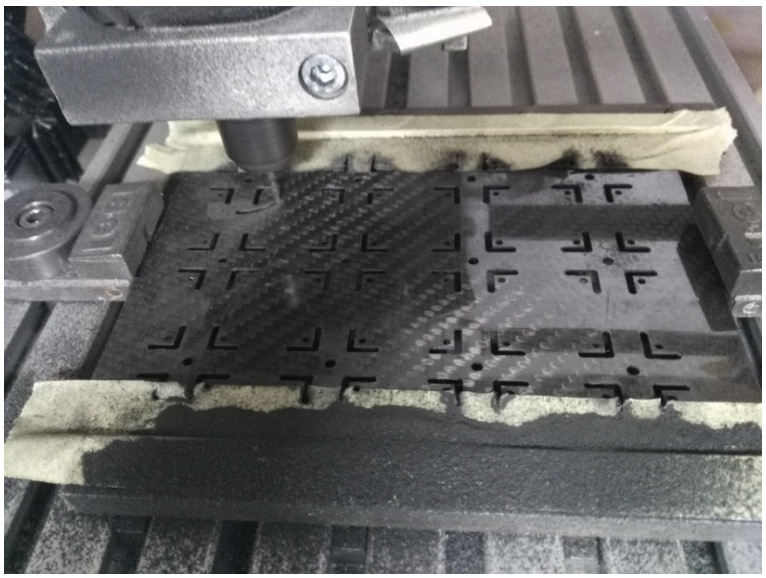

Figure 58: CNC milling

A milling in the air (see Figure 58) generates harmful dust. Helpful here would be an aspirator with a filter property of H700. However, to bind the dust particles in their entirety, a water bath (see Figure 59) was used. An surplus splash water formation could be avoided by the addition of tensides.

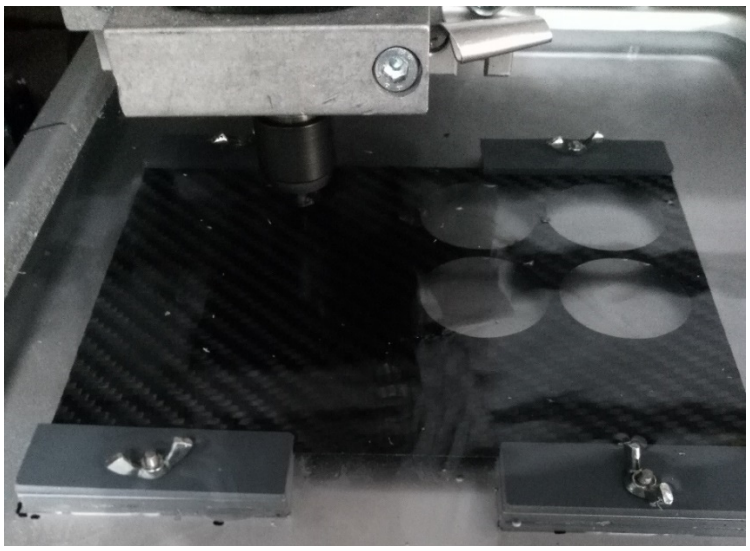

Figure 59: CNC milling in a water bath

After having soldered the motion carrier to the circuit boards (see Figure 60), they are screwed in the bottom of the housing.

Figure 60: Sensor units and covers prior to final assembly

Finally, a one-time calibration process is executed to determine the real neutral values of every sensor. These values are saved permanently and compared with the actual rest values after restart of the system. A deviation by more than 3 digits is detected as error. This procedure also detects a wrong handling of the user.

Figure 61: Finally assembled sensor of SG version 2

In the small serial production (see Figure 61) no demand for a constructive change of the prototype could be stated. All phases of the production process could be automated without problems.

4.5 Sensor test

To measure the quality and the possibility of sensor control, a simple but effective test was developed within the scope of this research work. The user has to follow a course (see Figure 62) with the EPW or draw a mouse cursor on the screen according to a template.

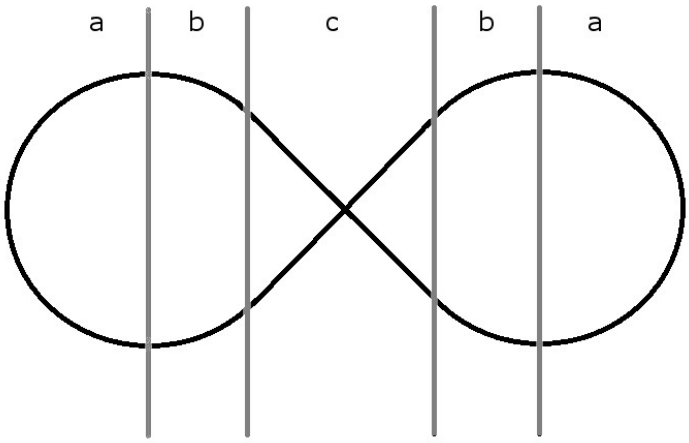

Figure 62: Test course-8

The source contains 3 areas with different requirements of input motion to be executed. While in area (a) an even radius must be followed, the curve radius changed in area (b) until it ends in a straight line, area (c). This requirement contains all variants of a possible change of direction. In another degree of difficulty, the course can also be followed backward. When the test is executed, an acceleration sensor and a video camera is fixed to the EPW. An optimally used sensor is characterized by the fact, that only very low sudden direction or velocity changes are recorded. The evaluated images of the camera show the accuracy by which the predefined lines were followed. Using a digital input device or the voice control will not make it possible to follow the predefined lines of the course with an even velocity. For example, a step-type driving distance would result at least in the areas (a) and (b) since the radius would be permanently corrected. An even motion is only possible with a proportionally working sensor.

4.6 Development of questionnaire

Since the use of the sensors developed in this thesis differs essentially from the use of traditional sensors of joystick-type, the resulting specific aspects should be further investigated. For this reason, a questionnaire was developed the questions of which are primarily dedicated to the usability and acceptance of the sensor. The focal points were the low deflection and the learning time to become familiar with the handling of the sensor. The questionnaire (refer to Chapter 7.3) first explains the user why the data is collected and how it supports the development and production process. The anonymous storage of the data and the promise that the data is not revealed to third parties, is secured, of course. The storage of the serial number would have been very helpful to detect possible errors in the production series but this would have been violated the anonymity. Because of the complexity of software of the optical sensor, the sensor could not be equipped with a bus protocol for traditional EPWs within the scope of this thesis. Also the construction of the housing must be left to a later thesis. For this reason, the SG variants were installed in the test tasks. Since the difference between the optical version and SG version 2 is not perceivable by the probands within the investigated application area, the results can also be projected to the optical variant. Only, after further advantages of the optical version have become known (high reproducible resolution, EMI and RFI resistant, etc.), e.g. in geophysical or military use, a differentiated investigation would be necessary.

3 probands worked with SG version 1 (SGD) and 13 probands with SG version 2. This distribution resulted from the available probands who did not get along with the hitherto input device or only with difficulties[1] (questions 4 and 5 of questionnaire). The questions on the same questionnaire allowed to be used for both SG variants. As described in chapter 1.2, the disease patterns are not only helpful to determine the frequency of their occurrence but also to find the gender-specific differences. This explains why only 5 of 15 probands are female. The Swiss Paraplegics Association (SPV Nottwil) states in a study [45] that the share of male paraplegics in the population increases significantly. The ratio is 32% to

[1] Exception proband 13. This proband had no problem with his input device.

68%. This study assumed that male persons generally live more dangerously or are more willing to take on risks. This risk does not exclusively refer to sportive risks, but also on the awareness of risks in the traffic on the road. This assumption is underlined by the fact that the gender distribution with non-traumatic paraplegics is balanced [46]. In this group of persons, however, it must be distinguished between para- and quadriplegics. While it is possible for paraplegics to further use their upper extremities after physical injury, this is not possible for quadriplegics. Further specialties such as artificial respiration, will not be handled since these factors are of no importance for this investigation. Special forms of plegie, e.g. hemiplegia or die hemiparesis, will be ignored similar to paraplegia since the necessity of a special sensor is missing [47]. In how far the general conversion of the involved people from the standardized joystick to the developed new joystick is target-oriented must be investigated in further tests. Below, the questions are listed with short comments, unless the question is self-explanatory.

*1. Would you please indicate your **gender and age**?*
□ *female* □ *male* *…….. age*

It must be assumed that the acceptance runs counter-proportional to the age. Young people see the sensor more as a toy. So, the habituation period will be shorter. The gender shall show in how far special actions are needed to get a better gender-specific access.

2. Which form of injury or illness do you suffer from?
……..

The category of illness will show for which disease patterns the sensor suits best. The severity of the illness should also be recorded although it will be rather subjective and hard to evaluate. It is assumed that the acceptance will increase with increasing illness symptoms while the selection of options will decrease.

*3. When has the **new** input device been installed?*
……. month, ……. year

This question about the installation time point shall clarify in how far the prevailing external temperature influences the acceptance of the sensor. Since the user can use the sensor also in external temperatures below 15 °C due to the learning function (with reference to a muscle illness), the acceptance can be influenced positively.

4. What do you control with your input device?
□ *Wheel chair*
□ *Environment*
□ *PC*
□ ……..

From this disease pattern, the illness stage can be derived. If the user does not control an EPW it must be assumed that the illness is in its final stage and that the option to use an EPW is not given anymore. In general, the recording of the application options shall reveal the support to be provided to access hitherto not yet utilized areas.

*5. Which input device have you used **formerly**?*
□ *None, this is the first one (go on with question 6)*
□ ……..

If formerly a standard joystick was used then it must be assumed that the familiarization period will be short (max. 2 weeks). If it is possible to collect data of first aid within the scope of this thesis, then a comparison will deliver important recognitions. The result would show in how far it would be reasonable to give a direct first aid via this sensor even if a standard input device would still be useable.

*6. Why have you received a **new input device**?*
□ ……..

The responses will deliver aspects of disease patterns and disease stage.

*7. Kindly comment your **first impression**.*

□ ……..

The first subjective impression shall reveal in how far non-problematic changes (modification of operating element, housing size, color, etc.) could be made to optimize the first impression.

*8. How long have you taken for a **safe use**?*

□ ……. *hour(s)*

□ ……. *day(s)*

□ ……. *weeks(s)*

□ ……. ……..

□ *I still cannot handle it (kindly give a short explanation in question 15)*

It could be possible that prior to the real use of the sensor, computer-aided learning programs would facilitate the handling.

*9. How important for you is the "**learning capability**" of the input device (adaptation to force and motion ability)?*

□ *very important*

□ *important*

□ *unimportant*

□ *irrelevant*

□ *don't know*

It must be assumed that the learning capability of the sensor will be of major importance only with progressing illness. Disease patterns with constant symptoms must only be adapted once to the user prior to its use; thereafter this function will be forgotten.

*10. How often do you **adapt** your input device to your needs?*

□ *daily*

□ *weekly*

□ *monthly*
□ *not at all*
□ *don't know*

Also this question will be answered depending on the disease pattern. The contraction capability of the muscles in case of muscle illnesses changes by a large number of factors. Therefore, the adaptation must be made in short intervals.

*11. Would you prefer a **larger motion stroke** for your input device? (This is the necessary distance from the initiation to the execution of an action)*
□ *yes*
□ *no*
□ *don't know*

Main sensor axes of different constructions (which can be exchanged on site without experts) can modify the perceived motion stroke. If e.g. a tension spring is integrated in the main sensor axis then a stroke of up to 15 mm results in every direction of motion. The stroke is reduced by a rigid execution whereby also the desired stroke from question 12 could be realized.

*12. Would you prefer a still **smaller stroke** for your input device? (This is the necessary distance from the initiation to the execution of an action)*
□ *yes*
□ *no*
□ *don't know*

Refer to question 11

*13. How do you rate the **force** to handle your input device?*
□ *convenient to me*
□ *is not convenient to me (kindly give a short explanation in question 15 or 16)*
□ *don't know*

If the user is satisfied with the force to be applied then the thickness of the motion carrier must be varied. The use of different material thicknesses results in force-windows which can cover all force options when they overlap.

*14. For which **period of time** can you use the input device **without fatigue**?*
□ *……. minute(s)*
□ *……. hour(s)*
□ *all the day*

Short periods of time can inform in how far the use of the relevant body part is not optimally positioned. If the shorter use is explained by sensor-related deficits then the reasons will probably be reflected in the response to question 16.

*15. How do you think can the **habituation time** be optimized?*
□ *no optimization required*
□ *don't know*
I have the following idea:
□ ……..

*16. How do you think can the **input device** be optimized?*
□ *no optimization required*
□ *don't know*
I have the following idea:
□ ……..

4.6.1 Evaluation of questionnaire

Within the scope of this thesis, 15 test positions and with it 15 questionnaires could be distributed. The age and gender can be taken from Figure 63. In the graph, the male probands are marked in blue and female probands are marked in red. As described in chapter 4.6, the distribution of gender in the test series reflects the real share of handicapped persons of the population.

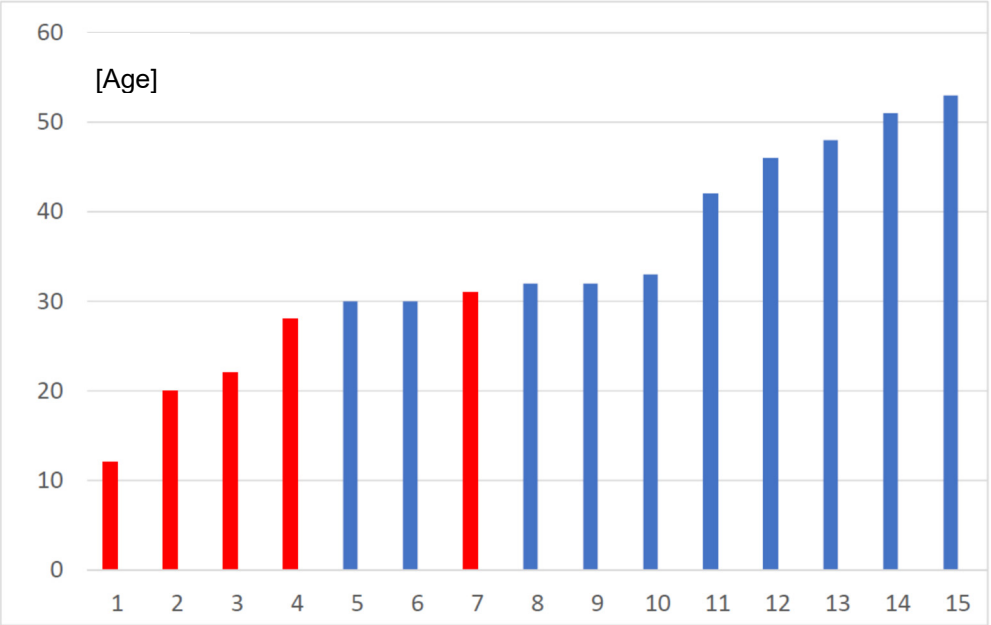

Figure 63: Age and gender of probands

Since, in particular, muscle illnesses develop progressively, the use of support becomes necessary only in a later stage of the illness and with it in an older age. The distribution of disease patterns in the test series can be taken from Table 24.

Table 24: Probands of test series

Prob.nr.	Age	Sex	Input Device	Disease
1	12	female	SG ver.2	Plegie
2	20	female	SG ver.2	Muscle
3	22	female	SG ver.2	Muscle
4	28	female	SG ver.1	Spastic
5	30	male	SG ver.2	Muscle
6	30	male	SG ver.2	Muscle
7	31	female	SG ver.2	Muscle
8	32	male	SG ver.2	Muscle
9	32	male	SG ver.1	Spastic
10	33	male	SG ver.2	Muscle
11	42	male	SG ver.1	Spastic
12	46	male	SG ver.2	Muscle
13	48	male	SG ver.2	Plegie
14	51	male	SG ver.2	Muscle
15	53	male	SG ver.2	Plegie

Three groups of illness could be included in the test series (see Table 25).

Table 25: Grouping of illness patterns

Muscle illness	Spastics	Plegie
Dystrophy, atrophy, progressive	Initiated by birth trauma and congenital	quadriplegia by accidents
Number: 9	Number: 3	Number: 3

The learning capability of the sensors is of special interest for the group of muscle illnesses, since in most cases the illness develops progressively. Therefore, a repeated adaptation is required. In the two other groups, the sensor is adapted in the initial state and then only relearned if needed. A need may come up if the patient uses the same sensor in the EPW as well as in bed. The force and stroke ratio varies which makes a new adaptation reasonable, as described by the probands in the questionnaire. The sensors were installed in a period from December 2016 to June 2017. The application spectrum is shown in Table 26.

Table 26: Application spectrum of sensors

EPW	PC-control mouse (keyboard emulation by mouse click)	Ambient control (light, multimedia, heating, air condition etc.)
Probands: 1-15	Probands: 1-12, 15	Probands: 1, 3-6, 8-12, 15

From Table 26 no conclusion can be derived in how far the application areas depend on age or gender. In general, it can be said however, that the probands can be assigned to the computer-affine generation because of their average age, that's why the utilization of all options rather depends on the individual performance carriers. The readiness to take over the described supply cost differs very much. It must also be noted that the described application options were already

available in all cases but were handled with other input devices. A new supply within the scope of this thesis was not possible since the total supply process normally spans over 1.5 years.

The first impression was collected from the answers to question 7. All probands initially perceived the sensor as very sensitive. Probands in an advanced age perceived the sensor rather negatively while younger probands perceived the sensor as a positive aid. In all cases, the initial learning process was started with strong reluctance of the probands which explained the above mentioned sensitive perception. The question why this predefined force was used for learning revealed that the probands were uncertain about the outcome. Only after a certain period of time the probands realized that this learning process could be repeated as often as desired. The total outcome improved with the time which passed between the initial use and the filling of the questionnaire. For this reason, the first impression was asked immediately after and/or during first use of the sensor. The priority of use was interpreted by the probands in that a safe handling must go in line with a comfortable handling, where the comfortable handling was assigned priority 1.

The answers of the probands can be taken from Figure 64 below.

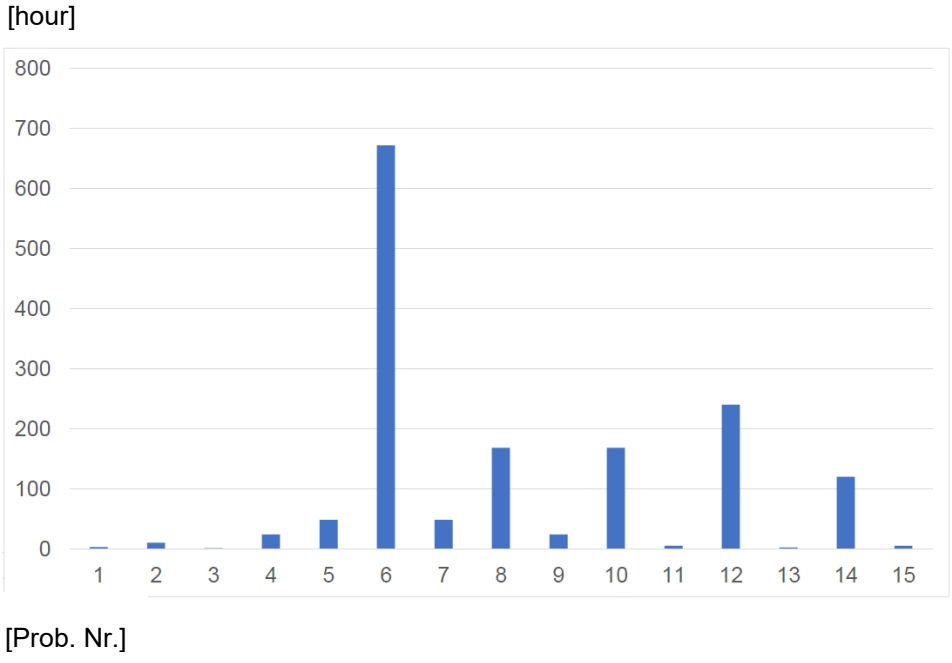

Figure 64: Habituation time

Not traceable is the answer of proband 6. Immediately after installation, he was able to control an EPW very accurately. He perceived that driving on a cobblestone pavement as difficult since the inertia of his hand generated a building-up effect. This effect could be eliminated by programming an acceleration ramp in the wheelchair electronics. The consequence, however, was a delayed response of the EPW to inputs. It is possible to program several driving programs independently on each other which could cause a different driving and contact response of the EPW. These programs could be selected by the user also when driving. In case of complex demands, only a combination of the described options would lead to an optimized result.

Probands 1, 4, 9, 11, 13 and 15 were not suffering from a muscle illness. Striking here is the low habituation time. This can be explained by the fact that working body parts with remaining functions are still available which enable a relatively fatigue-free use. To them belong primarily the head and the chin. Probands who suffer from a muscle illness, however, are normally in a progressive stage of the illness. Therefore, only very low forces are available to handle an input device. The extremities of persons with a plegie illness, however, were fixed and only allow a motion range which is needed to handle the device (e.g. fixing of the head). A person with a muscle illness in the above mentioned stage is not able anymore to master the inertia of the handling extremities. A fixing in this case is counterproductive since a fixing besides the desired motion is obstructive. In case of proband 6, the sensor was inserted in the operating table while the hands rested on the table. Ideally, a pad made of neoprene is used as support where the inertia of the hand is transferred to the table during the acceleration and slow-down.

If the habituation time is also considered under the aspect of different disease patterns then it can be stated that younger probands need less time to become familiar with the sensor. Probands without muscle illness generally need a very low habituation time. Question 9 deals with the learning capability of the sensor. Also here, the illness pattern could uniquely be used as rating factor (see Table 27).

Table 27: Rating of learning capability

Rating	Muscle illness	Spastic	Plegie
very important	2, 5-7, 10, 12, 14		
important	3, 8	4, 9	13, 15
unimportant			
irrelevant		11	
don't know			1

The group of probands with muscle illnesses thinks that the learning capability is as a very important instrument for the individual adaptation of the sensor while the other groups classifies this aspect "only" as important. Proband 1 is the youngest proband who used the sensor with relative gross motoric motions. She could not find any profit in the adaptation all the more since she used the learning function only once and immediately found the setting as appropriate. In principle, a quadriplegic can use a standard joystick with his chin, but it was difficult to find probands in this group who were willing to participate in the conversion test. The decisive argument in the persuasive phase was the low size of the sensor. Further advantages such as learning capability or low motion stroke were not recognized as advantages at that time. In the following discussions, it turned out that the indicated advantages were not imaginable at that time. The probands described the size of the sensor as very good since it was generally problematic to construct a standard joystick in this shape since a visual restriction (chin control) is missing. The simple fixing of the sensor (M4 threaded bushes inserted in the bottom (see Figure 56a)) facilitates the assembly at any location considerably.

The answers to question 10 (adaptation of sensor) are only evaluable with distinction. This is explained by the different disease patterns as well as by the frequency of the external temperature change. Probands who tested the sensor in the cold seasons of the year used the learning process rather seldom since they moved very seldom in the outdoor area. The learning process was also seldom used in the warm seasons of the year because the indoor and outdoor temperature was the same which made a new adaptation superfluous.

In spring, the learning process was used several times a day since the probands stayed in the outdoor area. Since the outdoor temperature at this time often fell below 15 °C, the related loss of force must be compensated by an adaptation process. In opposite case, the force increased which required a new learning process. A temperature-dependent automation of the learning process would be easy to execute, as described in details in Chapter 6.3. A graphic presentation of results was omitted since a clear statement could not be visualized, as already explained.

Questions 11 and 12 deals with the stroke of the sensor. It should be found out in how far a change of the stroke would be of advantage. It was stated that a smaller stroke would require a higher accuracy. This statement, however, is only valid in part since the applied force increases proportionally to the deflection. The sensor requires nearly the same force for deflection as a standardized joystick, if it is learned. Since a new supply has not been taken place in no case, the probands were working with standardized joysticks prior to the test. This generally required a habituation time anyway with respect to the stroke. Since this requirement was already recognized in the first test positions, it could be responded by a modification of the sensor axis (see Figure 65).

(a) *(b)*

Figure 65: (a) Sensor attachment with tension spring and (b) rigid

The rigid axis (see Figure 65 (b)) was replaced by a tension spring (see Figure 65 (a)). A motion conducts the applied force via the tension spring to the motion carrier. The exponentially applied force bends the tension spring which results in a higher stroke. This clearly facilitate the habituation phase and no probands desired a higher or lower stroke. 6 probands who were supplied with SG version 2, exchanged the sensor attachment within 15 days with the originally rigid sensor attachment. 2 probands with muscle illness kept the sensor with the tension spring since they were anyhow not able to apply such a high force to the sensor to bend the spring (statement of probands). One of the 2 last mentioned probands was of the opinion that a built-in tension spring would protect the sensor electronic. This assumption could be ascertained.

Question 13 deals with the applied force. Probands 7 and 10 were of the opinion that the needed force under certain conditions (uneven ground) would be too low. In general, however, a low force is essential since the force of the probands diminishes progressively. Also here, an automatic adaptation would be possible (refer to Chapter 6.3). All other probands were of the opinion that the force would be arbitrarily adaptable and could therefore be adapted to all needs.

The duration of fatigue-free use (question 14) was responded by the probands with additional notes. It was not of importance whether the statement referred to the driving with the EPW or to the working with a computer. The use would always be interrupted anyway which would generate a break for recovery. Proband 8 with a muscle illness indicated the lowest duration of use of 20 minutes. He further added that these 20 minutes was a longer drive with the wheelchair and that the driving could be continued after a short break[2]. Anyway, he achieved a longer use[3] than with the previous input device. Probands 11 and 13 left question 14 unanswered[4]. All other probands indicated that they could use the sensor the whole day. It must be assumed that a limited period of use for

[2] No written time information. A verbal question returned a rest period of 2-3 minutes

[3] No written time information. A verbal question returned a use time frame of 10-15 minutes with the previous input device.

[4] In a verbal question both probands indicated that they did not experience any fatigue and that they could continue working with the sensor at night in bed.

already mentioned reasons, can rather be assigned to the group of probands with muscle illness.

Question 15 referred to a possible optimization of the habituation phase. In summary, the probands desired a service engineer, at least on the first day of use. Not the sensor itself was concerned, but the programming of the wheelchair electronics. In many cases, a manual programming device is available for the users. Unfortunately, however, this programming cannot be done intuitively. But the actual development gives room to assume that in near future the R-NET of company Curtiss-Wright [48] will deliver the wheelchair electronic for all known electric wheelchair manufacturers so that once the setting is done it can be used for adaptation. These settings will then be loaded automatically after the sensor has been successfully recognized.

Probands 4 and 7 (question 16) would like to test different ball shapes of the axis attachment. Proband 7 with muscle illness described a warming attachment for the operating hand. These probands revealed that off-the-shelf handwarming devices are necessary but unfortunately inappropriate to use. Fan heaters need a lot of energy which strongly restricts the driving period of the EPW. Electric blankets would not be useable because of their material quality. This idea is retrieved in Chapter 6.3 where a possible execution is outlined.

14 of 15 probands desired to keep the new input device after the 8-week test period. Proband 13 (quadriplegic) principally assigned the new sensor a high potential but that it would not be exhaustible for him. This proband suffered from a complete injury of the spinal cord at cervical C4 level, parts of his shoulder muscles dispose of still working nerve cords. Therefore, the proband can handle a standard joystick without problem. The kind of injury, however, only allows gross motoric motions within the range of the hand since this motion is generated by the muscles of the shoulder. Another reason could be found in the fact that this proband uses the available input device neither to communicate with a computer nor with his environment. Since he disposes of functional hands [49] he can handle a touchpad, using an Internet access, and also controls his medical environment by hand. In case of a quadriplegia with remaining functionality in the shoul-

der muscles, the hands of the relevant person are broken multiple times in a chirurgic intervention and shaped in such a way that the grabbing and holding of assisting tools is facilitated. The proband was offered to test SG version 1 which will be installed in near future.

The z-axis in the new sensor was rated positively. While standardized joysticks use only the x- and y-axes, the installed new sensor also allows to use the z-axis. The options to use the sensor depend on the subsequent systems. To be able to use the function of the z-axis using a standard joystick, an additional switch or button need to be installed, which in turn prerequisites that another body part is available with sufficient remaining functions. This, in the opinion of the probands, would often be a handicap. A summarized comprehensive discussion can be found in Chapter 5.

5. Discussion of developments

5.1 Comparison of approaches

A direct comparison of the developed prototypes must be executed under different viewpoints. While the used technologies represent the first distinguishing criteria, the next criteria will be the purpose of use and the performance. Chapter 5.2 describes the advantages and disadvantages in the different application areas. The optical version generates and processes all measuring values fully digitally. The weighting of the projected shapes and the utilization of gray shades in the marginal area generate unique and reproducible coordinates while the SG versions change the resistance by deforming the motion carrier. This change of resistance results in a change of voltage which is converted in adequate voltage levels with the aid of differential amplifiers. Only thereafter, the measuring values are digitized via ADC, whereby both SG versions can be designated as analog systems. The measurement resolution of generated analog input parameters is theoretically infinitely high since the differential voltage of the SG changes steplessly. In fact, the described resolution is limited by the subsequent ADC. External influences such as temperature, air pressure and humidity modify the measuring

values of the SG versions with a constant deformation of the motion carrier. In the setting process, the temperature of the SG is compensated according to the carrier material, but in spite of this will never reach the reproduction accuracy of the optical variant, even not in part. In how far this production is needed, is discussed in Chapter 6.1. In medical engineering, the functionality of the optical sensor can be equaled to the functionality of SG version 2 since the accurate reproduction is of no major importance. Decisive is a high resolution which, however, can also be reached in SG versions using a suitable ADC (>= 10 bit). Only a high resolution enables a useful resolution of minimized strokes (refer to Chapter 4.2.9). In the optical sensor and in SG version 2, the motion carriers are made of CFRP. Since the thickness and the milling of both motion carriers are almost identical, also the applied forces are identical. It must be assumed that a user in context with the medical concept is not able to state a difference between these two versions. Both versions are especially suitable for users whose injury only allows the operating extremities to apply minor forces. Since all input forces can be individually adapted to the user, an application in other user groups is also thinkable.

SG version 1 considerably separates by design. This design was developed for users who suffer from a spastic injury. The construction was not designed for an as high sensitivity as possible but more for a high resistance against extreme load during spastics. In spite of this high load, the sensitivity was set in such a way that the forces of a healthy user must be sufficient to operate the sensor, free of fatigue. These forces can be compared with the forces of a spastic outside the spastic attacks. Since the principle design of construction of these three sensors aims at stability (difficult to damage) this shape should favor a safe handling under consideration of the different disease patterns. A standard joystick will make it impossible for a spastic to remove the cramped hand from the input device. But both, the optical and the SG version 2 could be able to resist these forces. Even in case of a complete damage of the sensor, the executed plausibility checks will prevent any safety-relevant handling. The velocity of the output signals in SG versions are clearly higher than in the optical variant. The reason is the generation process of the measuring data. To generate an optical measuring value (coordinates x, y, z) the total image of the image sensor must first be

transferred into the RAM of the microcontroller to search there for the size and position of projection. Then plausibility checks are executed before the coordinate are made available. To increase the processor speed to up to 180 fps, the AOI-procedure can be applied. The described process, however, implies a high computer load. The output signal speed of the SG version primarily depends on the ADC. A sample rate of 400 conversions per second can also be achieved with low-cost ADCs. The needed time for the following plausibility check does not delay the output. If, however, a use in the military or aerospace area is selected, then the only choice is the optical variant because of its interference stability against EMI and RFI.

In the geophysical area, the reproduction of the measuring values can be of major importance for deflection. The actually used systems are capacitive systems which only enable to record the relative changes but not the absolute values. A compensation of the optical variant by any external influence is not necessary.

5.2 Advantages and disadvantages

The advantages and disadvantages in comparison with off-the-shelf input devices primarily result from the application field in question. If a high resistance against interferences and/or a high reproducible resolution is needed, then the optical sensor should be selected. No other known input device is able to provide this performance spectrum, not even in part. The mechanical construction works without bearing in the conventional sense and therefore without moveable components, therefore no wear can be expected. Since the motion carrier is made of CFRP and since this material is predominantly used and tested in the aerospace industry, it can be assumed that the wear also here is very low. In the own test series (refer to Chapter 4.2.4) no fatigue of the CFRP-motion carrier could be stated. Because the z-axis is evaluated, an additional input device can be omitted which will extend the potential user group considerably. Especially in the area of severest disability, the remaining motoric of two body parts and their reasonable use is not self-explanatory. Because of the high spinal lesions, the major part of the quadriplegics [50] are just able to control the motion of their head. If an input

device is operated with the chin [51] then it is difficult to use a second input device (button) to initiate a mouse click. Especially the working with a PC will be clearly easier with a multi-axis input device.

The advantages of SG version 1 in the area of spastic illnesses have already been explained. Up to now, no input device is known which follows a similar approach. The low stroke can be seen as a disadvantage, at least in the initial or habituation phase. All known input devices use a clearly higher stroke which increases the technical solution. Since, however, 14 of 15 probands wanted to keep the installed new sensor after the test phase, it must be assumed that the stroke is only a temporary disadvantage.

Upon desire of the probands, the stroke could be improved by a modified sensor axis. The described disadvantage was not necessarily derived from the executed development steps but has been taken as necessary criterion at will. The reason can be found in the negative development of progressive muscle illnesses. The relevant users in their final phase of illness only have such a low force that a defined stroke of several centimeters is absolutely inacceptable. Healthy users will increase their working accuracy if they adapt the presented sensors to their individual needs. Simultaneously, the fatigue-free period of use can be extended. These aspects, however, should be assigned to further test jobs.

5.3 Probation of prototypes

The survey of the probands has proven that the used sensors represent a value-added to the previously installed input devices. In no case, a deterioration of the situation could be stated. Only in one case, the sensor was uninstalled after the test. The reasons were explained in Chapter 4.6.1. Installed new sensors should generally be equipped with a flexible axis to facilitate and shorten the habituation time. Since the full scope of performance of the optical- and of the SG version 2 sensor is only fully utilized in the last phase of the muscle illness of a user, further observations are still pending. No probands in the last illness phase could be found. It is understandable that this user group is physically instable

[52], that's why the supply should be made in a previous and more stable phase, if possible. It can be assumed that the low minimum force requirements favor a use of the presented sensor up to the last phase of the illness.

6. Summary

6.1 Conclusion

The objectives in the beginning of this research work could be realized completely. The initially favored acoustic research approach was not further discussed because of the unavoidable development of noise.

The primary problem of the executed developments was the reset feature of the motion carrier with its high demand for accuracy and stability. The solution of the problem using CFRP, was then transferred to the development of secondary SG sensors which increased the development speed tremendously. The advantages of the sensors could be documented by tests, accompanied by written surveys (questionnaires).

The inspirations and desired changes of the probands are executed still in the test phase, as far as this was possible. The high resolution of the optical sensors is needed only in some application areas. Therefore, image sensors with a lower resolution could be used. The needed processor time to determine the coordinates and in particular needed for the plausibility check was dramatically shortened. The production costs could be reduced considerably.

The individual adaptation to the users should be tested in other application areas to extend the fields of application. A use would also be thinkable in the area of consumer electronic where the problem of the low stroke in the introduction and habituation phase should be treated. Steven Jobs said: *„A lot of times, people don't know what they want until you show it to them.“* (25th of May 1998: Business Week). Optimistically, it can be assumed that traditional standard joysticks will be replaced by the here presented sensors in future.

6.2 Publications and award

Within the scope of this thesis, the Austrian patent was applied for to protect the optical sensor. After publication on 15th of March, 2017, the patent was granted on 15th of June, 2017, and registered under Patent No. 517 676 [53] (refer to Chapter 7.2.1). On 30th of August, 2016, a PCT registration was applied for at the European Patent Office in The Hague, under Reg.No. PCT/EP2016/070390. This claimed a temporary worldwide patent protection (refer to Chapter 7.2.2). The optical sensor was published, in addition, in the online Journal MDPI seated in Basel/Switzerland. These publications [54] can be found in Chapter 7.1.1. The same journal also published the SG version 1 [31] which can also be found in the Chapter 7.1.2 and online in the MDPI sensor journal. On the day of the last publication, the MDPI sensor journal reported an impact factor of 2.677. On 9th of March, 2017, the first price in the start-up idea competition 2017 was awarded. The application texts as well as some impressions of the award giving ceremony can be found in Chapter 7.4.

6.3 Forecast and further research options

To expand the application areas of the new sensors, the tests should be extended. This would first require to pass all test processes which are governed by the medical product law. This research work was executed at the Institute for Health Care Engineering at TU-Graz to which the European Testing Center of Medical Devices is connected. This enables executing the test on site. In the upfront, further developments are intended within the scope of two master theses (refer to Chapter 7.5). First task, the hardware and the circuit board layout will be developed. This must result in two variants at different quality levels. Second task, in parallel with the first task, the software must be optimized and adapted to the new microprocessor or signal processor. The development of housing can either be executed separately or assigned to the first development task.

If the optical sensor is used in highly sensitive areas, the two technologies can be combined. This research approach would most probably be executed without problems since the used motion carriers are equal in construction in both

variants. The SG movement carrier would then be provided with a projection unit in addition to the SG configuration, which compares the measured values of the SG with the measured values of the optically generated coordinates. The resulting redundancy of both technologies would in every respect be free of disturbance.

Inspired by the probands with muscle illnesses, a handwarming device could be targeted. Since the available force strongly degrades with progressing illness, the use of sensors in temperatures below 15 °C will not be possible anymore in spite of the low input forces. If the hand could be warmed up then this problem could at least be diminished. Known here are small handwarming fans. Since the warmed-up air rises too fast, too much energy is consumed to generate heat.

Pursuant to the statements of the probands, the use of these fans is disliked since the needed heat is only effective in a clearly smaller wheelchair range. Heating blankets are too inflexible and also create unintended control commands when they are jammed. A possibility would be to construct a hood on the forearm which, however, would need to be constructed individually which increases the costs. The problem could be solved by installing infrared panels [55]. Since the generated infrared rays exclusively warm-up solid and liquid bodies, the energy will be used efficiently. The arrangement of the infrared panels which are available in any size, could then be executed as needed by the individual user. Most easily, the infrared panel locates below the hand; lateral panels would also be thinkable.

The individual adaptation process of the presented sensors could be automated in a further development step. Not only should the available forces be taken into account here but also the ambient temperatures. Decreasing temperatures can increase the sensitivity of the sensor using a linear function. In general, it will be possible to calculate an average value of the maximum forces in every direction within a defined period of application time. The result will determine the factors or divisors for the adaptation of the sensitivity. Since the application time should at least be min. 10 minutes, also the temperature adaptation must be controlled to compensate the inertia of the system in sudden temperature changes.

7. Appendix

7.1 Publications MDPI sensor Journal

7.1.1 Publication of optical sensor

(15 pages)

sensors

MDPI

Article

A New, Adaptable, Optical High-Resolution 3-Axis Sensor

Niels Buchhold * and Christian Baumgartner *

Institute for Health Care Engineering, Graz University of Technology, Stremayrgasse 16, 8010 Graz, Austria
* Correspondence: 0603591990@t-online.de (N.B.); christian.baumgartner@tugraz.at (C.B.)

Academic Editor: Vittorio M.N. Passaro
Received: 13 December 2016; Accepted: 23 January 2017; Published: 27 January 2017

Abstract: This article presents a new optical, multi-functional, high-resolution 3-axis sensor which serves to navigate and can, for example, replace standard joysticks in medical devices such as electric wheelchairs, surgical robots or medical diagnosis devices. A light source, e.g., a laser diode, is affixed to a movable axis and projects a random geometric shape on an image sensor (CMOS or CCD). The downstream microcontroller's software identifies the geometric shape's center, distortion and size, and then calculates x, y, and z coordinates, which can be processed in attached devices. Depending on the image sensor in use (e.g., 6.41 megapixels), the 3-axis sensor features a resolution of 1544 digits from right to left and 1038 digits up and down. Through interpolation, these values rise by a factor of 100. A unique feature is the exact reproducibility (deflection to coordinates) and its precise ability to return to its neutral position. Moreover, optical signal processing provides a high level of protection against electromagnetic and radio frequency interference. The sensor is adaptive and adjustable to fit a user's range of motion (stroke and force). This recommendation aims to optimize sensor systems such as joysticks in medical devices in terms of safety, ease of use, and adaptability.

Keywords: tactile sensors; assistive technologies; power wheelchair; medical systems; robotic; joystick; optical sensor

1. Introduction

The use of sensors as an interface between people and machines is becoming increasingly important in our society. Joysticks can be operated practically in an intuitive manner and are found more and more often in a variety of controller systems as input devices. Areas of application such as medical technology require a high level of safety during use. Moreover, a wide spectrum is necessary for individual users. In particular, for people with physical disabilities such as quadriplegia, spasticity, and muscular dystrophy, using a sensor (joystick) is often a problem since the range of motion in terms of force and stroke undergoes constant changes as a result of such illnesses [1]. Depending on the specifications, off-the-shelf joysticks have a pre-determined accuracy (resolution); a certain amount of force is required to deflect it, and a certain stroke to overcome the necessary paths either by a fixed or very limited amount. Adapting the sensor to one individual is expensive and in some cases impossible when the user's range of motion and strength is affected by changes in temperature [2]. Standard joysticks are generally two-dimensional control systems for the x and y directions. In order to steer in the z direction, the controller is turned or an additional control element is required. Physically disabled people with spinal cord injury (SCI) [3] usually do not have the fine motor ability required to carry out such an action. A simple push along the z-axis is more likely to be possible. The sensor presented here can adapt to the desired strength and range of motion. Thus, there is no need for costly adjustments for individual users, thereby saving significant costs. There are currently 250,000 people living in the United States today with spinal injuries. A total of 47% of them are injured between C1 and C7 in the cervical spine area, rendering them quadriplegic. Each year, 11,000 people suffer a spinal injury [4,5].

In addition to this, there are muscular diseases such as muscular dystrophy. This disease affects between 1 in 3500 to 6000 male babies per year in the United States [6]. These diseases usually require a custom input device in order to enable users to operate electric wheelchairs or computers. However, the sensor can also be adapted to healthy users in the areas of diagnostic devices and surgical robotics, thus making it possible to achieve a higher level of user safety and precision while work is performed. If, for example, a powered wheelchair is used, new control systems such as eye tracking, voice control, and brain-computer interfaces tend to be problematic [7–11]. These types of input methods make it difficult to perform precise and complex control actions simultaneously. Voice controls can usually only process one command at a time and are unreliable in loud environments [12]. The exponential progression of the spring force and the very limited movement of the sensor axis generates a natural force feedback [13]. The user thus receives physical feedback pertaining to the deflection movement. The introduced sensor's potential areas of application can be expanded without limits. In addition to medical applications, fields such as the automotive, aeronautical, aerospace, marine, and military sectors in particular are conceivable here.

Optical methods for determining positions are well known and are described in the following selected patents and publications [14–17]. However, this paper introduces the prototype's hardware (see Figure 1) of a new optical, multi-functional, high-resolution 3-axis sensor and presents the sensor's novel features and components, and its methods of positioning. These include:

1. The specific construction of the projector unit
2. The minimal distance between projector unit and image sensor
3. The construction and formation of the movement carrier made of carbon fiber-reinforced polymer (CFRP)
4. The movement carrier's ability to return to its exact position of rest after deflection
5. Adherence to standard construction dimensions and the potential to establish the sensor in various areas of application
6. The algorithm to customize the device to changed clinical symptoms
7. The use of a software to increase frames per second (fps) to 150, which increases user safety and sensor responsiveness
8. Testing plausibility of projections to increase user safety
9. Using the natural force of feedback effect due to its construction
10. The increase in usable resolution by a factor of 100 through interpolation of the projected image using grey values and limits

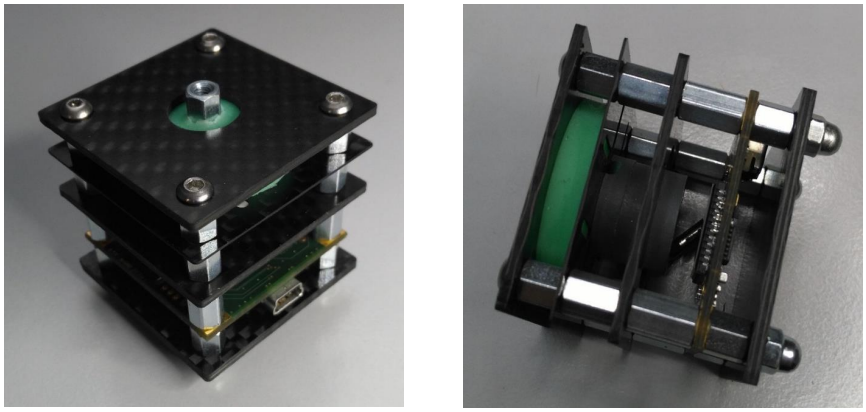

(**a**) (**b**)

Figure 1. The 3-axis sensor version 3 prototype V12.2 carbon fiber-reinforced polymer (CFRP), (**a**) front view (**b**) side view.

The applied optical approach substantially increases safety of use. Disruptive factors such as electromagnetic (EMI) and radio frequency interference (RFI) or differences in temperature have a marginal effect on the sensor if at all. Because the sensor can be manufactured very inexpensively, the consumer area is also an interesting option. With its very short axis movement of <1°, the operation and reaction time is substantially higher than that of off-the-shelf joysticks. The sensor is completely removable from its casing on the input side, making sterilization or disinfection very easy. The joystick also operates without a rubber boot. The sensor is, for the most part, free from wear and tear and can be placed in a waterproof casing.

2. Hardware of the 3-Axis Sensor

2.1. Basic Construction

The sensor consists of a force transducer 2 and a projection unit 3, which is firmly affixed to a movement carrier 4 (Figure 2). An image sensor is positioned underneath the projection unit at a set spacing. The angle of the movement carrier to the image sensor changes as a result of force applied to the force transducer. In doing so, the position of the projection on the image sensor shifts. Based on the position, size, and distortion of the projection, the current x, y, and z coordinates are calculated. This happens in relationship to the degree the angle changes and the pressure on the axis. In order to exchange the sensor for a commercially available joystick without further constructive problems, [18] standard designs have been adhered to during development. The 3-axis sensor casing measures (Length × Width × Height) 40 mm × 40 mm × 37 mm. Depending on the software configuration, the connection cables, which are located on the side or at the rear, can provide digital and/or analog data.

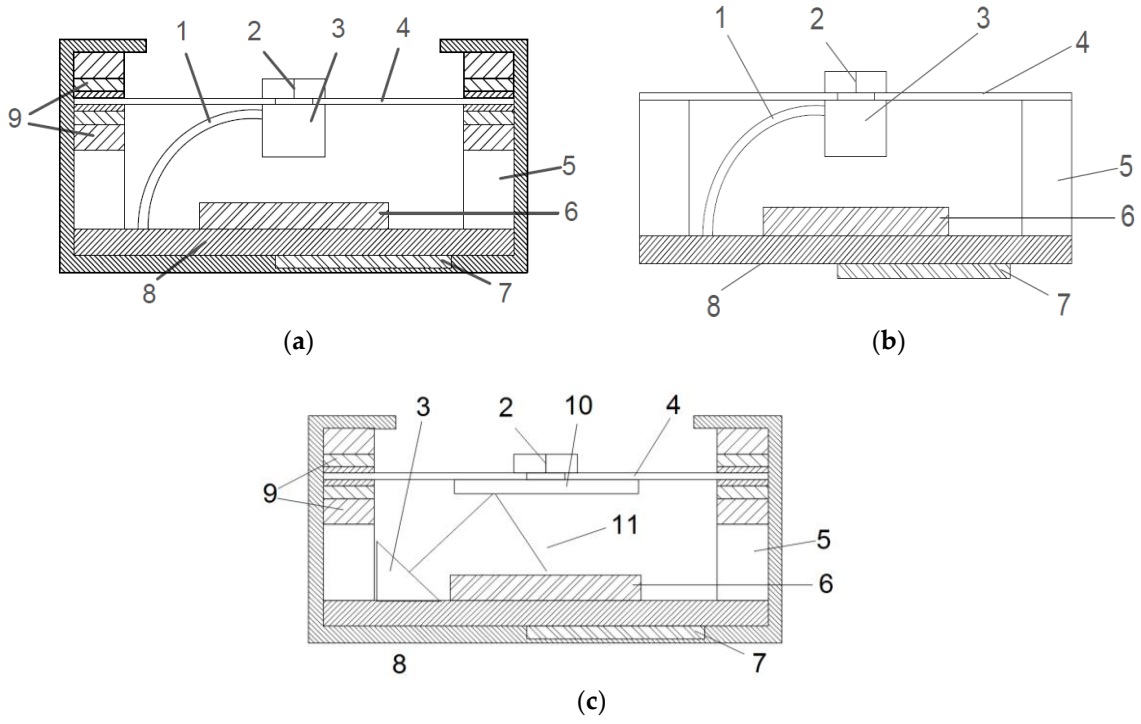

Figure 2. (**a**) The 3-axis sensor, version 1; (**b**) The 3-axis sensor, version 2; (**c**) The 3-axis sensor, version 4.

The 3-axis sensor consists of the following components:

1. power supply line, projection unit
2. force transducer
3. projection unit

4. movement carrier
5. spacer
6. image sensor
7. microcontroller
8. circuit board
9. polymer sandwich
10. mirror
11. laser beam

2.2. Projection Unit and Image Sensor

In its simplest construction, the projection unit consists of a laser diode with a downstream plano-convex lens [19]. This configuration can also be substituted by a collimator lens [19] and a shape template. The image sensor is positioned underneath the projection unit at a set spacing. Depending on the application and the image sensor that is used, frame rates up to 150 fps can be achieved. The sensor's maximum resolution depends on the image sensor type. For example, when using a 1/2 inch sensor with 1280 (horizontal) × 1024 (vertical) pixels, SXGA/1.3 MP [20], without further calculation, 1280/2 = 640 digits (horizontal) and 1024/2 = 512 digits (vertical) for each direction can be achieved. The structure of the projection unit is shown in Figure 3.

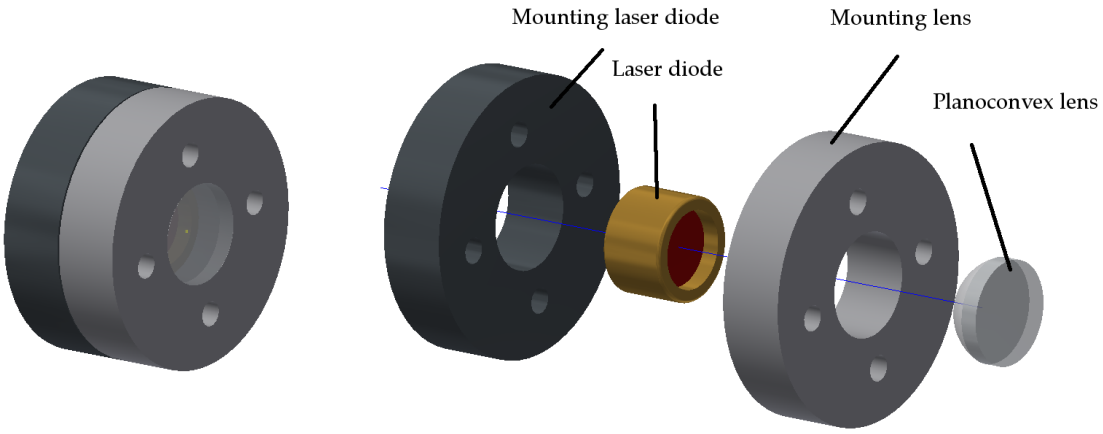

Figure 3. Left projection unit drawing; right projection unit exploded view drawing.

The projection unit has a diameter of 17 mm and a height of 10 mm. The relatively large diameter has no influence on the housing size. Since the movement carrier and the projection unit are to be connected to one another in a torsion-free manner, the supporting surface is necessary. With this structure, it is possible to place the focal point at a distance of 10 mm in front of the light output of the laser diode. When sub-pixels (gray tones) are included in the calculation and the resulting pool of light is interpolated, at least two decimal places can be added. The resolution is thus increased 100-fold with a resolution of 64,000 (H) und 51,200 (V) available in each direction. When using an off-the-shelf 18.1 MP sensor with 4912 (H) × 3684 (V) pixels [21], based on the calculation mentioned above, there is a resolution of 245.600 (H) × 184.200 (V) digits in each direction. These values should be sufficient even for highly sensitive measurements. In the consumer sector (personal computer joystick substitute), resolutions of 0.36 MP and frame rates of 30 fps are totally sufficient.

2.3. Different Versions

Depending on the purpose of use, the sensor can be operated in different variations:

Version 1 (see Figure 2a): The movement carrier is positioned in a polymer sandwich and consists of a rigid material such as steel or carbon fiber-reinforced polymer (CFRP). Through the force picked

up by the force transducer, the movement carrier tilts. The degree of tilt depends on the force being applied and the polymer's shore hardness (Figure 4).

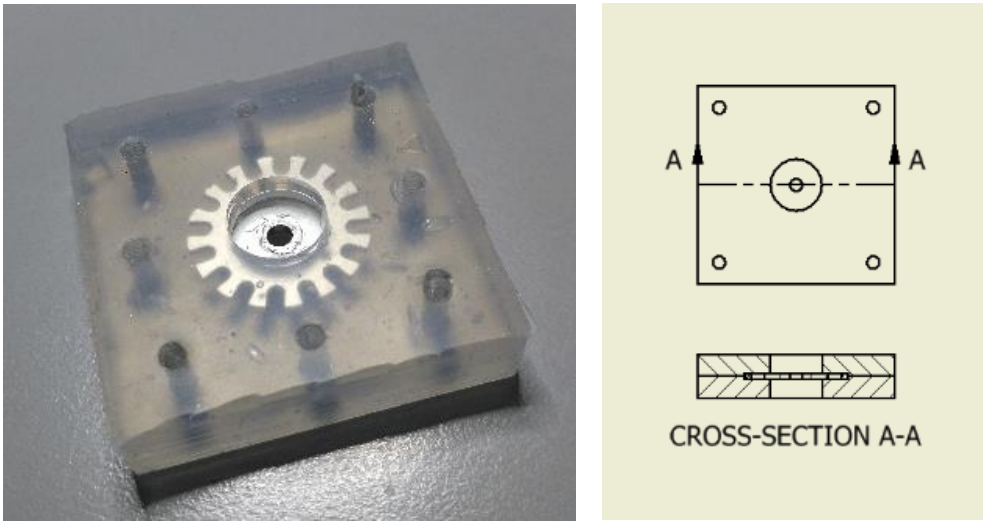

(**a**) (**b**)

Figure 4. (**a**) Polymer with encapsulated movement carrier, encapsulated version 1 (**b**) Polymer with movement carrier, cross-section, version 1.

Version 2 (see Figure 2b): The movement carrier is manufactured out of elastic material (e.g., CFRP in various strengths from 0.45 mm to 2 mm). The movement carrier is rigidly affixed to the casing and withstands bending and torsion. The cutout illustrated in Figure 5 is conducive to the movement carrier's deformation behavior.

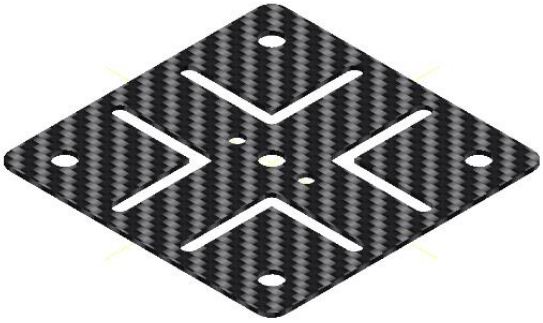

Figure 5. CFRP movement carrier, version 3.

Version 3: The same as Version 2 but includes an additional polymer cushion above the movement carrier.

Version 4 (see Figure 2c): The projection unit, which produces images, is replaced by a mirror. In order to generate a projection on the image sensor, the projection unit is affixed to the circuit board next to the image sensor and projects back over the mirror to the image sensor. The movement carrier's changed angle causes the projection to reposition according to the forces acting on the projection.

2.4. Movement Carrier

The movement carrier is selected depending on the application and the desired input force spectrum. In version 1, a rigid material such as steel (diameter > 1 mm) or CFRP (diameter > 1.5 mm) is integrated. In versions 2 and 3, flexible materials such as CFRP (0.3–1.1 mm) are used. The

materials used in version 2 and 3 should be characterized by excellent spring behavior, which is why CFRP is predestined for this application. The pivot point of the bearing is located at the height of the movement carrier. The distance between the movement carrier and the image sensor surface is 17 mm. For a diagonal of the image sensor of 1/2 inch (12.7 mm) and a resolution of 1.3 megapixels, the pixel size is 5.3 µm. The angular deviation of ~$17.86^\circ \times 10^{-6}$ can be calculated from the formula $x = r\ sin(\varphi)$, indicating the deflection of the laser beam by one pixel on the image sensor. The material and the shaping of the movement carrier were chosen such that after a deflection of the laser beam over the entire sensor surface, the resting position is found, with a drift of ±2 digits. Temperature influences of -30° to 80° Celsius produce an additional temperature drift of ±1 digit. Thus a maximum drift of ±3 digits is possible. The maximum angular writing of the laser beam then amounts to $\pm 53.58^\circ \times 10^{-6}$. In order to intercept this drift, a neutral window of ±5 digits is taken into account by the software. The output signals are not changed until the calculated coordinates are outside the described neutral window. The technical design consists of two layers of CFRP fabric which were installed in a unidirectional manner at $0^\circ/90^\circ$ to one another. The resin content is 35%. After 250,000 maximum deflections, the movement carrier's drift of ±2 digits did not change. Further tests will follow.

2.5. Polymer Sandwich

The movement carrier is positioned in a polymer sandwich in version 1. The movement carrier's spring is achieved through a particular arrangement of polymer layers. As a result, the Shore hardness increases (transition from soft to hard). Owing to the polymer arrangement (position 9) shown in Figure 2, the movement carrier is capable of absorbing a large spectrum of forces upon it (approximately 1 g to 5 kg). Due to the individual layer's varying degrees of Shore hardness, each becomes active under different forces. Once a layer's maximum compression is reached, the layer with the next degree of hardness becomes active and takes on the movement until it too reaches its maximum compression and so on.

3. Sensor Operations

3.1. Fundamentals

When forces act on the movement carrier's force transducer, the movement carrier changes its tilt and/or the spacing between it and the image sensor below. In doing so, the projection unit, which is firmly affixed to the movement carrier, generates an image of a filled circle on the image sensor (see Figure 6a for full view of a 1.3 MP image sensor without photo editing; Figure 6b shows a full view of the image sensor in binary mode).

(**a**) (**b**)

Figure 6. (**a**) Complete frame without image processing; (**b**) Complete frame with image processing to binary mode.

The movement carrier's restoring force occurs either through the arrangement of the polymer layers in version 1 or the resilience of the material used as in version 2 and version 3. Table 1 and Figure 7 show the deflection relative to the applied force. Different polymer arrangements and types are shown here as examples. Due to the fact that the measurement curves are identical in both directions, the measurement was carried out for one direction only. Force was applied by a 45-mm lever. In doing so, relatively soft polymer layers were used and a force up to 25 N was measured. "out" means that the light circuit has left the active sensor field.

Table 1. Selected measurements with different materials and versions.

Excerpt Test Series/ Force (N) 45-mm Lever	**0**	**0.05**	**0.1**	**0.2**	**0.5**	**1**	**2**	**3**	**5**	**10**	**20**	**25**
1 Mat.T13-44T1 V11.0	532	530	525	498	488	391	245	107	out	out	out	out
2 Mat.T13-44T1 V10.2	632	616	608	597	562	518	345	27	out	out	out	out
3 Mat.T11-55 V10.2	611	608	607	605	599	587	564	534	491	354	out	out
4 Mat.T13i-T1a V10.2	529	517	510	500	478	427	314	172	2	out	out	out
5 Mat.T1 V10.2	571	570	569	569	552	533	474	410	311	1	out	out
6 Mat.CFRP 055 V12.2	604	602	599	593	578	551	510	464	359	253	94	5

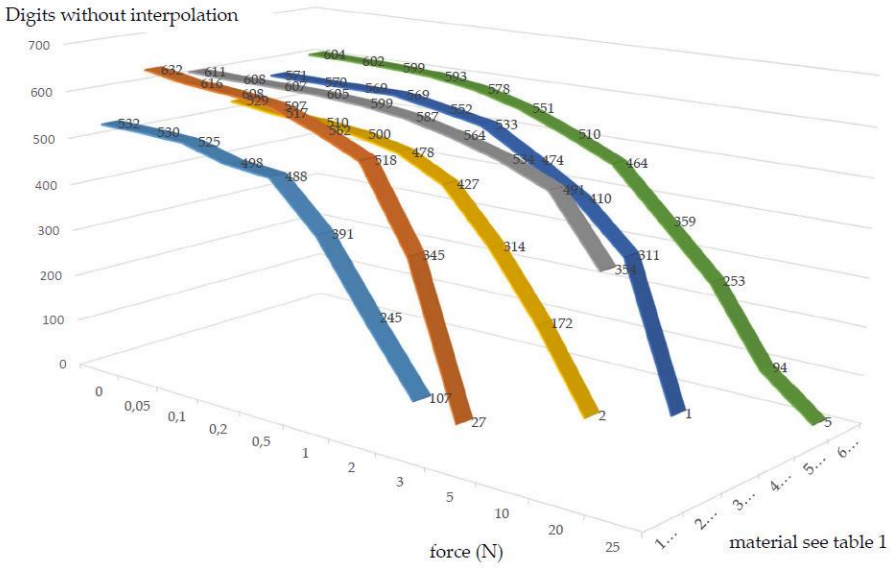

Figure 7. Visualized, measured values from Table 1.

3.2. Projection, Image Analysis and Data Output

3.2.1. Projection

As shown in Figure 8, geometric shapes of all kinds can be used for the projection (Figure 8a–c are shown in schematic form).

As an example, the simplest geometric shape (full circle; see Figure 8a on bottom left) was used for the prototype presented here. By using four dots (see Figure 8a top left) more than three axes can be measured. By measuring the four points with respect to each other as well as the measurement within the image sensor coordinate system, the change can be detected along any axis. Unfortunately, the measurement of the four points is very computation-intensive, which reduces the framerate of the prototype to about 12 fps. Faster processors can improve this. Figure 6 shows the resting state. As a result of the manufacturing allowances, it does not matter whether the projection of the circle is exactly in the middle of the image sensor or slightly off-center. The absolute zero position, or resting position, is set during calibration. The calibration process usually takes place only once after

production. This avoids higher production costs since the manufacturing allowances are relatively insignificant. Figure 8b shows the movement carrier in the x direction. A distorted ellipsis is produced due to the angle of the light. In addition, the diagonal deflections in the x and y directions are shown in Figure 8c.

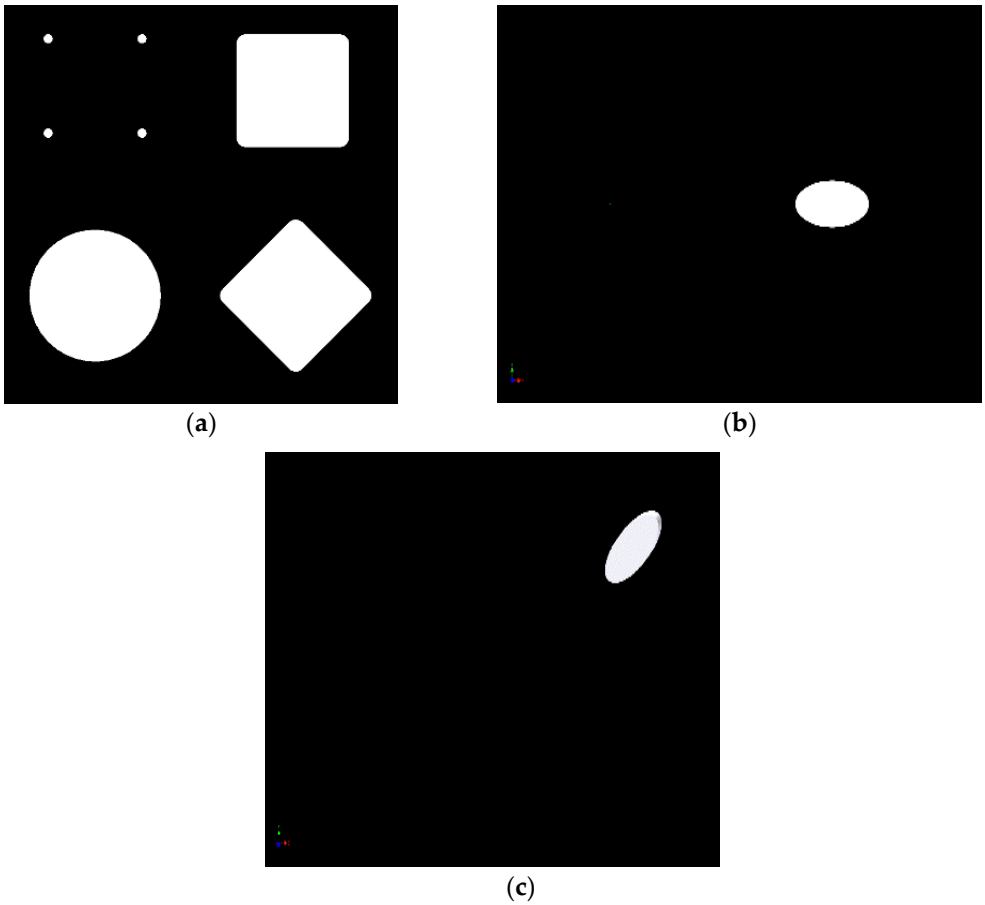

Figure 8. (**a**) Various projection images schematically; (**b**) Deflection of the circle (Figure 6b) on the x-axis schematically; (**c**) Deflection of the circle (Figure 6b) on the x- and y-axis schematically.

3.2.2. Image Analysis and Data Output

The image analysis software (Figure 9) first searches for the previously defined shape on the captured image. In order to reduce computation time, once the image is found, only the area of interest [22] around the object is examined. This approach increases the processing time substantially. If the image is no longer found in the scanned image area, the entire image is scanned again. The sub-pixels' brightness values are then analyzed and the center of the projection is calculated through interpolation. This increases the accuracy by two decimal places.

A button must be pressed in order to start the learning process for the individual adjustment. The microprocessor then records the maximum achieved coordinates in each direction. In addition, the distortion of the geometric figure is stored along with the maximum achieved coordinates. If it is a circle, the maximum x- and y-dimension of the figure is stored. In normal operation (Figure 9), the shape found is compared with the stored shapes and their coordinates. If the figure does not correspond to the expected figure, an error is generated to protect subsequent systems from malfunctions. The project focus is set in such a way that the focal point is below the image sensor's surface in a state of rest. As a result, a movement in the z direction removes the focal point from the image sensor or brings it closer. The projected circle thus changes in size depending on the force being

applied (Figure 10a, focusing without pressed *z*-axis). A pull of the *z*-axis decreases the size of the projection, while a push of the *z*-axis enlarges the projection (see Figure 10b).

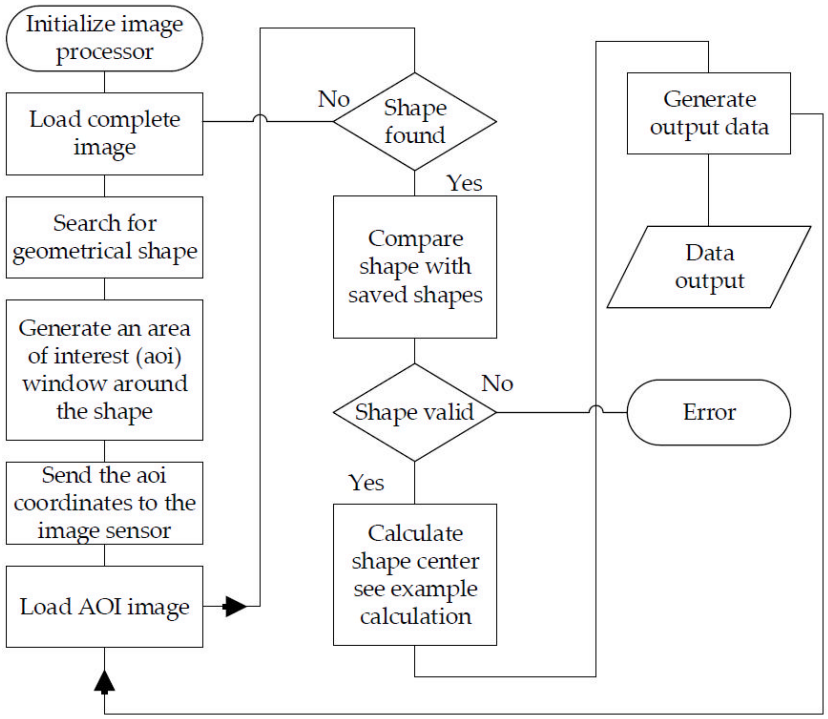

Figure 9. Schematic software procedure—normal use.

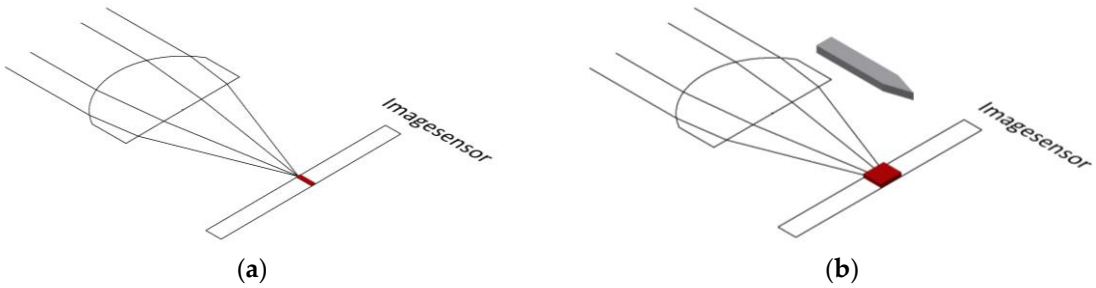

Figure 10. (**a**) Focusing without pressed *z*-axis; (**b**) Focusing with pressed *z*-axis.

The image analysis software detects either the smaller circle of light or the larger circle of light and then calculates the current *z*-axis coordinates (see Figure 11). These highly accurate coordinates are then passed on to the downstream system. While doing this, serial values or different bus protocols (CAN, SPI, I2C, analog voltage, etc. in the next step of development) can be generated.

Figure 11. Difference between neutral *z*-axis (**left**) and pressed *z*-axis (**right**).

3.3. Plausibility Check

The sensor should also be utilized in highly sensitive or safety-related areas. To do so, a plausibility check is performed. The projected shape is naturally distorted during the projection (Figure 8b,c). When the projected circle moves away from the middle of the image sensor, the circle becomes an ellipsis. Since an ellipsis has two focal points F1 and F2, the resulting spacing is calculated. The spacing of the focal points increases the further the movement carrier is moved. In order to identify the maximum allowable spacing between F1 and F2, the movement carrier is moved in each direction once with the maximum amount of force permitted. Ideally, it should be a circular movement with the maximum force permitted. This circular movement can be performed either manually or with a calibration device. During the calibration movement, the maximum distortions and their positions are extracted and saved permanently. All of the detected projections are compared to the previously saved images during normal operation. When a maximum position or a maximum distortion is exceeded, measures can be taken to protect the downstream system from malfunctions. Additionally, other special cases can be identified. In the event that the projection unit leaves its position of rest due to a hardware defect without being moved, the resulting projection would be distortion-free in another position. This is considered an error because it is not possible to detect a distortion-free projection at other coordinates such as the original position of rest. The plausibility check can be expanded depending on the performance of the image sensor and the microcontroller that are in use. In addition, motion patterns or speeds can be analyzed and checked for plausibility.

3.4. Individual Adjustment of the 3-Axis Sensor

Due to the various symptoms of individual medical conditions, different input forces and input lifts are required. Depending on the specifications, standard joysticks have a pre-determined accuracy (resolution), a certain amount of force is required to deflect it, and a certain stroke to overcome the necessary paths by a fixed amount. As described in the introduction, certain groups of physically disabled people are unable to use standardized joysticks. The issue has to do with this group of individuals' range of motion in terms of force and stroke. Moreover, the existing range of motion is affected by outside influences such as the ambient temperature [2]. A permanent readjustment of the sensor would be necessary for long-term use. In order to adapt the sensor to the patient's motion and stroke movement abilities, the user moves the 3-axis sensor at least once in each direction with a circular movement. The *z*-axis can also be configured through vertical pressure and tension applied to the movement carrier. The maxima of the *x*-, *y*-, and *z*-coordinates are then saved.

As an example, the force or the stroke of a patient suffering from muscular disease was documented. The result in Figure 12 shows an inhomogeneous progression of force applied in different directions.

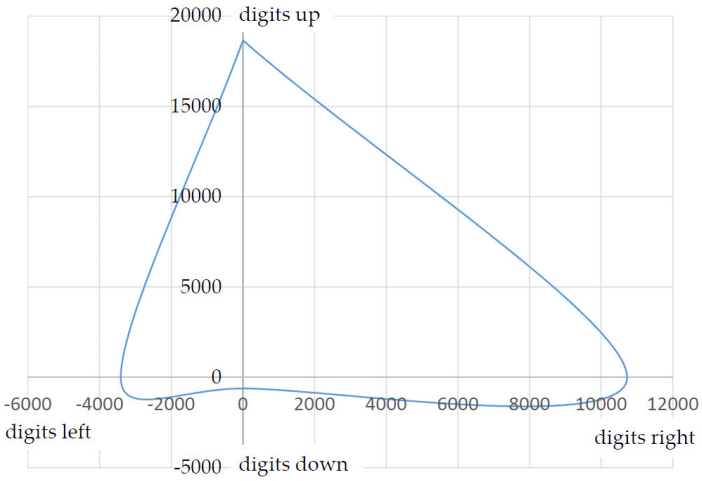

Figure 12. Force curve (force to digit); interpolated values.

When a reference was established (deflection and force to digit), Figure 12 can be used to directly determine the force and stroke the patient applied. The relationship between stroke and the change in coordinates is of course just as dependent on the length of the lever used. In a test case, the patient was able to carry out the following deflection, i.e. force (the *z*-axis is not taken into account here; Table 2).

Table 2. Patient measurements and applied force.

Direction To	Maximum Digits	Approximate Force
forward	18.653	3.92 N
back	611	0.07 N
left	3411	0.74 N
right	10.724	2.12 N

These values cannot be transmitted directly to a power wheelchair. The patient would simply drive the wheelchair forwards and to the right while traveling at a sufficient speed. The values achieved for reverse and left are not sufficient to move the wheelchair. Suitable factors or divisors can provide the desired consistent output signal. Example: Common output values are in the 10-bit range ((measured value/1024) 2 = divisor; Table 3).

Table 3. Patient measurements and calculated divisor.

Direction To	Maximum Digits	Divisor for Each Direction
forward	18.653	36,43
back	611	1,19
left	3411	6,66
right	10.724	20,95

All of the coordinates documented during use for this user, then have to be converted with the divisor to attain a consistent output signal.
Example calculation:
All values are multiplied by 100 by the interpolation of the image (right value, see Table 2; 10-bit output signal; image sensor 1280 × 1024).

$X_{MaxRes} = 128.000\ digits$; Maximum resolution in horizontal direction;
$X_{MaxResRight} = \frac{X_{MaxHorRes}}{2}$;
$X_{MaxResRight} = 64.000\ digits$; Half resolution, each direction;
$X_{Neutral} = 63.891\ digits$; Measured neutral value;
$X_{NeutHysteresis} = 500\ digits$; Hysteresis for a neutral window in the middle position;
$X_{MaxRight} = 74.615\ digits$; Learned maximum value to the right;
$X_{AbsolutMaxRight} = X_{MaxRightPat.1} - X_{Neutral}$;
$X_{AbsolutMaxRight} = 10.724\ digits$; Absolute maximum value to the right;
$Resolution_{OutMax10bit} = 1024\ digits$; Desired maximum output value;
$Resolution_{EachDirection} = \frac{Resolution_{OutMax10bit}}{2}$
$Resolution_{EachDirection} = 512\ digits$; Desired maximum output value, each direction;
$X_{DiviRight} = \frac{X_{AbsolutMaxRight}}{512\ \text{digits}}$;
$X_{DiviRight} = 20,95$; Calculated divisor;
$X_{RightExample} = 4.200\ digits$; Example value to the right;
$X_{OutRight} = \frac{X_{RightExample}}{20,95}$;
$X_{OutRight} = 200\ digits$ Digital output value;

By means of the algorithm shown above, the coordinates of the inhomogeneous input forces (see Figure 12) are converted into homogeneous output data (see Figure 13). The user can then, for example, move a computer mouse or an EPW (electric power wheelchair) at the same speed in all directions independently of its inhomogeneous force-lifting ratio. The output values calculated by the divisor are denoted in Table 4 and visualized in Figure 13.

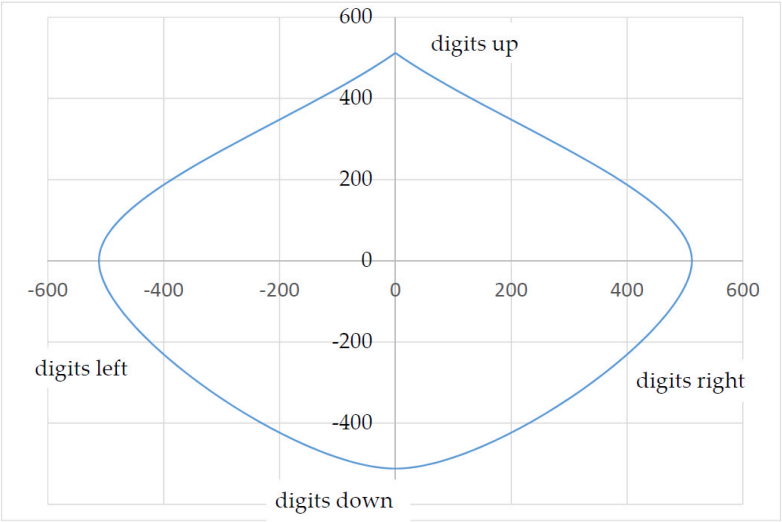

Figure 13. Output data curve.

Table 4. Maximum patient measurements and calculated output values.

Direction To	Maximum Digits	Divisor for Each Direction	Calculated Output Values
forward	18.653	36,43	512
back	611	1,193	512
left	3411	6,66	512
right	10.724	20,945	512

3.5. Hardware

The hardware (see Figure 14) consists of the image sensor, the image processor and a further microprocessor. The microprocessor first configures the image processor and then receives image data

for further processing (see Section 3.2.2). In order to increase the processing speed, x, y coordinates for the relevant image excerpt (AOI) are transferred to the image processor. The microprocessor generates the desired output data and obtains the learning command via an I/O port.

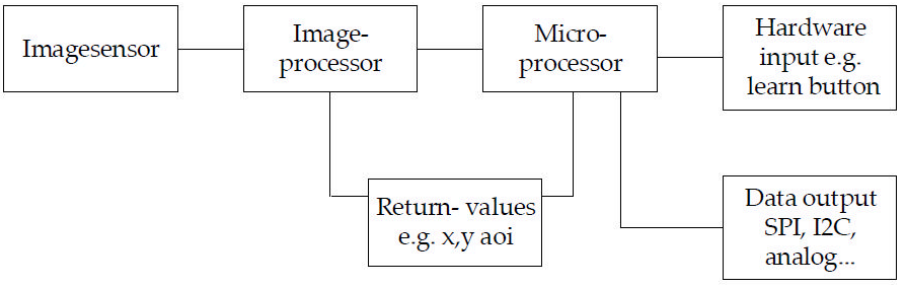

Figure 14. Schematic sensor hardware.

4. Results and Discussion

The sensor described here is in the prototype stage. Due to the optical implementation, it should be resistant to outside interference such as EMI or RFI. In version 1, hot, vulcanizing 2 components silicone rubber is used, which has optimal spring properties. Unfortunately, this ability is not sufficient to achieve a satisfactory result. Depending on the axis deflection, the neutral position is more or less difficult to reach. This circumstance can be compensated for because the neutral values can be reproduced exactly. In versions 2 and 4, the movement carrier is made of CFRP and firmly affixed to the casing. Compared to fiber-reinforced polymer (AFRP) and glass-fiber reinforced polymer (GFRP), CFRP has superb dynamic properties. The dynamic damping capacity of AFRP under a dynamic load is six times higher than GFRP and nine times higher than CFRP [23]. Using CFRP solves the problem described above and the spring precision is at ± 2 digits (without interpolation, image sensor 1.3 MP). The climate chamber was successfully completed (-30 degrees to 80 degrees). The deviation was at ± 1 digit (without interpolation, image sensor 1.3 MP). The first tests under laboratory conditions were successfully completed. During the tests, the 3-axis sensor was used in place of a mouse and to operate a power wheelchair [24]. As long as a physically disabled patient still has some type of physical capability (hand, finger, foot, toe, head, chin, etc.), it should be possible to use this sensor. Owing to the sensor's ability to learn, there are no additional costs. If the clinical symptoms change for the worse, the sensor can be adapted to the new conditions immediately. Thanks to the high resistance to interference, there is potential for application to areas other than the medical sector such as the automotive, aeronautics, aerospace, marine and military fields. Owing to its resolution and reproducibility (movement to digits), geophysical sensors could also be replaced by this sensor. A screwed-on rod or ball to receive the force can come into resonance oscillation when a defined oscillation frequency acts on the sensor. Thus, the system can begin to "vibrate". This particular case can also occur in off-the-shelf joysticks. To compensate, a polymer ring can be installed above the movement carrier (version 3), which functions as a shock absorber and dampens vibrations. For technical reasons, the force to be exerted increases exponentially to the deflection, causing a natural force feedback. This positive effect can be explained as follows: Since the movement carrier and thus also the axis of the sensor can only be moved by $<1^\circ$ in any direction, the user perceives it to be a rigid system. When a rigid system is subjected to an input force, the skin feels a pressure proportional to the applied input force. Users reported a very pleasant effect compared to conventional joysticks. Off-the-shelf joysticks are generally equipped with a reset spring. The effect of a proportional increase of the counterforce is very small. Without seeing a commercially available joystick, the user cannot derive a conclusion from the applied force to the actual deflection. Noise in the image sensor is also another issue. In a state of rest, the coordinates change by up to 2/100 digits (with interpolation, image sensor 1.3 MP). For the most part, this camera noise can be removed on a mathematical basis [22].

5. Conclusions

Our results show the feasibility and practicability of the new optical, multi-functional, high-resolution 3-axis sensor. Compared to standard, high-resolution sensors (resistive, inductive, or capacitive) the sensor presented here works on a completely digital basis. No compensation is required to adapt the sensor to fluctuations in temperature, for example. Depending on the intensity of the plausibility check, the software requires a substantial amount of calculation time. In the version shown here, the focus of the calculation can be on maximum frame rate or on maximum resolution. Because the different uses and applications usually only require one focus, the sensor's software can be optimized for each purpose. The current prototype can achieve a maximum resolution of 60 fps. When using the area of interest (AOI) function, 150 fps can be processed. This problem can be solved by using faster image sensors and faster microcontrollers. In addition, the sensor can also work with more than 3-axes, for example, when a square is used as the projected shape. The image analysis software then also detects a rotary movement of the axis, the computation time however increases substantially.

Author Contributions: The contributions of this paper are related to the PhD thesis of Niels Buchhold (conception, prototype design, paper writing). Christian Baumgartner is his thesis supervisor (conception, paper writing).

Conflicts of Interest: The authors declare no conflicts of interest except that the device described in this paper is patent pending (Austrian patent application A571/2015) and PCT (PCT/EP2016/070390) pending.

References

1. Cowan, R.E.; Fregly, B.J.; Boninger, M.L.; Chan, L.; Rodgers, M.M.; Reinkensmeyer, D.J. Recent trends in assistive technology for mobility. *J. Neuroeng. Rehabil.* **2012**, *9*. [CrossRef] [PubMed]
2. Balon, D. Facts about Myotonic Muscular Dystrophy. Available online: https://www.mda.org/sites/default/files/publications/Facts_MMD_P-212_0.pdf (10 January 2017).
3. Ramstein, C. *Combining Haptic and Braille Technologies: Design Issues and Pilot Study*; ACM: New York, NY, USA, 1996.
4. National Spinal Cord Injury Statistical Center. Spinal cord injury facts and figures at a glance. *J. Spinal Cord Med.* **2010**, *33*, 439.
5. Ginop, M. Spinal Cord Injury Facts & Statistics. Available online: http://www.sci-info-pages.com/facts.html (accessed on 10 January 2017).
6. Emery, A.E.H. The muscular dystrophies. *Lancet* **2002**, *359*, 687–695. [CrossRef]
7. Wolpaw, J.R.; Birbaumer, N.; Heetderks, W.J.; McFarland, D.J.; Peckham, P.H.; Schalk, G.; Donchin, E.; Quatrano, L.A.; Robinson, C.J.; Vaughan, T.M. Brain-computer interface technology: A review of the first international meeting. *IEEE Trans. Rehabil. Eng.* **2000**, *8*, 164–173. [CrossRef] [PubMed]
8. Kim, K.-N.; Ramakrishna, R.S. Vision-based eye-gaze tracking for human computer interface. In *IEEE SMC'99 Conference Proceedings*; IEEE Service Center: Piscataway, NJ, USA, 1999; pp. 324–329.
9. Malkin, J.; House, B.; Bilmes, J. Control of simulated arm with the vocal joystick. In *CHI 2007 Workshop on Striking a C [h] ord: Vocal Interaction in Assistive Technologies, Games, and More*; ACM: San Jose, CA, USA, 2007.
10. Malkin, J.; House, B.; Bilmes, J. The VoiceBot: A voice controlled robot arm. Vocal Interaction in Assistive Technologies, Games, and More. In *CHI 2007 Workshop on Striking a C [h] ord*; ACM: New York, NY, USA, 2007.
11. Buchhold, N. Apparatus for Controlling Peripheral Devices through Tongue Movement, and Method of Processing Control Signals. U.S. Patent 5,460,186A, 24 October 1995.
12. Martens, C.; Ruchel, N.; Lang, O.; Ivlev, O.; Graser, A. A friend for assisting handicapped people. *IEEE Robot. Autom. Mag.* **2001**, *8*, 57–65. [CrossRef]
13. Encarnacao, J.; Gobel, M.; Rosenblum, L. European activities in virtual reality. *IEEE Comput. Gr. Appl.* **1994**, *14*, 66–74. [CrossRef]
14. Furrer, B.; Ihlefeld, J.; Knaus, T.; Kluser, C.; Tiedeke, J. Messvorrichtung zum Messen von Verformungen Elastisch Verformbarer Objekte. EU Patent 2,395,320A1, 14 December 2011.
15. Klinger, D. Optoelectronic Measurement Arrangement. U.S. Patent 5,181,079A, 19 January 1993.
16. Uhlmann, E.; Seibt, M.; Haertwig, J.P.; Schaeper, E. Einrichtung zur Erfassung der Relative Position Zweier Zueinander Bewegbarer Körper. DE Patent 2002/002991, 14 August 2003.
17. Zeller, S. Dreiachsig Drehpositionierbarer Steuerknüppel. EU Patent 19970101788, 20 August 1997.

18. APEM Serie MS. Available online: http://www.apem.de/files/apem/brochures/DEU/Serie_MS_de_Low_Res.pdf (accessed on 11 January 2017).
19. Fischer, R.E.; Tadic-Galeb, B.; Yoder, P.R.; Galeb, R. *Optical System Design*; McGraw-Hill Education: New York, NY, USA, 2000.
20. IDS Imaging Development Systems GmbH. UI-1241LE. Available online: https://de.ids-imaging.com/store/ui-1241le.html (accessed on 10 January 2017).
21. IDS Imaging Development Systems GmbH. UI-3591LE. Available online: https://de.ids-imaging.com/store/catalogsearch/result/?q=UI-3591LE (accessed on 10 January 2017).
22. PRIESE, L. *Computer Vision: Einführung in Die Verarbeitung und Analyse Digitaler Bilder*, 1st ed.; Springer: Berlin/Heidelberg, Germany, 2015.
23. Ehrenstein, G.W. *Faserverbund-Kunststoffe: Werkstoffe, Verarbeitung, Eigenschaften*, 2nd ed.; Hanser Verlag: München, Germany, 2006.
24. Dynamic Controls. The DX2 System—Dynamic Controls. Available online: https://dynamiccontrols.com/en/dealers/products/dx2/the-dx2-system (accessed on 1 January 2017).

7.1.2 Publication SG version 1

(14 pages)

sensors

MDPI

Article

A New Input Device for Spastics Based on Strain Gauge

Niels Buchhold * and Christian Baumgartner *

Institute of Health Care Engineering with European Testing and Certification Body of Medical Devices, Graz University of Technology, Stremayrgasse 16/II, 8010 Graz, Austria

* Correspondence: 0603591990@t-online.de (N.B.); christian.baumgartner@tugraz.at (C.B.)

Academic Editor: Vittorio M. N. Passaro

Received: 13 February 2017; Accepted: 15 April 2017; Published: 17 April 2017

Abstract: This article presents a new sensor for use by people with spastic disorders and similar conditions and enables them to steer and control medical devices such as electric powered wheelchairs. As spastic patients often suffer from cramping of their extremities, which can then no longer be controlled, using a standard joystick while operating a powered wheelchair can lead to dangerous situations. To prevent this, we designed a sensor based on strain gauges, which is shaped like a flat disc that can be operated using any body part. By shifting weight along the x- and y-axis, the disc tilts in all directions thereby generating proportionate output signals. The disc can also be pressed downward (z-axis), for example, to open a wheelchair's menu. Thanks to the sensor's flat disc-like construction and the option of mounting it into a control panel, users are not in danger of becoming stuck on the disc during spastic episodes. In the event of a spasm, body parts simply slide over the disc reducing risk of unintended actions. The sensor is adaptive and adjustable enabling it to fit a user's range of strength and motion at any time. It was developed to ensure users can operate sensitive systems safely.

Keywords: tactile sensors; assistive technologies; power wheelchair; medical systems; robotic; joystick; strain-gauge; spastic; spasticity

1. Introduction

The role of sensors as interfaces between man and machine in today's world is gaining in importance. Joysticks and joystick-like sensors can be operated almost intuitively and are commonly used in a variety of control systems as input devices. Fields of application such as medical technology require the highest level of safety for operation. Using a sensor [1] (joystick) is problematic especially for physically disabled people suffering from spasms, as the range of motion (strength and hub) typically undergoes constant spasms. Cramp-like movements while using sensitive systems such as powered wheelchairs can result in uncontrollable and dangerous situations. Moreover, users are at risk of injury if their hand cramps around a joystick causing excessive strain on bones and tendons [2].

Therefore, the first task during development was to ensure the sensor had the proper ergonomics to prevent injury. To accommodate various medical conditions and the very different ranges of motion associated with them, a sensor should be adapted to each user. Making adjustments to a conventional sensor would be very costly and necessary for each progression of a medical condition. Moreover, for some medical conditions the success of such modifications would be only temporary because users' range of motion undergoes constant change. For that reason, the second task during development was to design the sensor in such a way that inhomogeneous forces (i.e., the maximum force a user can apply depending on the direction) can be converted into homogenous output signals. The goal in doing so was to generate consistent output signals for each direction despite varying degrees of force to drive an electric powered wheelchair, for instance, in each direction at the same speed. A computer mouse

could also move a pointer at the same speed on a screen in each direction. This development task, however, requires that the sensor be capable of processing a range of force between 0.05 N and 25 N.

When operating an electric powered wheelchair, new control systems such as eye tracking, voice control and brain-computer interfaces [3–6] are not usable for people with spastic conditions due to safety reasons. The reason is that the uncontrolled contraction of various muscle groups would cause the triggering of unintended actions. Tongue controls [7,8] are suitable for spastics to a limited degree since the tongue is affected only in rare cases. The aforementioned input methods make precise and complex control actions difficult as each change of direction or speed requires a new command. Moreover, eye tracking is affected by natural eye reflexes and completely unsuitable for safety critical control tasks. Voice control can usually only process one command at a time and is unreliable in loud environments [9].

In order to measure the quality and opportunities of sensor-based control, we developed a simple yet effective test during our research. The user is asked to navigate through an obstacle course with the electronic power wheelchair (EPW) (see Figure 1) or is tasked with moving a mouse pointer around a screen and tracing a shape.

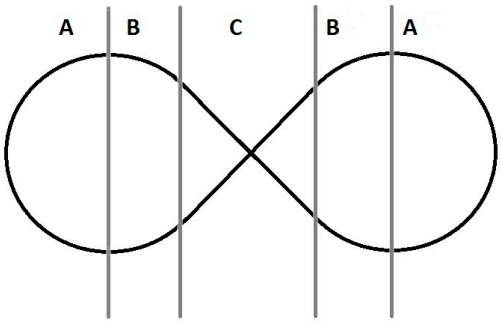

Figure 1. "Form 8" obstacle course.

The obstacle course consists of three areas with different requirements for specific input movements. While in area A the user is asked to drive in a consistent radius, in area B the radius of the curve changes and gradually transitions into a straight section in area C. This test includes all variations of possible changes in direction. For an increased level of difficulty, the obstacle course can be performed in reverse as well. During the tests, an acceleration sensor and a video camera are attached to the EPW. A sensor will have optimal effectiveness if it records only small jolts and spikes in direction and speed. A review of the pictures taken by the camera shows the degree of precision to which the line was traced. With digital input devices or voice control, it is not possible to follow the line through the obstacle course at a consistent speed. In area A and B the route driven would vary because the radius would be constantly adjusted. A consistent drive is only possible with a proportional sensor.

Until now, proportional sensors, such as joysticks, could only be used to a limited degree by people with spastic conditions due to the safety risk in case of cramping. Obstacle detection systems that helps users navigate [10,11] make sense but they are expensive. With these assistive systems, a user cannot complete an entire trip independently because the navigation aid takes over automatically when obstacles are encountered. After surveying users, we found that assistive systems often intervene in that desired route, making them more or less undesirable as aids. Control systems that record spastic movements over certain period [12] and use an algorithm with an averaging function to generate the next probable direction a user wants to move toward, could be combined with the strain-gauge disc presented here. But even this would hinder direct and independent control by users. Users only accept direct controls for wheelchair rides that take place in very narrow areas or for sporting activities such as EPW hockey.

US patents [13–15] describes input devices with strain-gauges (SG) that are designed like conventional joysticks. The method of determining positions with the help of strain gauges is therefore

commonly known [16]. The innovative aspect of this strain-gauge disc as compared to other sensors, their design and how they determine positions is listed below:

1. The sensor's flat disc-like design.
2. The construction and shape of the movement carrier constructed using carbon fiber reinforced composite (CFRP).
3. The movement carrier's highly precise ability to return to its original position after being deflected.
4. The software algorithm designed to adapt the sensor to a user's own range of strength and motion.
5. The differential processing of measurements for plausibility checks to increase user safety.
6. The sensor's range of sensitivity between 0.05 N and 25 N.
7. The sensor's unsusceptibility to excess strain (e.g., in case of spasms, it withstands loads up to 1400 N).

All of the features mentioned here were implemented in this development and are described in this article. This includes a description of the prototype's hardware (Figures 2 and 3) as well as a schematic look at the software and its algorithms.

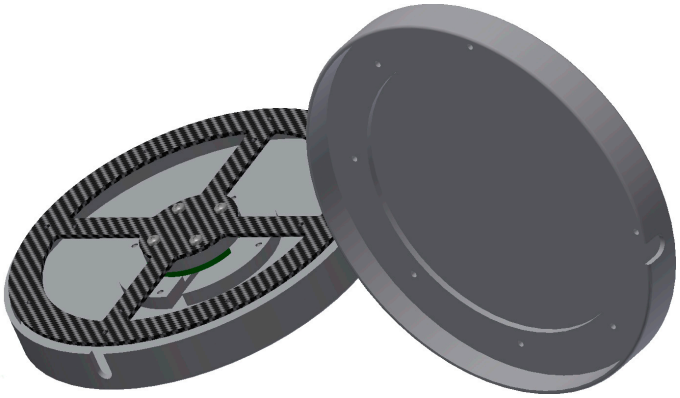

Figure 2. Strain-gauges device (SGD) drawing.

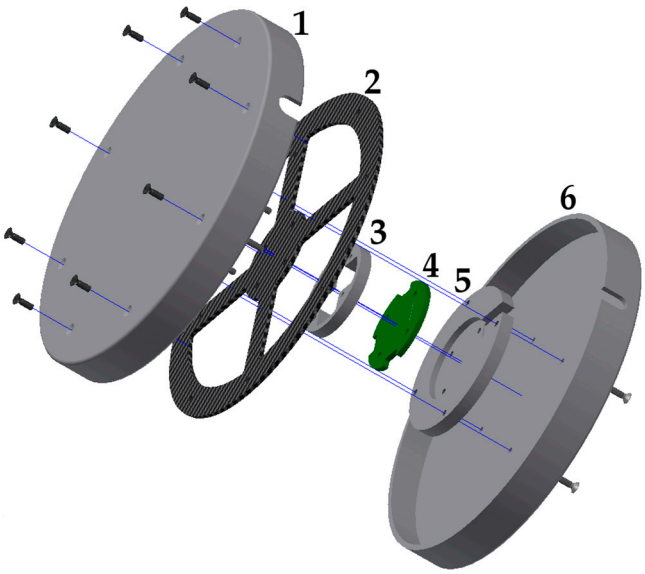

Figure 3. Exploded View of SGD.

2. Hardware of the SGD

2.1. Basic Construction

Because the sensor must sometimes undergo very high strain as in the case of spastic episodes, its construction needs to meet stability criteria. The strain gauge disc—SGD's maximum load capacity is 1400 N. This load limit can be increased by using a more sturdy housing (see Figure 3, Part 1 and Part 6), if needed. Despite the high load-bearing capacity, the sensor must be capable of processing a user's fine-motor movements since users with spastic disorders have a similar range of strength and motion as healthy people. It is very important that users do not trigger unintended actions during spastic fits. A flat disc (120 mm in diameter) seemed to make the most sense due to the aforementioned reasons. The actual sensor (see Figure 3) is made of a carbon fiber reinforced composite (CFRP) carrier (Figure 3, Part 2) that is attached to four strain gauges. A circuit board is positioned underneath the carrier (Figure 3, Part 4) with four differential amplifiers AD 623 [17] and an analog-to-digital converter (ADC) AD 7811 [18] with an integrated SPI (Serial Peripheral Interface) data output. The user can incline the disc in any direction by shifting its weight (x-, y-axis) on the upper cover (Figure 3, Part 1). As a result of the design, the edge of the CFRP carrier is pressed downwards during x- and y-axis movements, while the opposite side of the CFRP carrier lifts up. Due to this fact, a plausibility test can be carried out since a defined measured value of the opposite strain gauge must be present for each measured value. This software process is described in detail in Section 3.2. The upper housing (Figure 3, Part 1) can also be pressed down. In doing so, all four strain gauges are deflected in one direction (z-axis), which makes other control options possible, such as operating a computer mouse (mouse click). The sensor's parts labeled Part 3 and Part 5 (Figure 3) only serve as spacers. The entire sensor can also be integrated into a control panel in front of the user, such as in an electric powered wheelchair. In this case, for example, the entire control panel could be made of CFRP. The interlocking parts of the housing (see Figure 3, Part 1 and Part 6) protect the CFRP carrier against damage.

The SGD (see Figure 3) consists of the following components. Part 1 and Part 6 make up the upper part of the bottom casing. The CFRP movement carrier (Part 2) is screwed to the upper casing (Part 1). The circuit board (Part 4) is positioned between the spacers (Part 3 and Part 5) and soldered to the strain gauge.

2.2. CFRP Carrier

The prototype's CFRP carrier (Figure 4) is made of a CFRP plate measuring 1.3 mm in diameter. The material thickness can be adjusted depending on the application as CFRP has excellent durability compared to other materials. Compared to aramid fiber reinforced composite (AFRP) and glass fiber reinforced composite (GFRP), CFRP has superb dynamic properties [19]. The CFRP's reset behavior is of particular importance. When the sensor is overstrained, the interlocking parts of the casing (see Figure 3, Part 1 and Part 6) protect the CFRP carrier against damage. Thanks to the housing's design, the maximum stroke of the sensor can be mechanically limited. If the load is too high (max. 1400 N) or the stroke is too forceful, the incoming forces are distributed past the CFRP carrier via the housing. The CFRP compensated strain gauges are glued and soldered to the circuit board. Additional cross linking silicon can then be poured over the circuit board and the strain gauges. This makes the sensor usable in humid environments. For testing purposes, the CFRP carrier was also subjected to stretching. The design shown in Figure 5, which has a CFRP material thickness of 1.3 mm, broke under a tensile load of 102 N. It is not possible, however, to pull the sensor's housing without any aids. The 1.3 mm material thickness is a very good compromise between responsiveness and durability.

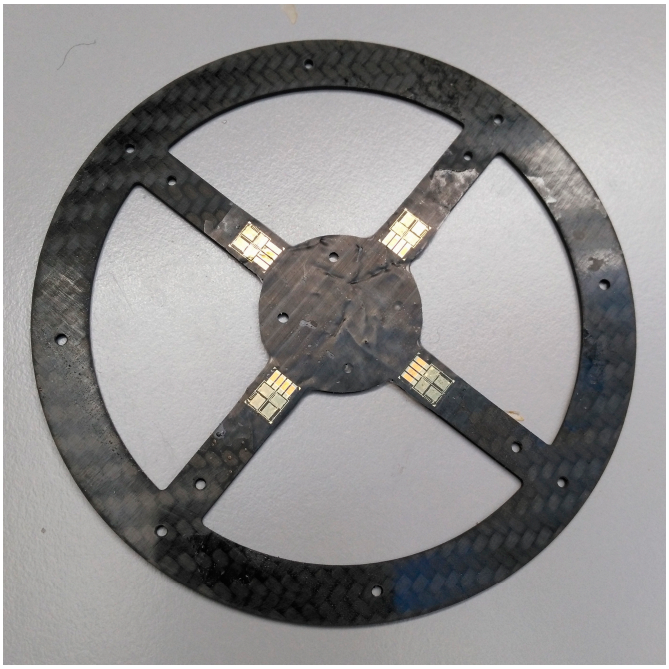

Figure 4. CFRP carrier with affixed strain-gauges.

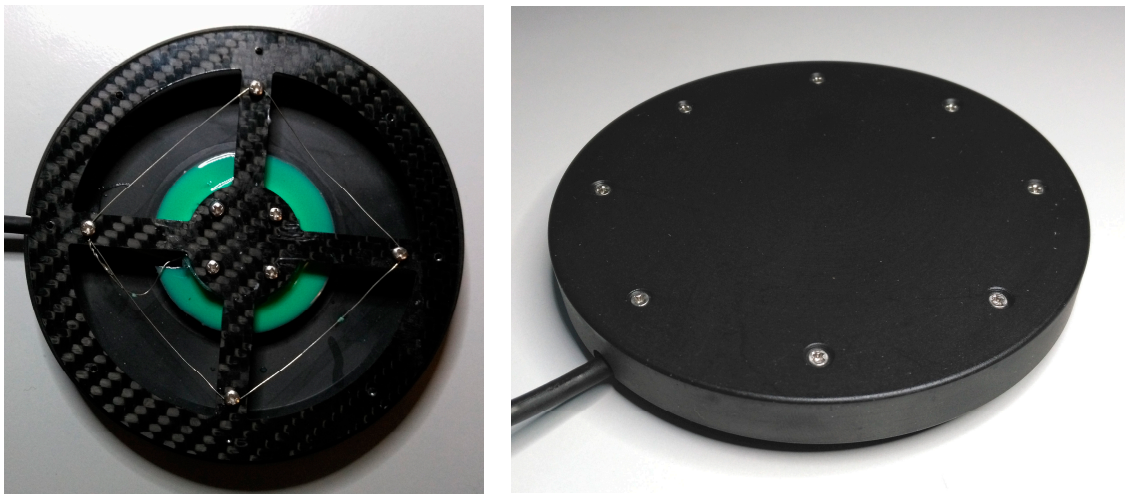

(**a**) (**b**)

Figure 5. SGD without upper cover (**a**) and with cover (**b**).

2.3. Circuit Board and Microcontroller

On the circuit board (Figure 3, Part 4) there are four differential amplifiers AD 623 [17], a 10-bit ADC AD 7811 [18] and a voltage stabilizer. The differential amplifiers' gain is set by an external resistor. All four values (see Figure 6) are constantly transmitted by the ADC via an SPI interface (slave) to a downstream microcontroller SPI (master). The microcontroller then generates the desired output signals for the hardware. The microcontroller's I/O pins, which are also connected to the downstream microcontroller, would activate in case of a malfunction. This makes it possible to initiate emergency measures.

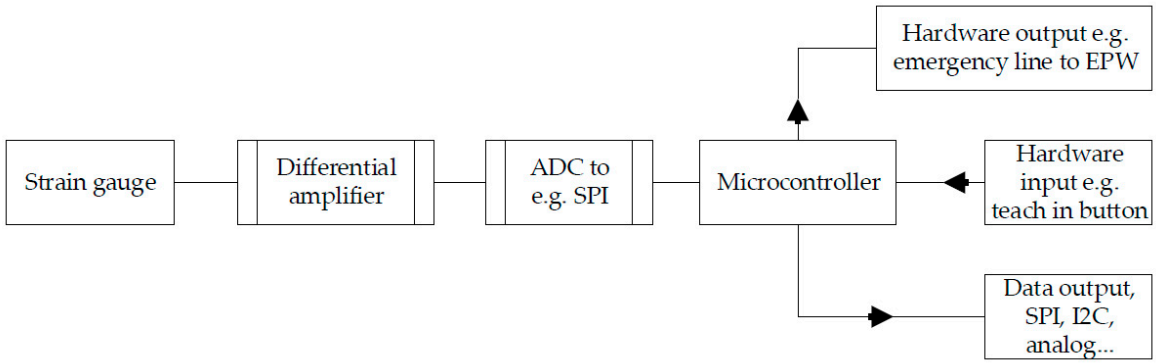

Figure 6. Schematic sensor hardware.

2.4. Different Versions

During development three different versions of the sensor were constructed for people with spastic conditions. Users can decide which version is most suitable for them.

Version 1: The CFRP carrier and its shaping would be adjusted to meet the requirements. The material thickness and the arrangement of the CFRP layers would be taken into account. The shaping reinforces stability and lends flexibility to the movement carrier.

Version 2: Setup is the same as version 1. In addition, the CFRP carrier is cast in an addition-crosslinked, thermally vulcanizing silicone rubber. The damping properties will vary depending on the Shore-hardness. Other damping materials, such as compression springs or other polymers, did not bring about the desired effect because the thermal expansion coefficients influenced the CFRP carrier in a counterproductive manner.

Version 3: The entire control panel of an EPW is made of CFRP. The strain gauges are attached to the panel using adhesive. Corresponding CNC milling patterns around the strain gauges influence the sensor's sensitivity.

During the series of tests, CFRP carriers with material thicknesses of 0.45 mm to 2 mm were tested. Thanks to the shaping, the sensitivity and the maximum load in regard to pulling in particular can be adapted.

3. Sensor Operations

3.1. Basics

If external forces act on the CFRP carrier (see Figure 3, Part 2) from outside the housing top (see Figure 3, Part 1), its tilt changes slightly. As a result, the opposite strain gauge is deflected differentially. The differential values that result are added together in the downstream controller, which then increases the resolution. Using a more powerful ADC would increase the resolution accordingly.

Example Calculation at the time of t = 1 (values dimensionless):

$X_{Neutral} = 512$ Measured neutral value;

$X_{Right\ t=1} = 640$ Measured value right strain gauges at t = 1;

$X_{Left\ t=1} = 430$ Measured value left strain gauges at t = 1;

$$X_{t=1} = \left|X_{Neutral} - X_{Right\ t=1}\right| + \left|X_{Neutral} - X_{Left\ t=1}\right|$$

$X_{t=1} = 210$ Output x-value to the microcontroller;

Depending on the version, the restoring force is caused by the CFRP on its own or additionally via silicone rubber. Table 1 and Figure 7 show the measured values of one SG in relation to the applied force. Various silicone rubber mixtures and different material thicknesses (see Table 2) are shown by way of example. Due to the fact that the measurement curves are identical in each direction, the measurement was carried out only for one SG. Depending on the CFRP motion carrier and the polymers shore hardness, the maximum value of the 10-bit ADC (1024) is achieved at different degrees

of force. Additional forces impact the housing beyond the maximum value of 1024 (see Figure 3, Part 1 and Part 6).

Table 1. Selected measurements with different materials and versions. (only X_{Right} is shown).

Test Series; Force (N) Disc Diameter of 120 mm Mat. (Material)	0	0.05	0.1	0.2	0.5	1	2	3	5	10	20	25
Mat. 1 CFRP 0.45 mm non silicon rubber	532	538	545	561	592	650	760	890	1024	1024	1024	1024
Mat. 2 CFRP 0.90 mm non silicon rubber	535	537	540	551	569	622	698	810	903	1024	1024	1024
Mat. 3 CFRP 1.30 mm non silicon rubber	510	511	513	516	529	550	611	675	776	895	1024	1024
Mat. 4 CFRP 2.00 mm non silicon rubber	521	521	521	521	522	528	549	607	673	790	897	1024
Mat. 5 CFRP 0.90 mm silicon rubber shore 20	505	506	507	511	558	611	670	796	881	982	1024	1024
Mat. 6 CFRP 0.45 mm silicon rubber shore 30	535	537	542	561	614	666	791	873	970	1024	1024	1024

Table 2. Explanation of materials used in Table 1.

Material	CFRP Thickness	Silicon Rubber	Shore Hardness
Material 1	0.45 mm	no	none
Material 2	0.90 mm	no	none
Material 3	1.30 mm	no	none
Material 4	2.00 mm	no	none
Material 5	0.90 mm	yes	20
Material 6	0.45 mm	yes	30

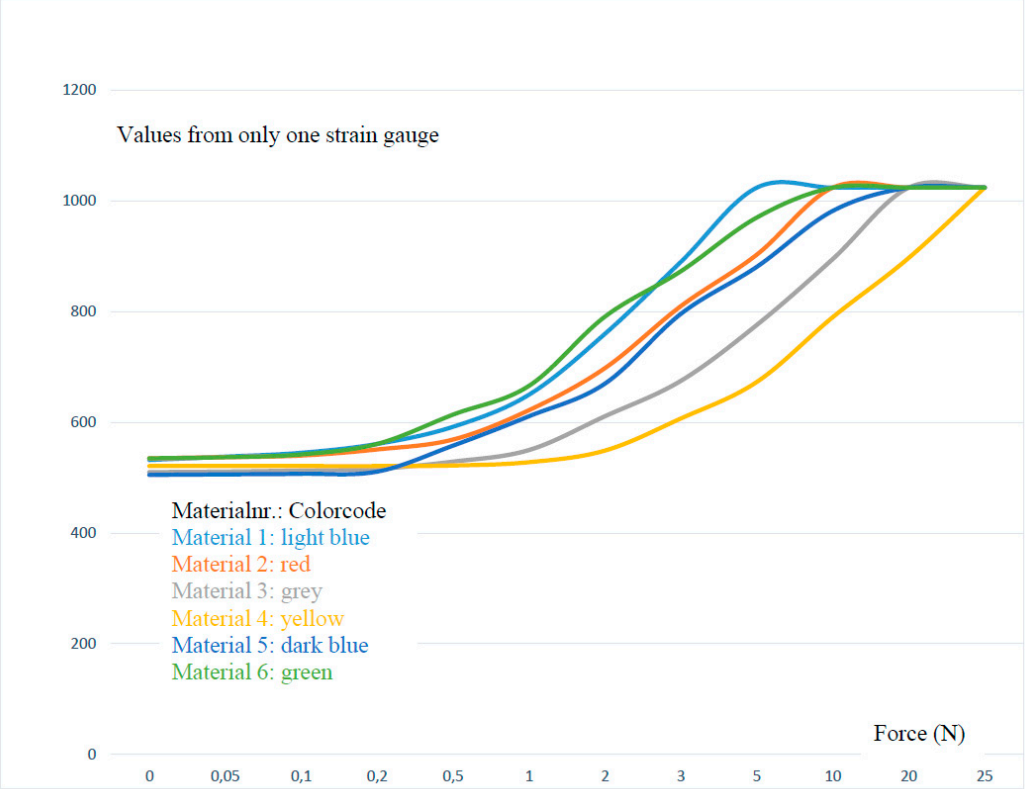

Figure 7. Visualized, measured values from Table 1.

3.2. *Plausibility Check*

The plausibility check constantly examines the values recorded by the sensor during operation. Directly after production, an initialization process is carried out. Under various loads, all of the strain

gauges' possible measured value combinations are stored during this phase. Under normal operating conditions, the measured values of the opposite strain gauge are compared to the previously registered value combinations. If the values deviate from the previous values, then there is an error.

This makes it possible to detect many errors or damage to the hardware immediately. A specific value is documented if a strain gauge loses contact with the CFRP carrier. The specific value of the strain gauge opposite that one is searched for. If the pair of values do not match, then there must be an error. Measures are then taken to protect the downstream system from malfunctions (see also Figure 6). Breakage also causes the currently measured value pair to not match a stored pair of values. All of the errors that occurred during the test phase were immediately detected by the plausibility check. In addition to breakage tests, the sensor was also immersed in water.

3.3. Individual Adjustment of the SGD

Due to the fact that symptoms vary from patient to patient, the sensor needs to be adapted to a user's own range of strength and motion. Conventional sensors, such as joysticks, have a certain accuracy (resolution), a certain amount of force required for deflection, and a certain stroke to overcome the necessary paths by a fixed amount. As described in the introduction, certain groups of physically disabled people are unable to use standardized joysticks for a variety of reasons. This issue has to do with this group of users' range of motion (force and stroke). Moreover, the existing range of motion is affected by outside influences such as ambient temperature [20]. A conventional sensor would have to undergo mechanical adjustments on a constant basis, which would be quite inconvenient. To adapt the sensor described here to the user's range of strength and motion, the SGD is moved once in each direction in a circular motion. During this 10-second learning process, the maximum x and y coordinates are stored. When vertical pressure is applied to the top of the housing (Figure 3, Part 1), the maximum values for z-axis can be stored as well. The absolute zero position or resting position, is set during a calibration process for each SGD after assembly, in conjunction with the initialization process (see Section 3.2 plausibility check). This eliminates excess production costs since production tolerances are relatively insignificant. To serve as a reference, a patient's strength and stroke were documented. The result in Figure 8 shows an inhomogeneous progression of force applied in different directions.

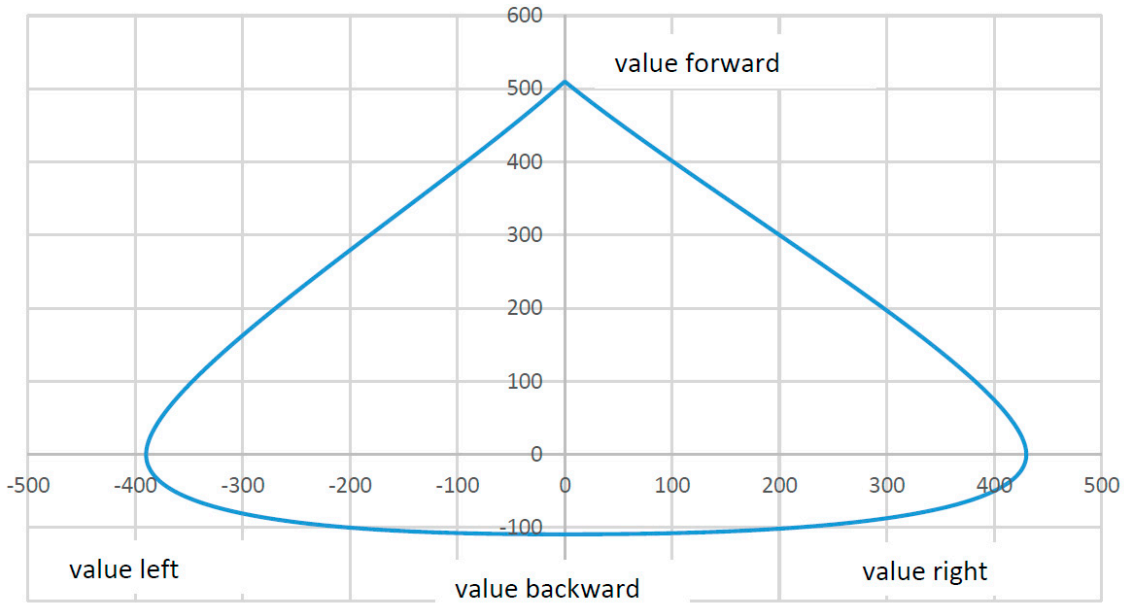

Figure 8. Force Curve (force to value), max. value from neutral position for Material 3 (see Table 3).

When a reference was established previously (deflection and force in relationship to the measured value), Figure 8 can be used to determine the force applied by the patient. In this test, the patient was able to apply the following maximum deflections, (force) without taking the z-axis into account:

Table 3. Patient measurements and applied force.

Direction	Maximum Values	Approximate Force
forward	510	18.4 N
backward	109	2.1 N
left	390	11 N
right	430	14.2 N

If the values in Figure 8 were sent directly to an EPW, the user would only be able to drive forward, right, and to the left at an acceptable speed. The maximum values for backwards are insufficient to move the wheelchair. The correct multiplication factors can help attain a consistent output signal.

Example:

The factor for a 10-bit ADC is calculated with this formula:

$$\frac{MaxValueADC}{MaxPatientMeasuredValue} = factor$$

$$(Sample\ calculation\ forward)\ \frac{1024}{510} = 2,007$$

All of the values documented during operation have to be converted by corresponding factor in Table 4 to attain a consistent output signal.

Example Calculation:

(Right value from Table 3; 10-bit ADC)

$X_{MaxRight} = 430$	Maximum right direction;
$X_{FactorRight} = 2,381$	Calculated factor see Table 3;
$X_{RightExample} = 200$	Example value to the right;
$X_{OutRight} = X_{RightExample} * X_{FactorRight}$	Digital output value;
$X_{OutRight} = 476$	Digital output;

Table 4. Maximum patient measurements and calculated output values.

Direction to	Maximum	Factor	Calculated Output Values
forward	510	2007	1024
back	109	9394	1024
left	390	2626	1024
right	430	2381	1024

These output values are then offset by the differential output value of the opposite strain gauge, as seen in the example calculation (see Section 3.1 Basics). At this time the plausibility check (see Section 3.2 Plausibility check) is also carried out. Using the algorithm shown above and its multiplication factors, the measured values of the input forces (see Figure 8) are converted to generate corrected values for the downstream systems. If the user applies his or her previously set maximum force, the output values reach the maximum value in each direction (see Figure 9). The user is thus able to move a computer mouse or an electric powered wheelchair in every direction at the same speed, despite different input forces.

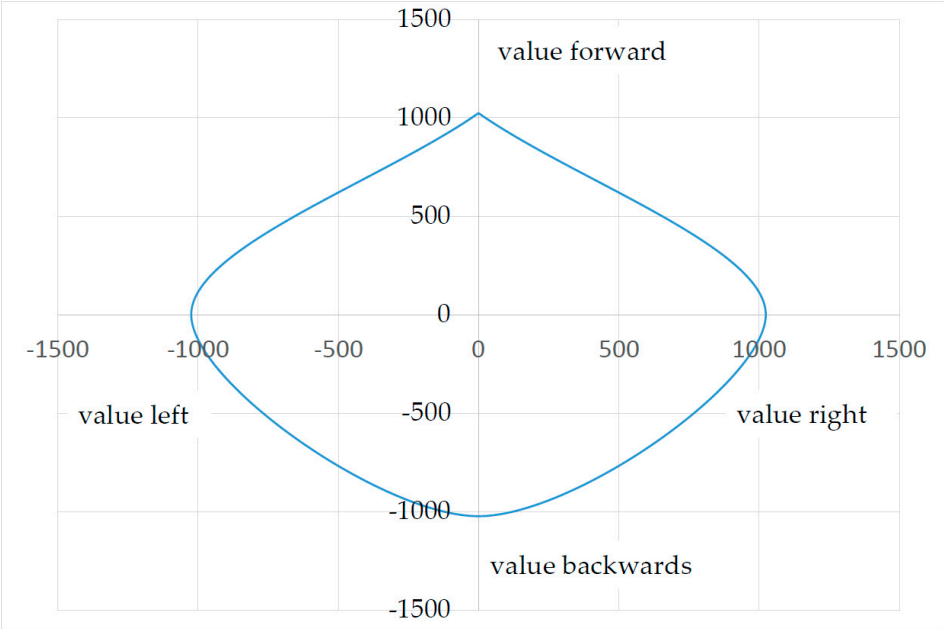

Figure 9. Maximum output data curve.

3.4. Software

The software procedures are divided into two separate processes. In order to adapt the strain gauge disc to a user (see Figure 10), the teach-in button (see Figure 6) must be pressed. After the resting values have been determined, the microcontroller stores the maximum values for each direction. In addition, various possible value combinations are saved for the opposite strain gauge, which are later used for plausibility checks (see Section 3.2 Plausibility check). After determining all the values mentioned, multiplication factors are calculated in order to generate homogeneous output signals (see Figure 9) from the inhomogeneous input signals (see Figure 8). An error will be generated if the resting values fall outside of a certain range (theoretical resting value ±100). This value window is used to eliminate manufacturing tolerances.

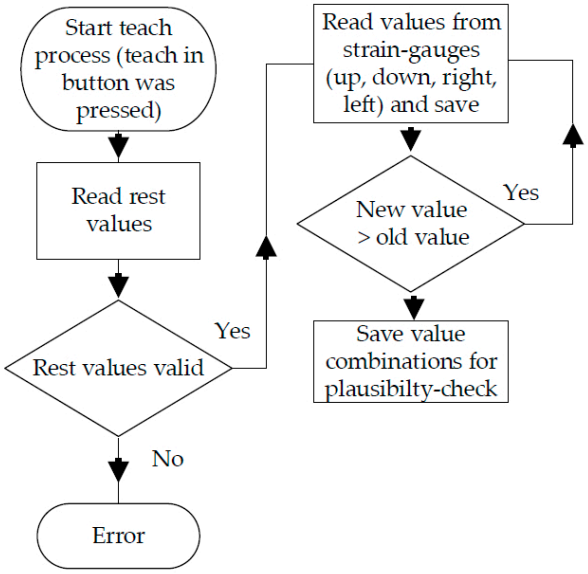

Figure 10. Schematic sensor software teach-in process.

During normal use (see Figure 11), the ADC's data are read via SPI. Afterward, a plausibility check is performed. In doing so, the values of two strain gauges opposite each other are combined. Theses pairs of values have to match the value pairs stored during the calibration process. This way, a very large portion of all the possible errors can be identified. If there is an error, the microcontroller sends neutral values to the systems that are connected to it and a separate error notification is sent via I/O pin.

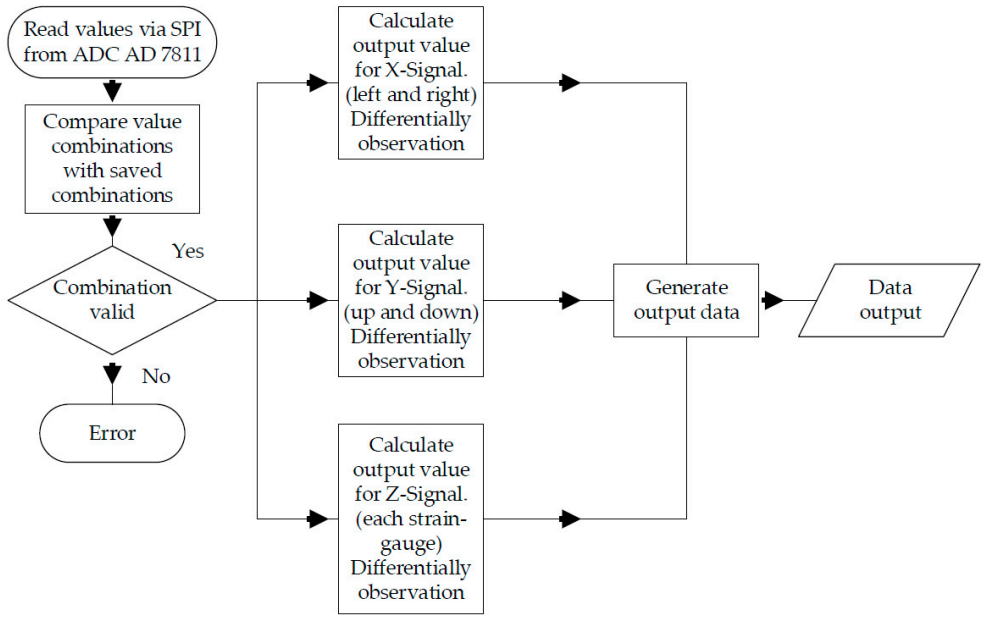

Figure 11. Schematic of sensor software under normal use.

4. Results and Discussion

The strain gauge disc described here is in a fully functional prototype stage. The main challenge was the execution of the movement carrier. First, the movement carrier was manufactured using aluminum and steel. Despite the fact that the strain gauges were designed for aluminum and steel, the test series could not be completed in a climate-controlled cabinet. The maximum deviation for aluminum was ±5 and for steel it was ±8 (measured using a 10-bit ADC). During the climate test, the strain gauge disc was subjected to a temperature range of −30 °C to +80 °C in a climate cabinet. During the first test phase (see Table 5) the SGD was not deflected.

Table 5. CFRP movement carrier, resting values in climate-controlled cabinet.

Temperature °C	Resting Values Forward	Resting Values Backward	Resting Values Right	Resting Values Left
−30	509	499	502	504
−20	509	499	502	504
−10	510	499	502	504
0	510	499	502	504
10	510	499	502	504
20	510	499	502	504
30	510	499	502	504
40	510	499	502	504
60	511	500	502	504
70	511	500	502	505
80	510	500	502	505

The test period lasted a total of 8 h. The maximum temperature-based deviation of resting values of ±1 could only be attained with a movement carrier made of CFRP. A static deflection of the SGD

during the second test (see Table 6) was conducted using a clamp (test period of 8 h). The deviations are within a maximum ±1 (measured with a 10-bit ADC).

Table 6. Fixed deflection of the SGD forward and to the right in a climate-controlled cabinet.

Temperature °C	Resting Values Forward	Resting Values Backward	Resting Values Right	Resting Values Left
−30	829	182	769	231
−20	829	182	769	231
−10	829	182	770	231
0	829	182	770	231
10	829	182	770	231
20	829	182	770	231
30	829	183	770	231
40	829	183	770	231
60	829	183	770	231
70	830	183	770	231
80	829	183	771	231

An additional series of tests examined the movement carrier's reset accuracy (see Table 7) after moving the SGD in all directions with varying degrees of force.

Table 7. Resting position after strain (temperature 21 °C).

Strain (N)	Resting Values Forward	Resting Values Backward	Resting Values Right	Resting Values Left
Resting Values	510	499	502	504
forward 25	510	499	502	504
forward 100	510	499	502	504
forward 500	511	499	502	504
forward 1400	511	499	502	504
backward 25	510	499	502	504
backward 100	510	499	502	504
backward 500	509	498	502	504
backward 1400	509	498	502	504
right 25	510	499	502	504
right 100	510	499	502	504
right 500	510	499	503	503
right 1400	510	499	503	503
left 25	510	499	502	504
left 100	510	499	502	505
left 500	510	499	502	505
left 1400	510	499	502	505

The results of the stress test show that the movement carrier's resting values deviate by a maximum of ±1 under different loads. The aluminum version had a deviation of ±6 whereas steel was ±4. Because deviations due to temperature and deviations after strain can occur simultaneously, a maximum deviation of ±2 needs to be accounted for. In order to counteract this problem, the strain gauges values have to deviate from the resting values by at least ±4, otherwise the downstream systems will not perform any actions. Tests under laboratory conditions were successfully completed. During the tests, the sensor was used as a substitute for a mouse and to operate an EPW [21]. As long as a physically disabled patient still has some type of physical capability [22] etc.) he or she should be able to use this sensor. If a patient's symptoms change, the SGD can immediately be adapted to the user's new range of strength and motion (without the help of service staff). This learning process takes a maximum of 10 s. The weight of the upper part of the casing can cause the SGD to vibrate when a certain oscillation frequency acts on the sensor. In laboratory tests, the resonance frequency was approximately 120 Hz. As a result the system might begin to vibrate. This rare case can also occur with conventional joysticks, but hardly occurs under normal conditions. In order to prevent this unlikely situation, we poured additional cross linking silicon-rubber underneath the CFRP carrier (version 2), which acts as a vibration damper. Owing to the design, the force to be exerted increases exponentially

with the deflection causing a natural force feedback. This positive effect can be explained as follows: because the movement carrier can only be moved a few millimeters (3.6 mm) in each direction, users experience the system as being rigid. When a rigid system is subjected to an input force, the skin feels pressure, which is proportional to the input force. Users reported a very soothing effect compared to conventional joysticks. Conventional joysticks are usually equipped with springs. A proportional increase in counterforce is only minimal with this design. Without seeing a conventional joystick, the user cannot determine the relationship between the applied force and the actual deflection.

5. Conclusions

This sensor provides a new input opportunity for spastic patients. Injuries or unintentional stops in operation due to sudden spastic episodes can be largely avoided. Used in combination with other recent developments cited in the introduction, this sensor could improve the human-machine interface for spastic conditions. Owing to the SGD's simple design, a high cost of production is not expected. Especially in countries with poor health systems, the strain gauge disc is highly beneficial since no costs or only minor follow-up costs are to be expected even if the SGD would be used by another user with a different disease pattern.

Author Contributions: The contributions of this paper are related to the PhD thesis of Niels Buchhold (conception, prototype design, paper writing). Christian Baumgartner is his thesis supervisor (conception, paper writing).

Conflicts of Interest: The authors declare no conflicts of interest.

References

1. Buchhold, N.; Baumgartner, C. A New, Adaptable, Optical High-Resolution 3-Axis Sensor. *Sensors* **2017**, *17*, 254. [CrossRef] [PubMed]
2. Hu, X.; Afsharipour, B.; Rymer, W.Z.; Suresh, N.L. Impairment of Muscle Force Transmission in Spastic-Paretic Muscles of Stroke Survivors. In Proceedings of the 2016 38th annual international conference of the IEEE Engineering in Medicine and Biology Society (EMBC), Orlando, FL, USA, 16–20 August 2016; pp. 6098–6101.
3. Wolpaw, J.R.; Birbaumer, N.; Heetderks, W.J.; McFarland, D.J.; Peckham, P.H.; Schalk, G.; Donchin, E.; Quatrano, L.A.; Robinson, C.J.; Vaughan, T.M. Brain-computer interface technology: A review of the first international meeting. *IEEE Trans. Rehabil. Eng. Publ.* **2000**, *8*, 164–173. [CrossRef]
4. Kim, K.-N.; Ramakrishna, R.S. Vision-Based Eye-Gaze Tracking for Human Computer Interface. In Proceedings of the IEEE SMC'99 Conference on Systems, Man and Cybernetics, Tokyo, Japan, 12–15 October 1999.
5. Malkin, J.; House, B.; Bilmes, J. Control of Simulated Arm with the Vocal Joystick. In Proceedings of the CHI 2007 Workshop on Striking a C [h] ord: Vocal Interaction in Assistive Technologies, Games, and More, San Jose, CA, USA, 28 April–3 May 2007.
6. House, B.; Malkin, J.; Bilmes, J. The VoiceBot: A Voice Controlled Robot Arm. In Proceedings of the SIGCHI Conference on Human Factors in Computing Systems, Boston, MA, USA, 4–9 April 2009; pp. 183–192.
7. Buchhold, N. Apparatus for Controlling Peripheral Devices through Tongue Movement, and Method of Processing Control Signals. U.S. Patent 5,460,186 A, 24 October 1995.
8. Kim, J.; Park, H.; Ghovanloo, M. Tongue-Operated Assistive Technology with Access to Common Smartphone Applications via Bluetooth Link. *Conf. Proc. IEEE Eng. Med. Biol. Soc.* **2012**, *2012*, 4054–4057. [PubMed]
9. Martens, C.; Ruchel, N.; Lang, O.; Ivlev, O.; Graser, A. A friend for assisting handicapped people. *IEEE Robot. Autom. Mag.* **2001**, *8*, 57–65. [CrossRef]
10. Huntemann, A.; Demeester, E.; Poorten, E.V.; van Brussel, H.; Schutter, J. Probabilistic Approach to Recognize Local Navigation Plans by Fusing Past Driving Information with a Personalized User Model. In Proceedings of the IEEE International Conference on Robotics and Automation (ICRA), Karlsruhe, Germany, 6–10 May 2013; pp. 4376–4383.
11. Kim, E.Y. Wheelchair navigation system for disabled and elderly people. *Sensors* **2016**, *16*, 1806. [CrossRef] [PubMed]

12. Cooper, R.A.; Widman, L.M.; Jones, D.K.; Robertson, R.N.; Ster, J.F. Force sensing control for electric powered wheelchairs. *IEEE Trans. Control Syst. Technol.* **2000**, *8*, 112–117. [CrossRef]
13. Kamentser, B.; Kamentser, E. Force Transducer with Co-Planar Strain Gauges. U.S. Patent 5,872,320, 16 February 1999.
14. Manara, A.; Scofield, M.C.; Cheal, B. Sensor and Circuit Architecture for Three Axis Strain Gauge Pointing Device and Force Transducer. U.S. Patent 6,243,077, 5 June 2001.
15. Nejedly, P.; Whitfield, D.W. Three Dimensional Strain Gage Transducer. U.S. Patent 4,217,569, 12 August 1980.
16. Ma, J.; Song, A. Fast estimation of strains for cross-beams six-axis force/torque sensors by mechanical modeling. *Sensors* **2013**, *13*, 6669–6686. [CrossRef] [PubMed]
17. Analog Devices Inc. AD623 (Rev. E). Available online: http://www.analog.com/media/en/technical-documentation/data-sheets/AD623.pdf (accessed on 1 January 2017).
18. Analog Devices Inc. AD7811/AD7812 (Rev. C). Available online: http://www.analog.com/media/en/technical-documentation/data-sheets/AD7811_7812.pdf (accessed on 1 January 2017).
19. Ehrenstein, G.W. *Faserverbund-Kunststoffe: Werkstoffe, Verarbeitung, Eigenschaften*, 2nd ed.; Hanser Verlag: München, Germany, 2006.
20. Muscular Dystrophy Association Inc. Facts about Myotonic Muscular Dystrophy. Available online: https://www.mda.org/sites/default/files/publications/Facts_MMD_P-212_0.pdf (accessed on 1 January 2017).
21. Dynamic Controls. The DX2 System—Dynamic Controls. Available online: https://dynamiccontrols.com/en/dealers/products/dx2/the-dx2-system (accessed on 1 January 2017).
22. Thorp, E.B.; Abdollahi, F.; Chen, D.; Farshchiansadegh, A.; Lee, M.-H.; Pedersen, J.P.; Pierella, C.; Roth, E.J.; Seanez Gonzalez, I.; Mussa-Ivaldi, F.A. Upper Body-Based Power Wheelchair Control Interface for Individuals With Tetraplegia. *IEEE Trans. Neural Syst. Rehabil. Eng. Publ.* **2016**, *24*, 249–260. [CrossRef] [PubMed]

7.2 Patents

7.2.1 National Patent

(9 pages)

(19) österreichisches patentamt

(10) **AT 517676 B1 2017-06-15**

(12) # Patentschrift

(21) Anmeldenummer: A 571/2015
(22) Anmeldetag: 31.08.2015
(45) Veröffentlicht am: 15.06.2017

(51) Int. Cl.: ***G05G 9/047*** (2006.01)
G06F 3/033 (2013.01)
G06F 3/0354 (2013.01)
G06F 3/038 (2013.01)
G01D 5/26 (2006.01)

(56) Entgegenhaltungen:
EP 0623884 A2
WO 03016817 A2
DE 10223019 A1
WO 2004114112 A1
US 6563101 B1
WO 2013065003 A1
EP 2693167 A2
WO 9833193 A1
EP 1696300 A1

(73) Patentinhaber:
Buchhold Niels Dipl.Ing.
6020 Innsbruck (AT)

(72) Erfinder:
Buchhold Niels Dipl.Ing.
6020 Innsbruck (AT)
Baumgartner Christian Dipl.Ing. Dr. techn.
8010 Graz (AT)

(54) **Optische, lernfähige Dreiachsensensorik**

(57) Eine Vorrichtung zur Drei-Achsen-Positionsbestimmung eines Kraftaufnahmeelements (2) umfasst einen hochauflösenden Bildsensor (6), einen dem Bildsensor gegenüber angeordneten Bewegungsträger (4), der mit dem Kraftaufnahmeelement (2) verbunden ist, eine mit dem Bewegungsträger (4) verbundene Projektionseinrichtung (3), welche auf den Bildsensor eine vordefinierte geometrische Form (10) projiziert, die entsprechend einer X/Y/Z-Neigung des Bewegungsträgers positioniert und verzerrt wird. Eine Recheneinrichtung (7) leitet aus der Position und Verzerrung der geometrischen Form (10) hochauflösende X/Y/Z-Koordinaten zur weiteren Verarbeitung ab.

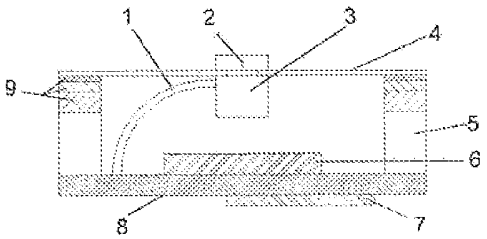

Fig. 1

AT 517676 B1 2017-06-15

Beschreibung

VORRICHTUNG UND VERFAHREN ZUR DREI-ACHSEN-POSITIONSBESTIMMUNG EINES KRAFTAUFNAHMEELEMENTS

[0001] Die Erfindung betrifft eine optische, lernfähige Dreiachsensensorik, welche jederzeit durch den Nutzer an die gewünschten Eingabekräfte angepasst werden kann.

[0002] Mehrachsensensoren im Allgemeinen und unter anderem auch Zweiachsensensoren (Joysticks, etc.) finden ihren Einsatz in sämtlichen privaten und industriellen Bereichen. Auch in den Bereichen Automobiltechnik, Luft- und Raumfahrt, Schifffahrt sowie in der Medizintechnik werden diese Sensorsysteme eingesetzt, da mehrere Funktionen gleichzeitig nahezu intuitiv gesteuert werden können. Je nach Anforderung wird dort eine bestimmte Präzision (Auflösung), eine bestimmte Kraft zur Auslenkung sowie ein bestimmter Hub zur Bewältigung der notwendigen Wege fest oder in gering variablem Rahmen vorgegeben.

[0003] Probleme entstehen u.a. und insbesondere dort, wo es nicht möglich ist mit gleichbleibendem Kraft- und Hubaufwand ein solches Sensorsystem zu bedienen bzw. zu nutzen. Zu schwach ausgelegte Sensorsysteme werden bei zu hohem Kraft- und Hubaufwand zerstört. Sehr robust ausgelegte Sensorsysteme reagieren bei sehr geringem Kraft- und Hubaufwand nicht oder nur in nichtverwertbarem Rahmen. Gängige mechanische Sensorsysteme unterliegen zudem einer bekannten Abnutzung, welche ebenfalls oder auch von der Art der Nutzung abhängt. Des Weiteren werden handelsübliche Sensorsysteme z.B. mit einem Gummibalg um die Achse ausgestattet um das Eindringen von Fremd- und Schadstoffen in die Mechanik zu verhindern. Hierbei entsteht eine zusätzliche Problematik hinsichtlich einer eventuell notwendigen Reinigung oder Desinfektion gerade im medizintechnischen Bereich da ein Balg oder andere Schutzgummis schwierig zu desinfizieren sind.

[0004] Aus z.B. EP 1 696 300 A1 und GB 2 334 573 A sind Sensorsysteme (Joysticks) bekannt, welche Ihre Position anhand von Lichtsensoren ermitteln die wiederum mittels einer an der Achse befestigten Lichtquelle entsprechend angestrahlt werden. Die dort beschriebenen Zeilen oder Matrizen sind je nach Dichte der verbauten Lichtsensoren in Ihrer Auflösung eingeschränkt. Auch wird dort ein fest definierter Hub und eine ebenso fest definierte Kraft benötigt um den Federmechanismus bis in die gewünschte Position zu bringen. Nur der Einbau eines anderen Rückholmechanismus oder die zwangsläufige Verringerung der möglichen Auflösung durch einen geringeren Weg, würden dort einen bedingt variablen Einsatz zulassen. Insbesondere sehen diese Sensorsysteme lediglich zwei Achsen vor (X- und Y-Achse).

[0005] Aufgabe der vorliegenden Erfindung ist es daher, einen Dreiachsensensor bzw. ein Verfahren zur Positionsbestimmung eines Bewegungsträgers zur Verfügung zu stellen, welches die genannten Nachteile weitestgehend bzw. vollständig vermeidet.

[0006] Diese Aufgabe wird erfindungsgemäß durch die Vorrichtung gemäß Anspruch 1 sowie durch das Verfahren gemäß Anspruch 6 gelöst. Vorteilhafte Weiterbildungen der Erfindung sind in den abhängigen Ansprüchen dargestellt.

[0007] Die Erfindung schafft eine optische, lernende Dreiachsensensorik, welche jederzeit durch den Nutzer an die gewünschten Eingabekräfte angepasst werden kann. Eine Projektionseinheit (projiziert eine definierte geometrische Form auf einen Bildsensor. Wirken Kräfte auf die Kraftaufnahme ein, verändert sich die Neigung und/oder der Abstand des Bewegungsträgers zum Bildsensor. Die mit dem Bewegungsträger fest verbundene Projektionseinheit projiziert je nach Neigung und Druck verschiedene verzerrte geometrische Formen auf den Bildsensor, woraus eine Bildanalysesoftware entsprechende X-, Y- und Z-Koordinaten berechnet. Die individuelle Anpassung der Eingabekräfte kann mittels eines Lernprozesses erfolgen, bei welchem der Nutzer alle Richtungen einmal betätigt und somit der Bildanalyse mitteilt, welche Maxima erreicht wurden. Alle Richtungen werden dann durch sukzessive Approximation in homogene Ausgangssignale gewandelt und dem nachgeschalteten System angepasst. Es sind sowohl analoge als auch digitale Signale und Busprotokolle möglich. Durch Interpolation der

verzerrten geometrischen Formen kann die Auflösung mindestens um einen Faktor 100 oder mehr erhöht werden.

[0008] Die Erfindung wird unter Bezugnahme zweier Ausführungsbeispiele, welche in den Zeichnungsfiguren schematisch dargestellt sind, weiter erläutert.

[0009] Fig.1 zeigt den schematischen Schnitt des Dreiachsensensors mit einem Bewegungsträger 4, welcher in einem geschichteten Material 9 gelagert ist.

[0010] Fig.2 zeigt den schematischen Schnitt des Dreiachsensensors mit einem Bewegungsträger 4, welcher fest mit der Bildsensoreinheit 5, 6, 7, 8 verbunden ist.

[0011] Fig.3 zeigt das projizierte Abbild einer geometrischen Form in Ruheposition 10 und das Abbild einer verzerrten geometrischen Form 11 bei Krafteinwirkung über die Kraftaufnahme 2 auf den Bewegungsträger 4, in X-Richtung.

[0012] Fig.4 zeigt das projizierte Abbild einer geometrischen Form in Ruheposition 10 und das Abbild einer verzerrten geometrischen Form 11 bei Krafteinwirkung über die Kraftaufnahme 2 auf den Bewegungsträger 4, in X- und Y-Richtung.

[0013] Fig.5 zeigt das projizierte Abbild einer geometrischen Form in Ruheposition 10 und das Abbild einer verzerrten geometrischen Form 11 bei Krafteinwirkung über die Kraftaufnahme 2 auf den Bewegungsträger 4, in Z-Richtung.

[0014] Gemäß der Erfindung bereitgestellt wird demnach eine Dreiachsensensorik, aufweisend einem Bildsensor 6 (aus heutigem Stand der Technik CMOS, CCD oder 3D Chips) mit einer beliebig hohen Auflösung, einer an dem Bewegungsträger 4 befestigten Projektionseinrichtung 3 oder Reflektionsfläche und einer nachgeschalteten Bildanalyse. Die Projektionseinrichtung 3 oder Reflektionsfläche erzeugt hierbei eine definierte geometrische Form 10 (z.B. Quadrat), welche auf dem Bildsensor 6, in Abhängigkeit der sehr geringen Bewegung des Bewegungsträgers ein entsprechend verzerrtes und neu positioniertes Abbild 11 projiziert dadurch gekennzeichnet, dass die auch im folgenden dargestellte Bildanalyse insbesondere aus dieser Verzerrung und Position der Projektion 11, gegenüber der Ursprungsform 10, die Neigung (X- und Y-Achse) des Bewegungsträgers 4 ableiten kann und zudem auch den Druck, welcher orthogonal auf den Bewegungsträger 4 (Z-Achse) einwirkt, bemisst. Im Falle der Z-Achse verkleinert sich optisch bedingt das Abbild Fig.5, 11 der definierten geometrischen Ursprungsform Fig.5, 10 auf dem Bildsensor 6, da sich der Bewegungsträger 4 in diesem Fall dem Bildsensor 6 nähert. Nach der vollständigen Analyse der Einzelbilder, welche je nach Bildsensor 6 und Anwendungsbereich mindestens mit einer definierten Abtastrate (10 fps (frames per second)) erfolgt, werden für das Endgerät angepasste Signale oder Protokolle erstellt und ausgegeben.

[0015] Durch die extrem hohe Dichte der einzelnen Punkte auf dem Bildsensor 6 (nach aktuellem Stand der Technik ca. 5000x4000 Punkte) ist nur eine kaum durch den Menschen feststellbare und sehr geringe Neigung des Bewegungsträgers 4 nötig um eine entsprechende Veränderung 11 der Projektion auf dem Bildsensor 6 zu erzeugen. Bei o.g. Bildsensoren werden somit physikalische Auflösungen des Dreiachsensensors von ca. 2.000 digits in jede Bewegungsrichtung der X-, und Y-Achse möglich (Mittelposition in jede Richtung). Die Auflösung der Z-Achse ist optisch und mechanisch bedingt geringer und liegt bei ca. 200 digits. Durch die softwareseitige Interpolation werden bis zu 200.000 digits in X-, und Y-Bewegungsrichtung erreicht. Da die Lagerung bzw. die Materialeigenschaften des Bewegungsträgers 4 nach einem der Ansprüche 2 oder 3 einen exponentiellen Kraftaufwand erfordern um den Bewegungsträger 4 entsprechend zu neigen oder zu drücken wird ein weiter Einsatzbereich ermöglicht bei sehr hoher Auflösung. Inwieweit diese hohe Auflösung tatsächlich benötigt wird, hängt ganz vom Einsatzzweck ab und lässt sich softwareseitig individuell anpassen. Der beschriebene Dreiachsensensor lässt sich zu jeder Zeit neu kalibrieren bzw. dem Nutzer oder dem Einsatzzweck individuell anpassen (siehe Bildanalyse Anpassung). Insbesondere Personen, welche krankheitsbedingt nur inhomogene Kräfte aufbringen können (z.B. Muskeldystrophie, Muskelatrophie, Tetraplegie) oder deren Kräftevermögen einer temperatur- bzw. krankheitsbedingten dauernden oder temporären Änderung unterliegt, werden mit dem hier beschriebenen Dreiachsensensor

dauerhaft Steuerungsaufgaben vollziehen können (Rollstuhl, PC, Umwelt, etc.). Kostspielige, individuelle Anpassungen entfallen somit. Durch die sehr geringe Neigung des Bewegungsträgers, steigt die Gegenkraft der Mittelachse des Dreiachsensensors proportional zum Kraftaufwendung des Nutzers. Eine sonst nur schwierig und kostspielig umzusetzende Kraftrückkopplung (force feedback) wird somit ohne weitere Mechanik realisiert. Sofern ein Hub vom Nutzer gewünscht wird, kann dieser durch eine auf der Kraftaufnahme 2 befestigte Zugfeder simuliert werden. Die Möglichkeiten der Reinigung und Desinfektion (z.B. Einsatz in Operationssälen, oder Reinraumtechnik) sind ebenfalls optimiert, da keine Gelenke oder Achsen nötig sind. Auch der Betrieb der Dreiachsensensorik in Flüssigkeiten stellt kein Problem dar, da eine vollständige Kapselung vorliegt. Da der Dreiachsensensor optisch arbeitet, ist der Einsatz innerhalb elektromagnetischer Störfelder unproblematisch. Bauartbedingt benötigt der Dreiachsensensor keine beweglichen, bzw. gelagerten Teile, womit die Herstellung kostengünstig ausfällt. Mit dem vorliegenden Prototyp kann ein Eingangskräftespektrum von 0,01 N bis 100 N abgedeckt werden.

BILDVERARBEITUNG

[0016] Normalbetrieb:

[0017] 1. Laden eines einzelnen Bildes in den Arbeitsspeicher.

[0018] 2. Umwandlung des Bildes in ein Binärbild anhand eines definierten schwarz/weiß Schwellwertes.

[0019] 3. Suchen der geometrischen Form in dem Binärbild.

[0020] 4. Vergleich der erkannten geometrischen Form und Position 11 mit der Ursprungsform 10 (im Ruhezustand).

[0021] 5. Aus dem Grad der erkannten Position und Verzerrung 11 gegenüber der Ursprungsform 10 werden die Werte für die X/Y/Z-Veränderungen des Bewegungsträgers 4 errechnet.

[0022] 6. Anpassung der errechneten X/Y/Z-Werte an das gewünschte Eingangsformat des angeschlossenen Endgerätes, bzw. des Gerätes für die weitere Verarbeitung der Daten. Hierbei können sowohl analoge Werte, als auch digitale Werte oder Busprotokolle erzeugt werden.

[0023] Erster und einmaliger Initialisierungsprozess:

[0024] 1. Betätigung des Bewegungsträgers 4 mit maximal zulässigem Kraftaufwand in jede Achsrichtung.

[0025] 2. Bilderfassung wie im Normalbetrieb mit Speicherung der maximalen Positionen und Verzerrungen der erfassten geometrischen Form 11.

[0026] 3. Wird im Normalbetrieb die zuvor gespeicherte maximale Position oder die maximale Verzerrung der geometrischen Form 11 überschritten, werden entsprechend dem Endgerät Sicherheitsmaßnahmen eingeleitet (Totmann, Notaus, etc.).

[0027] Beliebig oft durchführbarer Lern- bzw. Anpassungsprozess durch den Nutzer:

[0028] 1. Betätigung des Bewegungsträgers 4 mit dem gewünschten Kraftaufwand in jede Richtung.

[0029] 2. Bilderfassung wie im Normalbetrieb mit Speicherung der maximalen individuellen Position und Verzerrung der erfassten geometrischen Form 11 für jede Achse, entsprechend der vom Nutzer aufgebrachten Kräfte.

[0030] 3. Die nun möglicherweise sehr inhomogene Kräfteeinwirkung auf den Bewegungsträger 4 durch den Nutzer in die verschiedenen Richtungen, wird softwaremäßig durch sukzessive Approximation in homogene Ausgangssignale umgewandelt. Somit kann sich der Dreiachsensensor zu jederzeit an den Nutzer höchst individuell anpassen.

VERWENDETE BEZUGSZEICHEN

1	Zuleitung
2	Kraftaufnahme
3	Projektionseinheit
4	Bewegungsträger
5	Abstandhalter
6	Bildsensor
7	Mikrocontroller
8	Platine
9	Geschichtetes Material
10	Ursprungsform
11	Verzerrte Form

Patentansprüche

1. Vorrichtung zur Drei-Achsen-Positionsbestimmung eines Kraftaufnahmeelements (2), aufweisend einen hochauflösenden Bildsensor (6), einen dem Bildsensor gegenüber angeordneten Bewegungsträger (4), der mit dem Kraftaufnahmeelement (2) verbunden ist, eine mit dem Bewegungsträger (4) verbundene Projektionseinrichtung (3), welche eine vordefinierte geometrische Form (10) auf den Bildsensor projiziert, wobei diese entsprechend der X/Y/Z-Neigung des Bewegungsträgers positioniert und verzerrt wird (11), sowie eine Recheneinrichtung (7), welche dazu eingerichtet ist, aus der Position und Verzerrung der geometrischen Form (10) hochauflösende X/Y/Z-Koordinaten zur weiteren Verarbeitung abzuleiten.

2. Vorrichtung nach Anspruch 1, **dadurch gekennzeichnet**, dass der Bewegungsträger (4) am Außenrand fest mit der Bildsensoreinheit (5, 6, 7, 8) verbunden ist und aus einem biegsamen Material besteht, welches sich bei Krafteinwirkung auf das Kraftaufnahmeelement (2) hinsichtlich ihres Neigungswinkel und ihrer Entfernung zum Bildsensor (6) verformt.

3. Vorrichtung nach Anspruch 1, **dadurch gekennzeichnet**, dass der Bewegungsträger (4) in einem geschichteten Material (9) eingelagert ist, welches schichtweise verschiedene Dichte und/oder Viskosität aufweist und bei Krafteinwirkung auf das Kraftaufnahmeelement (2) hinsichtlich ihres Neigungswinkel und ihrer Entfernung zum Bildsensor (6) verformbar ist.

4. Vorrichtung nach einem der Ansprüche 1 bis 3, **dadurch gekennzeichnet**, dass die Projektionseinrichtung (3) mit dem Bewegungsträger (4) fest verbunden ist und die vordefinierte geometrische Form (10) direkt auf den Bildsensor (6) projiziert.

5. Vorrichtung nach einem der Ansprüche 1 bis 3, **dadurch gekennzeichnet**, dass der Bewegungsträger (4) fest mit einer Reflektionsfläche (3) verbunden ist, welche bei Beleuchtung mit der Projektionseinrichtung (3) die vordefinierte geometrische Form indirekt auf den Bildsensor (6) projiziert.

6. Verfahren zur Drei-Achsen-Positionsbestimmung eines Kraftaufnahmeelements (2) in einer Vorrichtung nach Anspruch 1, **dadurch gekennzeichnet**, dass von einem Nutzer auf das Kraftaufnahmeelement (2) inhomogen angewandte Kräfte durch sukzessive Approximation in homogene Ausgangssignale, passend zum angeschlossenen Endgerät, umgewandelt werden.

7. Verfahren nach Anspruch 6, **dadurch gekennzeichnet**, dass es dem Nutzer ermöglicht, zu jeder Zeit den Dreiachsensensor mit dem gerade gewünschten Kraftaufwand über das Kraftaufnahmeelement (2) neu zu kalibrieren.

8. Verfahren nach Anspruch 1, **dadurch gekennzeichnet**, dass eine Bildanalysesoftware in Echtzeit die vordefinierte geometrische Form (10, 11) in jedem aufgenommenen Bild des Bildsensors sucht, dessen Form hinsichtlich Position und Verzerrungen (11) analysiert, und daraus die entsprechende Neigung und die orthogonale Veränderung des Bewegungsträgers (4) zum Bildsensor (6) ableitet.

9. Verfahren nach Anspruch 8, **dadurch gekennzeichnet**, dass vor der ersten Nutzung der Dreiachsensensorik ein Initialisierungsprozess stattfindet, bei dem alle möglichen Richtungen des Bewegungsträgers (4) X/Y/Z mindestens einmal mit einer vorbestimmten, maximal zulässigen Kraft über das Kraftaufnahmeelement (2) betätigt werden, wodurch der Bildanalysesoftware die maximal zulässige Position und Verzerrungen der vordefinierten geometrischen Form (11) dargestellt werden.

10. Verfahren nach Anspruch 9, **dadurch gekennzeichnet**, dass die Bildanalysesoftware in Echtzeit die vordefinierte geometrische Form (10,11) in jedem aufgenommenen Bild des Bildsensors sucht und dessen Form hinsichtlich Position und Verzerrungen (11) analysiert, und anhand dessen eine Plausibilitätsprüfung durchführt, inwieweit die erkannte Form (11) den maximal zulässigen Positionen und Verzerrungen entspricht.

11. Verfahren nach einem der Ansprüche 9 und 10, **dadurch gekennzeichnet**, dass die Bildanalysesoftware in Echtzeit bei erkannten unzulässigen Positionen oder Verzerrungen (11) Maßnahmen zum Schutz angeschlossener Endgeräte vor Fehlfunktionen auslöst, wie Totmann- oder Notausschaltung.
12. Verfahren nach Anspruch 8, **dadurch gekennzeichnet**, dass die Bildanalysesoftware in Echtzeit durch Interpolation der erkannten geometrischen Form (11) die daraus abgeleitete Auflösung für die daraus resultierenden X/Y/Z-Koordinaten erhöht.
13. Vorrichtung nach Anspruch 1, **dadurch gekennzeichnet**, dass der Bewegungsträger (4) als ein hermetischer Abschluss zum Inneren der Vorrichtung ausgeführt ist, wodurch ein Betrieb in Flüssigkeiten ermöglicht wird.

Hierzu 2 Blatt Zeichnungen

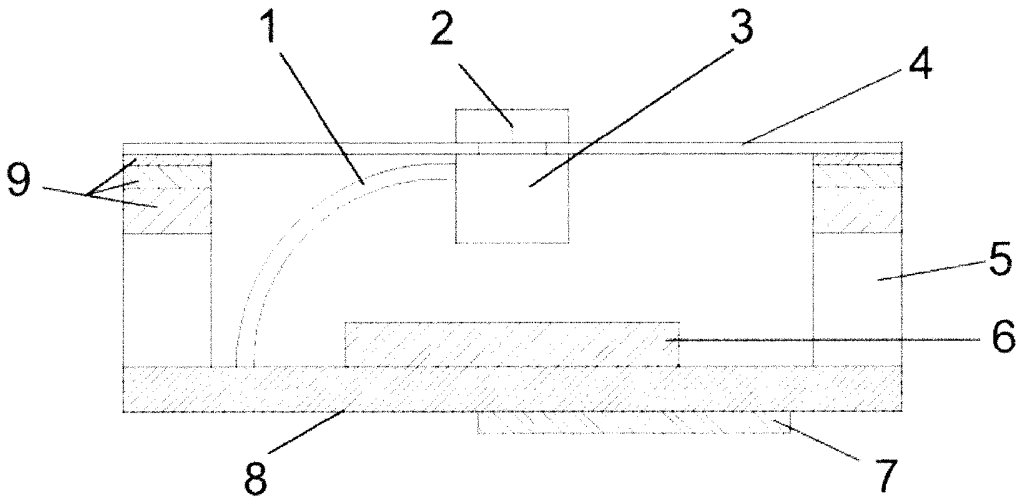

Fig. 1

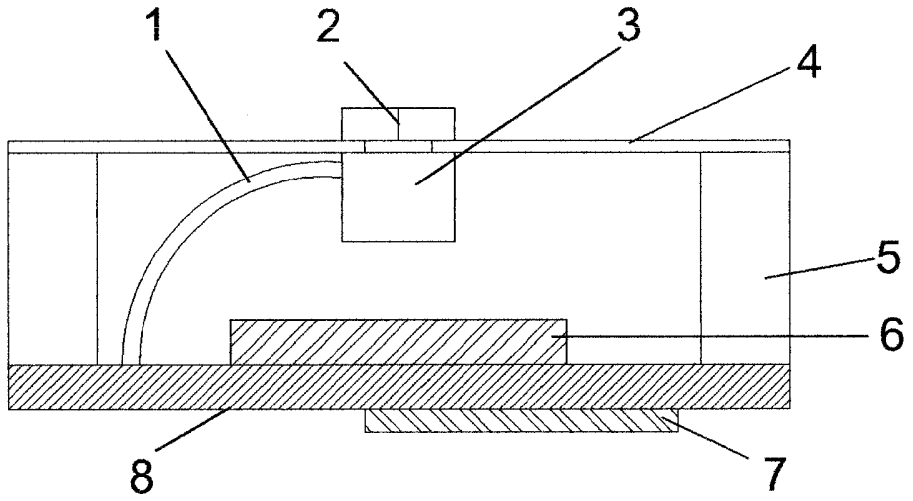

Fig. 2

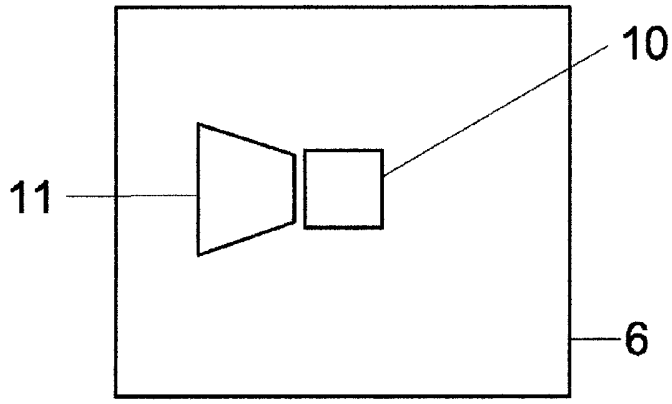

Fig. 3

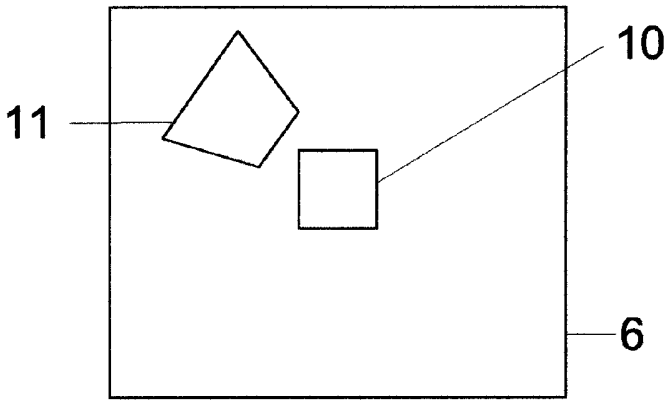

Fig. 4

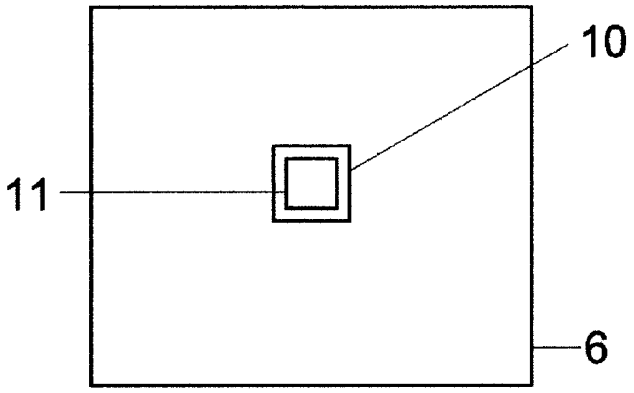

Fig. 5

7.2.2 PCT Application

(29 pages)

(12) NACH DEM VERTRAG ÜBER DIE INTERNATIONALE ZUSAMMENARBEIT AUF DEM GEBIET DES PATENTWESENS (PCT) VERÖFFENTLICHTE INTERNATIONALE ANMELDUNG

(19) Weltorganisation für geistiges Eigentum
Internationales Büro

(43) Internationales Veröffentlichungsdatum
9. März 2017 (09.03.2017)

WIPO | PCT

(10) Internationale Veröffentlichungsnummer
WO 2017/037048 A1

(51) Internationale Patentklassifikation:
G05G 9/047 (2006.01)

(21) Internationales Aktenzeichen: PCT/EP2016/070390

(22) Internationales Anmeldedatum:
30. August 2016 (30.08.2016)

(25) Einreichungssprache: Deutsch

(26) Veröffentlichungssprache: Deutsch

(30) Angaben zur Priorität:
A 571/2015 31. August 2015 (31.08.2015) AT

(72) Erfinder; und
(71) Anmelder : **BUCHHOLD, Niels** [DE/AT]; Sankt-Nikolausgasse 13, 6020 Innsbruck (AT).

(72) Erfinder: **BAUMGARTNER, Christian**; Burggasse 5, 8010 Graz (AT).

(74) Anwalt: **PATENTANWALTSKANZLEI MATSCHNIG & FORSTHUBER OG**; 36 Biberstraße 22, 1010 Wien (AT).

(81) Bestimmungsstaaten *(soweit nicht anders angegeben, für jede verfügbare nationale Schutzrechtsart)*: AE, AG, AL, AM, AO, AT, AU, AZ, BA, BB, BG, BH, BN, BR, BW, BY, BZ, CA, CH, CL, CN, CO, CR, CU, CZ, DE, DK, DM, DO, DZ, EC, EE, EG, ES, FI, GB, GD, GE, GH, GM, GT, HN, HR, HU, ID, IL, IN, IR, IS, JP, KE, KG, KN, KP, KR, KZ, LA, LC, LK, LR, LS, LU, LY, MA, MD, ME, MG, MK, MN, MW, MX, MY, MZ, NA, NG, NI, NO, NZ, OM, PA, PE, PG, PH, PL, PT, QA, RO, RS, RU, RW, SA, SC, SD, SE, SG, SK, SL, SM, ST, SV, SY, TH, TJ, TM, TN, TR, TT, TZ, UA, UG, US, UZ, VC, VN, ZA, ZM, ZW.

(84) Bestimmungsstaaten *(soweit nicht anders angegeben, für jede verfügbare regionale Schutzrechtsart)*: ARIPO (BW, GH, GM, KE, LR, LS, MW, MZ, NA, RW, SD, SL, ST, SZ, TZ, UG, ZM, ZW), eurasisches (AM, AZ, BY, KG, KZ, RU, TJ, TM), europäisches (AL, AT, BE, BG, CH, CY, CZ, DE, DK, EE, ES, FI, FR, GB, GR, HR, HU, IE, IS, IT, LT, LU, LV, MC, MK, MT, NL, NO, PL, PT, RO, RS, SE, SI, SK, SM, TR), OAPI (BF, BJ, CF, CG, CI, CM, GA, GN, GQ, GW, KM, ML, MR, NE, SN, TD, TG).

Veröffentlicht:

— *mit internationalem Recherchenbericht (Artikel 21 Absatz 3)*

(54) **Title**: DEVICE AND METHOD FOR DETERMINING THE POSITION OF A FORCE-ABSORBING ELEMENT IN THREE AXES

(54) **Bezeichnung** : VORRICHTUNG UND VERFAHREN ZUR DREI-ACHSEN-POSITIONSBESTIMMUNG EINES KRAFTAUFNAHMEELEMENTS

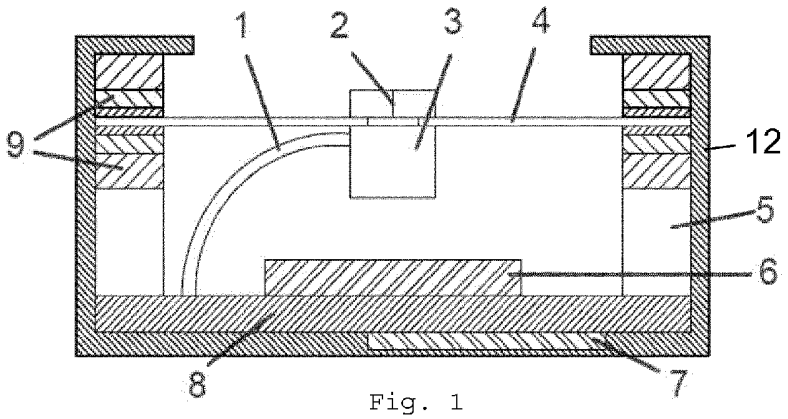

Fig. 1

(57) **Abstract**: A device for determining the position of a force-absorbing element (2) in three axes comprises a high-resolution image sensor (6), a movement support (4) which is arranged opposite the image sensor and is connected to the force-absorbing element (2), a projection device (3) which is connected to the movement support (4) and projects, onto the image sensor, a predefined geometric shape (10) which is positioned and distorted according to an x/y/z inclination of the movement support. A computing device (7) derives, from the position and distortion of the geometric shape (10), high-resolution x/y/z coordinates for further processing.

(57) **Zusammenfassung**: Eine Vorrichtung zur Drei-Achsen-Positionsbestimmung eines Kraftaufnahmeelements (2) umfasst einen hochauflösenden Bildsensor (6), einen dem Bildsensor gegenüber angeordneten Bewegungsträger (4), der mit dem Kraftaufnahmeelement (2) verbunden ist, eine mit dem Bewegungsträger (4) verbundene Projektionseinrichtung

[Fortsetzung auf der nächsten Seite]

WO 2017/037048 A1

(3), welche auf den Bildsensor eine vordefinierte geometrische Form (10) projiziert, die entsprechend einer X/Y/Z-Neigung des Bewegungsträgers positioniert und verzerrt wird. Eine Recheneinrichtung (7) leitet aus der Position und Verzerrung der geometrischen Form (10) hochauflösende X/Y/Z-Koordinaten zur weiteren Verarbeitung ab.

Vorrichtung und Verfahren zur Drei-Achsen-Positionsbestimmung eines Kraftaufnahmeelements

Die Erfindung betrifft eine Sensorvorrichtung mit einer optischen, lernfähigen Dreiachsensensorik, sowie ein Verfahren zur Positionsbestimmung eines Kraftaufnahmeelements (zumindest) hinsichtlich dreier Achsen.

Mehrachsensensoren im Allgemeinen und unter anderem auch Zweiachsensensoren (Joysticks, etc.) finden ihren Einsatz in sämtlichen privaten und industriellen Bereichen. Auch in den Bereichen Automobiltechnik, Luft- und Raumfahrt, Schifffahrt sowie in der Medizintechnik werden diese Sensorsysteme eingesetzt, da mehrere Funktionen gleichzeitig nahezu intuitiv gesteuert werden können. Je nach Anforderung wird dort eine bestimmte Präzision (Auflösung), eine bestimmte Kraft zur Auslenkung sowie ein bestimmter Hub zur Bewältigung der notwendigen Wege fest oder in gering variablem Rahmen vorgegeben.

Probleme entstehen insbesondere dort, wo es nicht möglich ist, mit gleichbleibendem Kraft- und Hubaufwand ein solches Sensorsystem zu bedienen bzw. zu nutzen. Zu schwach ausgelegte Sensorsysteme werden bei zu hohem Kraft- und Hubaufwand zerstört. Sehr robust ausgelegte Sensorsysteme reagieren bei sehr geringem Kraft- und Hubaufwand nicht oder nur in einem nichtverwertbarem Ausmaß. Herkömmliche mechanische Sensorsysteme unterliegen zudem einer Abnutzung. Des Weiteren werden handelsübliche Sensorsysteme z.B. mit einem Gummibalg um die Achse ausgestattet, um das Eindringen von Fremd- und Schadstoffen in die Mechanik zu verhindern. Hierbei entsteht eine zusätzliche Problematik hinsichtlich einer eventuell notwendigen Reinigung oder Desinfektion, besonders im medizintechnischen Bereich, da ein Balg oder andere Schutzgummis schwierig zu reinigen bzw. desinfizieren sind.

Aus z.B. EP 1 696 300 A1 und GB 2 334 573 A sind Sensorsysteme (Joysticks) bekannt, welche ihre Position anhand von Lichtsensoren ermitteln, die wiederum mittels einer an der Achse befestigten Lichtquelle entsprechend angestrahlt werden. Die dort beschriebenen Zeilen oder Matrizen sind je nach Dichte der verwendeten Lichtsensoren in ihrer Auflösung eingeschränkt. Auch wird dort ein vordefinierter Hub und eine vordefinierte Kraft benötigt, um den Federmechanismus bis in die gewünschte Position zu bringen. Außerdem sehen diese Sensorsysteme lediglich zwei Achsen vor (X- und Y-Achse).

Aufgabe der vorliegenden Erfindung ist es daher, einen Dreiachsensensor bzw. ein Verfahren zur Positionsbestimmung eines Bewegungsträgers zur Verfügung zu stellen, welches die genannten Nachteile vermeidet. Zudem soll ein Anpassen des Sensors an die gewünschten Eingabekräfte und den gewünschten Bewegungshub ermöglicht werden.

Diese Aufgabe wird erfindungsgemäß durch die Vorrichtung gemäß Anspruch 1 sowie durch das Verfahren gemäß Anspruch 6 gelöst. Vorteilhafte Weiterbildungen der Erfindung sind in den abhängigen Ansprüchen dargestellt.

Die Erfindung schafft eine optische, lernfähige bzw. anpassungsfähige Dreiachsensensorik, welche jederzeit durch den Nutzer an die gewünschten Eingabekräfte und den gewünschten Bewegungshub angepasst werden kann. Eine Projektionseinheit projiziert eine definierte geometrische Form auf einen Bildsensor. Wirken Kräfte auf die Kraftaufnahme ein, verändert sich die Neigung und/oder der Abstand des Bewegungsträgers zum Bildsensor. Die mit dem Bewegungsträger fest verbundene Projektionseinheit projiziert je nach Neigung und Druck verschiedene verzerrte geometrische Formen auf dem Bildsensor, woraus eine Bildanalysesoftware entsprechende X-, Y- und Z-Koordinaten berechnet.

Der Projektionseinheit ist eine Lichtquelle (z.B. LED oder Laser) zugeordnet; beispielsweise beinhaltet die Projektionseinheit selbst die Lichtquelle. Der Lichtquelle kann vorteilhafter Weise eine Optik nachgeschaltet sein (z.B. Plankonvexlinse, Kollimatorlinse und /oder Schablone zur Erzeugung einer geometrischen Figur), welche auf dem Bildsensor eine entsprechende geometrische Form projiziert. Diese Lichtfigur bzw. Projektion kann eine beliebige geometrische Form annehmen, aber auch aus Punkten bestehen. Wird als Lichtquelle ein Laser genutzt, kann auf eine formgebende Schablone verzichtet werden, da als Lichtfigur naturgemäß eine Kreisscheibe (ausgefüllter Kreis) entsteht.

Die individuelle Anpassung der Eingabekräfte kann vorprogrammiert sein oder mittels eines Lernprozesses erfolgen, bei welchem der Nutzer alle Richtungen einmal betätigt und somit der Bildanalyse mitteilt, welche Maxima erreicht wurden. Alle dann erkannten Koordinaten werden durch sukzessive Approximation in geeignete Ausgangssignale für das nachgeschaltete System gewandelt. Es sind sowohl analoge als auch digitale Signale und Busprotokolle als Ausgangssignal möglich. Durch Interpolation der verzerrten geometrischen Formen kann die Auflösung der erkannten Koordinaten um den Faktor 100 erhöht werden, in Abhängigkeit von der Qualität des eingesetzten Bildsensors.

Die Erfindung wird im Folgenden unter Bezugnahme auf nicht einschränkend zu verstehende Ausführungsbeispiele, welche in den beigelegten Zeichnungen schematisch dargestellt sind, weiter erläutert.

Fig.1 zeigt einen Dreiachsensensor gemäß einem ersten Ausführungsbeispiel in einer Schnittansicht entlang der Mittelachse des Sensors.

Fig.2 zeigt einen Dreiachsensensor gemäß einem zweiten Ausführungsbeispiel in einer Schnittansicht entlang der Mittelachse des Sensors.

Fig.3 zeigt das projizierte Abbild einer geometrischen Form in Ruheposition und das Abbild einer verzerrten geometrischen Form bei Krafteinwirkung über die Kraftaufnahme auf den Bewegungsträger in X-Richtung.

Fig.4 zeigt das projizierte Abbild einer geometrischen Form in Ruheposition und das Abbild einer verzerrten geometrischen Form bei Krafteinwirkung über die Kraftaufnahme auf den Bewegungsträger in einer Richtung diagonal zur X- und Y-Richtung.

Fig.5 zeigt das projizierte Abbild einer geometrischen Form in Ruheposition und das Abbild einer verzerrten geometrischen Form bei Krafteinwirkung über die Kraftaufnahme auf den Bewegungsträger in Z-Richtung.

Fig. 6 zeigt vier Beispiele von Lichtfiguren.

Fig. 7a zeigt eine Variante der Sensorvorrichtung der Fig. 1 mit horizontal geschichtetem Material der Trägerhalterung.

Fig. 7b zeigt eine andere Variante der Sensorvorrichtung mit vertikal geschichtetem Material der Trägerhalterung.

Fig. 8 zeigt eine weitere Ausführungsform der Erfindung, mit einem Gelenklager zur bewegbaren Halterung in des Kraftaufnahmeelements und der Projektionseinrichtung.

Fig. 9 zeigt eine weitere Ausführungsform mit einer Reflektionsfläche zur Erzeugung der Lichtfigur.

Gemäß der Erfindung wird eine Dreiachsensensorik vorgeschlagen, aufweisend einen Bildsensor, einer an dem Bewegungsträger befestigten Projektionseinrichtung oder

Reflektionsfläche und einer dem Bildsensor nachgeschalteten Recheneinheit mit Bildanalysesoftware.

Bezugnehmend auf Fig.1 umfasst ein Dreiachsensensor gemäß einem ersten Ausführungsbeispiel ein Kraftaufnahmeelement 2, das z.B. die Form einer Taste oder eines Stabes haben kann. Ein Träger (Bewegungsträger) 4 trägt z.B. außenseitig das Kraftaufnahmeelement 2 und ist hier als starre Platte ausgebildet. Der Bewegungsträger 4 ist z.B. in einem geschichteten Material 9 gelagert, das über Seitenteile (Abstandhalter) 5 mit einem Bodenteil 8 verbunden, das hier z.B. von einer Platine gebildet ist, die zudem mit der bereits erwähnten Recheneinheit 7 (z.B. einem Mikrocontroller) ausgestattet ist. Die Recheneinheit kann in einer Variante auch gesondert von der Sensorvorrichtung vorgesehen sein. Der Dreiachsensensor weist zudem eine von dem Träger 4 gehaltene Projektionseinrichtung 3 auf, sowie einen Bildsensor 6 (z.B. ein CMOS, CCD oder 3D Chip), der auf dem Bodenteil 8 positioniert ist. Über eine Zuleitung 1, z.B. in Form eines flexiblen Kabels, wird die Projektionseinheit 3 elektrisch versorgt.

Während des Betriebs ist die Projektionseinrichtung 3 mit dem Kraftaufnahmeelement 2 starr verbunden und folgt somit den Bewegungen des letzteren. Das Schichtmaterial 9 kann beispielsweise aus einem Polymer, wie z.B. additionsvernetztem Silikon, bestehen. Durch die Schichtung verschiedener Polymere mit wiederum verschiedener Dichte und/oder Festigkeit (Elastizitätsmodul) und/oder Viskosität kann das geschichtete Material ein großes Eingabekraftspektrum, z.B. 0,01N bis 50N, aufnehmen. Hierbei wird bei kleinen Kräften, welche auf die Kraftaufnahme 2 einwirken, zunächst nur das weiche Polymer komprimiert und mit zunehmenden Kräften die weiteren härteren Schichten. Die auf die Kraftaufnahme 2 einwirkenden Kräfte erzeugen eine umgekehrt exponentielle Auslenkung des projizierten Bildes 11 (Fig. 3-5) auf dem Bildsensor 6.

Fig.2 zeigt eine zweite Ausführungsform den schematischen Schnitt des Dreiachsensensors mit einem Bewegungsträger 4, welcher fest mit der Bildsensoreinheit 6 über Seitenteile 5 und dem Bodenteil 8 verbunden ist. In dieser Ausführung ist der Träger 4 biegsam, vorzugsweise elastisch verformbar; beispielsweise ist er aus einem verformbaren Material hergestellt, wie z.B. aus Polymer, Kunststoff, CFK, GFK oder Metall (z.B. einer Metallfolie). Die Materialauswahl hängt von dem gewünschten Einsatzgebiet ab. Wird beispielsweise eine maximale Krafteinwirkung von 30N auf den Kraftaufnehmer 2 gewünscht wird ein Federstahl eingesetzt. Um ein geringere Kräfte bis 5N aufzunehmen wird beispielsweise ein CFK oder Kunststoff Bewegungsträger 4 eingebaut.

Der erfindungsgemäße Dreiachsensensor kann zusätzlich in einem Gehäuse 12 untergebracht sein, wie am Beispiel der Fig. 1 ersichtlich ist. Das Gehäuse ist in Fig. 2 und 7-9 der deutlicher Darstellung halber nicht gezeigt.

Die Schichtung des Materials kann horizontal ausgeführt sein, wie in Fig. 7a gezeigt ist, oder vertikal, wie in Fig. 7b. Entsprechend dem Anwendungsgebiet kann auf eine Schichtung des Materials verzichtet werden und nur ein Material eingebracht werden. Hierdurch wird die Differenz zwischen den Werten der aufzubringenden Kraft für den minimalen und maximalen Hub verringert.

Wie in Fig. 3 bis 5 illustriert ist, wird durch die Projektionseinrichtung 3 oder Reflektionsfläche (siehe Fig. 9) eine definierte geometrische Form 10 erzeugt (z.B. Quadrat, Kreis, in beliebiger geometrischer Form angeordnete Punkte, siehe die vier in Fig. 6 gezeigten Beispiele), welche auf dem Bildsensor 6, in Abhängigkeit der Bewegung bzw. Auslenkung des Bewegungsträgers ein entsprechend verzerrtes und neu positioniertes Abbild 11 projiziert. Dadurch kann die Bildanalysesoftware der Recheneinheit 7 aus dieser Verzerrung

und Position der Projektion 11, gegenüber der Ursprungsform 10, die X-, Y- und Z- Koordinaten der Projektion 11 ableiten. Fig. 3 zeigt beispielhaft eine Verzerrung/Verschiebung infolge Bewegung bzw. Auslenkung in der X-Richtung, und Fig. 4 bei einer diagonalen Auslenkung. Im Falle der Z-Achse verändert sich optisch bedingt das Abbild 11 wie beispielhaft in Fig.5 gezeigt, z.B. verkleinert sich das Abbild 11 da sich der Bewegungsträger 4 in diesem Fall dem Bildsensor 6 nähert. Nach der vollständigen Analyse der Einzelbilder, werden für das nachfolgende System Signale oder Protokolle erstellt und ausgegeben.

Die Abtastrate des Bildsensors erfolgt mit einer dem nachgeschalteten System angepassten Geschwindigkeit (fps, frames per second). Um ein sicherheitsrelevantes Nachfolgesystem anzusteuern (z.B. medizinische Geräte, Flugzeug, Auto) ist eine hohe Abtastrate notwendig (mindestens 40 fps). Wird der Sensor im Consumer-Bereich eingesetzt (z.B. Computerspiele) kann die Abtastrate auf 10-20 fps abgesenkt werden.

Der Bildsensor 6 ist bevorzugt Weise ein hochauflösender Sensor. Durch die hohe Dichte der einzelnen Punkte auf dem Bildsensor 6 ist nur eine kaum durch den Menschen feststellbare und sehr geringe Neigung des Bewegungsträgers 4 nötig, um eine entsprechende Veränderung 11 der Projektion auf dem Bildsensor 6 zu erzeugen. Durch softwareseitige Interpolation kann zudem die Auflösung der erkannten Koordinaten erhöht werden, beispielsweise um einen Faktor von mindestens 100. Da die Lagerung bzw. die Materialeigenschaften des Bewegungsträgers 4 bevorzugt einen exponentiellen Kraftaufwand erfordern, um den Bewegungsträger 4 entsprechend zu neigen und/oder zu drücken, wird ein weiter Einsatzbereich bezüglich der aufzuwendenden Eingabekräfte ermöglicht. Inwieweit diese hohe Auflösung tatsächlich benötigt wird, hängt vom Einsatzzweck ab und lässt sich softwareseitig individuell anpassen.

Der beschriebene Dreiachsensensor lässt sich zu jeder Zeit neu kalibrieren bzw. dem Nutzer oder dem Einsatzzweck individuell anpassen (siehe weiter unten zur Bildanalyse-Anpassung). Insbesondere Personen, welche den Sensor krankheitsbedingt mit verschiedenen Kräften in jede Richtung betätigen (z.B. Muskeldystrophie, Muskelatrophie, Tetraplegie) oder deren Kräftevermögen einer temperatur- bzw. krankheitsbedingten dauernden oder temporären Änderung unterliegt, werden mit dem hier beschriebenen Dreiachsensensor dauerhaft Steuerungsaufgaben vollziehen können (Rollstuhl, PC, Umwelt, etc.). Kostspielige, individuelle Anpassungen entfallen somit.

Die Lernfähigkeit des optischen Sensors soll nachfolgend anhand eines Beispiels erklärt werden, wobei hierbei nur eine Auslenkungsrichtung beschrieben wird, welche sich analog zu den übrigen Richtungen verhält.

Ausgehend von einem X,Y-Koordinatensystem befindet sich der Mittelpunkt der von der Recheneinheit gefundenen geometrischen Form Fig. 6 auf der Position (0,0) im Ruhezustand (in der Mitte des Sensors). Hat der Bildsensor beispielsweise eine maximale Auflösung 5000x5000 Bildpunkten, stehen für jede Richtung (vom Mittelpunkt ausgehend) 2500 Bildpunkte zur Verfügung. Erreicht der Nutzer während dem Lernprozess beispielsweise maximal 500 Bildpunkte nach rechts, multipliziert die Recheneinheit im Normalbetrieb mit dem Faktor 5 um ein volles Ausgangssignal bei maximal möglicher Auslenkung durch den Nutzer zu erreichen (5x500=2500). Die übrigen Richtungen werden analog dazu berechnet, wodurch beliebig ungleiche Eingabekräfte stets zu einem optimierten Ausgangssignal umgerechnet werden.

Weitere Anwendungen sind beispielsweise in den Bereichen Aviation und Automotive denkbar. Hierbei steht die Störsicherheit im Vordergrund. Da EMI und RFI keinen Einfluss auf die hier beschriebene Projektion haben, wäre ein solches

System zur Steuerung prädestiniert. Zudem entfällt der Aspekt der Abnutzung.

Auch in geophysikalischen Bereichen kann der optische Sensor aufgrund seiner hohen Auflösung (z. B. nach aktuellem Stand der Technik 19.580 x 12.600 Bildpunkte) eingesetzt werden. Hierbei könnten geringste relative Bewegungen der Erdkruste erkannt werden. Bei der oben genannten Auflösung und einem Bildsensordiagonalen von 1 Zoll entspricht 1mm Auslenkung der Projektion 11 bereits ca. 770 Bildpunkten. Wird dazu noch ein Hebelsystem eingesetzt, erhöhen sich die Auslenkung (gemessen in Bildpunkten) beliebig. Zudem erhöht sich die Auflösung durch Interpolation der gefundenen geometrischen Form. In diesem Einsatzgebiet kann auf das geschichtete Material 9 verzichtet und die Projektionseinheit direkt über ein Gelenklager angesteuert werden, wie in Fig. 8 gezeigt ist. In dieser Ausführungsvariante sind das Kraftaufnahmeelement 2, z.B. als Knopf ausgebildet, und die Projektionseinrichtung 3 durch eine Achse 13 verbunden, die durch ein Gelenklager 14 geführt ist. Bei Krafteinwirkung auf den Knopf (durch den Doppelfeil in Fig. 8 angedeutet) wird die Achse 13 in dem Gelenklager 14 verkippt, wodurch die Projektionseinrichtung 3 ausgelenkt wird und wie bereits beschrieben eine Änderung der Lichtfigur 10, 11 erzeugt.

In anderen Ausgestaltungen der Erfindung kann die Projektionseinrichtung als optische Einrichtung, z. B. ein Spiegel oder ein anderes optisch wirksames Element, ausgebildet sein, das ein von einer Quelle erzeugtes Lichtbild als Lichtfigur auf den Sensor lenkt.

Fig. 9 zeigt eine Ausführungsform mit einer optischen Einrichtung, im gezeigten Fall einen Spiegel 31, mit dem der Bewegungsträger 4 fest verbunden ist. Eine Lichtquelle 30, die beispielsweise auf dem Bodenteil 8 neben dem Sensor 6 angeordnet sein kann, erzeugt einen Lichtstrahl L (z. B.

Laser-Strahl), und beleuchtet über diesen Spiegel 31 den Sensor 6. Auf diese Weise wird die vordefinierte geometrische Form indirekt über die Reflektionsfläche auf den Bildsensor (6) projiziert, aufgrund dessen die weitere Auswertung der Lichtfigur wie weiter oben beschrieben erfolgt.

Ein weiteres mögliches Material für einige oder alle Komponenten der erfindungsgemäßen Vorrichtung ist Silikonkautschuk mit ausreichender Materialsteifigkeit, welcher in geeigneten Metallformen vulkanisiert wird, beispielsweise in einem Formpressverfahren; geeignete Formpressverfahren sind aus dem Stand der Technik wohlbekannt.

Im Gegensatz zu bislang eingesetzten Sensortechniken (kapazitiv, induktiv und resistiv), bietet der optische Sensor hohe Genauigkeit, sehr gute Positionsreproduzierbarkeit und unterliegt keiner Abnutzung bei hoher Störsicherheit.

Durch die sehr geringe Neigung des Bewegungsträgers, steigt bedingt durch das Elastizitätsmodul des Bewegungsträgers 4 die Gegenkraft des Dreiachsensensors proportional zur Kraftaufwendung des Nutzers. Eine sonst nur schwierig und kostspielig umzusetzende Kraftrückkopplung (force feedback) wird somit ohne weitere Mechanik realisiert. Sofern ein Hub vom Nutzer gewünscht wird, kann dieser beispielsweise durch eine auf der Kraftaufnahme 2 befestigte Zugfeder (Knickelement) simuliert werden. Diese verbiegt sich je nach Krafteinwirkung und simuliert so einen Bewegungshub. Die Möglichkeiten der Reinigung und Desinfektion (z.B. Einsatz in Operationssälen, oder Reinraumtechnik) sind ebenfalls optimiert, da eine vollständige Kapselung durch das geschichtete Material 9, bzw. dem Bewegungsträger 4 zusammen mit den Seitenteilen 5 bzw. einem Gehäuse 12 vorliegt. Auch der Betrieb der Dreiachsensensorik in Flüssigkeiten stellt somit kein Problem dar. Durch den einfachen Aufbau des Dreiachsensensors fällt die Herstellung kostengünstig aus. Mit

dem vorliegenden Prototyp kann ein Eingangskräftespektrum von 0,01 N bis 250 N abgedeckt werden.

Nachstehend sind in Kürze beispielhafte Abläufe der Bildverarbeitung und der Konfigurierung der erfindungsgemäßen Vorrichtung dargestellt.

Normalbetrieb:

1. Laden eines einzelnen Bildes in den Arbeitsspeicher.

2. Umwandlung des Bildes in ein Binärbild anhand eines definierten schwarz/weiß Schwellwertes.

3. Suchen der geometrischen Form in dem Binärbild.

4. Vergleich der erkannten geometrischen Form und Position 11 mit der Ursprungsform 10 (im Ruhezustand).

5. Aus dem Grad der erkannten Position und Verzerrung 11 gegenüber der Ursprungsform 10 werden die Werte der aktuellen X/Y/Z-Koordinaten errechnet.

6. Anpassung der errechneten X/Y/Z-Werte an das gewünschte Eingangsformat des angeschlossenen Endgerätes, bzw. des Gerätes für die weitere Verarbeitung der Daten. Hierbei können sowohl analoge Werte, als auch digitale Werte oder Busprotokolle erzeugt werden.

Erster und einmaliger Initialisierungsprozess:

1. Betätigung des Bewegungsträgers 4 mit maximal zulässigem Kraftaufwand in jede Achsrichtung.

2. Bilderfassung wie im Normalbetrieb mit Speicherung der maximalen Positionen und Verzerrungen der erfassten geometrischen Form 11.

3. Wird im Normalbetrieb die zuvor gespeicherte maximale Position oder die maximale Verzerrung der geometrischen Form 11 überschritten, wird ein digitaler Ausgang aktiviert um beispielsweise einen elektrischen Rollstuhl zu stoppen.

Beliebig oft durchführbarer Lern- bzw. Anpassungsprozess durch den Nutzer:

1. Betätigung des Bewegungsträgers 4 mit dem gewünschten Kraftaufwand in jede Richtung.

2. Bilderfassung wie im Normalbetrieb mit Speicherung der maximalen individuellen Position und Verzerrung der erfassten geometrischen Form 11 für jede Achse, entsprechend der vom Nutzer aufgebrachten Kräfte.

3. Die nun möglicherweise sehr unterschiedliche Kräfteeinwirkung auf den Bewegungsträger 4 durch den Nutzer in die verschiedenen Richtungen, wird softwaremäßig durch sukzessive Approximation, sowie durch Multiplikation mit einem entsprechend dem Eingangssignal errechneten Faktors in gleichförmige Ausgangssignale umgewandelt. Der Nutzer ist dann in der Lage, trotz unterschiedlicher Eingabekräfte (z.B. 0,03N nach rechts, 0,1N nach links, 1N nach oben, 0,5N nach unten) ein nachfolgendes System (z.B. elektrischer Rollstuhl) in jede Richtung mit der gleichen Geschwindigkeit bzw. Drehgeschwindigkeit zu steuern. Somit kann sich der Dreiachsensensor zu jederzeit an den Nutzer individuell anpassen.

Patentansprüche

1. Vorrichtung zur Drei-Achsen-Positionsbestimmung eines Kraftaufnahmeelements (2), aufweisend einen Bildsensor (6), einen dem Bildsensor gegenüber angeordneten Bewegungsträger (4), der mit dem Kraftaufnahmeelement (2) verbunden ist, eine mit dem Bewegungsträger (4) verbundene Projektionseinrichtung (3), welche eine vordefinierte geometrische Form (10) auf den Bildsensor projiziert, wobei diese entsprechend der X/Y/Z-Neigung des Bewegungsträgers positioniert und verzerrt wird (11), sowie eine Recheneinrichtung (7), welche dazu eingerichtet ist, aus der Position und Verzerrung der geometrischen Form (10) X/Y/Z-Koordinaten zur weiteren Verarbeitung abzuleiten.

2. Vorrichtung nach Anspruch 1, dadurch gekennzeichnet, dass der Bewegungsträger (4) am Außenrand fest mit der Bildsensoreinheit (5,6,7,8) verbunden ist und aus einem biegsamen Material besteht, welches sich bei Krafteinwirkung auf das Kraftaufnahmeelement (2) hinsichtlich ihres Neigungswinkel und ihrer Entfernung zum Bildsensor (6) verformt.

3. Vorrichtung nach Anspruch 1, dadurch gekennzeichnet, dass der Bewegungsträger (4) in einem geschichteten Material (9) eingelagert ist, welches schichtweise verschiedene Dichte und/oder Härte (Shore) aufweist und bei Krafteinwirkung auf das Kraftaufnahmeelement (2) hinsichtlich ihres Neigungswinkel und ihrer Entfernung zum Bildsensor (6) verformbar ist.

4. Vorrichtung nach einem der Ansprüche 1 bis 3, dadurch gekennzeichnet, dass die Projektionseinrichtung (3) mit dem Bewegungsträger (4) fest verbunden ist und die vordefinierte geometrische Form (10) direkt auf den Bildsensor (6) projiziert.

5. Vorrichtung nach einem der Ansprüche 1 bis 3, dadurch gekennzeichnet, dass der Bewegungsträger (4) fest mit einer als Reflektionsfläche ausgebildeten Projektionseinrichtung (31) verbunden ist, über welche die vordefinierte geometrische Form indirekt auf den Bildsensor (6) projiziert.

6. Verfahren zur Drei-Achsen-Positionsbestimmung eines Kraftaufnahmeelements (2) in einer Vorrichtung nach Anspruch 1, dadurch gekennzeichnet, dass von einem Nutzer auf das Kraftaufnahmeelement (2) angewandte Kräfte, gegebenenfalls mit verschiedenen Kraftamplituden in verschiedene Richtungen, durch die Recheneinheit in gleichförmige Ausgangssignale, passend zum angeschlossenen Endgerät, umgewandelt werden.

7. Verfahren nach Anspruch 6, dadurch gekennzeichnet, dass es dem Nutzer ermöglicht, zu jeder Zeit den Dreiachsensensor mit dem gerade gewünschten Kraftaufwand über das Kraftaufnahmeelement (2) neu zu kalibrieren.

8. Verfahren nach Anspruch 6, dadurch gekennzeichnet, dass die Recheneinrichtung (7) durch eine Bildanalysesoftware in Echtzeit die vordefinierte geometrische Form (10,11) in jedem aufgenommenen Bild des Bildsensors sucht, dessen Form hinsichtlich Position und Verzerrungen (11) analysiert, und daraus die entsprechende Neigung und die Veränderung des Bewegungsträgers (4) zum Bildsensor (6) ableitet.

9. Verfahren nach Anspruch 8, dadurch gekennzeichnet, dass vor der ersten Nutzung der Dreiachsensensorik ein Initialisierungsprozess stattfindet, bei dem alle möglichen Richtungen des Bewegungsträgers (4) X/Y/Z mindestens einmal mit einer vorbestimmten, maximal zulässigen Kraft über das Kraftaufnahmeelement (2) betätigt werden, wodurch der Bildanalysesoftware die maximal zulässige Position und Verzerrungen der vordefinierten geometrischen Form (11) dargestellt werden.

10. Verfahren nach Anspruch 9, dadurch gekennzeichnet, dass die Bildanalysesoftware in Echtzeit die vordefinierte geometrische Form (10,11) in jedem aufgenommenen Bild des Bildsensors sucht und dessen Form hinsichtlich Position und Verzerrungen (11) analysiert, und anhand dessen eine Plausibilitätsprüfung durchführt, inwieweit die erkannte Form (11) den maximal zulässigen Positionen und Verzerrungen entspricht.

11. Verfahren nach einem der Ansprüche 9 und 10, dadurch gekennzeichnet, dass die Bildanalysesoftware in Echtzeit bei erkannten unzulässigen Positionen oder Verzerrungen (11) ein digitales Signal erzeugt, um nachgeschaltete Systeme vor Fehlfunktionen zu schützen.

12. Verfahren nach Anspruch 8, dadurch gekennzeichnet, dass die Bildanalysesoftware in Echtzeit durch Interpolation der erkannten geometrischen Form (11) die daraus resultierenden X/Y/Z-Koordinaten präzisiert.

13. Vorrichtung nach Anspruch 1, dadurch gekennzeichnet, dass der Bewegungsträger (4) als ein hermetischer Abschluss zum Inneren der Vorrichtung ausgeführt ist, wodurch ein Betrieb in Flüssigkeiten ermöglicht wird.

14. Vorrichtung nach Anspruch 1, dadurch gekennzeichnet, dass die Positionsbestimmung des Bewegungsträger (4) auf zwei Achsen (X/Y-Koordinaten) beschränkbar ist.

15. Vorrichtung nach Anspruch 1, dadurch gekennzeichnet, dass die Positionsbestimmung des Bewegungsträger (4) auf eine Achse (X oder Y oder Z -Koordinate) beschränkbar ist.

16. Vorrichtung nach Anspruch 1, dadurch gekennzeichnet, dass die Projektionseinheit über ein Gelenklager (14) gelagert ist und direkt mit einer Kraft beaufschlagt werden kann.

17. Vorrichtung nach Anspruch 1, dadurch gekennzeichnet, dass eine Laserdiode als Lichtquelle vorgesehen ist, die der mit dem Bewegungsträger (4) verbundenen Projektionseinrichtung (3, 31) zugeordnet ist, wobei die Laserdiode über eine Plankonvexlinse einen Kreis auf den Bildsensor (6) projiziert.

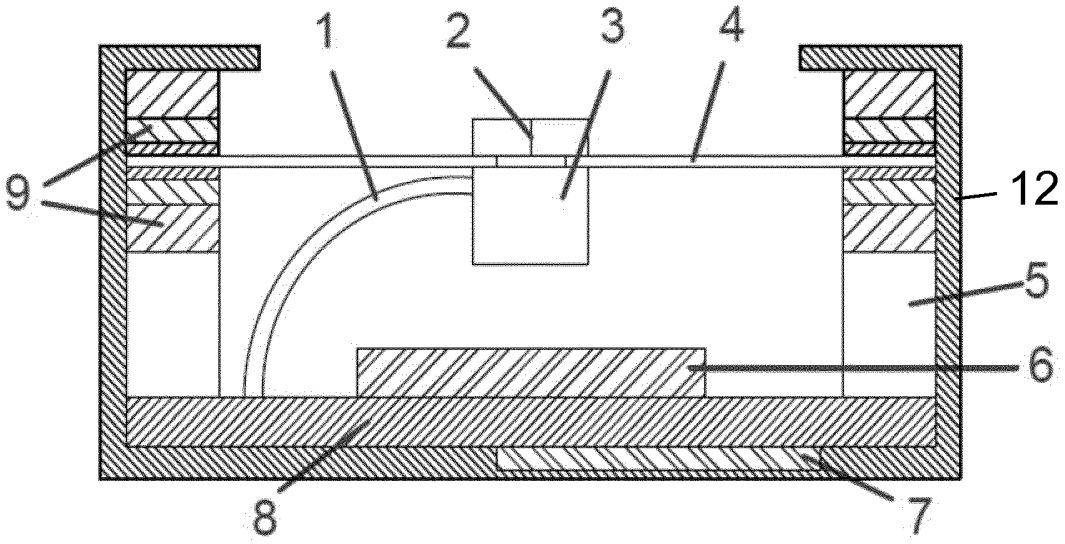

Fig. 1

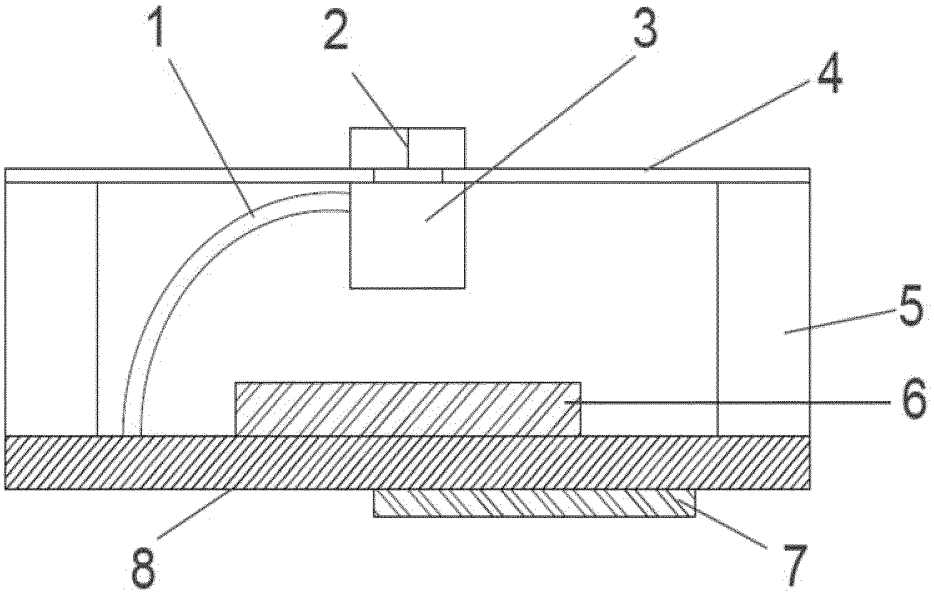

Fig. 2

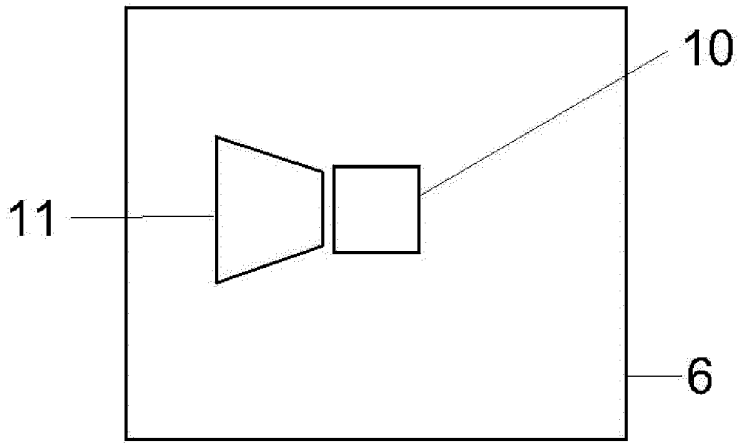

Fig. 3

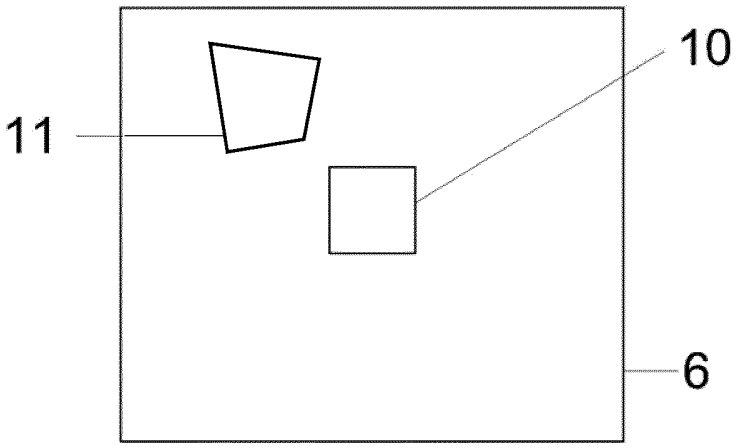

Fig. 4

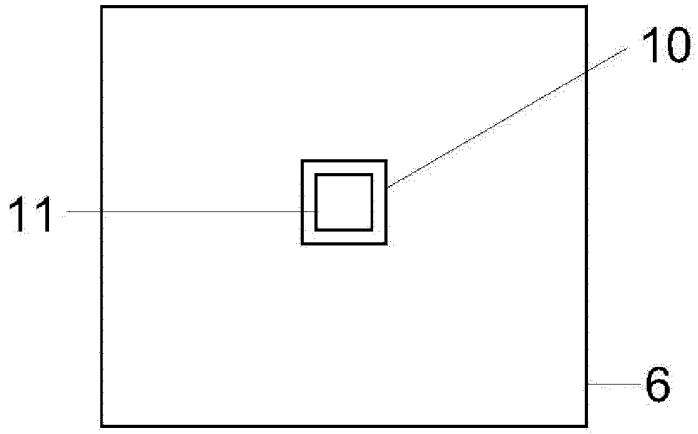

Fig. 5

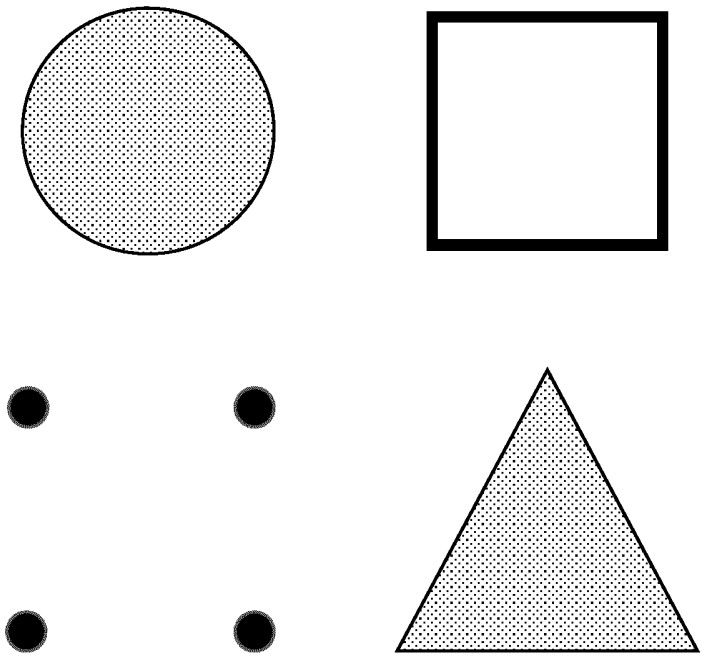

Fig. 6

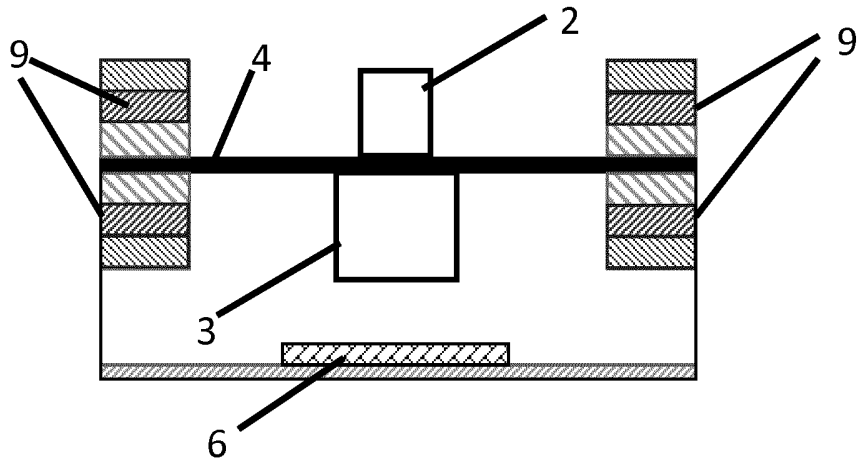

Fig. 7a

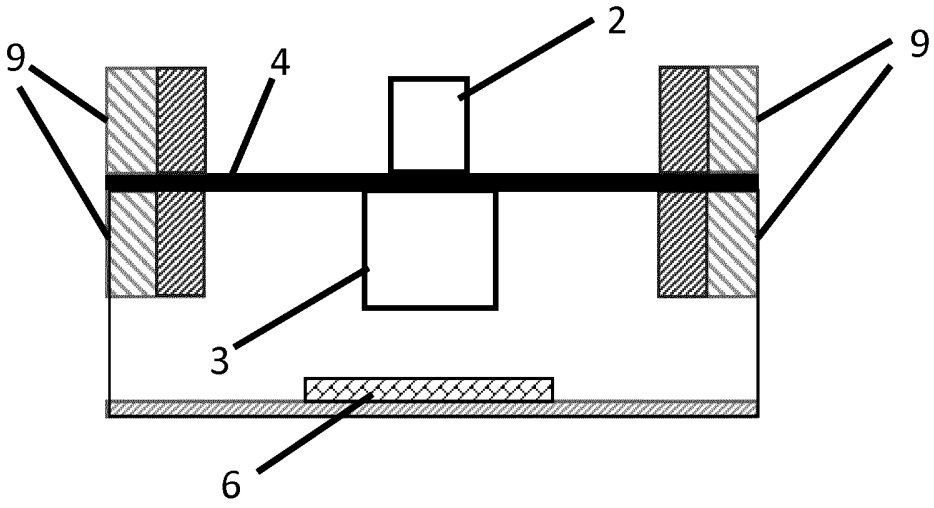

Fig. 7b

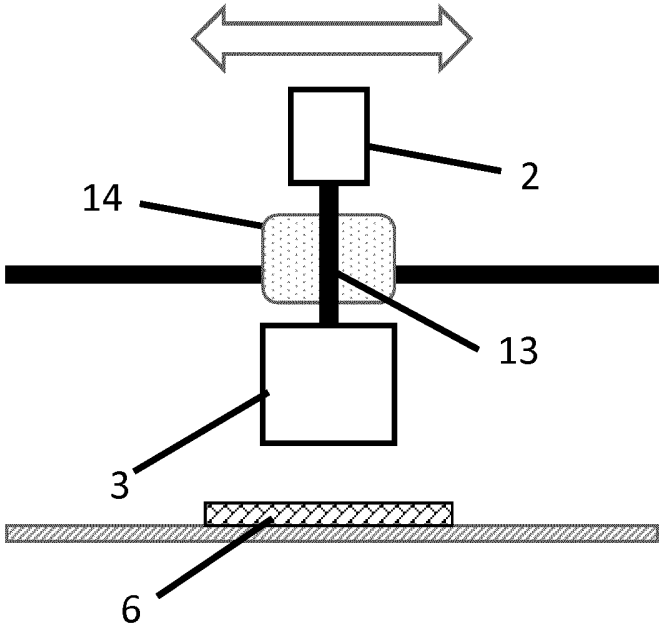

Fig. 8

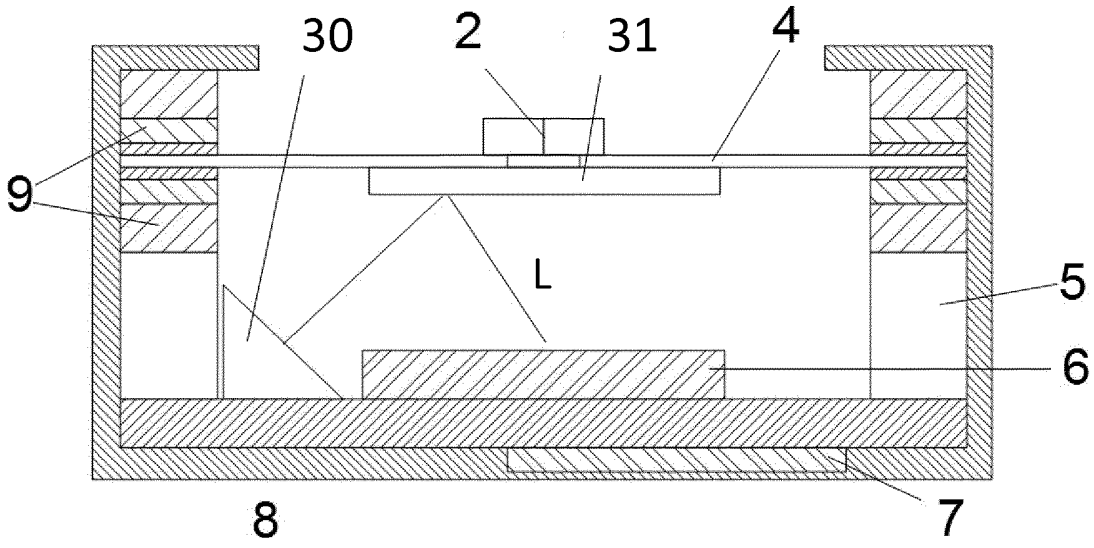

Fig. 9

INTERNATIONAL SEARCH REPORT

International application No
PCT/EP2016/070390

A. CLASSIFICATION OF SUBJECT MATTER
INV. G05G9/047
ADD.

According to International Patent Classification (IPC) or to both national classification and IPC

B. FIELDS SEARCHED

Minimum documentation searched (classification system followed by classification symbols)
G05G

Documentation searched other than minimum documentation to the extent that such documents are included in the fields searched

Electronic data base consulted during the international search (name of data base and, where practicable, search terms used)
EPO-Internal, WPI Data

C. DOCUMENTS CONSIDERED TO BE RELEVANT

Category*	Citation of document, with indication, where appropriate, of the relevant passages	Relevant to claim No.
X	US 2010/053070 A1 (TSAI MENG-CHE [TW] ET AL) 4 March 2010 (2010-03-04) paragraphs [0034], [0036], [0037], [0039]; claim 1; figure 1b	1-17
X	WO 03/016817 A2 (UHLMANN ECKART [DE]; SEIBT MARTIN [DE]; HAERTWIG JENS-PETER [DE]; SCHA) 27 February 2003 (2003-02-27) the whole document	1-17
X	EP 0 790 488 A2 (EUROCOPTER DEUTSCHLAND [DE]) 20 August 1997 (1997-08-20) the whole document	1-17
X	US 5 181 079 A (KLINGER DIETMAR [DE]) 19 January 1993 (1993-01-19) the whole document	1-17

-/--

[X] Further documents are listed in the continuation of Box C.

[X] See patent family annex.

* Special categories of cited documents :

"A" document defining the general state of the art which is not considered to be of particular relevance

"E" earlier application or patent but published on or after the international filing date

"L" document which may throw doubts on priority claim(s) or which is cited to establish the publication date of another citation or other special reason (as specified)

"O" document referring to an oral disclosure, use, exhibition or other means

"P" document published prior to the international filing date but later than the priority date claimed

"T" later document published after the international filing date or priority date and not in conflict with the application but cited to understand the principle or theory underlying the invention

"X" document of particular relevance; the claimed invention cannot be considered novel or cannot be considered to involve an inventive step when the document is taken alone

"Y" document of particular relevance; the claimed invention cannot be considered to involve an inventive step when the document is combined with one or more other such documents, such combination being obvious to a person skilled in the art

"&" document member of the same patent family

Date of the actual completion of the international search	Date of mailing of the international search report
1 December 2016	13/12/2016

Name and mailing address of the ISA/	Authorized officer
European Patent Office, P.B. 5818 Patentlaan 2 NL - 2280 HV Rijswijk Tel. (+31-70) 340-2040, Fax: (+31-70) 340-3016	de Beurs, Marco

1

Form PCT/ISA/210 (second sheet) (April 2005)

INTERNATIONAL SEARCH REPORT

International application No
PCT/EP2016/070390

C(Continuation). DOCUMENTS CONSIDERED TO BE RELEVANT

Category*	Citation of document, with indication, where appropriate, of the relevant passages	Relevant to claim No.
X	US 2005/275623 A1 (CHADHA LOVLEEN [US]) 15 December 2005 (2005-12-15) the whole document -----	1-17

1

INTERNATIONAL SEARCH REPORT

Information on patent family members

International application No
PCT/EP2016/070390

Patent document cited in search report	Publication date	Patent family member(s)	Publication date
US 2010053070 A1	04-03-2010	TW 201009651 A	01-03-2010
		US 2010053070 A1	04-03-2010
WO 03016817 A2	27-02-2003	AT 338265 T	15-09-2006
		DE 10139878 A1	06-03-2003
		EP 1415130 A2	06-05-2004
		WO 03016817 A2	27-02-2003
EP 0790488 A2	20-08-1997	DE 19605573 A1	21-08-1997
		EP 0790488 A2	20-08-1997
		US 6081257 A	27-06-2000
US 5181079 A	19-01-1993	DE 3827719 A1	22-02-1990
		EP 0429514 A1	05-06-1991
		JP H076768 B2	30-01-1995
		JP H03502605 A	13-06-1991
		US 5181079 A	19-01-1993
		WO 9002313 A1	08-03-1990
US 2005275623 A1	15-12-2005	US 2005275623 A1	15-12-2005
		WO 2005124528 A2	29-12-2005

INTERNATIONALER RECHERCHENBERICHT

Internationales Aktenzeichen
PCT/EP2016/070390

A. KLASSIFIZIERUNG DES ANMELDUNGSGEGENSTANDES
INV. G05G9/047
ADD.

Nach der Internationalen Patentklassifikation (IPC) oder nach der nationalen Klassifikation und der IPC

B. RECHERCHIERTE GEBIETE

Recherchierter Mindestprüfstoff (Klassifikationssystem und Klassifikationssymbole)
G05G

Recherchierte, aber nicht zum Mindestprüfstoff gehörende Veröffentlichungen, soweit diese unter die recherchierten Gebiete fallen

Während der internationalen Recherche konsultierte elektronische Datenbank (Name der Datenbank und evtl. verwendete Suchbegriffe)
EPO-Internal, WPI Data

C. ALS WESENTLICH ANGESEHENE UNTERLAGEN

Kategorie*	Bezeichnung der Veröffentlichung, soweit erforderlich unter Angabe der in Betracht kommenden Teile	Betr. Anspruch Nr.
X	US 2010/053070 A1 (TSAI MENG-CHE [TW] ET AL) 4. März 2010 (2010-03-04) Absätze [0034], [0036], [0037], [0039]; Anspruch 1; Abbildung 1b	1-17
X	WO 03/016817 A2 (UHLMANN ECKART [DE]; SEIBT MARTIN [DE]; HAERTWIG JENS-PETER [DE]; SCHA) 27. Februar 2003 (2003-02-27) das ganze Dokument	1-17
X	EP 0 790 488 A2 (EUROCOPTER DEUTSCHLAND [DE]) 20. August 1997 (1997-08-20) das ganze Dokument	1-17
X	US 5 181 079 A (KLINGER DIETMAR [DE]) 19. Januar 1993 (1993-01-19) das ganze Dokument	1-17

-/--

[X] Weitere Veröffentlichungen sind der Fortsetzung von Feld C zu entnehmen [X] Siehe Anhang Patentfamilie

* Besondere Kategorien von angegebenen Veröffentlichungen :
"A" Veröffentlichung, die den allgemeinen Stand der Technik definiert, aber nicht als besonders bedeutsam anzusehen ist
"E" frühere Anmeldung oder Patent, die bzw. das jedoch erst am oder nach dem internationalen Anmeldedatum veröffentlicht worden ist
"L" Veröffentlichung, die geeignet ist, einen Prioritätsanspruch zweifelhaft erscheinen zu lassen, oder durch die das Veröffentlichungsdatum einer anderen im Recherchenbericht genannten Veröffentlichung belegt werden soll oder die aus einem anderen besonderen Grund angegeben ist (wie ausgeführt)
"O" Veröffentlichung, die sich auf eine mündliche Offenbarung, eine Benutzung, eine Ausstellung oder andere Maßnahmen bezieht
"P" Veröffentlichung, die vor dem internationalen Anmeldedatum, aber nach dem beanspruchten Prioritätsdatum veröffentlicht worden ist
"T" Spätere Veröffentlichung, die nach dem internationalen Anmeldedatum oder dem Prioritätsdatum veröffentlicht worden ist und mit der Anmeldung nicht kollidiert, sondern nur zum Verständnis des der Erfindung zugrundeliegenden Prinzips oder der ihr zugrundeliegenden Theorie angegeben ist
"X" Veröffentlichung von besonderer Bedeutung; die beanspruchte Erfindung kann allein aufgrund dieser Veröffentlichung nicht als neu oder auf erfinderischer Tätigkeit beruhend betrachtet werden
"Y" Veröffentlichung von besonderer Bedeutung; die beanspruchte Erfindung kann nicht als auf erfinderischer Tätigkeit beruhend betrachtet werden, wenn die Veröffentlichung mit einer oder mehreren Veröffentlichungen dieser Kategorie in Verbindung gebracht wird und diese Verbindung für einen Fachmann naheliegend ist
"&" Veröffentlichung, die Mitglied derselben Patentfamilie ist

Datum des Abschlusses der internationalen Recherche	Absendedatum des internationalen Recherchenberichts
1. Dezember 2016	13/12/2016

Name und Postanschrift der Internationalen Recherchenbehörde	Bevollmächtigter Bediensteter
Europäisches Patentamt, P.B. 5818 Patentlaan 2 NL - 2280 HV Rijswijk Tel. (+31-70) 340-2040, Fax: (+31-70) 340-3016	de Beurs, Marco

1

INTERNATIONALER RECHERCHENBERICHT

Internationales Aktenzeichen
PCT/EP2016/070390

C. (Fortsetzung) ALS WESENTLICH ANGESEHENE UNTERLAGEN

Kategorie*	Bezeichnung der Veröffentlichung, soweit erforderlich unter Angabe der in Betracht kommenden Teile	Betr. Anspruch Nr.
X	US 2005/275623 A1 (CHADHA LOVLEEN [US]) 15. Dezember 2005 (2005-12-15) das ganze Dokument -----	1-17

INTERNATIONALER RECHERCHENBERICHT

Angaben zu Veröffentlichungen, die zur selben Patentfamilie gehören

Internationales Aktenzeichen
PCT/EP2016/070390

Im Recherchenbericht angeführtes Patentdokument	Datum der Veröffentlichung	Mitglied(er) der Patentfamilie	Datum der Veröffentlichung
US 2010053070 A1	04-03-2010	TW 201009651 A	01-03-2010
		US 2010053070 A1	04-03-2010
WO 03016817 A2	27-02-2003	AT 338265 T	15-09-2006
		DE 10139878 A1	06-03-2003
		EP 1415130 A2	06-05-2004
		WO 03016817 A2	27-02-2003
EP 0790488 A2	20-08-1997	DE 19605573 A1	21-08-1997
		EP 0790488 A2	20-08-1997
		US 6081257 A	27-06-2000
US 5181079 A	19-01-1993	DE 3827719 A1	22-02-1990
		EP 0429514 A1	05-06-1991
		JP H076768 B2	30-01-1995
		JP H03502605 A	13-06-1991
		US 5181079 A	19-01-1993
		WO 9002313 A1	08-03-1990
US 2005275623 A1	15-12-2005	US 2005275623 A1	15-12-2005
		WO 2005124528 A2	29-12-2005

7.3 Questionnaire

Fragebogen zu Ihrem neuen Eingabegerät

Sehr geehrte Anwenderin, sehr geehrter Anwender,
die Beurteilung Ihres neuen Eingabegerätes ist sehr wichtig. Nur so ist es uns möglich die Qualität unserer Neuentwicklungen zu optimieren. Durch Serviceupdates der Hard- und Software können wir nicht nur Neuentwicklungen, sondern auch bereits installierte Eingabegerät auf den neuesten Wissenstand der Ergonomie und Technik bringen. Alle Angaben werden selbstverständlich anonym weiterverarbeitet. Das ausgefüllte Formular senden Sie bitte per Mail oder per Post (frankierter Rücksendeumschlag liegt diesem Schreiben bei) an:

Postalische Adresse:

Mailadresse:

Weitere Informationen zu dem anhängenden Fragebogen:
Bitte versuchen Sie möglichst alle Fragen zu beantworten. Wenn es Ihnen nicht möglich ist eine Frage zu beantworten, verraten Sie uns bitte warum. Gerne können Sie die Antworten in einem digitalen Dokument verfassen. Vermerken dazu lediglich die Nummern der Fragen vor Ihren Antworten. Gerne können Sie jederzeit weitere Ideen und Anregungen formlos verfassen und uns zusenden.

Vielen Dank für Ihre Mithilfe.

1. Würden Sie uns bitte Ihr **Alter** und **Geschlecht** nennen?

□ weiblich □ männlich …….. Alter

2. Unter welcher Form einer Behinderung oder Krankheit leiden Sie?

……

3. Wann wurde das **neue** Eingabegerät installiert?

……. Monat, ……. Jahr

4. Was **steuern** Sie mit Ihrem Eingabegerät?

□ Rollstuhl

□ Umfeld Steuerung

□ PC

□ …….

5. Welches Eingabegerät haben Sie **zuvor** genutzt?

□ Keines, ist mein Erstes (bitte weiter mit Frage 5)

6. Weshalb haben Sie ein **neues Eingabegerät** bekommen?

7. Schildern Sie bitte Ihren **ersten Eindruck**.

8. Wie lange haben Sie benötigt um das neue Eingabegerät **sicher nutzen** zu können?

□ ……. Stunde/n

□ ……. Tage

□ ……. Woche/n

□ ……. …….

□ kann es noch immer nicht sicher nutzen (Bitte um eine kurze Erläuterung in Frage 14)

9. Wie wichtig ist für Sie die „**Lernfähigkeit**“ des Eingabegerätes (Anpassung an Ihr Kraft- und Bewegungsvermögen)?

□ sehr wichtig

□ wichtig

□ unwichtig

□ egal

□ weiß nicht

10. Wie oft **passen** Sie das Eingabegerät an Ihre Bedürfnisse **an**?

□ täglich

□ wöchentlich

□ monatlich

□ gar nicht

□ weiß nicht

11. Wäre es für Sie angenehmer, wenn Ihr Eingabegerät durch einen **größeren Bewegungshub** zu betätigen wäre? (Der notwendige Weg des Eingabegerätes, welchen Sie aufwenden müssen um eine Aktion auszuführen.)

□ ja

□ nein

□ weiß nicht

12. Wäre es für Sie angenehmer, wenn Ihr Eingabegerät durch einen noch **kleineren Bewegungshub** zu betätigen wäre? (Der notwendige Weg des Eingabegerätes, welchen Sie aufwenden müssen um eine Aktion auszuführen.)

□ ja

□ nein

□ weiß nicht

13. Wie bewerten Sie den **Kraftaufwand** um das Eingabegerät zu bedienen?

□ passt mir gut

□ passt mir nicht (Bitte um eine kurze Erläuterung dazu in Frage 14)

□ weiß nicht

14. Über welchen **Zeitraum** können Sie das Eingabegerät **ermüdungsfrei** nutzen?

□ ……. Minute/n

□ ……. Stunde/n

□ über den ganzen Tag

15. Wie könnte Ihrer Meinung nach die **Eingewöhnungsphase** optimiert werden?

□ Es muss nichts optimiert werden

□ weiß nicht

Dazu habe ich folgende Idee:

16. Wie könnte Ihrer Meinung nach das **Eingabegerät** optimiert werden?

□ Es muss nichts optimiert werden

□ weiß nicht

Dazu habe ich folgende Idee:

Vielen herzlichen Dank für Ihre Mühe. Wir werden Ihre Meinung und Ihre Anregungen in unseren Entwicklungs- und Fertigungsprozess einfließen lassen und somit die Qualität unserer Eingabegeräte optimieren. Bitte wenden Sie sich jederzeit mit Ideen und Anregungen an uns.

Mit freundlichen Grüßen

Ihr Vertriebs- und Entwicklungsteam

7.4 Start-up idea competition 2017

7.4.1 Article WIRTSCHAFTSZEIT 13.03.2017

WIRTSCHAFTS|zeit

Hier informiert sich die Wirtschaft!

Science Park Graz-Geschäftsführer Martin Mössler mit den Preisträgern Niels Buchhold (l.), Julia Pötsch und Michael Haas

IDEENWETTBEWERB 2017 DES SCIENCE PARK GRAZ: INNOVATIONEN BIS ZUM MOND

13. März 2017 | 10:49 Autor: Science Park Graz Österreich, Steiermark

Graz (A) **Vom selbstbremsenden Kinderwagen über futuristische E-Ultra-Leichtfahrzeuge bis hin zur kabellosen Stromübertragung: Mit Teilnehmerrekord ging der elfte Ideenwettbewerb der Hightech-Schmiede Science Park in Graz über die Bühne. Erstmals wurde auch die beste Idee mit Weltraumbezug prämiert: Ein Bus, der Komponenten zwischen Erde und Welt-All transportieren soll.**

Beim „Ideenwettbewerb" der Hightech-Schmiede Science Park katapultierten sich gestern in den Räumlichkeiten der Technischen Universität Graz zukunftsträchtige Start-Ups und ihre Technologien in den Mittelpunkt: Über 10.000 Euro wurden in der bereits elften Auflage des Wettbewerbs an findige Entwickler ausgeschüttet, schon im Vorfeld zeichnet sich mit 127 Einreichungen ein neuer Teilnehmerrekord ab: „Start-Ups sind die neuen Rockstars – wir wollen mit Wettbewerben wie diesen die hohe Innovationskraft der steirischen Gründerszene aufzeigen, Lust auf das Unternehmertum machen und so den Anstoß zum Unternehmen von Morgen geben", erklärt der Geschäftsführer des Science Park Graz, Martin Mössler.

Bediengerät für beeinträchtigte Personen

Auf dem Weg zum Industrie-Unternehmen von morgen ist auch Niels Buchhold, Sieger in der Kategorie „technologie-orientiert": Sein neuartiges Bediengerät unterstützt hochgradig behinderte Menschen etwa bei der Steuerung von elektrischen Rollstühlen oder Computern. Ein Vorteil: „Das Bediengerät ist lernfähig und so in der Lage, sich auf den Grad der Behinderung individuell einzustellen", erklärt Buchhold.

7.4.2 Article KLEINE ZEITUNG 13.03.2017

KLEINE ZEITUNG

START-UP-WETTBEWERB

Zahnfüllung bis Jackeneinsatz: Science Park prämiert Ideen

127 Einreichungen und 5 Gewinner. Der Science Park Graz hat bereits zum elften Mal, Ideen junger Unternehmensgründer ausgezeichnet.

Von **Roman Vilgut** | 13.58 Uhr, 10. März 2017

Die Gewinner des Ideenwettbewerbs des Science Park Graz © (c) The Schubidu Quartet

Es ist ein bisschen wie in der Show „2 Minuten 2 Millionen“, nur statt im TV-Studio kämpfen Start-ups in einem Büroraum des Inkubators Science Park an der Neuen Technik in Graz für ihre Idee. Millionen gibt es zwar keine, doch beim Start-up-Wettbewerb des Science Park werden über 10.000 Euro ausgeschüttet, ganz ohne Zugeständnisse.

Das Teilnehmerfeld ist bunt gemischt. 127 Ideen wurden eingereicht, 15 durften sich einer neunköpfigen Jury aus Wissenschaftlern, Juristen, Journalisten und

Bankern stellen. Der Ideenwettbewerb ist für alle offen, daher sind manche Projekte in der Ideenphase, andere haben für ihre Produkte bereits Abnehmer gefunden. Prämiert wurden die Start-ups in drei Kategorien, dazu kommen zwei Sonderpreise.

Rollstühle, Zahnfüllung und Babys

Die Kategorie "Technologie-Orientiert" konnte **Niels Buchhold** für sich entscheiden. Er hat ein Bediengerät für hochgradig behinderte Menschen entwickelt, für welche die bisher üblichen elektrischen Rollstühle nicht geeignet sind. Mit einem hochsensiblen Joystick oder Touchpad können Betroffene Rollstühle steuern. Das Gerät ist sehr robust und lernfähig und kann sich so dem Grad der Behinderung anpassen.

7.4.3 Impressions of the award ceremony

Dipl.-Ing. Christoph Adametz, Deputy head F&T Haus Graz, Niels Buchhold form right to left

Reprinted by kind permission of Thomas Raggam, The Schubidu Quartet, A-8020 Graz

Reprinted by kind permission of Thomas Raggam, The Schubidu Quartet, A-8020 Graz

7.4.4 Application text optical version

(3 pages)

Science Park Graz

Einreichdatum:	
Teilnehmernummer: (nicht ausfüllen)	

TEILNAHMEFORMULAR IDEENWETTBEWERB 2016 | 2017

1) PERSÖNLICHE DATEN

Name der Ansprechperson:	Niels Buchhold		
Telefonnummer:	0660 441 5867		
Email-Adresse:			
Bildungseinrichtung, an der studiert wird/ wurde: (Mehrfachnennung möglich)	☒ TU Graz ☐ Med Uni Graz ☐ Uni Graz	☐ FH Joanneum ☐ Campus02 ☐ Sonstige (bitte angeben)	
Studienrichtung(en):	Institute of Health Care Engineering		
Beschäftigungs-verhältnis an folgender Bildungseinrichtung:	☐ TU Graz ☐ Med Uni Graz ☐ Uni Graz	☐ FH Joanneum ☐ Campus02 ☒ Sonstige PhD Doktorand (bitte angeben)	
Teammitglieder:	Name Christian Baumgartner	Studienrichtung(en) und Bildungseinrichtung(en) Institute of Health Care Engineering	Bildungseinrichtung, an der Anstellungsverhältnis besteht Professor
Phase der Geschäftsidee: (bitte nur Einfachnennung)	☐ Nur Idee, Umsetzung nicht geplant ☐ Ich plane meine Idee in nächster Zeit umzusetzen ☐ Ich werde meine Idee später einmal realisieren ☒ Befinde mich bereits in der Umsetzungsphase		

2) BESCHREIBUNG DER IDEE

(Bitte beantworten Sie die Fragen nach Ihrem aktuellen Wissenstand. Wenn Sie derzeit noch nicht alle Fragen beantworten können, lassen Sie die betreffenden Felder einfach frei.)

Kurzzusammenfassung der Idee

(max. 2.500 Zeichen inkl. Leerzeichen)

Bei der hier vorgestellten Entwicklung handelt es sich um eine neuartige Eingabemöglichkeit (human-machine interface) für die Krankheitsbilder Muskeldystrophie und Muskelatrophie sowie alle weiteren Formen der Muskelkrankheiten (allgemein bekannt unter Muskelschwund).
Personen mit verschiedenen Formen der Muskelkrankheiten sind in den Anfangsstadien der Krankheit grundsätzlich in der Lage Standardjoysticks zur Bewältigung verschiedener Alltagsaufgaben zu nutzen (Elektrorollstuhl, Computerbedienung, etc.).
Leider verändert sich das Krankheitsbild in unvorhersehbaren Zeitintervallen wodurch der Patient dann nicht mehr in der Lage ist einen Standardjoystick zu nutzen. Die Hilfe von Pflegepersonal ist dann zu jeder Zeit unumgänglich. Durch die notwendige aber dauerhafte Anwesenheit dieser Personen wird die Intimsphäre der erkrankten Personen empfindlich eingeschränkt (selbständiges Telefonieren, Mails schreiben, etc.). Nicht zuletzt dem beschriebenen Umstand geschuldet wurde im Rahmen einer Doktorarbeit ein neuartiges Eingabegerät entwickelt um die Intimsphäre der betroffenen Personen in einem menschenwürdigen Rahmen zu schützen. Der hier beschriebene Sensor wird grundsätzlich wie ein handelsüblicher Joystick verwendet. Der Unterschied liegt jedoch

in seiner extrem hohen Auflösung und in dem Umstand, dass nur ein kaum spürbarer Hub (Weg) vollzogen werden muss. Gerade für körperlich behinderte Menschen mit Muskelkrankheiten wird die Nutzung eines Standardjoysticks im Verlaufe des Krankheitsbildes unmöglich da das Bewegungsspektrum (Kraft und Hub) mit jedem Krankheitsschub abnimmt. Aus diesem Grund ist der neu entwickelte Sensor unter anderem lernfähig und kann zu jeder Zeit an das gewünschte Kraft- und Bewegungsspektrum des Nutzers angepasst werden. Dieser Lernvorgang kann vom Nutzer selbst angestoßen werden und ist innerhalb von 15 Sekunden abgeschlossen. Keinesfalls außer Acht zu lassen ist hierbei die Entlastung des Gesundheitswesens. Bislang mussten Eingabegeräte bei den geringsten Änderungen des Krankheitsbildes neu und individuell angepasst werden. Zu den hohen Kosten der Fachkräfte kam zusätzlich der Umstand, dass Patienten möglicherweise während der Neuanpassung einen weiteren Krankheitsschub erfuhren und die gerade vollzogene Modifikation nicht mehr passend war. Auch in Entwicklungsländern wäre ein Einsatz dieses Sensors denkbar da nach einer Versorgung vor Ort meist keine weiteren Mittel und kein Fachpersonal für die Nachsorge bereitstehen. Selbst die Weitergabe an andere Personen ist durch den Lernvorgang in wenigen Sekunden erledigt.
Der Sensor dient grundsätzlich zur Positionsbestimmung und kann ebenso als hochpräziser „Joystickersatz“ in jeder Art von medizinischen Geräten zum Einsatz kommen (Operationsroboter, medizinische Diagnosegeräte, etc.). Hierbei kann der Sensor auch höchst individuell an den gesunden Nutzer angepasst werden. Dadurch entsteht ein hohes Maß an Nutzungssicherheit und Präzision während der Arbeit.
Zum Aufbau des Sensors: Eine Lichtquelle (z.B. Laserdiode) ist an einer beweglichen Achse befestigt und projiziert eine beliebige geometrische Figur auf einen Bildsensor (CMOS, CCD, etc.). Die Software in dem nachgeschalteten Mikrocontroller erkennt den Mittelpunkt, die Verzerrung und die Größe der Projektion und errechnet daraus X-,Y- und Z-Koordinaten. Diese Koordinaten können dann in den angeschlossenen Geräten weiterverarbeitet werden. Der 3-Achsensensor zeichnet sich durch eine extrem hohe Auflösung und eine sehr präzise Reproduzierbarkeit (Positionierung-> Koordinaten) aus. Durch die optische Signalverarbeitung besteht erhöhte Sicherheit gegenüber EMI (Elektromagnetische Störungen) und RFI (Hochfrequenzstörungen).
Besonderes Augenmerk wurde auf die Plausibilität (erkennen von Fehlfunktionen) der erzeugten Koordinaten gelegt. Fehlfunktionen können nach aktuellem Erkenntnisstand weitestgehend ausgeschlossen werden.
Im direkten Vergleich zu bestehenden Steuerungsmöglichkeiten sind Systeme wie Eye-Tracking, Sprachsteuerung und Gehirn-Computer-Schnittstellen eher problembehaftet. Mit diesen Eingabemethoden ist es schwierig präzise und gleichzeitig komplexe Steuerungen vorzunehmen. Eye-Tracking ist zudem Reflexen (Augenreflex) unterworfen und für sicherheitsrelevante Steueraufgaben gänzlich ungeeignet. Sprachsteuerungen können in der Regel nur einzelne Befehle entgegennehmen und funktionieren in lauten Umgebungen unzuverlässig.
Eine gut bewertbare Aufgabe ist das Fahren eines Kurses mit einem Elektrorollstuhl in Form einer „8“. Um diesen Kurs einwandfrei abfahren zu können sind proportionale Ausgangssignale wie die des hier vorgestellten Sensors oder die Ausgangssignale eines Joysticks notwendig.
Systeme welche den Nutzer bei der Navigation unterstützen (Hinderniserkennung) sind sinnvoll aber ebenso kostenintensiv. Zudem ist eine freie Wahl des Fahrweges nicht möglich da die Navigationshilfe bei bestimmten programmierten Situationen eingreift. Bei sportliche Aktivitäten wie z. B. Elektrorollstuhl Hockey sind direkte Steuerungen unumgänglich.

Innovationsgrad	
Was ist der Innovationskern Ihrer Idee? Was macht Ihre Idee einzigartig?	Weil es der weltweit erste und einzige volldigitale optische Sensor (Joystick) mit extrem hoher Auflösung ist (Patentierung läuft). Absolut störsicher
In welchem Entwicklungsstadium befindet sich Ihre Innovation?	Prototyp ist bereits fertiggestellt.

Kundennutzen

Welchen Nutzen hat Ihr Angebot aus der Sicht der KundInnen?	Sehr hohe Sicherheit, extrem hohe Auflösung, kann an den Patienten angepasst werden
Welche ZielkundInnen sprechen Sie an?	Alle Bereiche mit dem Einsatz von Sensoren zur Positionbestimmung.

Marktpotential	
Welche Trends kann man am Zielmarkt beobachten?	Kosten im Gesundheitswesen müssen eingespart werden. Leider oft zu Lasten der Patienten. Die eingereichte Lösung hilft dem Gesundheitswesen und den Patienten.
Wie groß ist Ihr Zielmarkt, lässt er sich in Zahlen ausdrücken?	Schwierig zu bemessen.
Welche KonkurrenzanbieterInnen gibt es bereits am Markt?	Keine. Beleg dafür ist die Patentierung. Prüfung national ist bereits positiv abgeschlossen. Gerade läuft die Einspruchsfrist.

Wirtschaftliche Verwertung	
Wie viele Ressourcen (Zeit und Geld) benötigen Sie, um die Idee vermarktungsreif zu machen?	ca. 200.000€
Welche Möglichkeiten des Schutzes (Patente, Markenschutz usw.) bestehen?	Nationales Patent ist bereits eingereicht und befindet sich nach positiver Prüfung in der Einspruchsfrist.

3) STATISTIK

Wie sind Sie auf den Science Park Graz Ideenwettbewerb aufmerksam geworden?	☐ Plakat ☐ Flyer ☒ Email von Sonja Buchegger (bitte angeben) ☐ Newsletter von (bitte angeben) ☐ Ankündigung auf Website von (bitte angeben) ☐ Facebook ☐ Sonstiges (bitte angeben)

4) NEWSLETTER

Science Park Graz Newsletter	☒ Ja, ich möchte regelmäßig zum Thema Innovation und Gründung rund um den Science Park Graz informiert werden und bestelle den Science Park Graz Newsletter.

Hiermit nehme ich am Science Park Graz Ideenwettbewerb teil und versichere, dass meine Angaben wahrheitsgemäß erfolgt sind.

Der Science Park Graz ist berechtigt diese Daten im Rahmen der Evaluierung zu vervielfältigen und den Mitgliedern der Jury zur Verfügung zu stellen. **Alle am Wettbewerb beteiligten Personen (Science Park Graz MitarbeiterInnen und Jurymitglieder) unterliegen einer Vertraulichkeitsvereinbarung zum Schutz Ihres geistigen Eigentums!**

Ort, Datum/ Unterschrift	Graz, 20.12.2016

7.4.5 Application text SG version 1

(3 pages)

Science Park Graz

Einreichdatum:	
Teilnehmernummer:	

(nicht ausfüllen)

TEILNAHMEFORMULAR IDEENWETTBEWERB 2016 | 2017

1) PERSÖNLICHE DATEN

Name der Ansprechperson:	Niels Buchhold		
Telefonnummer:	0660 441 5867		
Email-Adresse:			
Bildungseinrichtung, an der studiert wird/ wurde: (Mehrfachnennung möglich)	☒ TU Graz ☐ Med Uni Graz ☐ Uni Graz	☐ FH Joanneum ☐ Campus02 ☐ Sonstige (bitte angeben)	
Studienrichtung(en):	Institute of Health Care Engineering		
Beschäftigungs-verhältnis an folgender Bildungseinrichtung:	☐ TU Graz ☐ Med Uni Graz ☐ Uni Graz	☐ FH Joanneum ☐ Campus02 ☒ Sonstige PhD Doktorand (bitte angeben)	
Teammitglieder:	Name Christian Baumgartner	Studienrichtung(en) und Bildungseinrichtung(en) Institute of Health Care Engineering	Bildungseinrichtung, an der Anstellungsverhältnis besteht Professor
Phase der Geschäftsidee: (bitte nur Einfachnennung)	☐ Nur Idee, Umsetzung nicht geplant ☐ Ich plane meine Idee in nächster Zeit umzusetzen ☐ Ich werde meine Idee später einmal realisieren ☒ Befinde mich bereits in der Umsetzungsphase		

2) BESCHREIBUNG DER IDEE

(Bitte beantworten Sie die Fragen nach Ihrem aktuellen Wissenstand. Wenn Sie derzeit noch nicht alle Fragen beantworten können, lassen Sie die betreffenden Felder einfach frei.)

Kurzzusammenfassung der Idee

(max. 2.500 Zeichen inkl. Leerzeichen)

Bei der hier vorgestellten Entwicklung handelt es sich um eine neuartige Eingabemöglichkeit (human-machine interface) für Spastiker und oder Personen mit ähnlichem Krankheitsbild.
Bislang ist es Spastikern nicht oder nur stark eingeschränkt möglich sensitive Hilfsmittel wie z. B. einen Elektrorollstuhl eigenständig zu bedienen. Da bei eintretender Spastik die Extremitäten verkrampfen und nicht mehr kontrollierbar sind kann die Benutzung eines Standardjoysticks während einer Elektrorollstuhlfahrt, zu gefährlichen Fahrsituationen führen. Zudem kann sich der Nutzer verletzen da beispielsweise die Hand um einen Joystick verkrampft und die Knochen und Sehnen übermäßig belastet werden (häufiges Verletzungspotential dieser Personengruppe). Auch die Bedienung eines Computers (Tastatur- Mausemulation) bereiten dieser Personengruppe zumeist unüberwindbare Schwierigkeiten, wodurch sie auf die Hilfe von Pflegepersonal angewiesen sind. Ein weitere Grund für das Vorantreiben dieser Entwicklung ist die Tatsache, dass die Intimsphäre durch dritte anwesende Personen empfindlich eingeschränkt wird (selbständiges Telefonieren, Mails schreiben, etc.). Der Wunsch zu einer solchen Entwicklung wurde von betroffenen Personen direkt an uns herangetragen. Um das so erkannte Problem zu lösen wurde innerhalb einer Doktorarbeit ein

Sensor entwickelt welcher die Form einer Scheibe mit 120 mm Durchmesser und eine Höhe von 20 mm hat. Auf diese Scheibe kann ein beliebiger Körperteil (Hand, Fuß, Kopf) aufgelegt werden. Durch Druckverlagerung (x- und y-axis) kann sich die Scheibe zu allen Seiten neigen und erzeugt dabei proportionale Ausgangssignale. Die Scheibe kann ebenso zentrisch gedrückt werden (z-axis) um z. B. ein Menü aufzurufen (Mausklick). Der entwickelte Sensor kann somit Standardjoysticks in medizinischen Geräten wie z. B. elektrischen Rollstühlen (EPWs) ersetzen. Bei einer eintretenden Spastik ist es nicht mehr möglich, dass der Nutzer an dem Eingabegerät (in der Regel Joystick) hängen bleibt da die Scheibe flach ist und zudem in einem Bedientisch eingelassen werden kann. Der Körperteil rutscht bei einer Spastik lediglich über die Scheibe und eine Fehlbedienung ist somit weitestgehend ausgeschlossen.
In Einsatzgebieten wie z. B. der Medizintechnik wird höchste Sicherheit während der Nutzung gefordert. Zudem ist ein großes Spektrum hinsichtlich individueller Nutzung notwendig (Anpassung an den Patienten). Gerade für körperlich behinderte Menschen wie Spastiker wird die Nutzung eines Sensors (Joystick) oftmals zum Problem, da das Bewegungsspektrum (Kraft und Hub) krankheitsbedingt ständigen Veränderungen und unvorhersehbarer Spastik unterworfen ist. Aus diesem Grund ist der neu entwickelte Sensor zudem lernfähig und kann zu jeder Zeit an das gewünschte Bewegungsspektrum des Nutzers angepasst werden. Dieser Lernvorgang kann vom Nutzer selbst angestoßen werden und ist innerhalb von 15 Sekunden abgeschlossen. Keinesfalls außer Acht zu lassen ist hierbei die Entlastung des Gesundheitswesens. Bislang mussten Eingabegeräte bei den geringsten Änderungen des Krankheitsbildes neu und individuell angepasst werden. Zu den hohen Kosten der Fachkräfte kam zusätzlich der Umstand, dass Patienten möglicherweise während der Neuanpassung einen weiteren Krankheitsschub erfuhren und die gerade vollzogene Modifikation daducrh nicht mehr passend war. Auch in Entwicklungsländern wäre ein Einsatz dieser Scheibe denkbar da nach einer Versorgung vor Ort meist keine weiteren Mittel und kein Fachpersonal für die Nachsorge bereitstehen. Selbst die Weitergabe an andere Personen ist durch den Lernvorgang ebenso in wenigen Sekunden erledigt. Der Sensor ist sehr robust und kann derzeit ohne Schäden einer Belastung von 120 kg standhalten.
Im direkten Vergleich zu bestehenden Steuerungsmöglichkeiten sind Systeme wie Eye-Tracking, Sprachsteuerung und Gehirn-Computer-Schnittstellen eher problembehaftet. Mit diesen Eingabemethoden ist es schwierig präzise und gleichzeitig komplexe Steuerungen vorzunehmen. Eye-Tracking ist zudem Reflexen (Augenreflex) unterworfen und für sicherheitsrelevante Steueraufgaben gänzlich ungeeignet. Sprachsteuerungen können in der Regel nur einzelne Befehle entgegennehmen und funktionieren in lauten Umgebungen unzuverlässig.
Eine gut bewertbare Aufgabe ist das Fahren eines Kurses mit einem Elektrorollstuhl in Form einer „8“. Um diesen Kurs einwandfrei abfahren zu können sind proportionale Ausgangssignale wie die des hier vorgestellten Sensors oder die Ausgangssignale eines Joysticks notwendig.
Systeme welche den Nutzer bei der Navigation unterstützen (Hinderniserkennung) sind sinnvoll aber ebenso kostenintensiv. Zudem ist eine „freie Nutzung“ nicht möglich da die Navigationshilfe bei programmierten Situationen eingreift. Steuerungen welche die spastischen Bewegungen über einen definierten Zeitraum beobachten und durch einen Algorithmus mit Mittelwertbildung den wahrscheinlichen Richtungswunsch generieren, könnten mit der entwickelten Scheibe als Eingabemedium kombiniert werden. Jedoch wäre auch in diesem Fall die direkte Steuerung unterbunden. Bei sportliche Aktivitäten wie z. B. Elektrorollstuhl Hockey sind direkte Steuerungen unumgänglich.

Innovationsgrad	
Was ist der Innovationskern Ihrer Idee? Was macht Ihre Idee einzigartig?	Weil es keine geeigneten bzw. sichere Eingabegräte für Spastiker gibt.
In welchem Entwicklungsstadium befindet sich Ihre Innovation?	Prototyp ist bereits fertiggestellt und funktioniert einwandfrei.

Kundennutzen	
Welchen Nutzen hat Ihr Angebot aus der Sicht der KundInnen?	Sehr hohe Bediensicherheit für den Patienten.

Welche ZielkundInnen sprechen Sie an?	Spastiker und ähnliche Krankheitsbilder, Medizintechnik

Marktpotential	
Welche Trends kann man am Zielmarkt beobachten?	Kosten im Gesundheitswesen müssen eingespart werden. Leider oft zu Lasten der Patienten. Die eingereichte Lösung hilft dem Gesundheitswesen und dem Patienten.
Wie groß ist Ihr Zielmarkt, lässt er sich in Zahlen ausdrücken?	Kann ich nicht belegen
Welche KonkurrenzanbieterInnen gibt es bereits am Markt?	Keine bekannt

Wirtschaftliche Verwertung	
Wie viele Ressourcen (Zeit und Geld) benötigen Sie, um die Idee vermarktungsreif zu machen?	ca. 50.000€
Welche Möglichkeiten des Schutzes (Patente, Markenschutz usw.) bestehen?	Noch keine

3) STATISTIK

Wie sind Sie auf den Science Park Graz Ideenwettbewerb aufmerksam geworden?	☐ Plakat ☐ Flyer ☒ Email von Sonja Buchegger (bitte angeben) ☐ Newsletter von (bitte angeben) ☐ Ankündigung auf Website von (bitte angeben) ☐ Facebook ☐ Sonstiges (bitte angeben)

4) NEWSLETTER

Science Park Graz Newsletter	☒ Ja, ich möchte regelmäßig zum Thema Innovation und Gründung rund um den Science Park Graz informiert werden und bestelle den Science Park Graz Newsletter.

Hiermit nehme ich am Science Park Graz Ideenwettbewerb teil und versichere, dass meine Angaben wahrheitsgemäß erfolgt sind.

Der Science Park Graz ist berechtigt diese Daten im Rahmen der Evaluierung zu vervielfältigen und den Mitgliedern der Jury zur Verfügung zu stellen. **Alle am Wettbewerb beteiligten Personen (Science Park Graz MitarbeiterInnen und Jurymitglieder) unterliegen einer Vertraulichkeitsvereinbarung zum Schutz Ihres geistigen Eigentums!**

Ort, Datum/ Unterschrift	Graz, 20.12.2016

7.5 Tender of Master Theses

(3 pages)

Hochinteressante Aufgabenstellung zu zwei Masterarbeiten

Im Rahmen der „start up idea competition 2017“ gewann ein optischer Joystick den ersten Preis.

START-UP IDEA COMPETITION

10K TOTAL PRIZES
SPECIAL ESA-PRIZE

Patenturkunde

Gemäß dem Patentgesetz
ist für die in der angefügten Patentschrift
beschriebene Erfindung
ein Patent unter der

Nummer 517 676

erteilt worden.

Die Jahresgebühren werden bei alljährlicher Zahlung am letzten des Anmeldemonats fällig.

Wien, am 15. Juni 2017

Mag. Mariana Karepova
Präsidentin des Österreichischen Patentamts

Dieser neu entwickelte 3-Achsen Sensor befindet sich in einem voll funktionsfähigen Prototypenstadium und soll weiterentwickelt werden. Das österreichische Patent wurde am 15.06.2017 erteilt und kann unter der Patentnummer 517 676 online eingesehen werden. Die Funktionsweise basiert auf der optischen Auswertung einer Laserprojektion, welche eine geometrische Figur auf einem Bildsensor abbildet. Die so gewonnenen Koordinaten, werden dann entsprechend dem angeschlossenem System aufbereitet und ausgegeben. Das Ziel der Weiterentwicklung liegt darin, möglichst nah an ein marktreifes Produkt zu gelangen. Die zu leistende Entwicklungsarbeit kann in zwei voneinander abhängige Masterarbeiten unterteilt werden. Der Vorschlag zur Aufteilung der einzelnen Tätigkeiten kann selbstverständlich variiert werden. Weitere Details zu dem Prototyp können der Publikation *„A New, Adaptable, Optical High-Resolution 3-Axis Sensor“* doi:10.3390/s17020254 unter www.mdpi.com entnommen werden. Nach der Neuentwicklung ist die Gründung eines „start-up“ Unternehmens durch die Verfasser dieser Masterarbeiten möglich. Ausreichende Hilfestellungen werden selbstverständlich zu beiden Arbeiten gegeben.

Masterarbeit 1:

Hierbei wird die Hardware des optischen Sensors neu designt. Sowohl der Bildsensor als auch der Mikrocontroller (Signalprozessor) werden neu definiert und auf einer Platine untergebracht. Es sollten mindestens zwei 2 Varianten baugleich entstehen (highres, lowres). Das Platinenlayout ist nach EMV-verträglichen Vorgaben zu konzipieren und wird anschließend im Komplettsystem einer MPG- Prüfung an der TU-Graz unterzogen. Somit muss auch ein geeignetes Gehäuse entworfen werden, wodurch der einfache Austausch von industrieüblichen Standardjoysticks möglich wird. Die Projektionseinheit kann in ihrer funktionsweise übernommen werden, muss aber ebenso neu konstruiert werden. Die Hardwaregrundkonzeption wird zunächst provisorisch in einer Testvariante realisiert um die parallele Entwicklung der zweiten Masterarbeit (Software) zu ermöglichen. Mögliche Hard- oder Softwareänderungen werden hauptsächlich in diesem Stadium kommuniziert und umgesetzt.

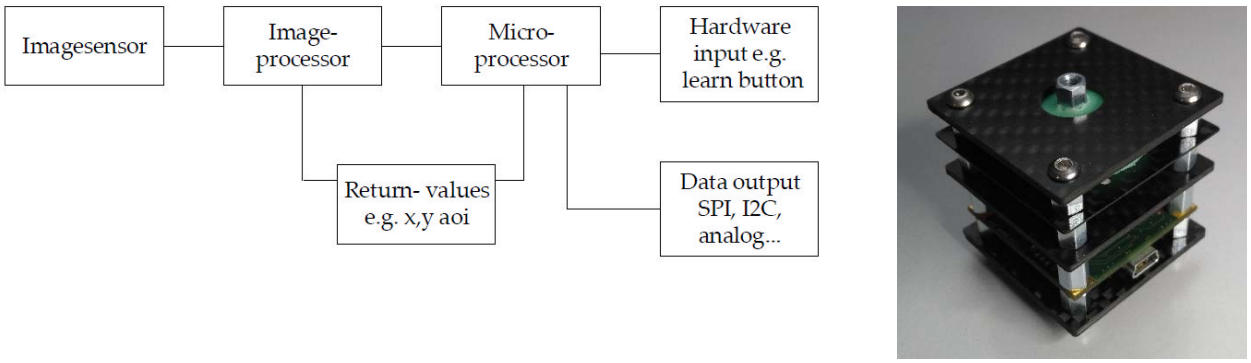

Abbildung 1: Möglicher Hardwareablauf und Prototyp

Masterarbeit 2:

Die grundlegende Vorgehensweise zur softwaretechnischen Verarbeitung der Bildinformation wird in Abbildung 2 dargestellt. Je nach eingesetztem Bildsensor werden die Bilddaten nach einer Initialisierung (Einstellung des Shutters, der Empfindlichkeit, etc.) im RAM eines Controllers durchsucht. Nach dem Auffinden einer zuvor definierten geometrischen Figur werden die Koordinaten des Mittelpunktes (Schwerpunkt) berechnet. Eine Ausgabe der Koordinaten erfolgt nach der erfolgreichen Plausibilitätsprüfung mittels eines an das Folgesystem angepassten Protokolls (SPI, I²C, seriell oder analog). Fehler während dem Betrieb werden grundsätzlich mit der Ausgabe von Ruhewerten und der Aktivierung einer I/O Leitung quittiert. Um den Sensor an das vorhandene Kraft- bzw. Bewegungsspektrum des Nutzers anzupassen, kann ein „teach-in“ durchgeführt werden. Die bislang eingesetzte Software wird dem Verfasser in Form des C++ Sourcecodes zur Verfügung gestellt.

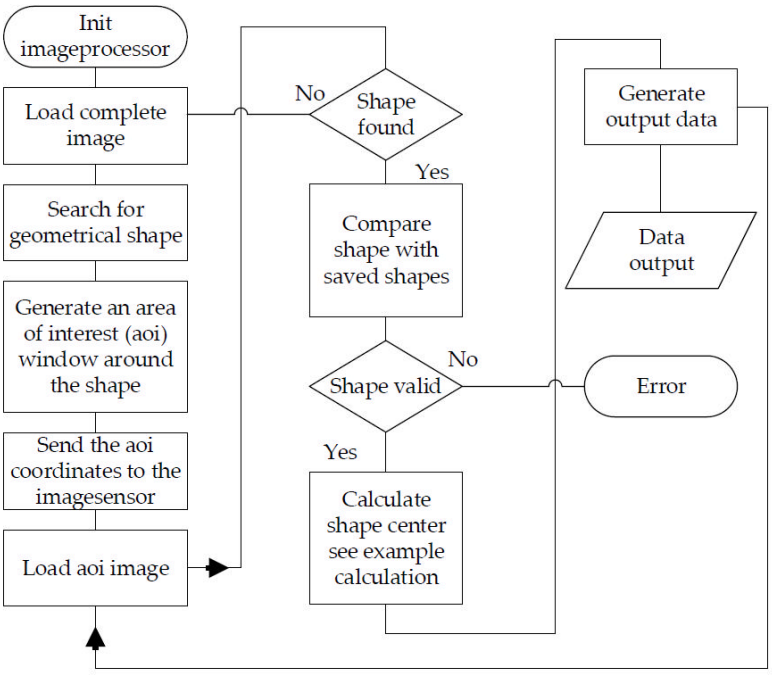

Abbildung 2. Möglicher Softwareablauf

Kontakt

Univ.-Prof. DI Dr. Christian Baumgartner

Institut für Health Care Engineering mit
Europaprüfstelle für Medizinprodukte
Technische Universität Graz
A-8010 Graz, Stremayrgasse 16

Tel: +43 316 873 7377
Fax: +43 316 873 107377
Email: christian.baumgartner@tugraz.at
Web: www.hce.tugraz.at

8. References

1. Freundorfer, S. *Joysticks: eine illustrierte Geschichte der Game-Controller 1972-2004*; Gameplan, 2004.
2. Analog Devices Inc. *AD7811/AD7812 (Rev. C)*. Available online: http://www.analog.com/media/en/technical-documentation/data-sheets/AD7811_7812.pdf (accessed on 1 January, 2017).
3. *fallpauschalenkatalog 2017 - Google-Suche*. Available online: https://www.google.de/?gws_rd=ssl#q=fallpauschalenkatalog+2017 (accessed on 28 June, 2017).
4. *Muskelerkrankungen | Deutsche Gesellschaft für Muskelkranke e.V. (DGM)*; 2017. Available online: https://www.dgm.org/muskelerkrankungen (accessed on 17 February, 2017).
5. *HCE - Home*; 2016. Available online: https://www.tugraz.at/institute/hce/home/ (accessed on 17 February, 2017).
6. Oréalys. *4000 Series APEM, industrial and professional switches, joysticks, switch panels, LED indicators*. Available online: http://www.apem.com/Robust-potentiometer-joysticks-v9-d-1023.html (accessed on 22 February, 2017).
7. Piot, J.; Favre, P.; Bidiville, M.; Kehlstadt, F.; Merminod, A. *Electromagnetic joystick using varying overlap of coils and conductive elements.* US Patent 08/956,840.
8. Zeller, S. *Dreiachsig drehpositionierbarer Steuerknüppel.* EU Patent 19970101788.
9. Uhlmann, E.; Seibt, M.; Haertwig, J.P.; Schaeper, E. *Einrichtung zur erfassung der relativposition zweier zueinander bewegbarer körper.* DE Patent 2002/002991.
10. Klinger, D. *Optoelectronic measurement arrangement.* US Patent 07/646,600.
11. Furrer, B.; Ihlefeld, J.; Knaus, T.; Kluser, C.; Tiedeke, J. *Messvorrichtung zum messen von verformungen elastisch verformbarer objekte.* EU Patent 2010/000738.
12. Kamentser, B.; Kamentser, E. *Force transducer with co-planar strain gauges.* U.S. Patent No. 5,872,320, 16. Febr. 1999.

13. Manara, A.; Scofield, M.C.; Cheal, B. *Sensor and circuit architecture for three axis strain gauge pointing device and force transducer.* U.S. Patent No. 6,243,077, 5. June 2001.
14. Nejedly, P.; Whitfield, D.W. *Three dimensional strain gage transducer.* U.S. Patent No. 4,217,569., 12. Aug. 1980.
15. IDS Imaging Development Systems GmbH. *UI-1241LE*. Available online: https://de.ids-imaging.com/store/ui-1241le.html (accessed on 10 January, 2017).
16. IDS Imaging Development Systems GmbH. *UI-3591LE*. Available online: https://de.ids-imaging.com/store/catalogsearch/result/?q=UI-3591LE (accessed on 10 January, 2017).
17. *uEye Cockpit - IDS Software Suite - IDS Imaging Development Systems GmbH*. Available online: https://de.ids-imaging.com/ueye-cockpit.html (accessed on 24 February, 2017).
18. Wacker Chemie AG. *Home*. Available online: https://www.wacker.com/cms/de/home/index.jsp (accessed on 24 February, 2017).
19. *Siglent SDG1050 2CH 50MHz Waveform Generator*. Available online: http://www.siglent.eu/siglent-sdg1050-functiongenerator.html (accessed on 26 February, 2017).
20. *Mixed Domain Oscilloscopes | Tektronix*. Available online: http://www.tek.com/datasheet/mixed-domain-oscilloscopes-3 (accessed on 26 February, 2017).
21. PETEC. *Flüssigmetall 25 ml SB - PETEC*. Available online: http://www.petec.de/index.php?id=610 (accessed on 26 February, 2017).
22. *ADAU1701 Datasheet and Product Info | Analog Devices*. Available online: http://www.analog.com/en/products/processors-dsp/sigmadsp-audio-processors/adau1701.html#product-overview (accessed on 27 February, 2017).
23. *EVAL-ADAU1701 Evaluation Board | Analog Devices*. Available online: http://www.analog.com/en/design-center/evaluation-hardware-and-software/evaluation-boards-kits/EVAL-ADAU1701.html#eb-overview (accessed on 27 February, 2017).

24. *SigmaStudio* | *Analog Devices*. Available online: http://www.analog.com/en/design-center/processors-and-dsp/evaluation-and-development-software/ss_sigst_02.html (accessed on 28 June, 2017).
25. *APEM Serie MS*. Available online: http://www.apem.de/files/apem/brochures/DEU/Serie_MS_de_Low_Res.pdf (accessed on 11 January, 2017).
26. Fischer, R.E.; Tadic-Galeb, B.; Yoder, P.R.; Galeb, R. *Optical system design*; Citeseer, 2000.
27. PRIESE, L. *Computer Vision*: *Einführung in die Verarbeitung und Analyse digitaler Bilder*, 1st ed; Springer Vieweg: Berlin, Heidelberg, 2015.
28. Balon, D. Facts About Myotonic Muscular Dystrophy. *MDA Muscular Dystrophy Association Inc* **2009**, 5.
29. Ehrenstein, G.W. *Faserverbund-Kunststoffe: Werkstoffe, Verarbeitung, Eigenschaften*, 2nd ed; Hanser Verlag: München, 2006.
30. Thorp, E.B.; Abdollahi, F.; Chen, D.; Farshchiansadegh, A.; Lee, M.-H.; Pedersen, J.P.; Pierella, C.; Roth, E.J.; Seanez Gonzalez, I.; Mussa-Ivaldi, F.A. Upper Body-Based Power Wheelchair Control Interface for Individuals With Tetraplegia. *IEEE transactions on neural systems and rehabilitation engineering : a publication of the IEEE Engineering in Medicine and Biology Society* **2016**, *24*, 249–260.
31. Buchhold, N.; Baumgartner, C. A New, Adaptable, Optical High-Resolution 3-Axis Sensor. *Sensors (Basel, Switzerland)* 2017, *17*.
32. Hu, X.; Afsharipour, B.; Rymer, W.Z.; Suresh, N.L. Impairment of muscle force transmission in spastic-paretic muscles of stroke survivors. In *2016 38th annual international conference of the IEEE Engineering in Medicine and Biology Society (EMBC)*: IEEE: Piscataway, NJ, 2016, pp. 6098–6101.
33. Huntemann, A.; Demeester, E.; Poorten, E.V.; van Brussel, H.; Schutter, J. de. Probabilistic approach to recognize local navigation plans by fusing past driving information with a personalized user model. In *IEEE International Conference on Robotics and Automation (ICRA), 2013*, *6 - 10 May 2013, Karlsruhe, Germany*: IEEE: Piscataway, NJ, 2013, pp. 4376–4383.
34. Kim, E.Y. Wheelchair navigation system for disabled and elderly people. *Sensors* **2016**, *16*, 1806.

35. Cooper, R.A.; Widman, L.M.; Jones, D.K.; Robertson, R.N.; Ster, J.F. Force sensing control for electric powered wheelchairs. *IEEE Transactions on Control Systems Technology* **2000**, *8*, 112–117.
36. Wolpaw, J.R.; Birbaumer, N.; Heetderks, W.J.; McFarland, D.J.; Peckham, P.H.; Schalk, G.; Donchin, E.; Quatrano, L.A.; Robinson, C.J.; Vaughan, T.M. Brain-computer interface technology: a review of the first international meeting. *IEEE transactions on rehabilitation engineering : a publication of the IEEE Engineering in Medicine and Biology Society* **2000**, *8*, 164–173.
37. Kim, K.-N.; Ramakrishna, R.S. Vision-based eye-gaze tracking for human computer interface. In *IEEE SMC'99 conference proceedings*: IEEE Service Center: Piscataway, NJ, 1999, pp. 324–329.
38. Malkin, J.; House, B.; Bilmes, J. Control of simulated arm with the vocal joystick. CHI 2007 Workshop on Striking a C [h] ord: Vocal Interaction in Assistive Technologies, Games, and More. *CHI 2007 Workshop on Striking a C [h] ord: Vocal Interaction in Assistive Technologies, Games, and More* **2007**.
39. Malkin, J.; House, B.; Bilmes, J. The VoiceBot: a voice controlled robot arm. Vocal Interaction in Assistive Technologies, Games, and More. *CHI 2007 Workshop on Striking a C [h] ord* **2007**, 183–192.
40. Buchhold, N. *Apparatus for controlling peripheral devices through tongue movement, and method of processing control signals.* US Patent 5460186 A, 24. Okt. 1995.
41. Kim, J.; Park, H.; Ghovanloo, M. Tongue-operated assistive technology with access to common smartphone applications via Bluetooth link. *Conference proceedings : … Annual International Conference of the IEEE Engineering in Medicine and Biology Society. IEEE Engineering in Medicine and Biology Society. Annual Conference* **2012**, *2012*, 4054–4057.
42. Martens, C.; Ruchel, N.; Lang, O.; Ivlev, O.; Graser, A. A friend for assisting handicapped people. *IEEE Robotics & Automation Magazine* **2001**, *8*, 57–65.
43. Analog Devices Inc. *AD623 (Rev. E)*. Available online: http://www.analog.com/media/en/technical-documentation/data-sheets/AD623.pdf (accessed on 1 January, 2017).

44. Dynamic Controls. *The DX2 System - Dynamic Controls*. Available online: https://dynamiccontrols.com/en/dealers/products/dx2/the-dx2-system (accessed on 1 January, 2017).
45. MACSPV. *merkblatt_d*. Available online: http://www.spv.ch/__/frontend/handler/document.php?id=245& (accessed on 4 July, 2017).
46. Marx, G.; Muhl, E.; Zacharowski, K.; Zeuzem, S. *Die Intensivmedizin*; Springer Berlin Heidelberg, 2014.
47. Schmitz, B.; Tettenborn, B. *Paroxysmale Störungen in der Neurologie*; Springer Berlin Heidelberg, 2006.
48. *R-Net Mobility Wheelchair Control System | Curtiss-Wright*. Available online: http://www.cw-industrialgroup.com/Products/Mobility-Vehicle-Solutions/R-net.aspx (accessed on 5 July, 2017).
49. Gohritz, A.; Turcsányi, I.; Fridén, J. Handchirurgie bei R?ckenmarkverletzungen (Tetraplegie). In *Handchirurgie*; Towfigh, H., Hierner, R., Langer, M., Friedel, R., Eds.: Springer-Verlag Berlin Heidelberg: Berlin, Heidelberg, 2011, pp. 1673–1694.
50. Zäch, G.A.; Koch, H.G. *Paraplegie*: *Ganzheitliche Rehabilitation*; Karger, 2006.
51. *Kinnsteuerung*. Available online: https://www.der-querschnitt.de/archive/fachbegriff/kinnsteuerung (accessed on 6 July, 2017).
52. Daut, V. Leben mit Duchenne-Muskeldystrophie. Eine qualitative Studie mit jungen Männern.
53. Buchhold, N.; Baumgartner, C. *Optische, lernfähige Dreiachsensensorik.* Austrian Patent Nr. A 571/2015, 15. Jun. 2017.
54. Buchhold, N.; Baumgartner, C. A New Input Device for Spastics Based on Strain Gauge. *Sensors (Basel, Switzerland)* 2017, *17*.
55. Matschiner, H.; Klätte, M., Eds. *Infrarotheizung*: *Ein Heizsystem mit Zukunft ; [Fachtagung Infrarotheizung - ein Heizsystem mit Zukunft ; Tagungsband]*; Jenaer Akad. Verl.-Ges: Jena, 2010.